Introduction to PV Development



History • Physics • Materials • Measurement • Research

Publication information and a note to the reader.

Alper Ferudun · Mercury Software GmbH

English teaching edition · 9 September 2026

This book is designed to guide readers with no prior knowledge of photovoltaics from basic concepts to research questions. In historical experiments, the setup and observations are explained, and in technical subjects, the mechanism, unit, example, and model limits are explained together. After the introductory explanations, the text moves on to more advanced details.

CC BY 4.0 · License and attribution

Copyright and similar rights that the publisher is authorized to license are licensed under the Creative Commons Attribution 4.0 International License, unless otherwise specified. Commercial use, sharing, translation, and adaptation are permitted. Preserve the attribution to Alper Ferudun and Mercury Software GmbH, the source and license links, and the copyright and warranty notices; indicate any changes. Do not imply that the publisher endorses your use; do not apply any additional condition or digital restriction that limits the permitted uses.

Creative Commons BY 4.0 license text · EulerSolve library

Third-party works cited in the bibliography, trademark and patent rights, and font software are not re-licensed by this notice. The freedoms of public domain elements are preserved. To the extent that no copyright arises in artificial intelligence elements, this notice does not create any new rights. The work is provided as is, to the extent permitted by law; no warranty of accuracy or specific results is given.

Editorial guidance and publication: Alper Ferudun. OpenAI tools were used in the preparation of the text and visuals. Conceptual illustrations are not actual sample photographs; numerical examples are synthetic unless otherwise specified. This work does not claim to be a peer-reviewed publication or to present experimental validation. It is not claimed that all literature has been reviewed; the limitations of access to sources are explained in the records.

Suggested citation: Ferudun, A. (Ed.). (2026). Introduction to PV Development. Translation of the Turkish teaching revision, 9 September 2026. Affiliation: Mercury Software GmbH. Specify the chapter and printed page used.



Contents

Chapter titles and page numbers are clickable. This volume is a standalone book in a two-book series.

BOOK I · Introduction to PV Development 1

I.01 To the reader: from understanding light to designing research 7

I.02 From light to electricity: the emergence of photovoltaics and its research culture 13

I.03 Solar source, spectrum, and photon accounting 26

I.04 The inner workings of a semiconductor: bands, statistics, and optical transitions 34

I.05 Junction and selective contact: how is the light-generated charge converted into work? 41

I.06 Recombination: where current and voltage are lost 50

I.07 Current-voltage curve: interpreting a cell's performance 58

I.08 Detailed balance and voltage losses: what does the theoretical limit restrict? 66

I.09 Multijunction cells: the physics of spectrum splitting 74

I.10 Crystalline silicon: transforming a good semiconductor into a good product 81

I.11 Thin films: low material consumption, intense interface physics 88

I.12 III-V and multijunction cells: the cost of spectral splitting 94

I.13 Halide perovskites: strong optoelectronics, dynamic chemistry 100

I.14 Perovskite tandem cells: why is simply combining two good cells not enough? 109

I.15 Organic, dye-based, quantum-dot and emerging absorbers 115

I.16 Optical, contact, and interface engineering: the common language of all technologies 121

I.17 From the laboratory to the module: area, encapsulation, and sustainable production 127



I.18 Photovoltaic measurement: how the correct value is obtained 135

I.19 Characterization: which question does each tool answer? 143

I.20 Durability: from one-hour curves to service life 151

I.21 First-principles materials research: the power and limits of DFT 158

I.22 From material to cell: optical and electrical modeling 166

I.23 Searching for materials with machine learning: from prediction to evidence 174

I.24 Experimental design and statistics: how do you distinguish an effective change? 180

I.25 From cell to module, to the field, and throughout the lifecycle 186

I.26 From literature review to research question 193

I.27 How is a research program established? 197

I.28 A twelve-week study route for researchers 202

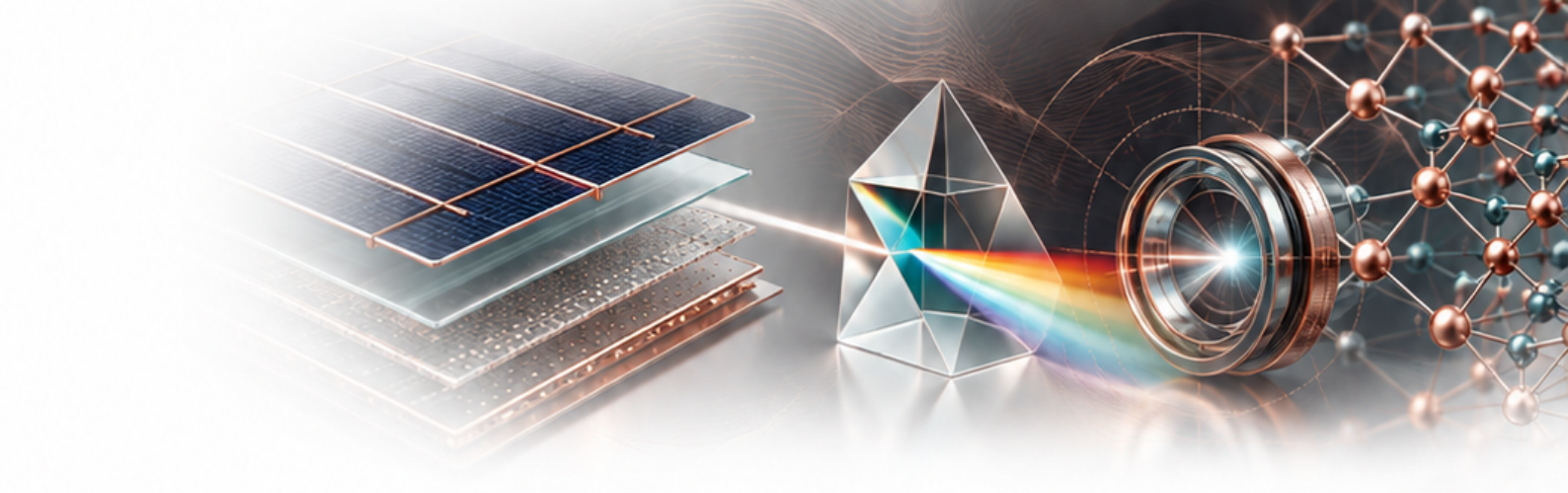
I.29 Clear limitations of the research and future perspectives 205

I.30 To analyze a device from start to finish 209

I.31 Solved research problems 214

I.32 Symbols, units, and a Turkish-English glossary 219

I.33 References and access notes 225



List of figures

Figures and calculated plots in the text. Each caption identifies the conceptual explanation, model or data source.

01 Four scales extending from photons to lifetime energy generation 9

02 A teaching illustration of the two-compartment setup described in Becquerel's 1839 paper 15

03 The upper circuit investigates the change in conductivity under external bias; the lower circuit investigates the current dependent on illumination without an external battery 18

04 The historical development of photovoltaic concepts and devices 20

05 The rationale behind three different experiments 23

06 From the reference spectrum to photon counting 28

07 The photon energy and absorption length represent different scales 29

08 The band structure and occupancy are distinct pieces of information 36

09 Charge, field and potential are three views of the same solution 43

10 A single Fermi level at equilibrium; separated quasi-Fermi levels in the ideal illuminated open-circuit limit 45

11 Generation and collection do not follow the same profile 48

12 Three recombination mechanisms and where the energy goes 52

13 Different injection regimes with the same material parameters 56

14 From the physical solar cell to the single-diode equivalent circuit 60

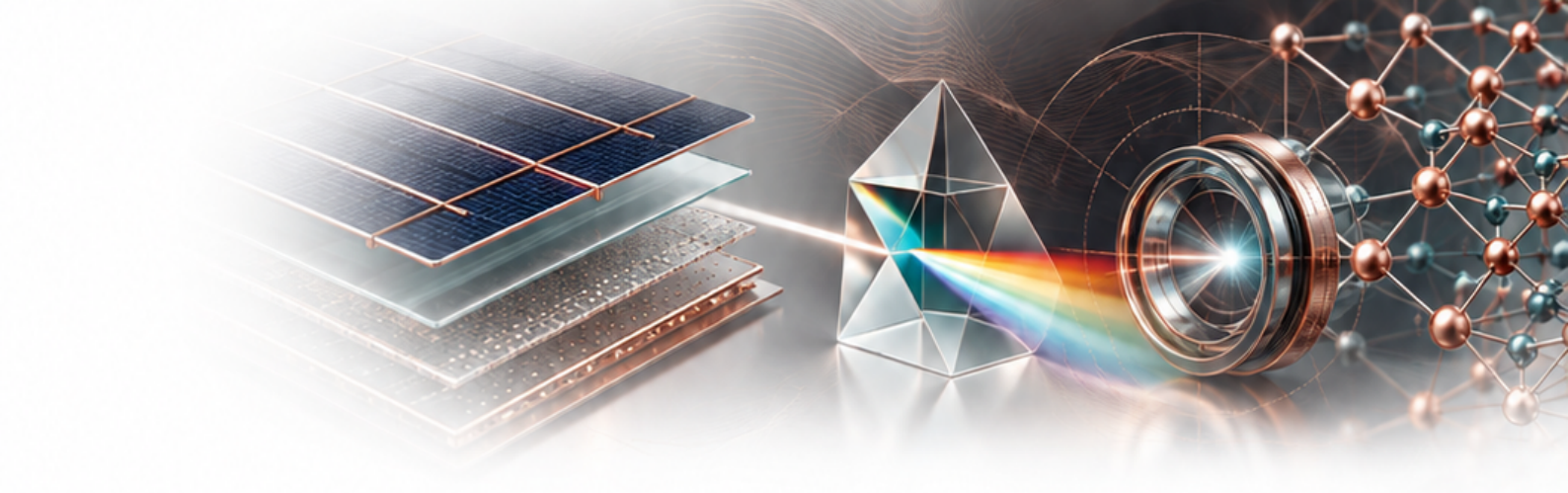
15 The distinct traces of series and parallel losses on the curve 64

16 Recalculation of the ideal single-junction limit 67

17 Isolating voltage losses 72

18 Optical sharing and electrical connection in a tandem 75

19 Cross-sections of four common silicon design concepts 82



20 Typical layer sequences for CdTe, CIGS, and amorphous silicon families 89

21 Spectrum and electrical connection sharing in a three-junction III-V device 95

22 The perovskite structure family and two device orientations 101

23 Transition from wet precursor to polycrystalline film 106

24 An illustrative diagram of slow ionic redistribution under bias 107

25 Representative layer cross-section for a monolithic perovskite-silicon tandem cell 110

26 Interface and connected transport pathways in an organic bulk heterojunction 116

27 Interference-based reflection reduction 125

28 Passivation and conductivity are two distinct design targets 126

29 Cell stripes and interconnection traces in a monolithic thin-film module 128

30 Two complementary measurement setups 136

31 The origin of spectral mismatch 141

32 Reading a signal requires a physical forward model 144

33 Analyze the stability in terms of time and mechanism 152

34 Testing DFT results at two distinct scales 159

35 The defect formation energy and the kinetic barrier have different roles 164

36 From a continuous device description to a conservative finite-volume calculation 167

37 An example of an optimum thickness with explicitly defined geometry 172

38 The data split must match the research question 175

39 Illustrative examples of blocking and interaction 181

40 From initial power to lifetime energy 187

41 The research cycle that tests the mechanism 198

42 The same efficiency, different physics 211

BOOK I · CHAPTER 01 / HISTORY AND PHYSICS

To the reader: from understanding light to designing research

To begin: the cell, the circuit, and energy

The large, glazed panel we see on a roof is usually a **module**. Inside the module, there are many interconnected solar **cells**. A cell is the smallest functional device that converts light into electrical energy. Many modules, along with cables, a supporting structure, and devices that convert the electricity into a usable form, form a **system**. An inverter is a power electronics device that converts the direct current produced by the cells into alternating current for the grid. A battery stores energy; however, not every system requires a battery for the cell to operate. [B16]

First, let's define the three key terms related to electricity. **Charge** is the property of particles that allows them to interact electrically; an electron has a negative charge. The net amount of charge passing through a cross-section of a wire in one second is the **current**. **Voltage** is the difference in energy that can be transferred per unit of charge between two points. Just as the water level in a reservoir and the amount of water flowing through a pipe are different, voltage and current are also different. This analogy only provides an intuitive understanding of the relationship; in an electrical circuit, electrons are not consumed like water, and the transfer of energy is explained in conjunction with the electromagnetic field.

The unit of current is the ampere, the unit of charge is the coulomb, and the unit of voltage is the volt. 1 ampere is 1 coulomb per second; 1 volt means 1 joule per coulomb. **Power** is the rate at which energy is transferred. Its unit is the watt, which is joules per second. In a direct current, the two fundamental relationships are as follows:

$$P = VI, \qquad E = Pt. \tag{I.1.1}$$

Here, P represents power, V represents voltage, I represents current, E represents energy, and t represents time. In the teaching example, a cell that provides 2 A at a voltage of 0.5 V provides 1 W of power. If the same conditions last for two hours, it provides 2 Wh of energy. This is 7200 J, because one hour is 3600 seconds. If the power changes over time, the energies in each small time interval are summed. The integral sign will be used later as a shorthand notation for this summation.

What changes inside when light is present?

We can examine light through its constituent **photons**, which carry energy. A **semiconductor** is a material whose properties are determined by the energy levels at which its electrons can exist and how easily they can move. When a photon with appropriate energy is absorbed, the electron can transition to a higher energy state. The resulting electron deficiency is called a **hole**. A hole is not a physical void within the crystal; it is an electronic deficiency whose movement we track as if it were a positive charge carrier.

The creation of these mobile charge carriers by light is the starting point. The **contacts** on both sides of the cell establish an electrical connection with the external cables. In a good cell, one contact preferentially collects electrons, while the other collects holes. This preference is called **selectivity**. If the charges return to a low-energy state without participating in the work, this is called **recombination**. We will discuss these concepts in order; for now, it should be remembered that the absorption of light, the creation of charge carriers, their arrival at the appropriate terminal, and the performance of work in the external circuit are four separate steps. [B16]

Percentage, area, and initial efficiency calculation

Efficiency is the ratio of the electrical output power to the incident light power. In the teaching example, the area of a 10 cm × 10 cm cell is 100 cm^2, which is 0.01 m^2. If 1000 W/m^2 of light falls on the cell, then 10 W falls on the cell. If the cell produces 2 W of electrical power, the efficiency is 2/10 = 0.20, which is 20%. The remaining energy does not disappear; some of it is reflected, transmitted, or converted into heat. The output from “20%” to “22%” is a 2 percentage point increase, which is a 10% relative increase compared to the beginning. These two statements in research papers are not the same number.

This book does not assume any prior knowledge of PV. It introduces the tools, such as ratio setting, scientific notation, graphical slope, and area under the curve, as they are used. More advanced derivations may require a slower pace during the initial reading. First, we will understand what the quantity represents, then its unit, and finally the assumption of the equation. The goal is not to memorize the formula, but to be able to test what it says with numbers of your own choosing.

Comprehension check: Did we generate electricity?

Does a cell displaying 0.6 V in an open circuit prove that it is currently supplying power? **No.** If the current in the external circuit is zero, then even if there is voltage, the power delivered to the external circuit is zero. When a load is connected, it is necessary to measure the voltage and current together. For 0.5 V and 0.1 A, the power is 0.05 W. This distinction is the first key to understanding subsequent experimental results.

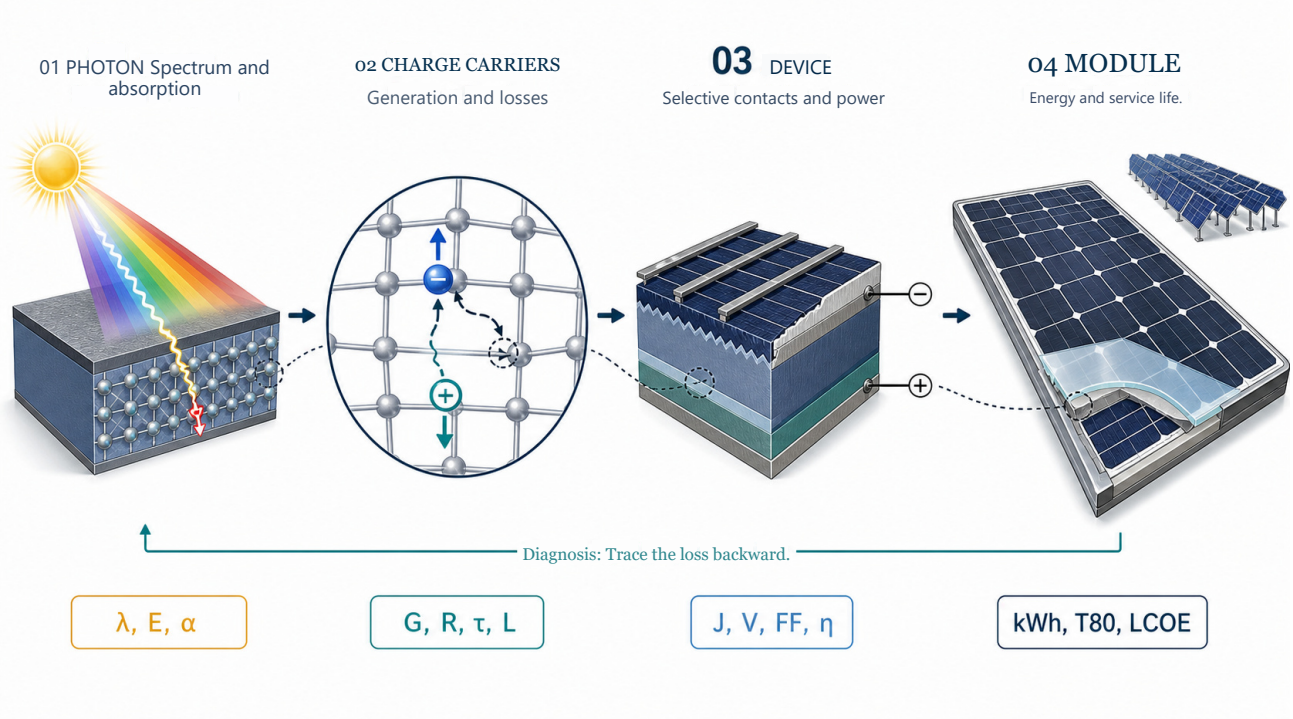


Figure 01. Four scales extending from photons to lifetime energy generation. Light absorption determines carrier generation; generation and recombination determine the current that can be collected; selective contacts determine device power; and encapsulation and durability determine service life. The return path along the bottom illustrates how a module loss can be traced to mechanisms at smaller scales. The dimensions of the structure, charges and layers are schematic. Conceptual illustration prepared with an image-generation tool; it is not a measurement image.

When we look at a solar cell, we see two different objects. The first is a structure a few micrometres or a few hundred micrometres thick that generates electricity under illumination. The second is the accumulated knowledge of almost two centuries of experiments, quantum physics, chemistry, precision measurement and manufacturing engineering. This book was written to make the second object visible. Its purpose is not merely to teach the names of technologies, but to establish a way of thinking that allows you to answer independently why a cell works, why it performs worse than expected, and how we can tell whether we have improved it.

Photovoltaics, or PV, is the direct conversion of light into electrical energy. Solar thermal systems first produce heat; PV cells use the interaction between photons and electronic states. A system does not automatically become photovoltaic simply because it runs on sunlight. Nor does a material's absorption of light mean that it makes a good

solar cell. Some of the absorbed energy must be transferred to the external circuit through selective contacts without losing the carriers. The chapters of this book examine the different links in this chain.

What does this book cover?

History and fundamental physics, the solar spectrum, semiconductors, carrier transport, recombination, current-voltage curves, thermodynamic limits, the main material families, tandems, optical and interface engineering, manufacturing, characterisation, measurement uncertainty, reliability, computational materials discovery, machine learning and field performance are considered together. The final part presents a method for reading the literature, examples of research design, a study programme and a Turkish-English glossary.

This breadth does not replace all the detail within a specialist field. A researcher is usually not an expert in the whole of PV; for example, someone specialising in defect calculations may work with colleagues on module ageing. The aim here is to understand the language connecting the fields, see where to position your own expertise, and ask about critical assumptions when assessing someone else's result.

Three reading routes

For the introductory route, read the chapters on history, the spectrum, basic semiconductor physics and J-V in sequence. Then compare the silicon and perovskite chapters. Finally, move on to measurement. This route teaches you what the Jsc, Voc, FF and PCE values in a paper mean, how they are obtained and when they should be questioned.

For the researcher's route, complete all the physics and measurement chapters, then choose a single material family. Analyse the supplementary information, characterisation data and methods section of an original paper in that family using the questions in this book. Then carry out a computational or experimental reproduction study. The strongest test of understanding a paper is being able to explain which alternatives you could have chosen in place of the author's decisions.

In the computational research pathway, focus particularly on the sections of computational discovery, interface, device modeling, uncertainty, and research design. Always keep in mind that verifying a chemical formula and verifying a cell are different tasks. The calculated band gap is not the performance of the entire system. The calculation is exemplified in the later research sections, which demonstrate that material, interface, device, and product verification each require different types of evidence.

Distinguishing types of knowledge

The book contains four types of knowledge. Established physics comprises charge conservation, energy conservation and the equations of well-defined models. A model-dependent inference is a result obtained under a particular spectrum, temperature and set of loss assumptions. An experimental finding belongs to a particular specimen and measurement arrangement. A research proposal is an idea that has not yet been tested. Whenever a paragraph moves between these types, the transition is stated explicitly.

Most of the figures are graphs generated using original educational diagrams and clear equations. The reference solar spectrum has been redrawn from numerical data with the source specified. The numbers used in the example calculations are synthetic values selected for teaching purposes, unless otherwise stated; they are not actual sample measurements or validated predictions for a new material. Historical achievements found in the sources are not presented as the current world record. Independent efficiency tables serve as the starting point for a current record comparison; the sample area and measurement conditions should still be checked. [B03]

Scope and method of the literature review

The cut-off date for the initial literature review is September 7, 2026. In this Turkish teaching revision, new historical source checks were performed on September 8, 2026. This work is not a systematic meta-analysis or a comprehensive review of all publications; it is a broad literature synthesis aimed at researcher training. Sources were selected based on historical milestones, original studies that elucidate mechanisms, measurement and reliability protocols, institutional data sources, and further reading materials. Publisher pages, DOI records, universities, and public research institutions were prioritized. No detailed results or standard items were extracted from inaccessible full texts.

The search clusters included: photovoltaic history and solar battery; semiconductor recombination and selective contacts; detailed balance and tandem current matching; silicon PERC TOPCon heterojunction; CdTe CIGS III-V; halide perovskite ion migration; organic DSSC quantum dot; JV EQE stabilized efficiency; ISOS IEC reliability; DFT defects convex hull phonons; machine learning materials leakage; photovoltaic energy yield LCA recycling. Backward and forward citations of foundational sources were used to connect these clusters. This method covers the main structure of the field; it does not claim to have searched all languages and patent databases exhaustively.

In the bibliography, the letters H, T, R, and B represent fundamental physics/history, technology, research/measurement, and editorial reference sources, respectively. The same source can be reused in different sections. DOIs or institutional links are provided in a clickable format. For some of the books, only the publisher's scope and bibliographic information have been verified; these are not indicated as fully read works.

Reading the scale of the field correctly

The IEA PVPS 2026 Snapshot report states that global installed PV capacity reached approximately 3 TW by the end of 2025. The summary chart in the main report gives 2025 additions as a range of 607-698 GW; the summary page highlights the upper estimate of approximately 698 GW. Here, 2026 is the publication year and 2025 is the data year; the values should be read in the context of the report's estimates and revisions. Installed capacity is not an amount of energy: the annual generation of a 1 GW plant depends on irradiance, temperature, losses and availability. [B02]

The Fraunhofer ISE report updated on 14 July 2026 presents indicators for cells, modules, manufacturing, cost and sustainability together. Such reports are useful for an overall picture of the technology; for the details of a research record, consult the original certificate or primary table. Not every number in the same report necessarily refers to the same date or uses the same denominator definition. [B01]

The researcher's reflex

When reading a result, first complete this sentence: "This material or structure, under these conditions and compared with this control, showed a difference in this observable quantity with this uncertainty." If you cannot complete the sentence, the result has not yet been fully understood. This reflex is a tool that will outlast even the equations in this book.

BOOK I · CHAPTER 02 / HISTORY AND PHYSICS

From light to electricity: the emergence of photovoltaics and its research culture

Let’s first familiarize ourselves with the experimental setup

The statement “1839: Becquerel” in the timeline raises the following question: When light falls on a material, does it only heat it, or can it also create an electrical change? The researcher in question is **Edmond Becquerel**. We will not interpret his 1839 work by assuming he knew about modern solar panels. First, we need to understand the function of the components he used, then the condition he modified, and finally the result he observed.

An **electrode** is a conductor that establishes contact between an electrical circuit and the medium being studied. An example of this is immersing a metal plate in a liquid. An **electrolyte** is a medium that can conduct current through the movement of charged atom or molecule groups, called ions. While current in a metal wire is primarily carried by electrons, ion movement is important in a solution. At the **interface** where the metal and the liquid meet, chemical reactions involving electron exchange can occur. The study of electricity and chemistry together is called **electrochemistry**.

A **galvanometer** is a measuring instrument that makes the magnetic effect of very small currents visible by deflecting a needle. In older texts, it is also referred to as a “multiplicateur.” A 10-degree deflection of the needle does not necessarily mean 10 amperes or 10% efficiency. To convert the degree to current, the instrument’s calibration, the circuit’s resistance, and the reading method must be known. **Calibration** is the process of establishing the relationship between the measuring instrument’s indication and a known reference value. This allows us to distinguish what the old observation was measuring and what result it could not provide on its own.

1839: What exactly did Becquerel do?

Becquerel's November 1839 text begins by recalling his research on the contact of two liquids in July, aiming to determine whether the electrodes also respond to light. In the described setup, a box with darkened interiors is divided into two compartments by a thin membrane. Each compartment contains the solution being tested and a platinum plate. The plates are connected to a sensitive galvanometer. The compartments are kept in the dark with separate lids, and the lids are opened sequentially to change which side is illuminated. He attempts to separate the effect of light from the thermal effect using colored filters. The weakening of the effect on very clean platinum surfaces demonstrates the importance of the surface condition. [H31]

As you read this sequence, consider the four steps in order. **First**, establish the behavior of both sides in the dark as a baseline. **Next**, change the illumination of only one side, keeping the other parts of the circuit the same. **Then**, observe the relationship between illuminating and turning off the other side and its effect on the indicator. **Finally**, choose a control to test another possible cause for the observed change. These four sentences represent a reading of the historical description in the language of modern design of experiments; it is not a data table fabricated later to account for missing historical measurements.

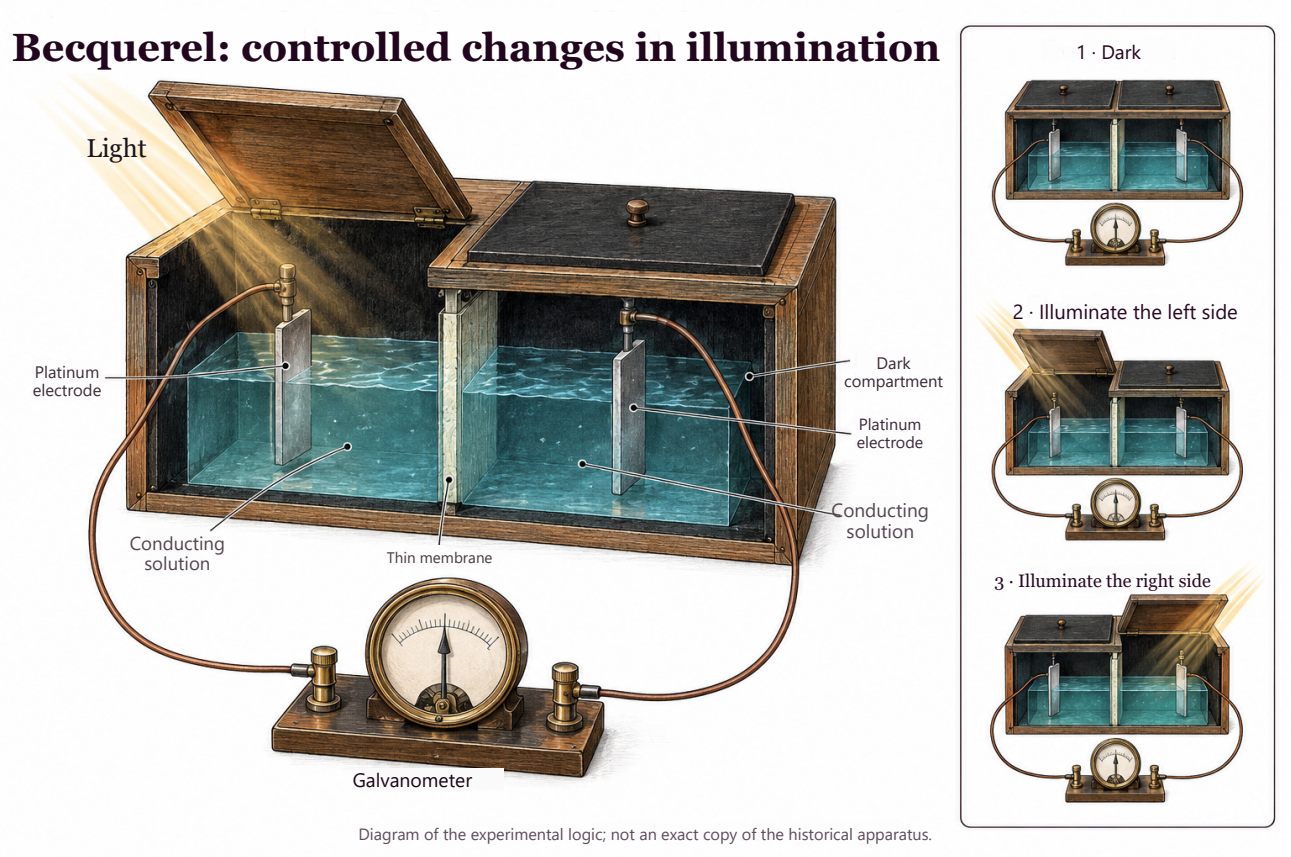


Figure 02. A teaching illustration of the two-compartment setup described in Becquerel's 1839 paper. The plates are connected externally via a galvanometer, and the liquids are connected internally via an ionic path across the membrane. The purpose of the covers is to change which side receives light; the source does not provide the exact dimensions of the historical device in this drawing. [H31] Conceptual illustration prepared with an image-generation tool; it is not a measurement image.

Why should the silver chloride experiment be explained separately?

In the subsequent part of the same text, a freshly prepared thin silver chloride layer is placed on platinum; the plate is then immersed in water to which acid is added, making it conductive. When illuminated, the layer darkens, and the galvanometer needle deflects. In this way, the visible chemical change and the electrical response are observed together. [H31] This description is not a procedural recipe but rather the experimental logic of the original work; it is not necessary to use the historical chemicals exactly as described in a modern laboratory experiment.

The formula for silver chloride is **AgCl**: Ag represents silver, and Cl represents chlorine. The chemical formula indicates the elements and their ideal stoichiometric ratio. A **photochemical reaction** is a chemical process that is initiated or altered by light energy. The change in photographic materials upon exposure to light provides a familiar example of this concept. Here, the metal plate should not only be considered as an "electrically conductive material"; it also provides electrical contact and mechanical

support to the light-sensitive layer. The liquid, on the other hand, is part of the electrochemical pathway.

The cautious conclusion from this experiment is that light can change the electrical behavior of a particular electrode-solution arrangement. It does not directly establish a modern silicon p-n junction, stable power over a long period, or a particular energy conversion efficiency. **Photovoltage** means a light-dependent voltage difference; **photocurrent** means a light-dependent current component. When establishing a continuous energy balance in an arrangement that also involves a chemical reaction, light, chemical change, and electrical output must be accounted for separately. Interpreting a needle deflection as an “everlasting solar cell” loses this distinction.

1873: How was a telegraph problem connected to selenium?

Willoughby Smith was searching for a material with high resistance to use in the testing and signaling system employed during the laying of submarine cables. His brief note, published on February 20, 1873, describes selenium rods with a length of 5-10 cm and a diameter of approximately 1-1.5 mm. The rods are enclosed in glass tubes, and platinum wires extend from their ends for electrical connection. The light-dependent electrical resistance of selenium unexpectedly became a significant focus of the research. [H02]

Selenium is a chemical element with the symbol Se. It can exist in different structural forms, such as amorphous and crystalline; therefore, knowing only the element's name does not provide all the electrical properties of the sample. **Resistance** is a measure of how much current flows through a material for a given voltage under specific conditions. Its unit is the ohm. In a simple ohmic element, the relationship is as follows:

$$I = \frac{V}{R}. \tag{I.2.1}$$

I represents the current, V is the voltage across the element, and R is the resistance. The statement “the resistance decreased in the light” means that more current can flow at the same voltage. This increase is called **photoconductivity**. Here, “photo” refers to light, and “conductivity” refers to the ability of electric charges to move. When the conductivity of a material changes with light, it can be used as a light sensor; however, this observation alone does not prove that the material is a solar cell that provides energy to an external circuit.

Let’s examine the same phenomenon using numerical data

Synthetic example, not a measurement by Smith: assume that a selenium element has a resistance of 10 megaohms in darkness and 2 megaohms under illumination. “Mega” means one million. If an external battery applies a constant 10 V across the terminals, the dark current is 1 microampere and the illuminated current is 5 microamperes. “Micro” means one millionth. The instrument detects an increase of 4 microamperes. The battery supplies the electrical power; light has changed the conditions under which the material conducts that power. This calculation does not show that the same current will continue after the battery is removed.

In today’s semiconductor terminology, light can increase the number of mobile charge carriers. The lifetime of these charge carriers, whether they are trapped in defects, and how easily they move, all affect conductivity. In a simple crystal model, conductivity depends on the weighted sum of the electron and hole densities multiplied by their mobilities. This is not to claim that Smith used the current band theory in 1873; rather, it is an attempt to interpret a historical observation using the physics language developed later.

Furthermore, not every selenium device is an ideal, voltage-independent resistor. The contacts and the previous electrical processing history can alter its behavior. The Ohm’s law example above was chosen to illustrate the meaning of the decrease in resistance under illumination; it does not assume that all selenium samples behave linearly at every voltage.

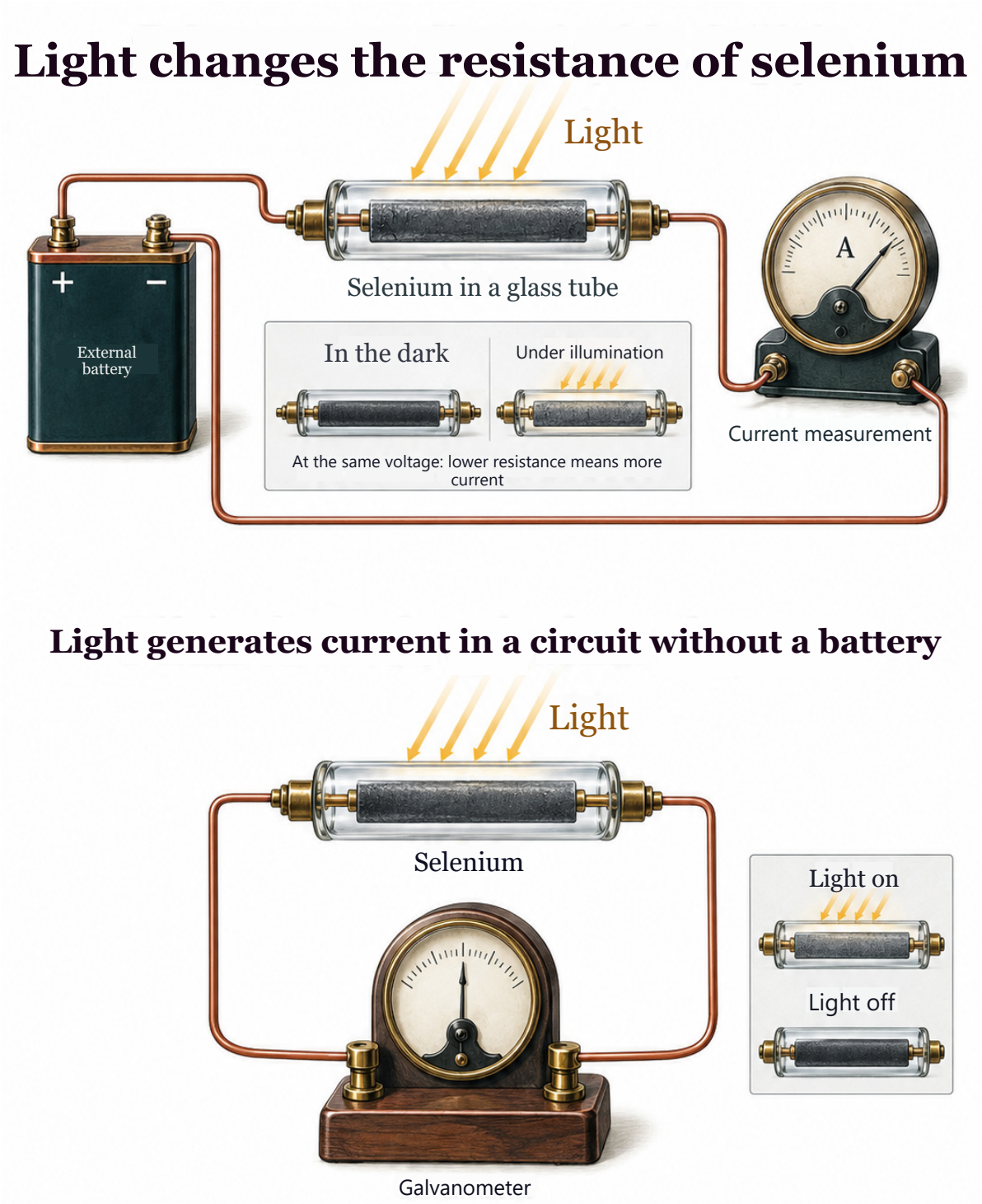


Figure 03. The upper circuit investigates the change in conductivity under external bias; the lower circuit investigates the current dependent on illumination without an external battery. The diagrams illustrate the logic of the experiments. The geometry, contact condition, and instrument calibration of the actual historical samples cannot be inferred from this schematic. [H02] [H32] Conceptual illustration prepared with an image-generation tool; it is not a measurement image.

1876-1877: What additional question did Adams and Day pose?

William Grylls Adams and Richard Evans Day treated the behavior of selenium in darkness and the question of whether light could generate a current as separate questions. They used annealed samples with platinum contacts. In the critical test they reported, the selenium was connected directly to a galvanometer: there was no deflection in darkness, but candlelight produced a deflection, which returned to its initial position when the light was removed. They also tested three similar samples through which no battery current had previously passed; two responded to light and one did not. The short communication was received in 1876, and the full study was published in 1877. [H32] [H03]

Annealing is the process of altering the structure of a material by subjecting it to a specific thermal history. The **contact** is the region where the platinum wire makes contact with the selenium. Why are these two terms important? Because what is being measured is not just the name of the element; it is a device consisting of the element's structure, surface, contacts, and processing history. The fact that the samples react differently requires the researcher to initially question the difference between "the same recipe" and "the same result."

The battery-less experiment provides evidence that is distinct from simply transmitting the current provided by an external battery. Nevertheless, to convert an electrical response into a useful power source, voltage and current under load, illumination intensity, area, and stability over time must be measured. Therefore, the historical record includes different stages of evidence, starting with photo-conductivity and then moving to the photovoltaic device. A single sentence like "light generates electricity" obscures this progression.

1883 and 1905: Surface design and the quantum idea

Charles Fritts' early selenium cell with a very thin gold layer exemplifies the transition from effect to device design. The ability for light to enter and for electrical contact to be established must be resolved on the same surface. Thick metal can block light, while insufficient contact can hinder charge extraction. The challenge in modern transparent-contact and metal-grid designs is also to address these two requirements simultaneously. [H01]

In Einstein's 1905 approach, the energy exchange of light is explained through quanta. In the **external photoelectric effect**, light with sufficient energy can eject electrons from a surface. The energy threshold required to eject an electron from a metal is the **work function**. A single photon below the threshold does not become more energetic simply because we increase the light intensity; an increase in intensity mostly increases the number of photons. In a solar cell, however, the electron does not need to escape

into a vacuum. The use of charges generated within the semiconductor with selective contacts is another device operation. [H06]

Today, these observations can be interpreted as three distinct phenomena: light can alter the **conductivity** of a circuit, it can generate **photovoltage** and **photocurrent** in a device, and it can extract **electrons** from a surface. When we establish the energy source, the measurement circuit, and the outcome separately, we are ready to understand why the silicon cell of 1954 represented a new stage in engineering.

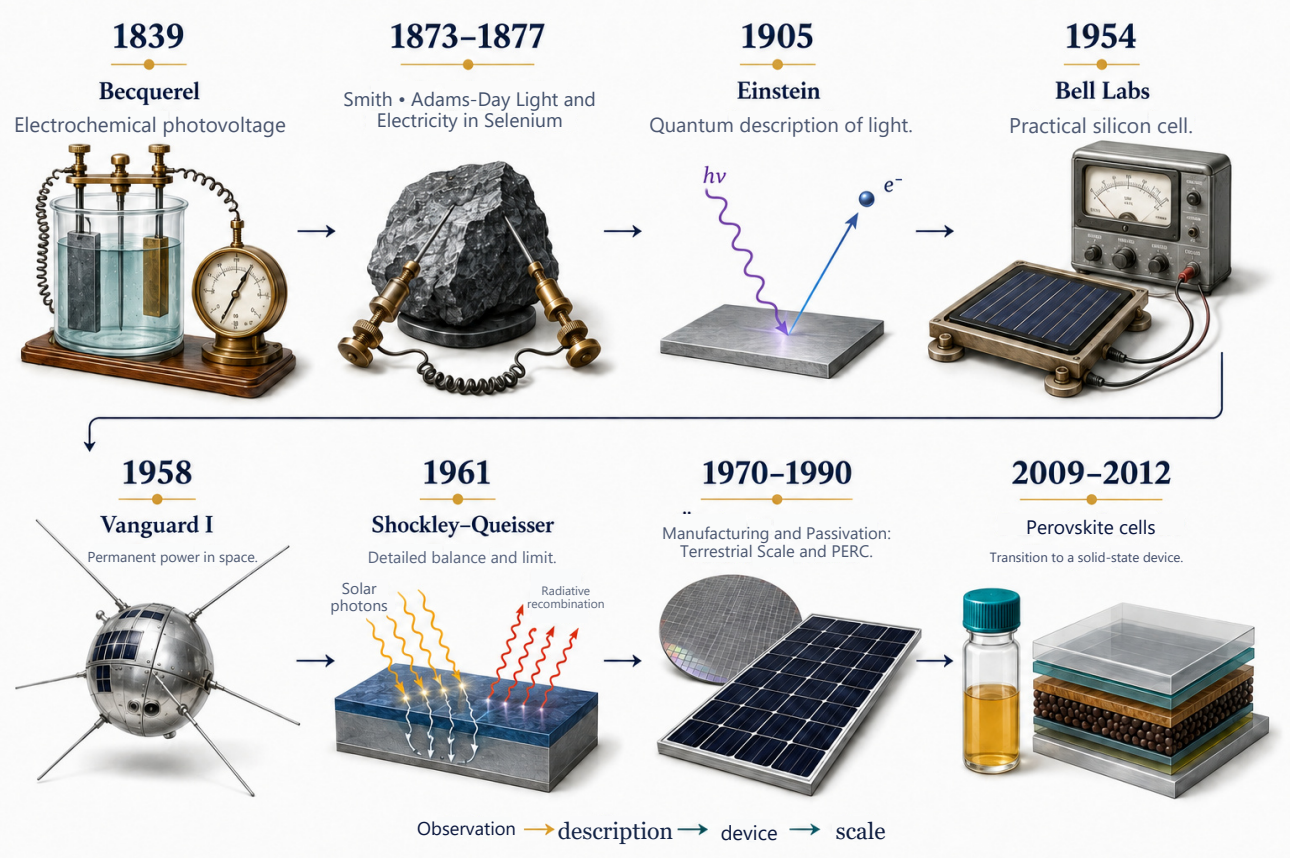


Figure 04. The historical development of photovoltaic concepts and devices. The top row is read from left to right, and the connecting arrow turns to the left of the bottom row. The milestones collectively illustrate observation, quantum explanation, semiconductor engineering, and the need for application. The intervals are not proportional to time; the diagrams should not be used as exact reconstructions of historical objects. [H01] [H02] [H03] [H04] [H07] [H25] [T10] [T11] Conceptual illustration prepared with an image-generation tool; it is not a measurement image.

Comprehension check: explain the experiment to someone

When describing Becquerel's experiment, instead of saying "he captured the light," describe the electrode, the solution, the galvanometer, and the sequentially opened covers. When describing Smith's experiment, use the 10 V example to demonstrate why the photocurrent increases under constant voltage. For Adams-Day, explain why the removal of the external battery constitutes a separate piece of evidence. If you can distinguish between the three, it means you have learned the historical events not just by their names, but by understanding the logic of the experiments.

1954: The intersection of material purity and device physics

Twentieth-century semiconductor research advanced the ability to control the number of charge carriers by adding controlled atoms to the crystal (doping), to extend the same atomic arrangement to a large volume (single crystal growth), and to create regions where current flows differently depending on the direction (rectifying junction). Without this accumulated knowledge, simply searching for a "good light-absorbing material" would not have been sufficient. The 1954 paper by Chapin, Fuller, and Pearson presented a silicon p-n junction photovoltaic cell for electricity generation. The bibliographic identifier of the paper serves as a reliable primary source for tracing the beginning of a class of devices. [H04]

The record of the experimental cell in the Smithsonian collection demonstrates Chapin's shift at Bell Labs towards generating electricity from the sun and the role of Russell Ohl's previous silicon work in this development. According to the institution's records, the practical cell emerged from the joint work of Chapin, Fuller, and Pearson. Bell Labs' approximately [H05] efficient cell, 6%, does not derive its historical significance solely from its numerical value; it represented a converter that could power a specific load and be further developed for engineering purposes. The efficiency of that era should not be interpreted as a record subject to today's certification and field regulations. [H08]

The lesson to be learned from this transition is clear. A material that appears to have a desirable band gap may not be suitable for a solar cell if it cannot be produced in an electrically clean manner. Even a perfect crystal may be useless without proper contacts. A successful device requires the simultaneous presence of desirable properties within the same sample and after the same processing sequence.

Why were purity, junctions, and the idea of an efficiency limit turning points?

Purity refers to the low concentration of unwanted atoms in a crystal; doping, on the other hand, is the deliberate addition of specific atoms. These are not mutually exclusive: we can control a beneficial doping while minimizing random contamination. In the **n-type** region, mobile electrons are dominant, while in the **p-type** region, holes, which represent an electron deficiency, are dominant. The boundary between these two regions is called the **p-n junction**. The internal structure that forms when charges redistribute at the boundary helps in the collection of electrons and holes from different contacts during illumination. "n" and "p" do not mean that the entire wafer is uniformly negatively or positively charged. In electrically neutral regions, the charge of mobile charge carriers is balanced by other charges in the crystal.

This brief mechanism explains why the 1954 device differs from a simple rod whose resistance changes only in light. To utilize the charge carriers generated by photons, both the internal structure and the external electrical contacts must be optimized. In subsequent periods, **passivation** enabled higher voltage and power to be obtained from the same cell by reducing effective defects that cause charge carrier loss on the surfaces or by reducing access to these defects. The goal here is not to increase the light, but to reduce the early loss of the generated excitation. [H04] [T01]

In 1961, Shockley and Queisser asked another question: Even if we could ideally eliminate manufacturing defects, why can't a single junction convert all solar energy into electricity? The inability to utilize low-energy photons, the dissipation of excess energy from high-energy photons as heat, and the emission of light from the cell itself are all considered together. The **detailed balance** is the foundation of this calculation, which consistently addresses absorption and reverse emission. The result is an upper limit that depends on specific assumptions; it is not an invariant efficiency percentage for all technologies. The 1961 marker on the timeline therefore indicates not a new cell sale, but the method of calculating the inevitable losses of the device. [H25]

From space to Earth

Vanguard 1, launched on March 17, 1958, was the first satellite to use solar power. In space applications, lightness and long operational life represented a value distinct from the cost per unit of electricity. NASA's historical record confirms this early application. [H07] A technology may be expensive in its initial market; however, it remains meaningful if no other solution can perform the same task under similar mass and maintenance conditions.

The requirements changed with terrestrial applications. Remote communication points, stand-alone power sources, and later grid-connected generation created new demands in terms of durability and cost. The U.S. Department of Energy historically examines the role of federal research and development efforts in the development of solar technologies in the 1970s. [H08] Research now had to consider not only efficiency improvements but also material consumption per wafer, production rate, the elimination of defective cells, encapsulation, and years of operation in the field.

This date does not imply that a single material will reign supreme forever. The advantage of a material family may vary at different times. Thin films can offer strong absorption with less material, thanks to their direct band gap. Silicon can offer improved manufacturing infrastructure and high electronic quality. Multijunction devices may require more complex optical and electrical matching in exchange for higher efficiency. The researcher's task is to determine which problem each approach solves and which new problem it creates.

A historical calculation: the area required for the same amount of electricity

This is an illustrative example, not a historical sample measurement. Let's assume an irradiance of 1000 W/m^2 and a target electrical power of 100 W. The required area, A, will be P/(ηG). With an efficiency of 6%, A = 100/(0.06 × 1000) = 1.67 m^2; with an efficiency of 20%, 0.50 m^2 is required. The efficiency has increased by 14 percentage points; the required area has decreased by approximately 70%. However, without knowing the cell cost, charge carrier structure, and maintenance costs, it cannot be said that the electrical cost has also decreased by 70%. The same equation teaches us how to identify which economic variable is directly affected by a particular development.

Reading history as a chain of cause and effect

Learning the history of a field by simply memorizing names and dates is insufficient for understanding subsequent technical choices. In the history of PV, four distinct challenges emerge sequentially. The first challenge is to reliably demonstrate that light creates an electrical change. The second challenge is to differentiate whether this change is an externally powered conductivity effect or an energy conversion that can supply an electrical load. The third challenge is to quantitatively explain the energy and charge flow within the device. The fourth challenge is to repeatedly manufacture this device over a large area and with a long lifetime. The same scientific idea cannot, on its own, overcome all these challenges.

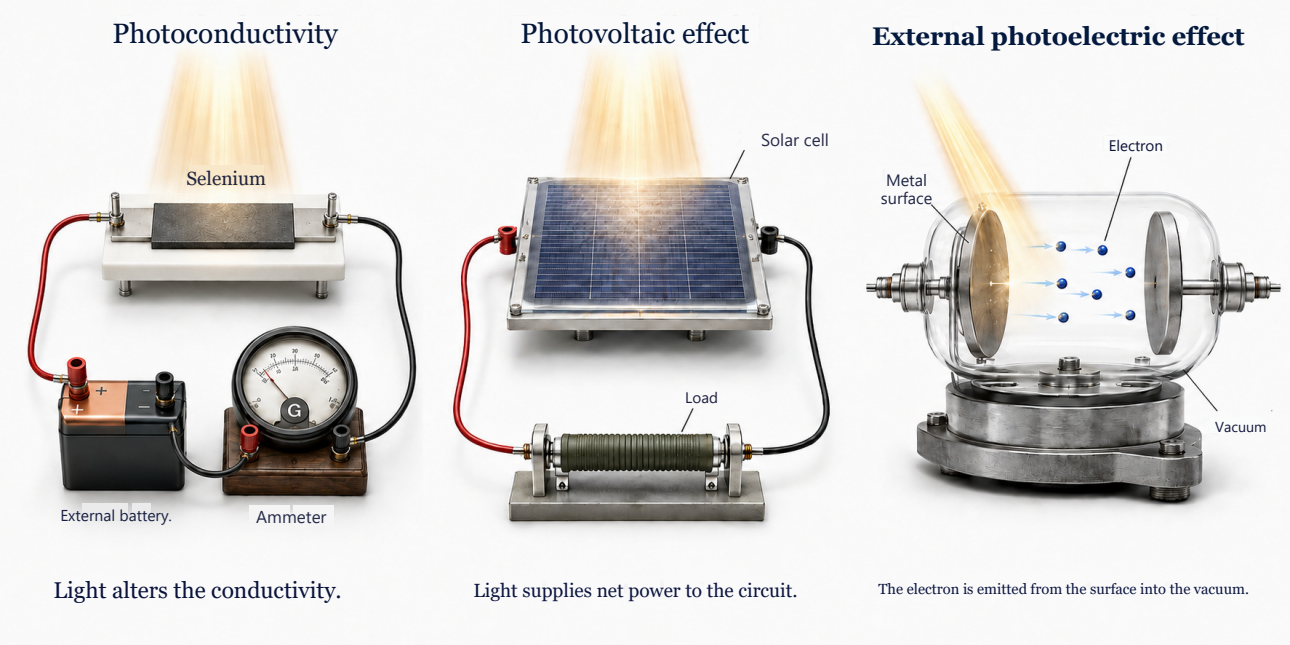


Figure 05. The rationale behind three different experiments. On the left, the energy for the current is provided by an external battery; light alters the conductivity of the sample. In the middle, the energy consumed by the load comes from illumination. On the right, electrons are emitted from the surface into a vacuum. This distinction ensures that selenium experiments are not confused with modern solar cells under the same terminology. Original educational illustration. [H01] [H02] [H03] [H06] Conceptual illustration prepared with an image-generation tool; it is not a measurement image.

The historical significance of selenium lies in this distinction. When a material is exposed to light and the current changes, it indicates that the light is interacting with electrons; however, the source of the changing current must also be investigated. In modern research, a similar concept is interpreted as a detector with a photoconductive gain, where the external quantum efficiency can exceed one, similar to a solar cell that provides the same gain as free power. The work done by external biasing also contributes to the detector's gain. Without an energy balance, the number of electrons per photon cannot be substituted for the energy conversion efficiency.

The instructive aspect of the 1954 silicon cell is not that it revealed a previously unknown law of nature. Rather, it demonstrated the convergence of sufficient crystal quality, controlled doping, junction formation, and electrical contact within a single device. The manufacturing tools of semiconductor technology made it possible to transform a physical effect into a usable product. The 1958 Vanguard application, however, demonstrates a shift in research priorities: in an environment where limited battery life is a problem, the ability to reuse incident light is highly valuable. The first customer of a technology is not always the one seeking the cheapest electricity. [H04] [H05] [H07]

Terrestrial deployment has shifted these priorities. While power per unit mass and radiation resistance may be critical for a device in space, on Earth, production cost, area, assembly, material availability, and long-term energy generation become important considerations together. Therefore, the “higher efficiency” trend in the history of research is not sufficient on its own. During the same period, cell efficiency, module efficiency, manufacturing yield, and field life can improve at different rates. In the later sections of this book, we will examine how passivation affects voltage gain, how tandem structures affect spectral gain, and how module design affects area loss, all within the same energy accounting framework.

> Historical reading experiment: Choose a turning point and write three sentences: What was the obstacle? What tool or physical understanding overcame this obstacle? What obstacle remained unresolved? This exercise translates historical knowledge into research design.

Common misconceptions and practice questions

The statement “Photovoltaics, photoconductivity, and the photoelectric effect are the same thing” is incorrect. In one, conductivity changes under external bias; in the other, usable photovoltage and power are generated; and in the external photoelectric effect, electrons are emitted from the surface. The statement “The date of invention explains everything” is also incorrect; scientific observation, a working prototype, and a scalable product are distinct steps.

1. Does a selenium sample whose resistance halves under illumination count as generating power without an external battery? **Answer:** No; a separate photovoltage measurement and a measurement of net power under load are required.

2. What is the increase in efficiency from 10% to 15%, expressed as both absolute percentage points and relative percentage? **Answer:** 5 percentage points; the relative increase is 50%.

3. Why can’t a space-qualified solar cell automatically be used as a suitable rooftop module? **Answer:** The spectrum, radiation, area, and mass priorities, as well as cost, encapsulation, and operating conditions, are different.

Reading path: First, read the brief timeline [H01], then the identification and scope of the 1954 article [H04], and finally the object and application history [H05] [H07]. Do not directly add the historical efficiency figures to the modern certification table.

BOOK I · CHAPTER 03 / HISTORY AND PHYSICS

Solar source, spectrum, and photon accounting

How do we count the photons in a beam of light?

The fact that we perceive sunlight as white does not mean that all the photons within it are the same. A prism makes this visible by creating a color spectrum. **Wavelength** is the distance between two successive equivalent points on a wave; it is denoted by λ. **Frequency** is the number of oscillations per second; it is denoted by ν. Since the speed of light in a vacuum is c, the relationship $c = \lambda\nu$ applies. A short wavelength means a higher frequency and higher energy per photon. The difference between violet and red is not just our eye's perception of color.

Spectrum illustrates how the intensity of light is distributed across different wavelengths. In the graph, the horizontal axis represents the wavelength in nanometers (nm), and the vertical axis represents the power in $W/(m^2 \cdot nm)$. The vertical value alone does not represent the total power at that specific wavelength; instead, it indicates the power density for each nanometer interval. Multiplying the vertical value by the interval width yields the power in W/m^2. Therefore, summing only the heights while adding boxes with different widths is incorrect.

Teaching example: Let's assume that the spectral irradiance in the range of 500-510 nm is constant at 1 $W/(m^2 \cdot nm)$. Since the range is 10 nm, the incident power is 10 W/m^2. The photon energy can be approximately calculated using 505 nm, which is the middle of this narrow range. Since 1 nm = 10^{-9} m, the energy per photon is approximately 3.93×10^{-19} J. If we divide the value of 10 J/s by this energy, we find approximately 2.54×10^{19} photons per second per square meter. We have converted a power measurement into a photon count; we have not yet calculated the electrical power generation.

From incident photon to collected electron

If we assume that each photon contributes to the transition of one electron in the external circuit, we multiply the photon flux by the magnitude of the electron charge. The example above yields approximately 4.07 A/m^2, which is 0.407 mA/cm^2. In reality, photons can be reflected, not absorbed in the active layer, or the generated charge can be lost. The **external quantum efficiency** is the ratio of the number of charge carriers collected in the external circuit per incident photon, measured under appropriate conditions; it is denoted by EQE. If EQE is 80%, then the current is approximately 0.326 mA/cm^2. This is not an energy efficiency: to convert from flux to power, the operating voltage is also required.

As sunlight passes through the atmosphere, some wavelengths are absorbed by gases, and a portion of the light is scattered. **Direct light** comes from the direction of the sun, while **diffuse light** comes from different directions in the sky. AM (air mass) is a measure that describes the ratio of the path length of light through the atmosphere to a reference path length. AM1.5G is a laboratory reference spectrum; it does not mean "1.5 hours every day" or "1.5 times the solar power." The spectrum, total irradiance, and sample temperature are specified separately.

Large numbers and the integral sign

10^{3} is 1000; 10^{-3} is 0.001. This **scientific notation** allows us to manage very large numbers of photons and very small energies at the atomic scale within the same calculation. For example, when multiplying 2×10^{3} by 3×10^{-2}, we first find $2 \times 3 = 6$, and then we add the powers of ten: the result is $6 \times 10^{1} = 60$. In formulas, we will see these exponents as actual superscripts.

Σ represents the sum of discrete terms. ∫ is the integral sign, representing the continuous sum obtained by reducing the intervals to very small values. To calculate the area under a spectrum, one multiplies the width by the height of each narrow band and sums the results. **dλ** represents a very small wavelength interval in a continuous expression, while **Δλ** represents the finite difference between two wavelengths in a table. When the curve is approximated linearly, multiplying the average of adjacent heights by the interval width is the **trapezoidal rule**. The following integral formulas are a shorthand notation for this counting process.

Comprehension check: which area of the graph?

If a band with an irradiance of 2 W/(m^2·nm) remains constant over 20 nm, this band carries 40 W/m^2. If the same power is shifted to a longer wavelength, the number of photons increases because each photon carries less energy. However, if this falls below the absorption threshold of the cell, having more photons does not necessarily provide more current. When interpreting the spectrum, we must consider the number of photons, the photon energy, and the EQE together.

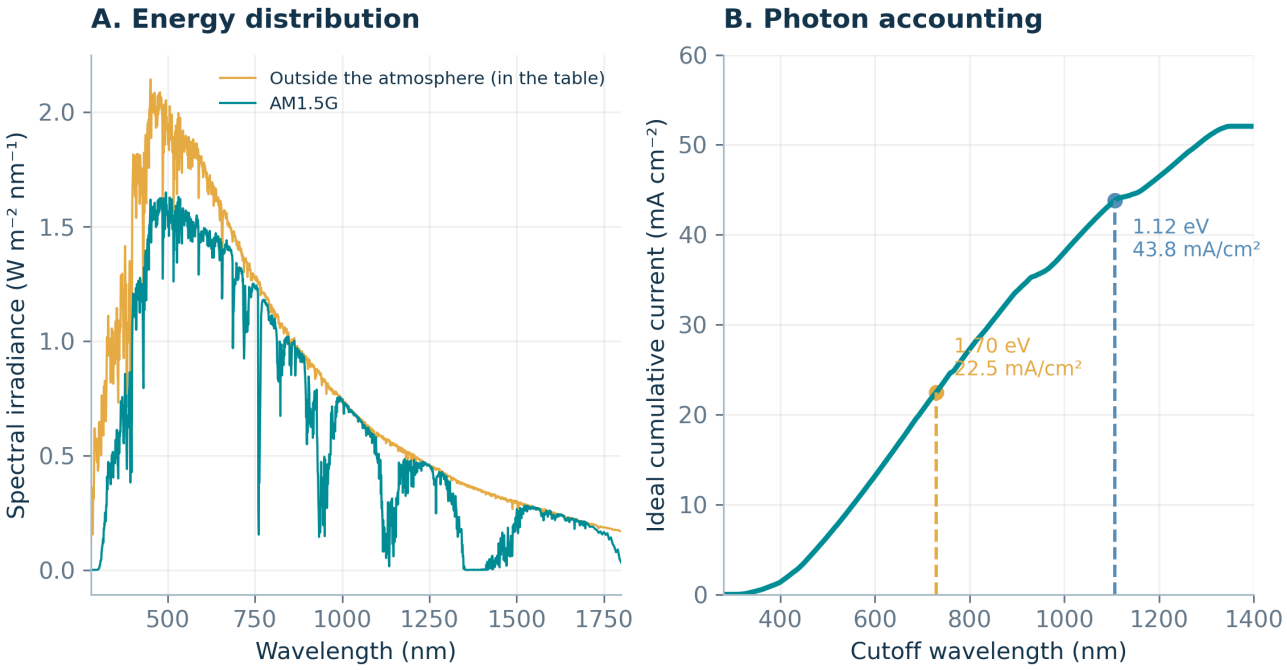


Figure 06. From the reference spectrum to photon counting. Panel A shows the extraterrestrial and global spectra from the ASTM G173 table; panel B shows the ideal current integral of the global spectrum. Threshold lines are plotted for 1.12 and 1.70 eV. Data from the pvlib repository; curves and integrals were reproduced for this book. [H09] [B10]

Power density and energy should be treated as distinct concepts

The initial input for cell research is not simply “sunlight is present”; rather, it is the distribution of light arriving at the surface with respect to time, wavelength, angle of incidence, and polarization. The irradiance, G, is the power per unit area arriving at the surface per unit time and is expressed in W/m^2. The irradiance energy, $H = \int G(t)dt$, is expressed in J/m^2 or kWh/m^2. 1 kWh = 3.6 MJ. The instantaneous power of a module is expressed in watts, and the electricity it generates in a day is expressed in kilowatt-hours. Confusing these two is one of the most common errors when transitioning from cell measurements to power plant calculations.

The spectral irradiance, $E\lambda$, represents the distribution of this power across different wavelengths. For example, if you sum a table with units of $W\ m^{-2}\ nm^{-1}$ across the wavelengths, you obtain W/m^2. A high value at a specific point in the table does not necessarily mean that that particular wavelength carries a large amount of power on its own; the bandwidth is also taken into account. The measure in the integral is a part of the physical quantity.

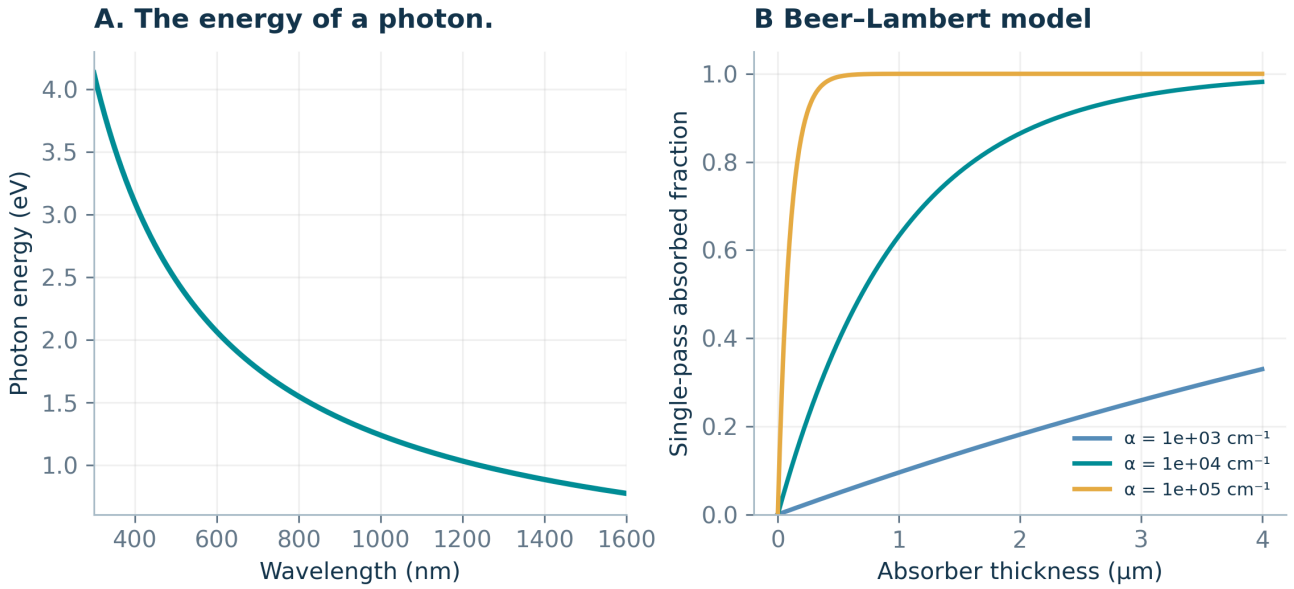


Figure 07. The photon energy and absorption length represent different scales. On the left, hc/λ is shown, and on the right, 1 - exp(-αd) is calculated for a constant α. It is not assumed that a material has the same α value for all wavelengths; the right panel is intended to illustrate the effect of thickness for a single wavelength. [H10] [H13]

The energy of a photon and the number of charge carriers

The photon energy is $E = h\nu = hc/\lambda$. In the SI definition, $h = 6.62607015 \times 10^{-34}$ J s, $c = 299792458$ m/s, $q = 1.602176634 \times 10^{-19}$ C, and $k_B = 1.380649 \times 10^{-23}$ J/K are the exact values. [H10] In practical terms, the conversion is $E[\text{eV}] \approx 1239.842/\lambda[\text{nm}]$. Therefore, a 500 nm photon has approximately 2.480 eV, and a 1000 nm photon has approximately 1.240 eV.

The number of photons and energy are not the same. Two narrow-band sources with the same optical power will produce a greater number of photons from the source with the longer wavelength, because each photon has lower energy. The incident photon flux is given by $\varphi\lambda = E\lambda/(hc/\lambda)$. Here, λ must be converted to meters consistently with hc; the fact that $E\lambda$ is expressed "per nanometer" only applies to the spectral bandwidth. The unit of the resulting $\varphi\lambda$ is photons m^{-2} s^{-1} nm^{-1}.

For a conventional device, where a single photon generates at most one collected electron, the short-circuit current density, Jsc, is calculated as $J_{sc} = q \int \varphi\lambda \, EQE(\lambda) d\lambda$. EQE is the external quantum efficiency: the number of electrons collected in the external circuit per incident photon on the device. This definition also includes the loss of incident photons due to reflection or parasitic absorption. The internal quantum efficiency, on the other hand, uses the number of absorbed photons appropriately defined in the denominator. [H24]

What do AM0, AM1.5G, and AM1.5D represent?

AM stands for air mass, which is an approximate measure of the optical path length that light travels through the atmosphere. In the plane atmosphere approximation, and for the Sun when it is not very close to the horizon, AM ≈ 1/cosθz, where θz is the zenith angle. The AM0 spectrum outside the atmosphere is not the same as the standard spectrum on the Earth's surface. AM1.5G represents the global reference, including both direct and diffuse components, while AM1.5D represents the direct irradiance reference.

The ASTM G173 reference provides a common baseline calculated with specific atmospheric and surface orientation assumptions. NLR's reference page, accessible from the former NREL address, describes the 37° tilted surface, specified water vapor and ozone amounts, air mass, and the generation of the spectrum using the SMARTS model. This spectrum is not identical to the actual light observed everywhere and at every hour. [H09]

A total power of 1000 W/m^2 does not necessarily mean that the spectrum is accurate. Two lamps may produce the same total irradiance, but one may provide more power to the top tandem cell, while the other provides more power to the bottom cell. Calibrating a lamp with a silicon reference cell does not guarantee that a new material with a different spectral response is measured accurately. The necessary correction is made by knowing both the lamp's spectrum and the spectral responses of the test and reference devices.

Geometry and the real-world environment

On a horizontal surface, the total irradiance can be expressed as GHI = DNI cosθz + DHI, where DNI represents the direct irradiance on a surface perpendicular to the sun, and DHI represents the diffuse irradiance on a horizontal surface. When transitioning to a tilted module, the projection of the direct component onto the surface, as well as the sky diffuse and ground-reflected components, are evaluated separately. On a cloudy day, the total power decreases, while the proportion of the diffuse component may increase. Concentrating optics cannot utilize diffuse light as easily as flat-plate modules; therefore, the same weather data does not provide the same production advantage for both technologies.

As the distance from the sun changes, the power in free space decreases approximately in inverse proportion to the square of the distance. It would be incorrect to directly apply this simple law to the field, as the atmosphere, clouds, aerosols, and surface geometry are also factors. The purpose of the spectral model is not to conceal these effects behind a single "solar constant."

Worked example: from a spectral band to current

Illustrative example. Consider a band with a width of 20 nm centered around 600 nm, where the spectral irradiance, Eλ, is assumed to be constant at 1.50 W m^{-2} nm^{-1}. The band power is 30 W/m^2. Using the central wavelength approximation, the photon energy is 3.31 × 10^{-19} J, and the photon flux is approximately 9.06 × 10^{19} m^{-2} s^{-1}. If EQE = 0.90, the current density is approximately 13.07 A/m^2, which is equal to 1.307 mA/cm^2. In this final conversion, the equality 1 mA/cm^2 = 10 A/m^2 is used.

If we shift the same 30 W/m^2 to 1200 nm, the number of photons doubles. However, an ideal single-photon absorber with a band gap of 1.12 eV cannot utilize the approximately 1.033 eV photons at 1200 nm through interband transitions. More photons do not necessarily mean more electricity. Both the photon energy threshold and the quantum yield are required.

It is also incorrect to simply rename the horizontal axis when converting a spectrum from the wavelength axis to the energy axis. Since E = hc/λ, a Jacobian is required for spectral density transformation: φE = φλ |dλ/dE|. Ordering a list that goes from high to low energy on the energy axis in ascending order helps maintain the correct integration sign and data order. The fact that two numerical codes written with different spectral units yield the same current is a good test of independent consistency.

Calculating the spectral integral

To sum the area under a spectrum graph, the unit of the axis must be used in conjunction with the sampling interval. If the wavelengths are not equally spaced, directly summing the irradiance values in the rows is incorrect. The total power and ideal short-circuit current from the discrete table can be calculated using the trapezoidal rule as follows:

$$G \simeq \sum_i \frac{E_{\lambda,i} + E_{\lambda,i+1}}{2}(\lambda_{i+1} - \lambda_i). \tag{I.3.1}$$

$$J_{\mathrm{sc}} \simeq q \sum_i \frac{\phi_i Q_i + \phi_{i+1} Q_{i+1}}{2}(\lambda_{i+1} - \lambda_i), \qquad \phi_i = \frac{E_{\lambda,i}\lambda_i}{hc}. \tag{I.3.2}$$

Here, Q represents the EQE at the point in question. In the second equation, when calculating the photon energy, the wavelength is converted to meters; however, in the integration step, nanometers are used, consistent with the “per nm” unit of the spectral table. If the result is in A/m^2, it is divided by 10 to convert it to mA/cm^2. Explicitly writing these two conversions prevents errors of a factor of one thousand or ten thousand.

The spectrum plot in this edition was redrawn from the 2002-line numerical representation of ASTM G173 distributed in the pvlib repository. The trapezoidal integral of the global spectrum yielded 1000.371 W/m^2. The table was not rescaled to hide the small difference from 1000; the same integral was used in the denominator in the detailed balance calculation. This choice ensures the reproducibility of the results. The integral of the extra-atmospheric column in the table, from 280-4000 nm, is approximately 1347.93 W/m^2; it should not be assumed that the integral of this finite wavelength range is identical to the Sun's irradiance across all wavelengths. The data source and file summary are kept in the book's accompanying package. [H09] [B10]

The cumulative current plot of the device is particularly valuable. An ideal device capable of collecting all photons up to the Eg = 1.12 eV threshold yields approximately 43.8 mA/cm^2; for Eg = 1.70 eV, it yields approximately 22.5 mA/cm^2. These are not material record values. They are the results of photon counting, assuming complete absorption, complete collection, and one electron per photon. The EQE curve of a real cell is lower and smoother than this step function.

Why do we express the loss in mA/cm^2? If a 3% reduction in reflection is not uniform across all wavelengths, we cannot simply assume a 3% increase in current. The gain must be weighted by the photon flux at the wavelength where the change occurs:

$$\Delta J_{\mathrm{sc}} = q \int \phi_\lambda \, \Delta \mathrm{EQE}(\lambda) \, d\lambda. \tag{I.3.3}$$

This formula links an optical design decision to a measurable electrical outcome. When comparing two coatings, using this weighted integral instead of just the average reflectance prevents the region that the human eye perceives as bright from unduly influencing the numerical evaluation.

Common misconceptions and practice questions

The statement "Since a sun provides 1000 W/m^2, the spectrum is irrelevant" is incorrect. The statement "W/m^2 can be obtained from the lux value using the same coefficient for each lamp" is also incorrect; lux is weighted by the wavelength-dependent sensitivity of the human eye. Radiometric and photonic quantities are required for photovoltaic measurements.

1. If the average irradiance is 800 W/m^2 and lasts for 5 hours, what is the total energy received? **Answer:** 4 kWh/m^2; efficiency and other losses are also required for electricity generation.

2. What is the ideal cutoff wavelength for a band gap of 1.55 eV? **Answer:** Approximately 800 nm.

3. If the Eλ table is written as W m^{-2} μm^{-1} instead of W m^{-2} nm^{-1}, how will the numbers change? **Answer:** They will be multiplied by 1000; the correct integral will yield the same total power.

Instructions: Open the spectral table [H09] and first calculate the total power, then the photon flux. Read the definition of quantum efficiency in [H24]. The MIT course outline presents a learning sequence that progresses from the solar source to optics and charge carrier excitation. [H11]

BOOK I · CHAPTER 04 / HISTORY AND PHYSICS

The inner workings of a semiconductor: bands, statistics, and optical transitions

An energy band is not a stripe inside the crystal

The electrons of a single atom can only exist in specific energy states. When a large number of atoms come together and form a regular **crystal**, these states interact, resulting in closely spaced, allowed energy clusters. We call these clusters **bands**. The vertical axis of the band diagram represents electron energy, not the height of the material. The **valence band** contains the filled states that participate in chemical bonding; the **conduction band** contains the higher energy states that allow excited electrons to move. The energy difference between the edges of these two groups is the **band gap**.

The band gap is not simply “the space between two layers.” It signifies the absence of allowed electron states within a specific energy range in an ideal crystal. In a real material, defects can introduce localized states within this range. The excitation of an electron from the valence band to the conduction band creates an electron and a hole. The total electric charge is conserved: since a negatively charged electron and a hole, which behaves like a positive charge, are created together, light does not fill the neutral crystal with an unlimited negative charge.

The electronvolt is the unit corresponding to the energy gained by a single electron across a potential difference of 1 V. **Teaching example:** In an ideal absorber with a band gap of 1.1 eV, a 1.0 eV photon is not sufficient for interband transition. A 2.0 eV photon can induce a transition; however, not all of the excess 0.9 eV is collected as electrical energy at the contacts. In a conventional cell, the excess energy of hot charge carriers is mostly transferred to crystal vibrations. This relaxation is called **thermal relaxation**.

Why are the concepts of holes and doping useful?

Imagine a nearly full row with only one empty seat. As people take turns moving to the empty seat, the empty space moves in the opposite direction. A hole provides a similar means of tracking; the actual movement is the change in state of many electrons. This analogy does not explain energy bands, but it illustrates the logic of tracking the absence as a charge carrier.

Doping is the process of changing the number of charge carriers by adding a very small and controlled amount of another atom to the crystal. In silicon, a suitable donor impurity provides electrons that can easily move to the conduction band: the material becomes **n-type**. A suitable acceptor impurity facilitates the formation of holes in the

valence band: it becomes **p-type**. These names do not mean that the material is entirely negatively or positively charged; the mobile charges are approximately balanced in a large volume by the fixed impurity ions. The majority carriers are electrons in n-type material and holes in p-type material.

The **Fermi level** is not a surface; it is an energy parameter that determines the probability of electron state occupancy. **Mobility** describes how much average drift velocity the electric field imparts to the charge carrier. The **lifetime** is related to the dynamics of excess charge carriers before they disappear. A charge that moves quickly but disappears rapidly may not reach the contact. In the following equations, we will consider these two different material properties together.

In statistical formulas, **exp(x)** represents the x-th power of the number e; e is approximately 2.718. exp(0) = 1, and exp(-1) is approximately 0.368. This function is used to illustrate how the probability of high-energy states being occupied rapidly decreases as the energy difference increases. **kT** is the product of the Boltzmann constant k and the absolute temperature T, and it has units of energy. On the Kelvin scale, room temperature is approximately 300 K, and kT is approximately 0.026 eV. Dividing an energy difference by kT yields a dimensionless number; we can then substitute this ratio into the exponential function.

Comprehension check: Does the same band gap imply the same cell?

The band gap of two materials can be 1.4 eV; however, this does not mean that they absorb the same light at the same thickness. The probability of the transition, the required momentum change, defects, and transport properties are different. The band gap is the initial threshold. For good cell design, we also need to know the absorption coefficient, charge carrier lifetime, selective contacts, and stability.

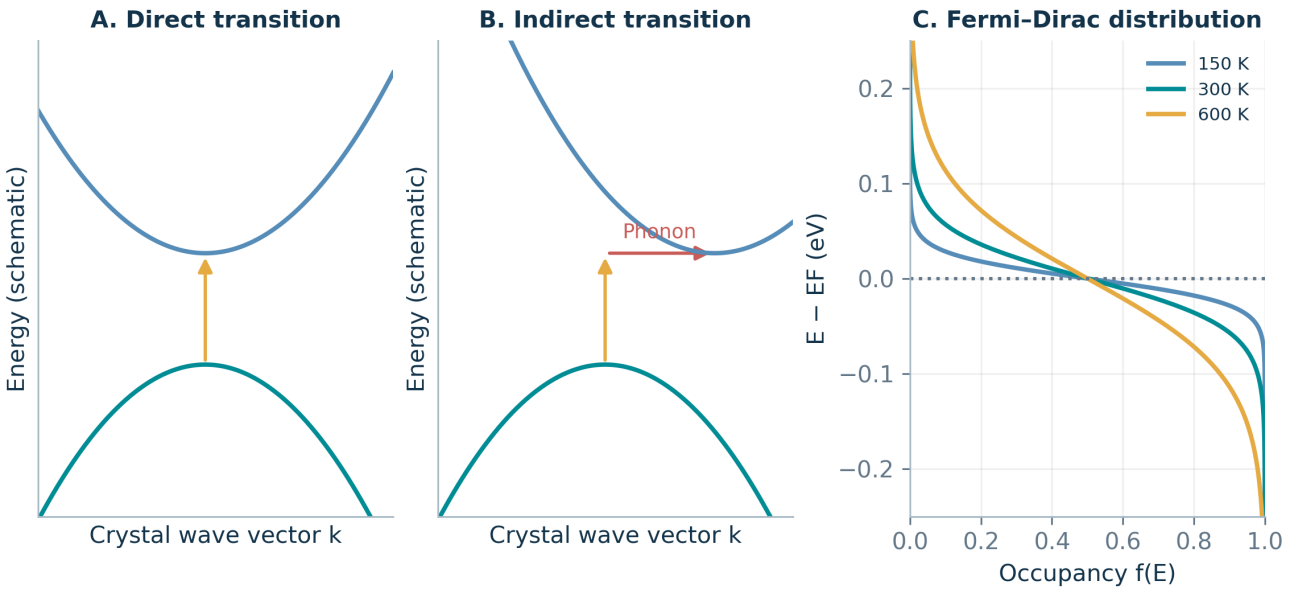


Figure 08. The band structure and occupancy are distinct pieces of information. Panels A and B are conceptual drawings of direct and phonon-assisted indirect transitions, respectively; they are not actual material band calculations. Panel C calculates the Fermi-Dirac distribution: temperature broadens the occupancy transition around the Fermi level. [H12] [H14]

From atom to crystal, from crystal to band

In an isolated atom, electrons occupy specific energy levels. When a large number of atoms combine to form a regular solid, the interaction of atomic orbitals creates a multitude of closely spaced energy states. We treat these as energy bands. The number of electrons, the symmetry of the states, and the interactions within the crystal determine the filling of the bands. This picture does not imply that every solid behaves like a free electron gas; strong correlations, disorder, and electron-lattice coupling can limit the validity of the simple band approach.

The difference between the upper limit of the valence band, Ev, and the lower limit of the conduction band, Ec, is the band gap, Eg = Ec - Ev. Excitation of an electron between the bands creates an electron in the conduction band and a hole in the valence band. A hole is not a “real positive fundamental particle” within the material; it is an effective description that tracks the charge and movement of a missing electron in the nearly full band. The band gap is the primary guide for determining which portion of the light can be utilized. [H12]

However, knowing only Eg is not enough. How the band structure changes with crystal momentum k, whether the transitions are strong, how easily charge carriers move, and their interactions with defects are all separate questions. Two materials may have the same band gap but exhibit very different absorption depths and charge carrier lifetimes.

Direct, indirect, and optically weak transitions

In an optical transition, both energy and crystal momentum must be conserved. Due to the small momentum of the photon compared to the electrons in the solid, a simple direct transition connects states near the same k-vector. If the conduction band minimum and the valence band maximum are at different k-points, a phonon, which is a lattice vibration, may also need to be involved in the process for an indirect transition. This can reduce the probability, especially near the absorption edge.

A direct band gap does not necessarily mean that the transition will be very strong. The symmetry of the initial and final states can make the dipole matrix element small or forbidden. Conversely, strong transitions can be found at higher energies. Therefore, the result of "direct Eg = 1.4 eV" in a computational scan is not a complete optical evaluation without the α(E) absorption coefficient.

In a simple, single-pass, non-reflective medium, $I(x) = I0 \exp(-\alpha x)$. The unit of α is m^{-1} or cm^{-1}; the absorption length is $1/\alpha$. In a multi-layer, real cell, due to interference, texturing, reflection, and the back mirror, this expression does not solve the entire optical problem; however, it is useful for understanding the thickness scale. The absorption coefficient section of PVEducation demonstrates the importance of the dependence on wavelength and material type. [H13]

Carrier density is an occupation problem

In equilibrium, the probability of occupancy of an electronic state is given by the Fermi-Dirac distribution: $f(E) = 1/[1 + \exp((E - EF)/(kBT))]$. EF is the Fermi level, which represents the electronic chemical potential. Do not think of EF as a single energy level where all electrons reside; it is the occupancy scale of the distribution. The density in the conduction band is the integral of the density of states multiplied by f(E).

In the non-degenerate limit, the following equations can be used: $n = Nc \exp[-(Ec - EF)/(kBT)]$ and $p = Nv \exp[-(EF - Ev)/(kBT)]$. Nc and Nv are the effective density of states of the conduction and valence bands, respectively, and have the same units as the charge carrier densities. This approach requires caution when the Fermi level is very close to the band edges or when the doping is very high. The equilibrium relation $np = ni^2$, relates the electron and hole populations through the intrinsic charge carrier density ni. [H14]

Donor impurities release electrons under appropriate conditions, while acceptor impurities increase the hole concentration. Not all of an n-type semiconductor is negatively charged; the charge of free electrons is balanced by the positive charge of ionized donors. The dopant concentration and the free charge carrier concentration are not always equal. Incomplete ionization, compensation of counter-dopants, and defects fixing the Fermi level can disrupt this equality.

Effective mass, mobility, and exciton

Near the band edge, the effective mass can be defined by the approximately parabolic dispersion relation $E(k) \approx Ec + \hbar^2k^2/(2m)$*. As the curvature increases, m* decreases. In an anisotropic crystal, a tensor may be required instead of a single number. The effective mass alone does not determine the charge carrier mobility: in a simple model, $\mu = q\tau m/m^*$, where τm is the momentum relaxation time. Even if the light charge carrier is strongly scattered, it may still exhibit low mobility. The lifetime τ and the momentum relaxation time τm are not the same quantity.

An electron and a hole can form an exciton, bound together by Coulomb attraction. The binding energy affects the conditions under which optical excitation transforms into free charge carriers. High dielectric screening and a small reduced effective mass tend to result in weaker binding in a simple hydrogenic model. This picture can change in molecular solids or low-dimensional systems. It is important not to use the onset of optical absorption, the quasiparticle band gap, and the DFT eigenvalue difference as the same quantity.

Worked example: two separate material filters

Illustrative example. Assume reflection is negligible and the target is 90% absorption in a single pass. From the condition $A = 1 - \exp(-\alpha d) = 0.90$, we obtain $d = \ln(10)/\alpha$. For $\alpha = 10^5\ cm^{-1}$, $d \approx 0.230\ \mu m$; for $\alpha = 10^3\ cm^{-1}$, $d \approx 23.0\ \mu m$ is required. A difference of only a factor of 100 in the absorption coefficient requires a difference of a factor of 100 in the thickness. This result is important for thin-film manufacturing, material consumption, and charge carrier collection distance.

As a second thought experiment, let's assume $n_i = 10^{10}\ cm^{-3}$ and a fully ionized net acceptor concentration of $10^{16}\ cm^{-3}$. In the low-injection and non-degenerate equilibrium approximation, $p \approx 10^{16}\ cm^{-3}$, and $n \approx n_i^2/p = 10^4\ cm^{-3}$. Although the concentration of the few minority electrons is small, it can be decisive for the collectable current under illumination and for recombination. These numbers are used as an example of a calculation with clear assumptions, rather than as precise values for a specific silicon wafer at a specific temperature.

From density of states to charge carrier density

Each line in the energy band diagram does not represent a single electron. In a large crystal, there are many allowed states; the density of states, g(E), gives the number of states per unit volume and per unit energy interval. In a three-dimensional parabolic band, g(E) increases with the square root of the distance from the band edge. The number of charge carriers is the sum of the product of the number of available states and the probability of occupancy of these states:

$$n = \int_{E_c}^{\infty} g_c(E) f(E)\, dE. \tag{I.4.1}$$

If the difference between the Fermi level and the conduction band is greater than a few kBT, f(E) reduces to the Boltzmann exponential form. The parabolic band integral is summed within the effective density of states, Nc, and the following result is obtained. For a simple isotropic single-valley case, spin degeneracy is included; multiple valleys or anisotropy modify the effective mass definition.

$$N_c = 2\left(\frac{2\pi m_e^* k_B T}{h^2}\right)^{3/2}, \qquad n = N_c \exp\left[-\frac{E_c - E_F}{k_B T}\right]. \tag{I.4.2}$$

For holes in the valence band, a similar operation yields Nv and p. When you multiply the two expressions, the Fermi level disappears:

$$np = N_c N_v \exp\left(-\frac{E_g}{k_B T}\right) = n_i^2. \tag{I.4.3}$$

This derivation shows the origin of the mass action law. It also explains why temperature has a strong influence: while Nc and Nv change approximately with T^(3/2), the band gap enters the exponential term. If degenerate doping, band gap narrowing, or strong disorder is present, the validity of these simplified expressions needs to be reassessed. The statement “If the doping amount is doubled, the free charge carrier concentration also doubles” is not true under all conditions.

Two time scales: mobility and lifetime

Mobility is related to how much acceleration a charge carrier can achieve under an electric field. Lifetime is related to how long an excess charge carrier population persists before recombination. An electron that loses momentum does not necessarily recombine; it may only have its direction or speed changed. Therefore, high mobility and long lifetime are investigated through different experiments.

If we substitute the Einstein relation into the diffusion length equation, we get:

$$L = \sqrt{D\tau} = \sqrt{\mu \frac{k_B T}{q} \tau}. \tag{I.4.4}$$

If we choose μ = 10 $cm^2/(V\ s)$ and τ = 1 μs at 298.15 K, we find D = 0.257 cm^2/s and L = 5.07 μm. Increasing the mobility by a factor of four only doubles L; increasing the lifetime by a factor of four also yields the same result. However, the contact, material, and temperature dependencies of these two interventions are different. For a research

program, what is important is not only the increase in L, but also how this is achieved, specifically which loss is reduced in the process.

> The derivation principle: The band gap affects the photon threshold, mobility affects carrier transport, lifetime loss, and the dielectric response affects electrostatic interactions. A single "good material" does not represent all four of these functions simultaneously.

Considering scattering, lifetime, and geometry together

Scattering is the change in the direction and momentum of a moving charge carrier due to crystal vibrations, defects, or other interactions. The electron does not necessarily undergo recombination with each scattering event. Therefore, the momentum relaxation time, which limits the mobility, is distinct from the lifetime of an excess charge carrier before recombination. The former determines how easily the charge carrier moves, while the latter determines how long it remains available for collection.

Geometry encompasses the film thickness, lateral dimensions, and distance to the contacts. The collection distances can differ in two devices made from the same material. For example, a diffusion length of 10 micrometers is suitable for reaching a contact 1 micrometer away, but it does not provide the same level of confidence for a distance of 100 micrometers. Lifetime alone does not indicate device quality; mobility, diffusion, and the required path length must be considered together.

Common misconceptions and practice questions

"If the band gap is correct, then the PV material has been found" is an incorrect inference. It cannot be said that "a high dielectric constant renders all defects harmless"; defect energy, capture cross-section, lattice relaxation, and concentration are also required. Calculated band edges do not inherently represent the actual chemical composition and interfaces after manufacturing.

1. For $\alpha = 2 \times 10^4\ cm^{-1}$, what is the 1/e absorption length? **Answer:** 0.50 µm.

2. Why might the Jsc values of two materials with the same Eg differ? **Answer:** The absorption coefficient, thickness, optical losses, and charge carrier collection probability may be different.

3. Why can an n-type crystal be macroscopically neutral? **Answer:** Free electrons balance the positive charge of the ionized donors.

Instructions: Read the sections on band gap [H12], absorption [H13], and equilibrium concentration [H14], noting the units for each formula. Then, in separate columns, list what information the material screening provides about the band structure and what experiments are still needed.

BOOK I · CHAPTER 05 / HISTORY AND PHYSICS

Junction and selective contact: how is the light-generated charge converted into work?

How is a junction formed?

Let's bring the n-type region, where electrons are concentrated, and the p-type region, where holes are concentrated, into proximity within the same crystal. The **concentration difference** determines the net result of the random movement of charge carriers: initially, electrons diffuse from the n-side to the p-side, and holes diffuse in the opposite direction. This spreading is called **diffusion**. The spreading of perfume from a concentrated area to a less concentrated area in a room is a similar statistical concept; an electric field is also present for electrons.

As mobile charge carriers move away from the junction, ionized impurities that cannot move remain behind. The donor ions on the n-side are positively charged, and the acceptor ions on the p-side are negatively charged. This creates an **electric field** directed from the n-side to the p-side. The field applies a force on the electrons in the opposite direction. When the diffusion tendency due to the charge carrier density difference is balanced by the field's drift tendency, the net current in the dark becomes zero. The movement never stops; opposing average flows balance each other.

Because the majority charge carrier concentration decreases in this region, it is called the **depletion region**. The region is not devoid of atoms. The atomic lattice and fixed charges are present there. The **built-in potential** is the internal electrostatic potential difference across the **junction**; potential is related to energy per unit charge. We should not mistake this for a battery voltage that we could obtain by connecting a voltmeter to the two ends in the dark and continuously draw energy. When all contacts and energy differences in equilibrium are considered together, no free power is obtained.

How does illumination alter the equilibrium?

Light generates excess electrons and holes. The electric field around the junction and diffusion in other regions helps these charge carriers reach the respective selective contacts. If a surface is created where holes can easily be lost at the electron contact and electrons can easily be lost at the hole contact, energy conversion will be impaired. Therefore, the fact that a metal is highly conductive alone does not make it a good solar cell contact. It is necessary to allow charge to pass with low resistance and to block the wrong charge carrier.

In an open circuit, the external path is disconnected; charge accumulation at the terminals creates a voltage, but in a steady state, the excess charge carriers generated recombine within the device. **When a load is connected**, a portion of the charge carriers transfers energy in the external circuit. The cell does not deplete its electron reservoir. The return path from the external circuit, along with charge conservation and continuous energy input from light, maintains the cycle.

Under illumination, the electron and hole populations may not be described by a single equilibrium parameter. We use a separate **quasi-Fermi level** for each. Their separation indicates that there is free energy in the charge carriers that can be converted into electrical work. The voltage measured at the ends can track this separation with ideal selective contacts; poor interfaces and transport losses introduce additional differences. We will use the following advanced equations to calculate the magnitude of this physical phenomenon.

Reading the electric field and the sign of a derivative

In a graph, if the horizontal axis represents the x-position and the vertical axis represents the potential, then the slope is the potential difference between two nearby points divided by the distance. The **derivative** describes the limit of this slope over a very small interval. The electric field is related to the negative derivative of the potential with respect to position; the negative sign indicates that the field points in the direction of decreasing potential. **Representative example:** if the potential increases by 0.1 V over 1 µm, the average field is -0.1 V/µm, which is -100,000 V/m. The Poisson equation relates how this field changes with position to the local charge density. The ∂ symbol denotes the **partial derivative**, which indicates that when there are multiple variables, we take the change with respect to only the specified variable while keeping the others constant.

Comprehension check: Does a stronger field always lead to better performance?

If light-generated charge carriers are produced far from the junction, they may first need to reach the appropriate region through diffusion. Simply increasing the junction electric field does not automatically compensate for the detrimental effects of a short lifetime or poor surface quality. It is necessary to ask the following questions together: “Where were the charge carriers generated, how far did they travel, and how quickly did they recombine?”

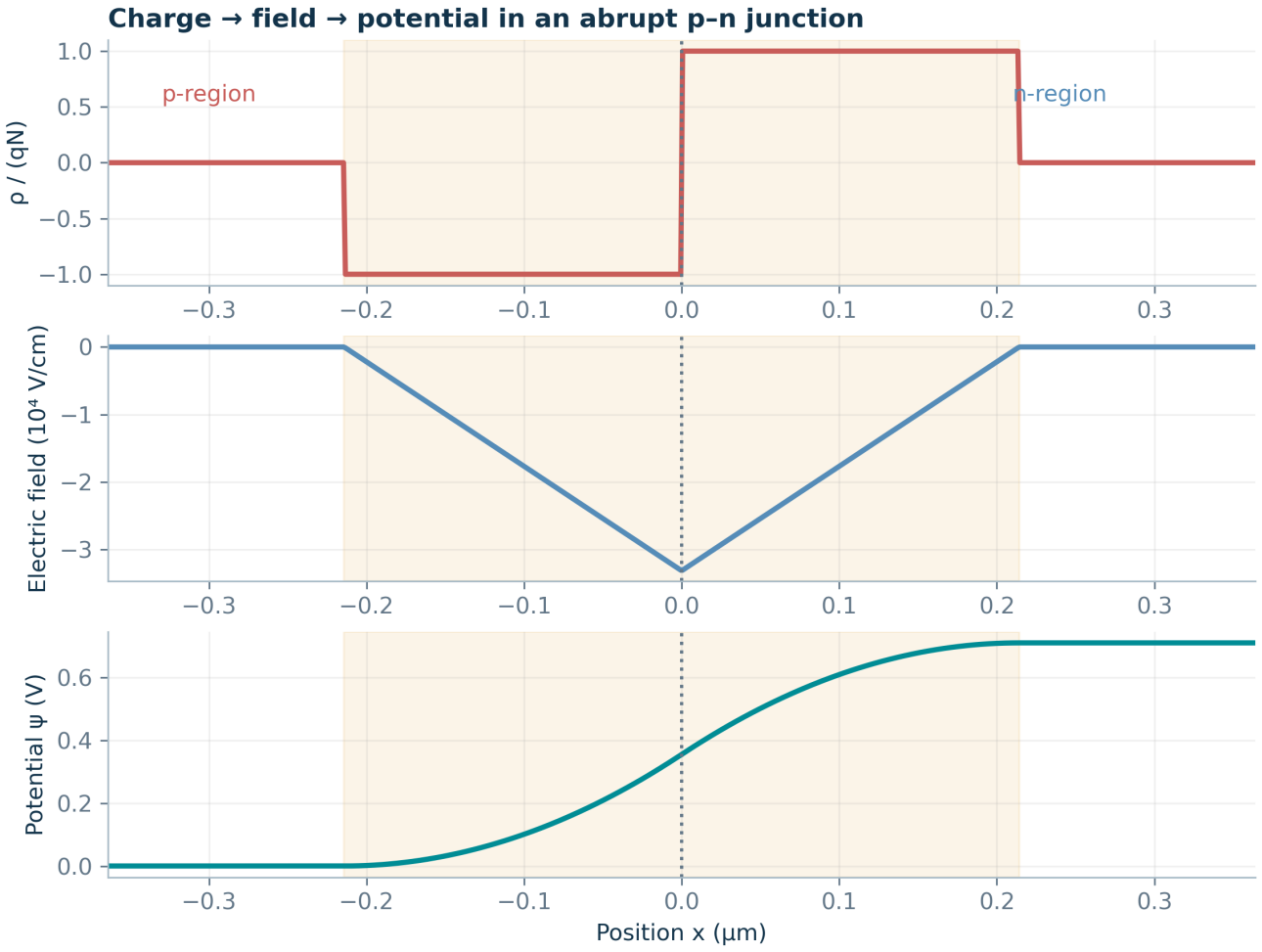


Figure 09. Charge, field and potential are three views of the same solution. For an abrupt junction with equal doping on both sides, Na = Nd = 10^{16} cm^{-3}, ni = 10^{10} cm^{-3}, εr = 11.7 and T = 298.15 K were used. The yellow region is the depletion region. Potential is the negative integral of the electric field. The derivation appears later in this chapter. [H15]

Why is an illuminated crystal not always a solar cell?

When we expose a homogeneous semiconductor to light, we can generate electrons and holes. However, simply connecting metal contacts randomly to both ends does not automatically produce useful photovoltage. A structure where electrons and holes can dissipate equally easily from both ends can consume the generated free energy through recombination at the contacts. One end should preferentially collect electrons, and the other should preferentially collect holes. This selectivity is achieved through different charge carrier conductivities and appropriate interface properties.

Würfel, Cuevas, and Würfel's selective transport analysis emphasizes that explaining a solar cell solely with the concept of "the internal electric field separates electrons and holes" is an incomplete approach. It is more general to consider transport in terms of quasi-Fermi energy gradients and selectivity in terms of different transport paths for the two charge carriers. [H21] This framework allows for considering p-n, p-i-n, heterojunction, and passivating contact architectures in a common language.

How is a p-n junction established in equilibrium?

When the p and n regions come into contact, the concentration differences lead to electron and hole diffusion. As some of the mobile charge carriers separate, ionized dopants remain in the space-charge region. The resulting electric field creates a drift current that opposes the diffusion. In thermal equilibrium, the total current is zero; however, the microscopic movement does not cease. The drift and diffusion currents are balanced.

For a simple, abrupt, non-degenerate homojunction, the built-in potential is given by $V_{bi} = (kBT/q) \ln(N_a N_d/n_i^2)$. This potential, when connected to a voltmeter, does not represent a hidden battery that provides power for free from an external source. Equilibrium contact potentials and a single Fermi level do not allow for net work production in a closed circuit. Shockley's 1949 junction theory systematized the role of potential distribution and minority charge carrier diffusion in the rectifying behavior. [H15]

In the depletion approximation, the mobile charge is neglected, and Poisson's equation is solved. The total width is given by $W \approx \sqrt{[(2\varepsilon_s/q)(1/N_a + 1/N_d)(V_{bi} - V)]}$, where V is the forward bias voltage. ε_s is the absolute dielectric permittivity of the semiconductor. If Na and Nd are in m^{-3}, then ε_s should be in F/m. The net space charge balance, $N_a x_p = N_d x_n$, indicates that the depletion region will be wider on the more lightly doped side.

Electric field, diffusion, and continuity equations

In one dimension, the conventional current densities are given by $J_n = q\mu_n nE + qD_n dn/dx$ and $J_p = q\mu_p pE - qD_p dp/dx$. Here, E is the electric field in V/m, mobility μ is in $m^2/(V\,s)$, and the diffusion coefficient D is in m^2/s. The direction of the electron particle flux and the conventional current of electrons are different; a significant portion of the sign confusions arises from this. In a non-degenerate equilibrium, the Einstein relation is $D/\mu = kBT/q$. The relationship between diffusion and the density gradient is discussed step-by-step in the relevant section of PVEducation. [H16]

The continuity equations combine charge carrier conservation with local generation G and recombination R: $\partial n/\partial t = (1/q)\partial J_n/\partial x + G - R$; $\partial p/\partial t = -(1/q)\partial J_p/\partial x + G - R$. The Poisson equation relates the electric field to the charge density: $dE/dx = \rho/\varepsilon_s$. In steady state, the time derivatives are zero. However, it is not necessary for G to equal R at every location; the difference between them is balanced by the change in the transport current. The accounting of generation, recombination, and the extracted current must be closed over the entire cell.

These three equations alone do not constitute a complete model. The boundary conditions at the contacts, mobile ions, interface charges, trap occupancy, optical generation profile, and temperature must also be specified. The convergence of the numerical solver does not prove that the physical parameters have been chosen correctly. First, it should be checked whether the analytical limits, charge conservation, and dark equilibrium are satisfied.

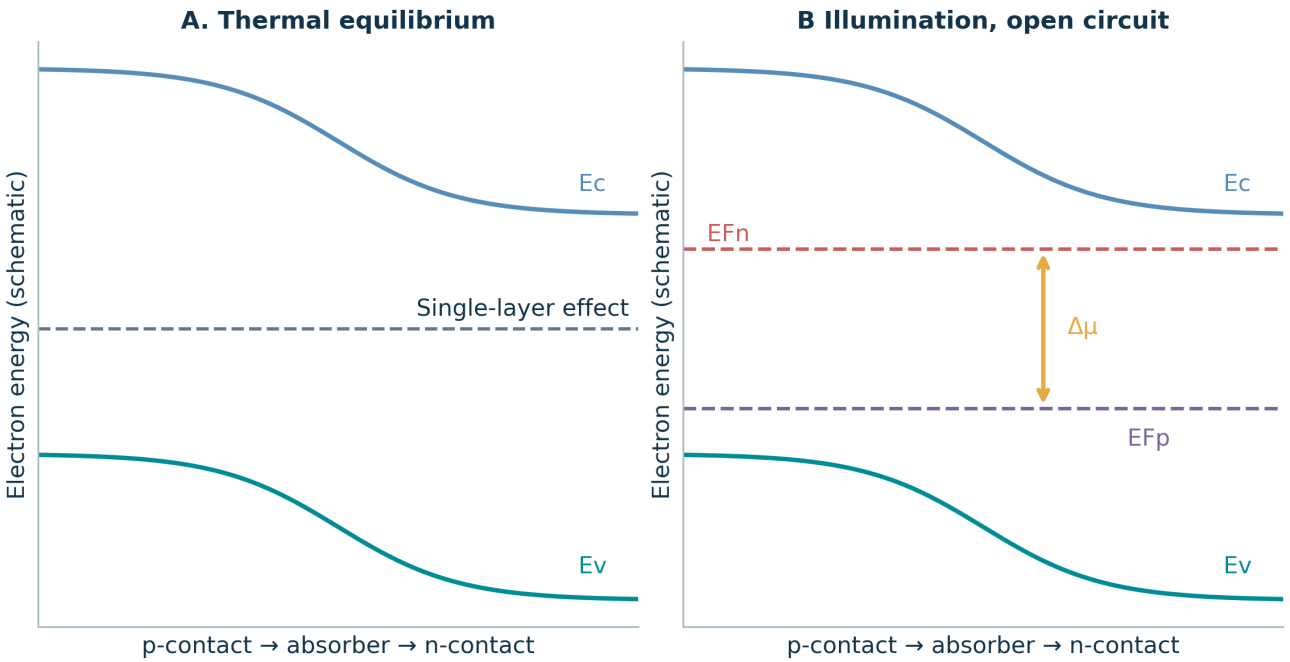


Figure 10. A single Fermi level at equilibrium; separated quasi-Fermi levels in the ideal illuminated open-circuit limit. Panel B is a conceptual limiting case with flat quasi-Fermi levels, not a self-consistently solved Poisson profile. Δμ describes the available chemical potential of the carrier pair. [H21] [H27]

Quasi-Fermi splitting and terminal voltage

Under illumination, the electron and hole populations can be described by separate quasi-Fermi levels, EFn and EFp. The local separation Δμ = EFn - EFp represents the available chemical potential of the charge carrier pair. In nondegenerate local equilibrium, np = n_i^2 exp(Δμ/kBT). Ideal, selective, and lossless contacts, under appropriate conditions, reflect this separation in the external circuit as qV. Due to recombination or transport loss at real interfaces, a high separation within the material does not necessarily mean that the same magnitude of open-circuit voltage, Voc, will be obtained.

A good contact performs two functions simultaneously: it minimizes the transition resistance of the desired charge carrier and limits the loss of the counter charge carrier. An insulating layer on the surface can perfectly passivate while also blocking the charge transport path. A highly conductive metal can also rapidly promote electron-hole recombination. Therefore, in contact research, low contact resistance and low recombination should be evaluated on the same sample.

Worked example: depletion width and collection distance

Illustrative example. Let kBT/q ≈ 25.693 mV for 298.15 K. If Na = 10^{16} cm^{-3}, Nd = 10^{18} cm^{-3}, and ni = 10^{10} cm^{-3} are used, then Vbi ≈ 0.828 V. With εr = 11.7 and ε0 = 8.854 × 10^{-14} F/cm, the width W ≈ 0.329 μm at zero applied voltage. Since xp/xn = Nd/Na = 100, almost the entire width is on the p-side. The numbers in this example are only the results of the specified model.

Now, consider a cell with a thickness of 150 μm. The depletion region being 0.329 μm does not mean that all charge carriers generated in the remaining thickness are lost. Minority carriers with sufficiently long lifetimes can reach the junction through diffusion. For example, for D = 10 cm^2/s and τ = 100 μs, L = √(Dτ) ≈ 316 μm. Reducing cell physics solely to the strong field region overlooks this important collection mechanism.

Solving the Poisson equation at a junction

In an abrupt homojunction, let's define the p-side as x < 0 and the n-side as x > 0. In the complete ionization and depletion approximation, mobile charges are neglected. The remaining acceptor charge on the p-side is -qNa, and the donor charge on the n-side is +qNd. By setting the electric field to zero in the remote neutral regions, we integrate the equation dE/dx = ρ/ε separately on both sides:

$$E_p(x) = -\frac{qN_a}{\varepsilon_s}(x + x_p), \qquad -x_p \le x \le 0. \tag{I.5.1}$$

$$E_n(x) = \frac{qN_d}{\varepsilon_s}(x - x_n), \qquad 0 \le x \le x_n. \tag{I.5.2}$$

The continuity of the field at the junction results in Na xp = Nd xn. This is not just an equation to be memorized; it expresses that the areas of the negative and positive fixed charge regions must be equal. The sum of the areas of the two triangles in the electric field graph is the potential drop; since E = -dψ/dx for ψ, the sign must be preserved.

$$V_{\text{bi}} - V = \frac{q}{2\varepsilon_s}\left(N_a x_p^2 + N_d x_n^2\right). \tag{I.5.3}$$

Using charge balance and W = xp + xn, the depletion width formula given earlier can be derived. For an equally doped sample with Na = Nd = 10^{16} cm^{-3}, ni = 10^{10} cm^{-3}, and εr = 11.7, Vbi = 0.710 V and W = 0.428 µm. The field in the middle of the region decreases to approximately -3.3 × 10^{4} V/cm. If you read the three panels of the figure in order, you will see how the rectangular charge-density profile creates a triangular electric-field profile, and how this, in turn, generates its curved potential. The equally doped example in the figure was specifically chosen to be different from the previous asymmetric numerical example.

Deriving the collection probability

Let Pcol(x) represent the probability that a minority charge carrier generated far from the junction reaches the junction. In a semi-infinite, neutral region with a constant diffusion coefficient and constant lifetime, where the electric field is neglected, this probability is described by the equation D Pcol'' - Pcol/τ = 0, with the boundary conditions Pcol(0) = 1 and Pcol = 0 at infinity.

$$P_{\text{col}}(x) = \exp(-x/L), \qquad L = \sqrt{D\tau}. \tag{I.5.4}$$

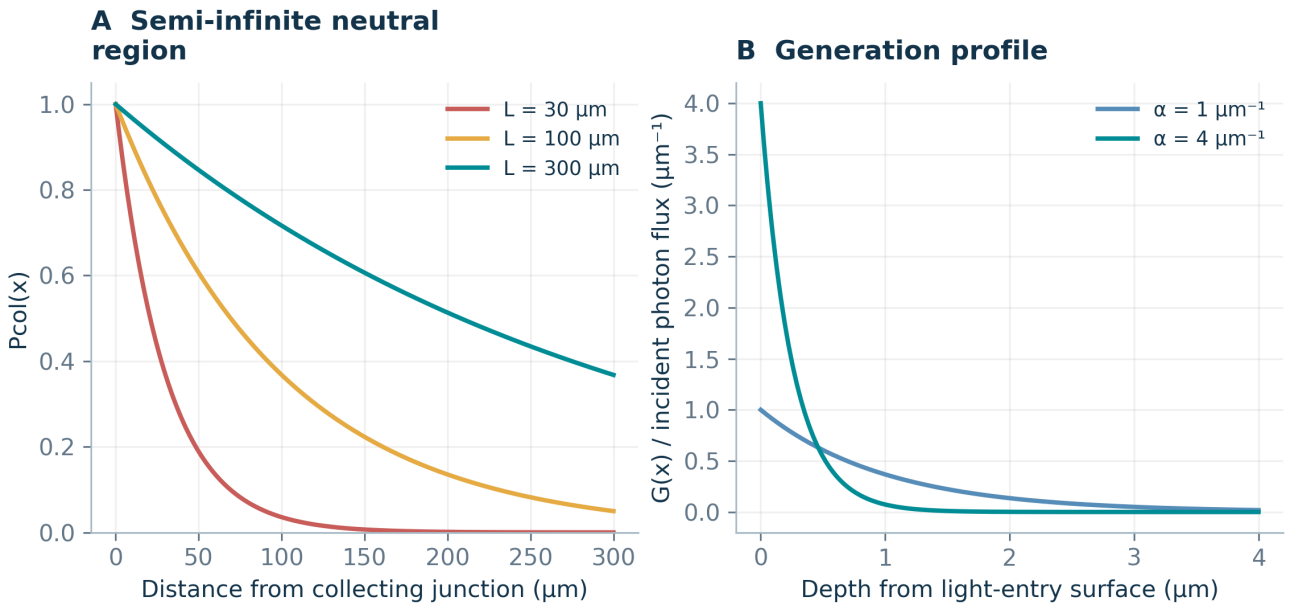


Figure 11. Generation and collection do not follow the same profile. In panel A, the probability of a charge carrier reaching the junction decreases as it moves away from the junction; as L increases, generation at greater depths becomes usable. In panel B, optical generation decreases from the point of light entry. The actual current is the integral of the product of G(x) and Pcol(x) in the same coordinate system. Analytical plots with explicitly stated assumptions. [H16]

Now write the generation rate per unit volume as G(x). Each thin slice dx produces a potential current contribution qG(x)dx, of which the fraction Pcol(x) is collected. Thus:

$$J_{\mathrm{ph}} = q \int_0^d G(x) P_{\mathrm{col}}(x)\, dx. \tag{I.5.5}$$

This statement brings the optical engineer and the device physicist into the same framework. Reducing front surface reflection increases G; rear surface passivation can change Pcol. Both can increase Jsc, but they do not produce the same change in the material. Front and rear illumination, along with EQE and thickness series measurements at different wavelengths, can be used to distinguish between these two explanations. The solution for finite thickness and finite rear surface recombination is not simply a single exponential; the two boundary conditions are solved together.

Control volume and flux at the boundary

We can analyze charge conservation by selecting a small **control volume** within the device. The number of charge carriers within this volume changes due to those generated inside, those recombining, and those entering and leaving through its boundaries. The **outward-pointing surface normal** at each point on the boundary indicates which direction we consider the positive outflow direction. In this notation, V represents the volume, S represents its surface, and the hat symbol on n represents the unit normal vector. This geometric n is not the same physical quantity as the electron density n.

Comparing the water entering and exiting a pipe segment is analogous to this accounting. However, in charge accounting, there is also production and recombination. The **boundary condition** specifies how the neighboring region or contact allows this flow. An ideal closed boundary, a constant contact voltage, and a recombining surface are not the same physical condition.

Common misconceptions and practice questions

It cannot be said that "the higher the doping concentration at the junction, the better"; high doping can lead to Auger recombination, band gap narrowing, and reduced mobility, along with some electrical advantages. Also, the statement "a thicker absorber always generates more current" is incorrect; increased generation can be offset by increased recombination.

1. Why is the net current zero when there is an internal electric field in a p-n junction at equilibrium? **Answer:** The drift and diffusion currents balance each other.

2. For $D = 2\ cm^2/s$ and $\tau = 5\ \mu s$, what is the diffusion length? **Answer:** Approximately 31.6 μm.

3. Which side has a wider depletion region? **Answer:** The side with the lower dopant concentration.

Reading path: First, read about the basics of junction history in [H15], then the concept of diffusion in [H16], and finally, a more general explanation of selective contacts in [H21]. When drawing a device schematic, indicate not only the band edges but also which end the electrons and holes can pass through.

BOOK I · CHAPTER 06 / HISTORY AND PHYSICS

Recombination: where current and voltage are lost

What is lost during recombination?

An electron transitioning from an excited state to a lower-energy, unoccupied state can eliminate the electron-hole pair. What disappears is not the matter or the total electric charge, but rather the **excited pair** capable of carrying energy. The energy is transferred to a photon, crystal vibrations, or another charge carrier. To understand the recombination loss in the cell, we must first trace this energy pathway.

In radiative recombination, energy is carried by a photon. The light emission of an LED is a familiar example of this process. The emitted photon can be reabsorbed within the cell; this is called photon recycling. However, not every emitted photon is recycled, and not every recycling process is lossless. The observation of light emission alone does not prove high power efficiency.

In **defect-assisted recombination**, the energy state created by an atom vacancy, a foreign atom, or a broken bond acts as an intermediate stop. The defect can first capture a charge carrier and then complete the cycle with the opposite charge carrier. In this way, energy can be transferred to lattice vibrations. The Shockley-Read-Hall model, abbreviated as **SRH**, is an important model for this capture and release equilibrium. Simply stating that a “trap exists” is not enough: the energy position, the number of traps, and the probability of charge carrier capture determine the effect.

In **Auger recombination**, the energy of the electron-hole pair is transferred to a third charge carrier. This carrier then releases its excess energy, mostly as heat. Since it is a process involving three charge carriers, it can become significant at high concentrations. On surfaces, broken or incomplete bonds can increase recombination. **Passivation** is the general term for processes that reduce these active defects or the access of unwanted charge carriers to the surface; it is not the same as simply covering the surface mechanically.

Understanding lifetime through a filling-and-draining calculation

Let's consider light generation as water entering a pool, and recombination as the outlet. In this analogy, the water level represents the excess charge carrier density. In a simple, single time constant, and homogeneous case, the steady-state condition for the excess density Δn, the generation rate per unit volume G, and the lifetime τ is given by $\Delta n = G\tau$. The generation unit is $cm^{-3}\ s^{-1}$, time is in seconds, and the result is in cm^{-3}. In a real cell, the current drawn at the contact and carrier transport dependent on position also enter the equation.

Synthetic example: For G = 10^{20} $cm^{-3}\ s^{-1}$ and τ = 1 µs, $\Delta n = 10^{14}$ cm^{-3}. If the lifetime is 10 µs, the density increases tenfold in the same simple model. However, the efficiency does not increase tenfold: the relationship between density and voltage is logarithmic, and there are also current, optical, and contact losses. We will examine the following rate equations to determine under which conditions different decay pathways become dominant.

Comprehension check: what does rapid luminescence decay tell us?

If a film exhibits faster luminescence decay, consider two possibilities: either the carriers are recombining more rapidly at defects, or a good contact is drawing the carriers away more quickly. Without electrical measurements and excitation conditions, it is not possible to simply label a cell as "good" or "bad" based solely on the decay time of contactless and contacted test samples.

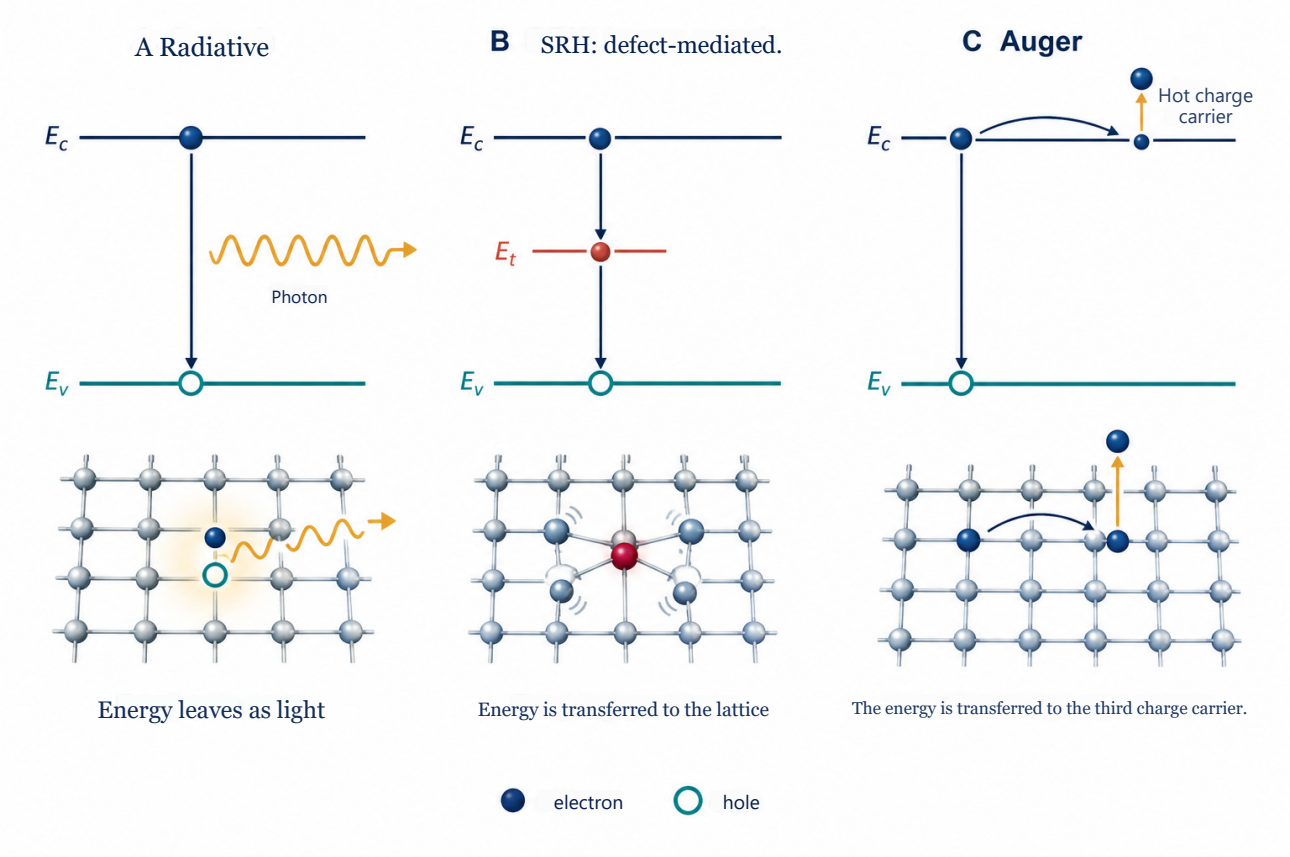


Figure 12. Three recombination mechanisms and where the energy goes. In the upper energy diagrams, Ec is the conduction-band edge and Ev the valence-band edge. In radiative recombination, a photon is emitted; in the SRH pathway, energy is transferred to the lattice via a defect; in the Auger process, energy excites another charge carrier. The lattices below are conceptual representations. The arrows indicate the sequence of events and are not a measure of rate or probability. [H17] [H18] [H19] Conceptual illustration prepared with an image-generation tool; it is not a measurement image.

Why is lifetime a central characteristic of good materials?

After an absorbed photon creates an electron-hole pair, two possibilities compete: the pair's free energy can be converted into work in the external circuit, or it can be lost through recombination. During the process where the electron fills the hole in the valence band, energy is transferred to a photon, lattice vibrations, or other charge carriers. The electron and hole do not simply disappear; the electronic system transitions to a lower free energy state. "Charge carrier loss" refers to the loss of this usable excitation.

The lifetime τ is, in most cases, defined as the ratio of excess charge carrier density to the recombination rate: $\tau_{eff} = \Delta n / R$. However, this is not a universal material constant. The apparent lifetime can change when the injection level, doping, temperature, surface condition, or measurement method changes. The differential decay time after a short laser pulse does not necessarily have to be the same as the effective lifetime obtained under continuous sunlight, in the case of non-linear recombination.

From the perspective of charge carrier collection, the product of μτ or Dτ is important. It is beneficial for a charge carrier to be able to move quickly; however, a very short lifetime can also lead to the loss of a fast-moving charge carrier. Therefore, a material study that reports only mobility or only photoluminescence decay does not fully determine the device collection quality.

Radiative recombination and recyclable photons

In radiative recombination, the energy of the electron-hole pair is emitted as a photon. The simple bulk model is expressed as $R_{rad} = B(np - n_i^2)$, where n and p are in cm^{-3}, and B is in cm^3/s. Since $np = n_i^2$ under zero illumination and thermal equilibrium, the net Rrad is zero; however, microscopic absorption and emission events continue.

The generated photon can be reabsorbed within the device, creating another charge carrier pair. This process, known as photon recycling, can become significant under conditions of specific optical geometry and high internal radiative efficiency. A photon that escapes from the cell has not contributed to the current in the external circuit; however, strong external emission capacity can also be an indication of low non-radiative losses. The answer to the question, “Why does a good cell emit light?” is that absorption and emission are the forward and reverse processes of the same optical transitions.

Internal radiative efficiency and external radiative efficiency are not the same. The escape cone of the photon, re-absorption, parasitic absorption at the metal contact, and the rear optical boundary all affect how much of the internal events can be observed from the outside. High material photoluminescence alone does not guarantee that a completed device with poor contacts will have a high Voc.

Trap-assisted Shockley-Read-Hall process

A localized defect state within the band gap can mediate the sequential capture of an electron and a hole. The electron is first trapped, and then it recombines with a hole; the reverse sequence is also possible. The statistical approach by Shockley and Read in 1952, along with Hall’s work in the same year, forms the classical basis of this mechanism. [H17] [H18]

For a single trap level and the steady state, $R_{SRH} = (np - n_i^2)/[\tau_p(n + n1) + \tau_n(p + p1)]$ is used. Here, $n1 = N_c \exp[-(E_c - E_t)/(kBT)]$ and $p1 = N_v \exp[-(E_t - E_v)/(kBT)]$, which are related to the trap energy Et. In the expressions $\tau_n \approx 1/(\sigma_n v_{th} N_t)$ and $\tau_p \approx 1/(\sigma_p v_{th} N_t)$, σn and σp represent the capture cross-sections, vth is the thermal velocity (length/time), and Nt is the trap density, expressed as the number of traps per unit

volume. The numerator ultimately yields density × time, while the denominator yields density/time.

From this equation, it does not follow that "every defect in the band gap is equally detrimental." The asymmetry of the capture cross-sections, as well as the charge carrier densities and trap occupancy, also play a role. One defect may be abundant but a very weak trap; another defect, even at low concentrations, can be the dominant loss mechanism. Therefore, computational defect studies cannot be reduced solely to the formation energy or transition level. The capture kinetics and experimental density limits are also required.

Auger recombination and surfaces

In the Auger process, the energy of the electron-hole pair is transferred to a third charge carrier; this carrier can then release its energy into the lattice. A simplified model is given by $R_{Auger} = (C_n n + C_p p)(np - n_i^2)$. The units of the coefficients C, when the density is in cm^{-3}, are cm^6/s. If it is assumed that $n \approx p \approx \Delta n$ in high injection, the rate increases approximately with Δn^3. Compared to the radiative recombination rate, which increases approximately with Δn^2, it can be seen why the dominant mechanism may change at high densities.

In real silicon, it may be necessary to go beyond the simple constant-coefficient model. Richter et al.'s 2012 study presents an improved intrinsic recombination parameterization for 300 K by examining the passivation, doping, and injection dependence in high-purity silicon. The 300 K condition of this source should not be considered identical to the set of parameters that perfectly match at 298.15 K. [H19]

The surface is the region where the periodic order of the crystal is interrupted and chemical bonds are altered. The surface recombination velocity, S, expressed in units of m/s or cm/s, is used to represent the surface recombination loss. This "velocity" is not the velocity of a single electron moving to the surface; it is the coefficient in the conversion of excess charge carrier density into surface current. Chemical passivation can reduce the density of active defects, while field-effect passivation limits the encounter by removing one of the electrons or holes from the surface. The effect of surfaces on the total lifetime is described in [H20].

Worked example: What are the benefits of surface modification?

Illustrative example. Consider a slab with a thickness of d = 150 μm = 0.015 cm and a bulk lifetime of τbulk = 1 ms, where the excess charge carrier density is approximately uniform. If the two surfaces have the same S, then $1/\tau_{eff} \approx 1/\tau_{bulk} + 2S/d$. For S = 1000 cm/s, τeff ≈ 7.44 μs. Very good bulk quality is rendered invisible in the measurement due to poor surfaces.

When S is reduced to 10 cm/s, τeff ≈ 429 μs. The effective lifetime increases by approximately 58 times, while the bulk material itself remains unchanged. Therefore, performing surface and contact control before changing the growth method may be more cost-effective and provide better differentiation in most experiments. However, if the uniform density approximation is invalid, the spatial diffusion and surface boundary conditions must be solved together instead of using this simple relationship.

Second simple calculation: for D = 2 cm^2/s and τ = 10 ns, $L = \sqrt{(D\tau)} \approx 1.41$ μm. If τ = 1 μs in the same material, then L ≈ 14.1 μm. While the lifetime increases by a factor of 100, the diffusion length increases by a factor of 10. Linear intuition is misleading here; the square root relationship directly affects the device thickness design.

Understanding the SRH expression through capture-emission balance

Consider a defect as an intermediate state that can be either filled with an electron or empty (a hole). An empty trap can capture an electron; a filled trap can release an electron or capture a hole, thereby annihilating the electron-hole pair. If, in a steady state, the probability of trap occupancy does not change, the accounting for these transitions ceases. The electron and hole capture coefficients, along with the trap density, are aggregated within the time scales τn and τp. This equilibrium yields the following net recombination rate for the single-level model:

$$R_{\mathrm{SRH}} = \frac{np - n_i^2}{\tau_p(n + n_1) + \tau_n(p + p_1)}. \tag{I.6.1}$$

$$n_1 = n_i \exp\left(\frac{E_t - E_i}{k_B T}\right), \qquad p_1 = n_i \exp\left(-\frac{E_t - E_i}{k_B T}\right). \tag{I.6.2}$$

The numerator explains why the net loss in the np - n_i^2 term is zero. Capture events maintain the equilibrium; however, generation equals recombination. The denominator includes not only the presence of the trap but also its access to both types of charge carriers. Therefore, the statement “there is a defect in the middle of the band

gap" alone does not represent a lifetime calculation. The defect density, capture cross-sections, and occupancy at the operating point are also required. [H17] [H18]

Let τn = τp = τ0 in a symmetric, mid-gap trap. In p-type, low-injection conditions, when p is approximately p0 and n is approximately Δn, R is approximately Δn/τ0. In high-injection conditions, when n is approximately p, and both are approximately Δn, R is approximately Δn/(2τ0). Therefore, the same trap system can yield different apparent effective lifetimes when the injection changes. The non-flatness of the lifetime curve does not automatically imply the emergence of a new type of defect.

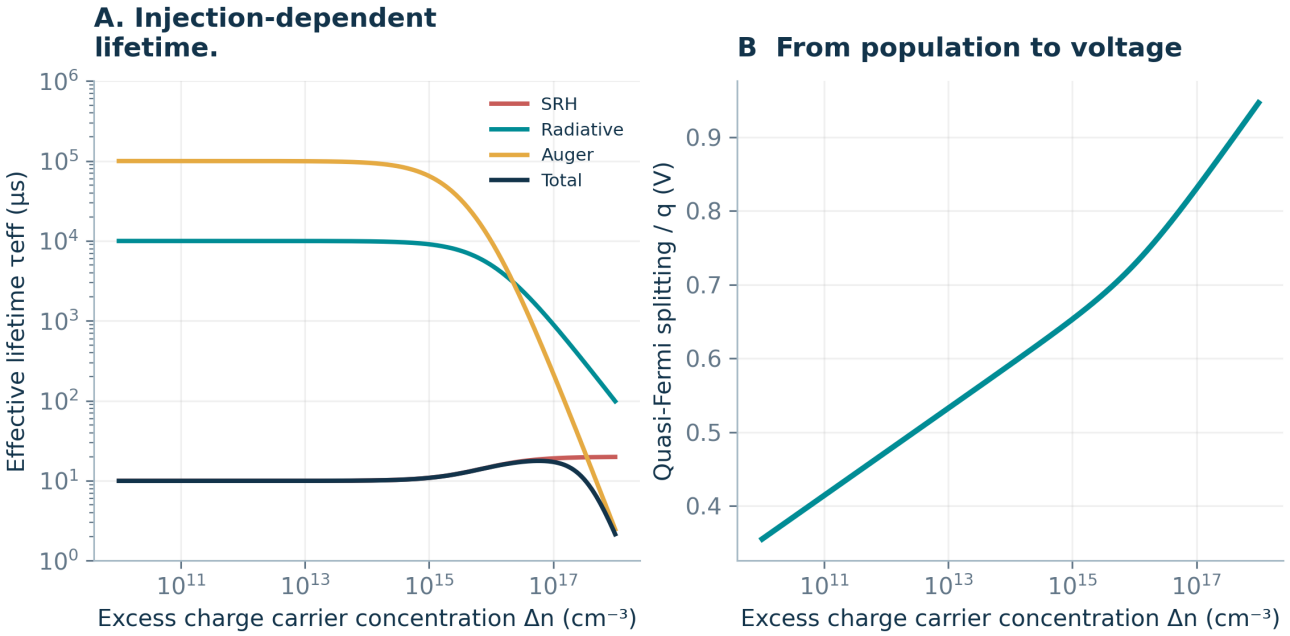


Figure 13. Different injection regimes with the same material parameters. The SRH lifetime is approximately 10 µs at low injection and changes when transitioning to high injection; the Auger contribution increases with strong injection. Panel B shows the quasi-Fermi splitting calculated from the same populations. The parameters are for instructional purposes: p0 = 10 ^{16} cm^{-3}, ni = 10 ^{10} cm^{-3}, τn = τp = 10 µs, B =) $^{-14}$ cm^3/s, Cn = 3 ×) $^{-31}$ and Cp =) $^{-31}$ cm^6/s. [H17] [H18] [H19]

Why isn't the ideality factor a unique identifier?

At a high forward bias, if the dominant recombination current, Jrec, behaves approximately as J0 exp[qV/(nid kBT)], then nid = (q/kBT) dV/d ln Jrec can be defined. Under specific assumptions, familiar results, such as one for diffusion in the neutral region at low injection and approximately two for the symmetric depletion region SRH model, can be derived. In a real heterostructure, voltage-dependent collection, contact barrier, ionic redistribution, and multiple recombination channels also modify the slope.

When a graph yields nid = 1.7, the researcher-level conclusion is not "SRH has been proven". First, one must ask in which voltage and illumination range the slope was calculated, whether it is affected by the series resistance, and whether the same physical model works at multiple temperatures. A stronger interpretation would be

that the same mechanism is also consistent with PL, charge carrier density dependence, and contact series. The ideality factor is useful when combined with other evidence.

What does changing the measurement condition test?

Bias voltage is the voltage applied to the device before a measurement; the voltage during the measurement also changes the density and distribution of charge carriers. In the same material, different recombination pathways may be dominant at low and high charge carrier densities. Therefore, the lifetime measurement should be provided along with the light intensity, temperature, and electrical conditions. A single lifetime value does not represent the dominant mechanism under all operating conditions.

Let's differentiate between the two distinct interventions in optimization. Defect reduction aims to minimize the number of effective trapping centers. **Contact selectivity**, on the other hand, aims to limit the loss of holes at the electron contact and electrons at the hole contact while allowing the desired charge carrier to pass through. A highly insulating coating can reduce recombination but also hinder the useful current. Therefore, success should be evaluated not only by luminescence or lifetime improvement but also by the voltage and power of the completed device.

Common misconceptions and practice questions

"Recombination is zero in a perfect cell" is incorrect. Radiative recombination is an unavoidable consequence of absorption in reciprocal optical systems. Also, "the sample with the longest carrier lifetime yields the best cell" is not reliable; the injection conditions and contacts must be matched. In an experiment, increasing photoluminescence may simultaneously indicate decreasing extraction efficiency; the measurement geometry and operating point must be specified.

1. If Nt increases by a factor of ten, while other capture parameters remain constant, how does the simple SRH lifetime parameter change? **Answer:** It decreases by a factor of ten.

2. If the charge carrier density doubles under high injection conditions, how do the rates of simple radiative recombination and Auger recombination change? **Answer:** They increase by approximately a factor of four and eight, respectively.

3. Why does the surface velocity S have units of cm/s without being a particle drift velocity? **Answer:** S is an effective boundary coefficient relating the surface loss flux to carrier density.

Reading path: First, review the original sources of the SRH model ([H17] [H18]), and then examine how the parameters are measured in a specific material ([H19]). Do not make comparisons without noting the injection level, temperature, surface treatment, and method next to each lifetime value.

BOOK I · CHAPTER 07 / HISTORY AND PHYSICS

Current-voltage curve: interpreting a cell's performance

How is the current-voltage curve actually formed?

Let's consider a scenario where we connect different electrical loads to a cell. With a very small resistance, the terminal voltage can be low, while the current is high. With a very large resistance, the current decreases while the voltage increases. The measuring instrument scans these operating points in a controlled manner. When we plot the voltage on the horizontal axis and the current on the vertical axis and connect the points, we obtain the **I-V curve**. If we divide the current by the measured area, we obtain the current density J, and we plot the **J-V curve**. In this way, we can compare cells with different areas using an appropriate area definition.

Short-circuit current is the current when the voltage is zero. **Open-circuit voltage** is the voltage when the current is zero. At both of these extreme points, the power is zero because power is the product of voltage and current. The useful operating point lies somewhere in between. At each measurement point, we calculate this product and select the largest one; this is called the **maximum power point**, or MPP in English. The electronic control that keeps the cell operating near this point is called maximum power tracking.

Extract four values from the measurement table

Synthetic measurement: Consider a 1 cm^2 cell with a short-circuit current density of 40 mA/cm^2 and an open-circuit voltage of 0.70 V. At the measured best operating point, we find 0.58 V and 36 mA/cm^2. The power density is $0.58 \times 36 = 20.88$ mW/cm^2. An irradiance of 1000 W/m^2 corresponds to 100 mW/cm^2; therefore, the efficiency is 20.88%. In this example, we compared electrical and optical power with reference to the same area.

The **fill factor** is the ratio of the area of the actual maximum power rectangle to the area of the larger rectangle formed by the short-circuit current and the open-circuit voltage. In the example, $20.88/(40 \times 0.70) = 0.746$, which is approximately 74.6%. The geometric intuition of how "square-like" the shape is comes from this. FF is not a voltage or a current; it is a dimensionless ratio. A high FF alone does not guarantee high efficiency: if the current and voltage are small, the power can still be low.

What do the components in the equivalent circuit represent?

The **current source** represents photogeneration; the **diode** represents the internal current that rises rapidly with voltage and the model's recombination behavior. **Series resistance** represents the loss encountered by charge along the conduction and contact path to the outside. **Shunt resistance** represents the unwanted leakage path between the two terminals. Lower series resistance reduces transport loss; higher shunt resistance reduces leakage. The diagram does not mean that separate battery and resistor components of this kind actually exist inside the cell; it is an electrical representation of physical processes.

Measurement software uses different conventions for the current sign. This book considers the current supplied to the external circuit as positive. Seeing the curve of the same cell oriented downwards in another publication does not necessarily mean that the device is defective; first, check the sign convention.

Comprehension check: why is multiplying short-circuit current by open-circuit voltage insufficient?

Writing $0.70 \times 40 = 28$ mW/cm^2 for the above cell does not give the actual power. 40 mA/cm^2 is measured at short circuit, and 0.70 V is measured at open circuit; they do not occur simultaneously. For the actual 20.88 mW/cm^2, the values of 0.58 V and 36 mA/cm^2 from the same measurement row should be used. The FF (Fill Factor) precisely reveals this difference.

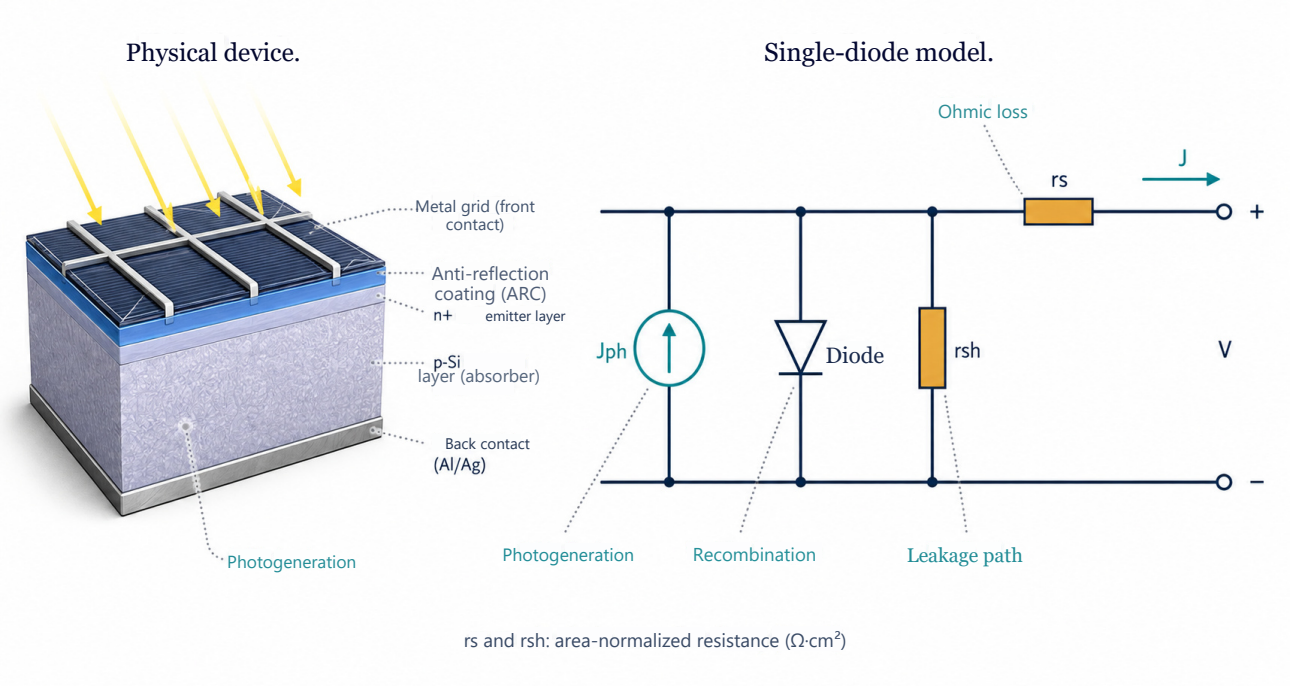


Figure 14. From the physical solar cell to the single-diode equivalent circuit. The photocurrent source, diode, and shunt resistance are all connected to the same two internal nodes; the series resistance is between the internal node and the positive external terminal. The dotted annotation lines are not electrical connections. J is the current density supplied to the external circuit; rs and rsh are normalized to the area. The thicknesses of the cell cross-section are not to scale. [B06] [B11] Conceptual illustration prepared with an image-generation tool; it is not a measurement image.

Four numbers and one curve

The electrical behavior of a solar cell is observed in the current-voltage curve measured under specific illumination and temperature conditions. The current I is expressed in amperes, and the current density J is expressed as J = I/A, in amperes per square meter or milliamperes per square centimeter. Whether the area is the active area, the aperture area, or the total area affects J and the efficiency; the denominator is not merely a detail but is part of the measurement.

In short-circuit conditions, V = 0 and the current is Isc or Jsc. In open-circuit conditions, I = 0 and the voltage is Voc. At both ends, the electrical power P = VI is zero. The maximum power occurs at a point along the curve: Pmpp = Vmpp Impp. The fill factor FF = Pmpp/(Voc Isc) measures how closely the curve approaches an ideal rectangle. The efficiency η = Pmpp/(GA) = Voc Jsc FF/G. These fundamental definitions should be applied consistently, regardless of the direction in which the measurement mark is chosen. [H23]

Jsc represents the current-collection capacity supplied by photons; Voc represents the chemical potential that can be established against recombination; and FF summarizes the current maintenance at the operating voltage. None of them can be directly attributed to a single defect. For example, a poor interface can reduce both Voc and FF; optical losses can reduce Jsc while causing a smaller logarithmic change in Voc.

The single-diode model and consistent units

If we define the generated current as positive, the commonly used equivalent circuit model is given by $J = Jph - J0\{\exp[(V + JRs)/(nid\ VT)] - 1\} - (V + JRs)/Rsh$, where $VT = kBT/q$ is the thermal voltage, nid is the ideality factor, Rs is the area-normalized series resistance, and Rsh is the area-normalized shunt resistance. If J is in A/cm^2, then Rs and Rsh must be in $\Omega\ cm^2$. In the model written in terms of current, the resistances are in Ω. Mixing the two representations introduces a systematic error that degrades the model when the area changes.

Jph is the current source generated by light and is assumed to be collected in the model. J0 is the dark saturation current density, and nid is the effective scaling factor for the exponential behavior. Values such as nid ≈ 1 or 2 can be associated with specific ideal mechanisms; however, it is not accurate to simply look at the number that fits the curve and definitively determine the dominant microscopic defect type. The single-diode model is a simplified representation of the physics of the device.

Rs can collectively represent the resistance of the metal and transparent conductive layers, contact losses, and some of the transport effects. Rsh, on the other hand, can reflect edge leakages, local short circuits, or similar parallel paths. On a curve, multiple parameters can compensate for each other, resulting in a similar fit. This identifiability problem demonstrates that adding more parameters does not automatically lead to a better understanding of the underlying physics.

Open-circuit condition and maximum power point

If Rs = 0, Rsh is infinite, and Jph is independent of voltage, then $Voc = nid\ VT \ln(Jph/J0 + 1)$. When the photocurrent doubles, under the condition that Jph is much larger than J0, the increase in Voc is $nid\ VT \ln 2$. Therefore, while the current increases approximately linearly with light intensity, the voltage increases logarithmically. Although VT increases during heating, J0 generally increases significantly; therefore, the conclusion that "if VT increases, Voc must increase" is incorrect.

For the ideal diode, normalized variables $v = V/(ni\ d\ VT)$ and $voc = Voc/(ni\ d\ VT)$ are used. The power density, $p = VJ$, is maximized by setting its derivative to zero, resulting in the maximum power condition $vmp + \ln(1 + vmp) = voc$. This equation can be easily solved using a single-variable root-finding method. The approximate fill factor expression $FF0 \approx [voc - \ln(voc + 0.72)]/(voc + 1)$ is a useful hand calculation for the ideal diode; Green's 1981 study addresses the general fill factor graph and empirical expressions. [H22]

This approximate formula does not inherently include the series resistance of the actual device, the multi-diode behavior, or the voltage-dependent collection. The fact

that the formula yields a result with several decimal places does not necessarily indicate that the model assumptions are also accurate to that degree. Directly finding the numerical maximum of the power curve is generally more accurate when measurement data is available; however, noise and scan history must still be taken into account.

Worked example: a complete ideal diode calculation

This is an illustrative example, not a measured cell. Let T = 298.15 K, n_{id} = 1, J_{ph} = 0.040 A/cm^2, J₀ = 10^{-13} A/cm^2, R_s = 0, and R_{sh} = ∞. Then, V_T = 0.0256926 V, and V_{oc} = 0.68637 V. Solving the above maximum power equation yields V_{mpp} = 0.60417 V and J_{mpp} = 0.038368 A/cm^2. The fill factor is 0.84434. For G = 0.100 W/cm^2, the efficiency is 23.181%.

This calculation includes two useful checks. First, the maximum power density is approximately 0.023181 W/cm^2; since the denominator is 0.100 W/cm^2, the efficiency is dimensionless. Second, it is verified that FF is less than one, Vmpp is less than Voc, and Jmpp is less than Jsc. These are not exhaustive verifications, but they can quickly identify unit or sign errors.

Consider a separate example where Voc = 0.720 V, Jsc = 40.0 mA/cm^2, and FF = 0.800. The efficiency is 23.04%. If FF is increased to 0.820, while the other parameters remain constant, the efficiency becomes 23.616%: the gain is 0.576 percentage points. It is incorrect to directly report a 0.02 increase in FF as "the efficiency increased by two points."

From the curve to diagnosis

The slope near the short circuit indicates shunt resistance, while the slope near the open circuit may be sensitive to series resistance and diode behavior; however, these observations alone do not constitute proof of the mechanism. An S-shaped curve can provide clues about charge carrier blocking or improper contact. Voc as a function of light intensity, temperature-dependent current, EQE, dark current, and steady-state power tracking should be interpreted together.

Especially in time-dependent devices, a fast sweep can make energy storage or ion redistribution appear to be device performance. The sweep direction, speed, preconditioning, and dwell time should be specified. The high value observed at a specific point in time and the steady-state power generation represent distinct observations. The static model in this section operates under the assumption that these dynamic effects are absent.

Finding the maximum power point using derivatives

In the ideal single-diode model, let J = Jph - J0[exp(V/VT) - 1]. Define the dimensionless voltage v = V/VT. At open circuit, exp(voc) = 1 + Jph/J0. At the maximum power density, p = VJ, dp/dV = J + V dJ/dV = 0. Substituting the diode derivative, we get:

$$\exp(v_m)(1+v_m) = \exp(v_{\mathrm{oc}}), \qquad v_m + \ln(1+v_m) = v_{\mathrm{oc}}. \tag{I.7.1}$$

Since the expression on the left increases monotonically with v, the root can be reliably found. It can also be written in closed form using the Lambert W function; however, this scalar root is sufficient to understand the physical meaning. For Jph = 40 mA/cm², J0 = 10^{-13} A/cm², and 298.15 K, we obtain Voc = 0.68637 V, Vmpp = 0.60417 V, and Jmpp = 38.368 mA/cm². The fill factor is 84.43%; at an incident power density of 100 mW/cm², the efficiency is 23.18%. Although the open-circuit voltage is higher, the power is zero because the current is zero.

Maintaining series and shunt resistances in the same equation

When the area-normalized series resistance, rs, and shunt resistance, rsh, are added, the internal voltage of the diode becomes V + Jrs. If the current supplied to the external circuit is chosen to be positive:

$$J = J_{\mathrm{ph}} - J_0\left[\exp\left(\frac{V + Jr_s}{nV_T}\right) - 1\right] - \frac{V + Jr_s}{r_{\mathrm{sh}}}. \tag{I.7.2}$$

Since J appears on both the left and right sides of the equation, this is an implicit equation. We can solve for J at the external voltage point numerically. If the current I were used, the resistance would be in ohms (Ω); however, since J is in A/cm², rs and rsh are in Ω·cm². Transferring the same numerical resistance between the two equations without performing a unit conversion will result in a significant error that depends on the sample area. [B06] [B11]

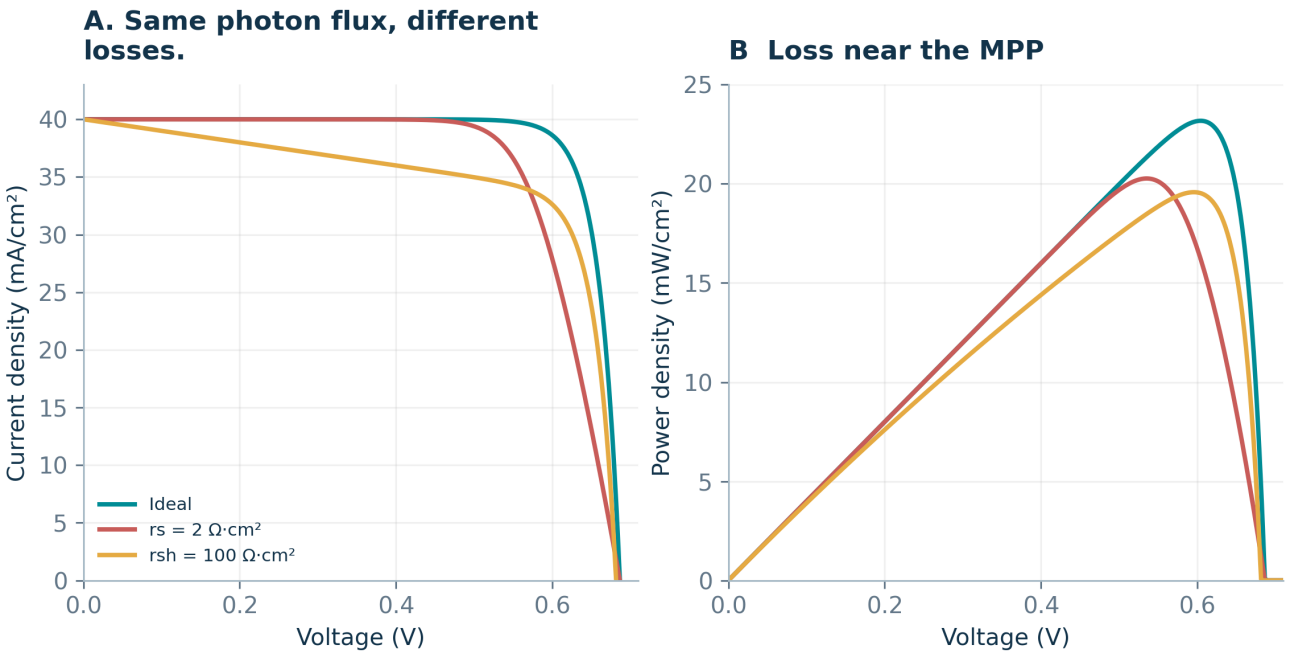


Figure 15. The distinct traces of series and parallel losses on the curve. All curves were calculated with the same Jph, J0, temperature, and ideality factor. Series resistance creates an internal voltage drop, especially at high current; the parallel path causes leakage current that depends on the voltage. Panel B directly shows the effect of the loss on the power maximum. The curves are solutions of the implicit equation, not measurements. [B11]

Do not limit yourself to the mnemonic "right slope is series resistance, left slope is shunt resistance." These approaches provide an approximate understanding within the appropriate operating regions. The combined fitting of the dark and illuminated curves, and the parameter stability under varying irradiance and temperature, more rigorously test the validity of the equivalent circuit. Two models that fit the same curve with a very large parameter uncertainty do not necessarily mean that a single physical mechanism is being measured.

> Quick design calculation: When Jmpp = 20 mA/cm², rs = 1 Ω·cm², this yields an ohmic loss scale of approximately 0.4 mW/cm². If J doubles, this loss quadruples. Therefore, concentrated cells and tandem contacts should be evaluated under the same current conditions.

Relating the curve to the cross-section of the cell

The cell's front coating reduces light reflected from the surface, allowing more photons to reach the absorber under the same illumination. The n and p regions have different majority carriers. In the **depletion region** between them, mobile carriers are depleted and the electric field of the fixed ionized dopants becomes important. The front and rear metal contacts carry current into the external circuit. Each feature can affect the curve; sometimes several different causes produce the same change in the curve.

Cross-validation involves testing the same physical result using a different measurement method. For example, the short-circuit current calculated from a spectral integration measurement is compared with the short-circuit point of the

current-voltage curve. Agreement supports the interpretation; disagreement requires re-examining factors such as the area, light spectrum, calibration, or measurement history.

Common misconceptions and practice questions

The statement "Voc × Isc is the power of the cell" is incomplete; these two quantities belong to different operating points, and their product is corrected by the fill factor (FF). The statement "the best curve fit means correct physics" is also incorrect. More independent measurements sometimes provide more information than a more complex equivalent circuit.

1. If 40 mA is measured in a 1 cm^2 cell and 160 mA is measured in a 4 cm^2 cell, what are the current densities? **Answer:** Both are 40 mA/cm^2.

2. At 298.15 K, when nid = 1 and Jph/J0 is large, if the light intensity is doubled, what is the ideal Voc gain? **Answer:** Approximately 17.81 mV.

3. What is the efficiency for Voc = 0.70 V, Jsc = 35 mA/cm^2, FF = 0.80, and G = 100 mW/cm^2? **Answer:** 19.6%.

Reading path: First, examine the geometry of the curve ([H23]), and then examine the mathematical approximation of the fill factor ([H22]). For each new model, verify power conservation, unit consistency, and the recovery of the ideal limit.

Detailed balance and voltage losses: what does the theoretical limit restrict?

How is a theoretical limit defined?

“What is the highest possible efficiency for a solar cell?” is an incomplete question. Is it a single absorber or multiple absorbers? Is it direct sunlight or concentrated light? What is the temperature and spectrum? Which losses are considered unavoidable? The **theoretical limit** is the highest result within a clearly defined family of models. It is not the value that a material will achieve in a factory, nor is it the single universal percentage that nature imposes on every device.

In the conventional single-junction model, low-energy photons with energies below the band gap do not contribute to useful interband generation. Very high-energy photons, on the other hand, largely dissipate their excess energy as heat after generating an electron-hole pair. Reducing the band gap allows more photons to be utilized, but it also reduces the voltage scale related to the energy that can be obtained per electron-hole pair. Increasing the band gap has the opposite effect. The **Shockley-Queisser calculation** quantitatively establishes this trade-off, including the device’s unavoidable radiative recombination. [H25]

What is being balanced in the “detailed balance”?

If, in the dark, an object at the same temperature as its surroundings only absorbed light and never emitted it, it would disrupt the equilibrium by drawing energy unidirectionally from its surroundings. The same relationship between absorption and emission through the same optical channels requires us to consider that the solar cell is also a light emitter. In equilibrium, the processes match. When additional light arrives from the sun, the device is driven out of equilibrium; electrical power generation, increased charge carrier density, and emission are resolved together. Saying “if we make the radiation loss zero, we will exceed the limit” can compromise the model’s own consistency under the same absorption conditions.

Representative energy calculation: When a 2 eV photon creates an electron-hole pair in a material with a band gap of 1.1 eV, a difference of approximately 0.9 eV is released during relaxation to the band edges. If the terminal voltage is 0.70 V, the energy transferred per electron in the external circuit is 0.70 eV. It is also necessary to consider the difference between 1.1 eV and 0.70 eV; the band gap is not directly equal

to the terminal voltage. This single-photon example does not represent a complete efficiency calculation but illustrates which energy differences are distinct.

The logarithmic nature of voltage loss also requires intuition. The **natural logarithm** tells us which power of the base e gives a number; e is approximately 2.718. For example, ln(10) is approximately 2.303. In some idealized relationships, reducing a loss channel by a factor of ten gives a voltage improvement of tens of millivolts at room temperature. This does not mean that power increases tenfold. Below, we will pay particular attention to the dimensionless ratios entering the logarithm and to the reciprocity assumptions used.

Comprehension check: graph exceeding the limit

If a result lies above a boundary curve, first check if it belongs to the same model class. Tandem, concentration, different spectrum, or area definition can alter the comparison. Measurement errors are also possible. Without indicating which assumption has changed, it is not possible to make statements such as “the fundamental physics has been exceeded” or “the result is definitely incorrect.”

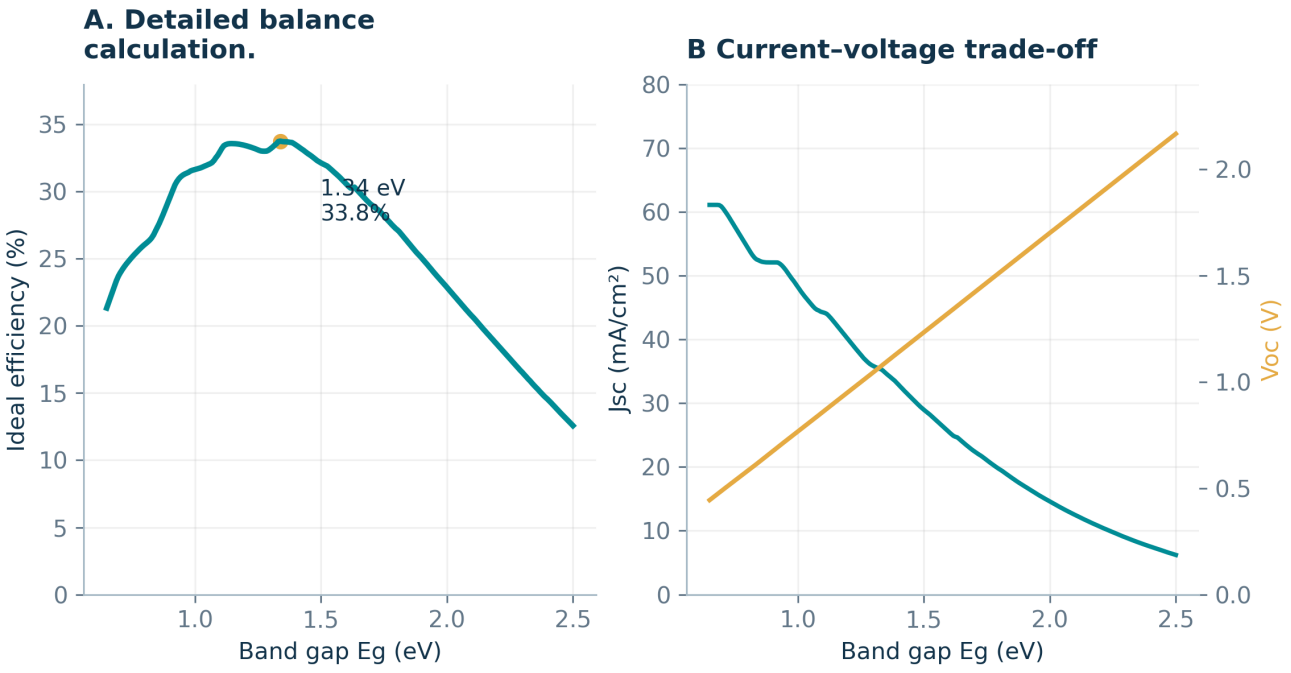


Figure 16. Recalculation of the ideal single-junction limit. Input: ASTM G173 global spectrum; temperature: 298.15 K; step-function absorption; ideal rear mirror; external emission into one hemisphere. Panel A shows the efficiency maximum, and panel B the current loss and voltage gain as the band gap increases. The curve is not a table of measured world records. [H09] [H25] [H26] [B10]

The value of an upper limit stems from its assumptions

The efficiency limit is not the only number that nature unconditionally imposes on a device. A limit can be calculated when it is defined which photons are absorbed, how many charge carriers are generated, how quickly the charge carriers cool down, how many independent chemical potentials exist, and from which angles the light enters and exits. If this definition is changed, the calculated limit can also change. Therefore, before presenting a result as "we have exceeded the limit," it should be asked whether the two calculations belong to the same category.

In their 1961 paper, Shockley and Queisser established the detailed balance limit for a p-n junction solar converter, considering the ideal case where only radiative recombination occurs. The original work treated the Sun with a blackbody approximation of 6000 K and the cell with 300 K; the historical approximate 30% result is dependent on these conditions. [H25] The fact that the single-junction limits calculated with current AM1.5G are approximately one-third of the original limit represents another spectral problem. Rühle's 2016 study presents, in tabular form, the current, voltage, and maximum power values as a function of the band gap. [H26]

Incident photons and unavoidable radiative emission

In an ideal step absorber, $a(E) = 0$ for $E < Eg$, and $a(E) = 1$ for $E \geq Eg$. The photocurrent is given by $Jph = q \int a(E)\, \varphi sun(E) dE$. In this single-photon model, photons with energy below the band gap do not generate electron-hole pairs. Photons with energy above the band gap generate one electron-hole pair each; the excess energy above Eg is lost through rapid thermalization. We have not yet calculated the voltage: if the energy of a pair is Eg, then the external electrical work that can be obtained is $qV = Eg$.

In an isotropic external environment, the blackbody photon flux emitted into a single hemisphere is given by $\varphi bb(E,T) = [2\pi E^2/(h^3c^2)]/[\exp(E/(kBT)) - 1]$, where energy is measured in joules. The saturation current, $J0,rad$, is calculated as $q \int a(E)\varphi bb(E,T) dE$. This expression assumes that the refractive index of the external environment is 1 and that there is no escape from the back side. If both surfaces radiate in the same manner, the corresponding geometric factor must be added.

When a voltage is applied, the chemical potential of the charge carriers enhances the emission. In the Boltzmann tail approximation, we obtain $Jrad(V) \approx J0,rad[\exp(qV/(kBT)) - 1]$. Thus, the detailed balance leads to the familiar ideal diode curve: $J(V) = Jph - Jrad(V)$. The maximum VI is found and divided by the incident optical power. This derivation shows that the limit is both a photon counting and a free energy calculation.

In the generalized Planck approach, E - μγ enters the exponential denominator of the emission expression; μγ is related to the electron and hole quasi-Fermi splitting under appropriate conditions. Würfel's 1982 study addresses thermal and luminescent emission by using the photon chemical potential in addition to the emitter's temperature. [H27] Thus, it is not necessary to assume that a light-emitting cell has a temperature thousands of degrees higher than it actually does.

Decomposing the voltage loss into its components

The total open-circuit voltage deficit, Woc, can be defined as Woc = Eg/q - Voc. This quantity encompasses the combined effect of all radiative and non-radiative causes; it is not solely due to defect loss. The optical absorption edge, angular emission, spectrum, temperature, and photon flux modify the radiative reference. Therefore, when comparing the Woc values of two materials, it is also necessary to know how Eg was determined.

Under a fixed radiative reference, the non-radiative voltage loss ΔVnonrad can be related to the external radiative efficiency ERE by the equation ΔVnonrad = -(kBT/q) ln(ERE). Here, ERE is a fraction between 0 and 1, not a percentage; the operating point and the definition of external optical escape must be specified. Rau's 2007 reciprocity study derives the relationship between photovoltaic quantum efficiency and electroluminescent emission, as well as the relationship between open-circuit voltage and emission efficiency. [H28]

Do not apply this relationship blindly to any photoluminescence intensity. Absolute calibration, the excitation conditions, device area, emission angle, and the relevant injection point are required. The quasi-Fermi splitting within the material, the open-circuit voltage (Voc) of the completed device, and the electroluminescence yield are all different observations. If the charge carrier collection is strongly dependent on the voltage, the assumptions of simple reciprocity must also be tested.

Worked example: percentage and logarithmic trap

Illustrative example. At 298.15 K, VT = 25.6926 mV. For ERE = 1% = 0.01, ΔVnonrad = 118.32 mV. For ERE = 0.01% = 0.0001, the loss is 236.64 mV. A hundredfold degradation of ERE does not increase the loss by a hundredfold; it adds approximately 118.32 mV. The physical meaning of the logarithm is the exponential relationship between charge carrier density and chemical potential.

In the reverse calculation, if ΔVnonrad = 200 mV is given, then ERE = exp(-0.200/0.0256926) ≈ 0.0004162, which means 0.04162% is obtained. Directly writing 0.0004162 as a percentage would lead to an error of 100 times. If this value

represents the total Woc, the same reverse transformation cannot be performed; first, the radiative component must be separated.

Another example of geometry: if, with everything else held constant, the number of external illumination channels doubles and J0,rad doubles, the ideal Voc decreases by approximately VT ln2 = 17.81 mV. This calculation shows that the rear mirror not only extends the light path but can also affect the external illumination geometry under appropriate conditions. However, the parasitic absorption and re-absorption effects of the actual mirror must also be modeled.

Turning an efficiency-limit code into a research tool

In a detailed balance calculation, the spectrum file, units, and integration range must be recorded. First, the total incident power is verified independently. Then, a band gap scan is performed; it is checked that the photocurrent decreases as the band gap increases, that the voltage scale is reasonable, and that the maximum power remains within the limits. When the energy grid is refined, the result should remain stable. Two calculations, written with Joule and electronvolt notations, should yield the same result; the factor q in the variable transformation should not be applied twice.

In the results table, T = 298.15 K and T = 300 K are listed as separate conditions. Optical concentration, one or two emission hemispheres, step or measured absorption, recycling, and the number of terminals are explained. Such a calculation does not predict the laboratory efficiency of a new material; it indicates how far one could go if losses in the specified architecture were eliminated. Actual production of the material and its operation as a device require separate verification.

Reconstructing the limit numerically

To utilize a theoretical limit, the inputs and optical geometry must be defined. Here, a single junction is used, with a step-function absorption profile a(E) = 1 (E ≥ Eg), one electron-hole pair per photon, a 298.15 K cell, an unconcentrated ASTM G173 global spectrum, and an ideal back reflector are selected. The cell emits into one external hemisphere. The geometry where the back surface can also emit light does not yield the same result.

First, Jsc is calculated based on the incident spectrum. Then, the equivalent current corresponding to the photon flux emitted outward is determined while the cell is in thermal equilibrium with its surroundings in the dark. When the energy E is expressed in joules, the blackbody photon flux for a hemisphere is used:

$$J_{0,\mathrm{rad}} = q\frac{2\pi}{h^3c^2}\int_{E_g}^{\infty}\frac{E^2}{\exp(E/k_BT)-1}\,dE. \tag{I.8.1}$$

In this equation, Eg is expressed in joules. Numerically, it is more convenient to evaluate the integral with the variable x = E/(kBT). When a voltage is applied, the number of emitted photons increases by the factor exp(qV/kBT) at the Boltzmann limit. The decrease in current as a function of voltage is not due to "defect generation" here; it is the unavoidable radiative recombination of the ideal cell. The accounting of incoming and outgoing photons yields J(V), and its maximum produces the ideal efficiency. [H25] [H26] [H27]

For Eg = 1.34 eV, the calculation in this book yields Jsc = 35.032 mA/cm^2, Voc = 1.08350 V, and Vmpp = 0.98905 V. With Jmpp = 34.145 mA/cm^2, the power density is approximately 33.77 mW/cm^2, and the efficiency is approximately 33.76% with respect to the applied input of 1000.371 W/m^2. The maximum of the band gap scan is around 1.34 eV. The digits after two decimal places are not universal constants but represent the reproducibility check of the specified numerical model.

Dividing the energy budget into four separate questions

In this model, photons with energy less than Eg are not absorbed. The excess energy of a photon with energy greater than Eg, beyond Eg, is largely transferred to the lattice as charge carriers relax to the band edges. Not all of the generated charge carrier pairs contribute to the external circuit; at the operating voltage, a portion undergoes radiative recombination. The electrical work done by each pair that emerges is not Eg, but rather qV. Separating these four steps clarifies why "absorbing all the light" yields different results than "converting all the light into electricity."

Consider the curve relating Jsc to the band gap as a diagnostic tool. As Eg decreases, the current increases, but Voc decreases. The maximum lies in the middle of this trade-off. A tandem cell modifies this single-threshold requirement of a single absorber; in return, it introduces optical and electrical matching between the layers. When discussing exceeding the SQ limit, it must be clearly stated which assumption is being changed. The fact that a two-junction device exceeds the single-junction limit does not violate energy conservation.

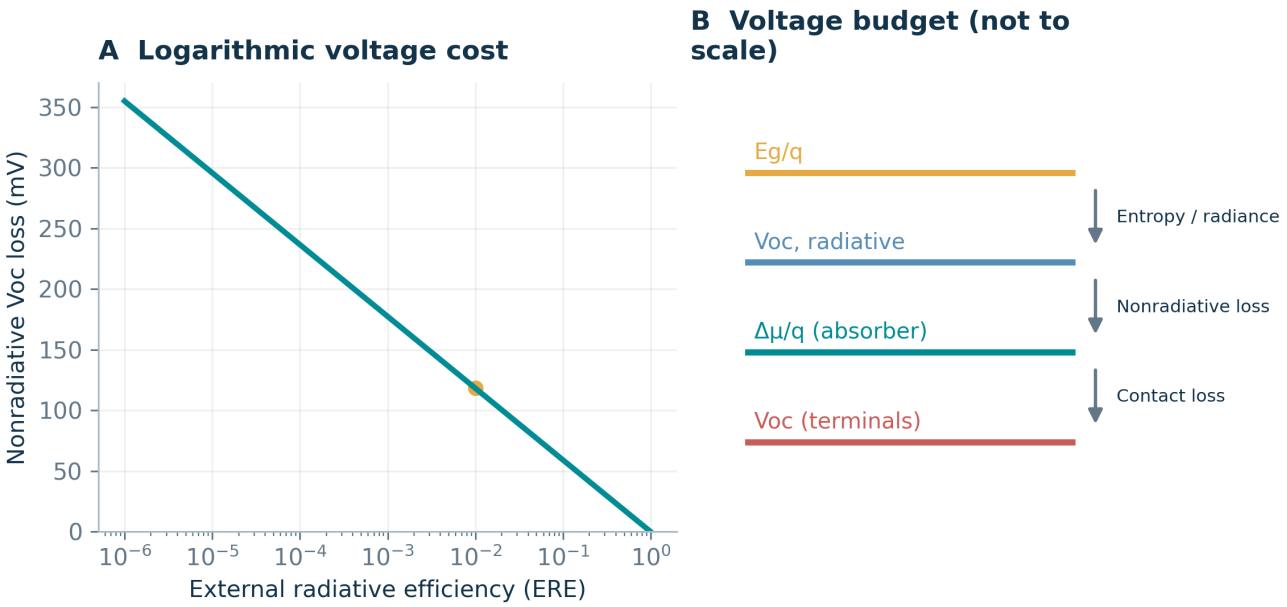


Figure 17. Isolating voltage losses. In panel A, each tenfold decrease in external radiative efficiency results in a loss of approximately 59.16 mV at 298.15 K. Panel B represents the theoretical budget from Eg/q to the terminal voltage; the intervals between the lines are not to scale. If a high quasi-Fermi splitting is observed in the absorber while the terminal Voc is low, the contacts and interfaces need to be investigated further. [H28] [T26]

How should reciprocity be utilized?

Under appropriate linear transport and reciprocity conditions, the relationship between the external optical channels determined by EQE and electroluminescence allows for the calculation of losses within the same framework. The external radiative efficiency (ERE) and the $\Delta V_{oc,nr} = -VT \ln(ERE)$ relationship provide a powerful means of interpretation. However, external emission does not solely reflect the internal recombination probability; photon escape and optical geometry are also important. Therefore, PLQY or ERE values of different optical stacks cannot be directly converted into a defect density ratio without a consistent experimental definition. [H28]

What is the meaning of chemical potential in this context?

Chemical potential describes the free energy cost of adding a particle to the system under appropriate equilibrium conditions; the presence of the term “chemical” does not necessarily imply that a chemical reaction is taking place. For electron and hole populations in an illuminated semiconductor, separate occupancy scales can be used. Quasi-Fermi levels represent these scales. As their separation increases, the device’s ability to perform electrical work increases; however, the actual terminal voltage is also limited by contact losses.

Thermalization is the process where high-energy charge carriers transfer their excess energy to crystal vibrations, bringing them closer to the band edges. This process is not the same as recombination: after thermalization, the charge carriers can still be

collected. A **radiative reference** is an ideal device that recombines only through light emission, under the same optical and electrical assumptions. In a real device, the additional non-radiative channels added compared to this reference are evaluated separately. Thus, the concepts of “energy,” “voltage,” and “additional loss” are not interchangeable. [H25] [H27] [H28]

Common misconceptions and practice questions

The inference that “we calculated an upper limit for high efficiency, therefore the candidate is highly efficient” is invalid. The statement that “the SQ limit constrains all energy converters” is also incorrect; an architecture that goes beyond the single-junction model is evaluated with new assumptions. This does not imply exceeding the conservation of energy.

1. If ERE decreases from 10% to 1%, what is the additional voltage loss at 298.15 K? **Answer:** $VT \ln 10 \approx 59.16$ mV.

2. Why is Eg/q - Voc not simply a direct, non-radiative loss? **Answer:** It also includes unavoidable radiative and entropic contributions.

3. Why does calculating only Jsc not provide the efficiency limit? **Answer:** The operating voltage and the maximum power point, which is determined by recombination, are also required.

Reading path: First, read the assumptions of the original model in [H25], then the spectral tabulation of the same problem in [H26], and finally, the connection between chemical potential and reciprocity in [H27] [H28]. Being able to write the conditions before a numerical limit in a single paragraph is more valuable than memorizing the result.

BOOK I · CHAPTER 09 / HISTORY AND PHYSICS

Multijunction cells: the physics of spectrum splitting

How do two absorbers share the light?

Tandem, a multijunction device in which two cells are used together in the same light path. The top cell typically has a wider band gap; it utilizes sufficiently energetic photons while allowing some lower-energy photons to pass through to the bottom cell. The bottom cell, with its narrower band gap, utilizes some of this remaining light. The layers do not necessarily have to be of equal thickness, nor does each color have to belong entirely to one cell. The actual sharing is determined by wavelength-dependent absorption, reflection, and layer thickness.

The aim of this approach is to mitigate the trade-off between "many photons, low voltage" and "few photons, high voltage" at a single junction. Evaluating high-energy photons at a higher voltage in the top cell can reduce the loss of excess energy as heat. The bottom cell also provides a means of utilizing the light that passes through the top cell. However, additional layers introduce optical and electrical losses. The fact that both cells perform well individually does not guarantee that their power will simply add up when combined.

The number of terminals indicates the type of electrical connection

The **terminal** is the lead connected to the external circuit. In a two-terminal (**2T**) configuration, the sub-cells in a tandem structure are connected in series. In a steady state, the same current flows through both series-connected cells; their voltages add up at this common current. In a four-terminal (**4T**) optical stack, each cell has two leads brought out separately. The power of the two cells can be monitored independently. In return, additional transparent contacts, wiring, and power electronics may be required.

Synthetic example: Two sub-cells with the same area, when operating at a selected common current of 15 mA/cm^2, yield 1.00 V and 0.60 V, respectively. The 2T power density is then $15 \times (1.00 + 0.60) = 24$ mW/cm^2. This is just one operating point; to see if it is the maximum, we must also scan around the common current. If the maximum for the top cell alone is at 18 mA/cm^2 and the maximum for the bottom cell alone is at 16 mA/cm^2, we cannot use these two different currents simultaneously in a series connection.

In a 4T arrangement, the powers at the separate maxima can be added; however, the bottom cell's power must be measured **under light filtered through the top cell**. Adding the bottom cell's power under direct sunlight to the top cell's power counts some photons' energy twice. **Current matching** means bringing the usable currents of series-connected subcells into alignment. Matching can change with clouds, angle of incidence, and spectrum. A single efficiency value under standard conditions and annual energy production therefore address different questions.

Comprehension check: why did the bottom cell become weaker?

A decrease in the bottom cell's current after adding the top cell is not automatically a manufacturing defect; the top cell has used some of the photons. To distinguish whether there is a defect, compare the filtered spectrum, the bottom cell's expected current in that spectrum, and the actual measurement. This separates the natural effect of sharing energy from a new loss mechanism.

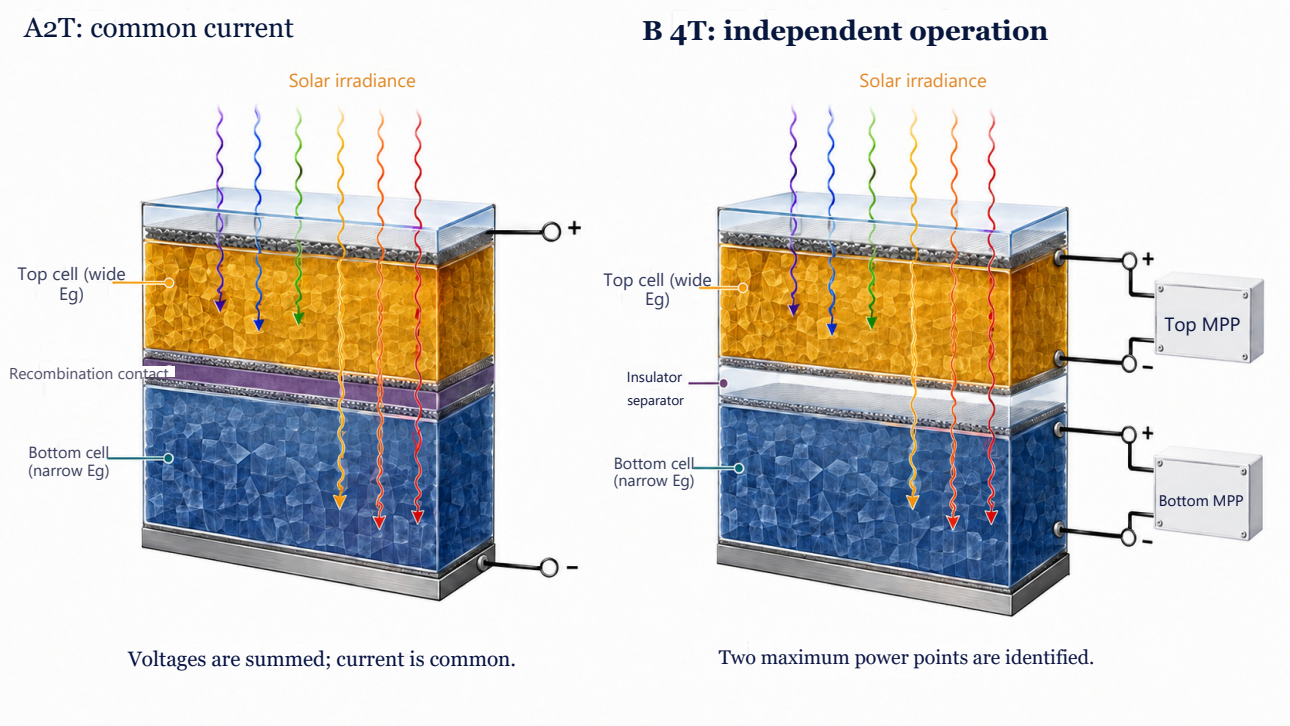


Figure 18. Optical sharing and electrical connection in a tandem. The 2T structure on the left has two external terminals, a common current and summed voltages. In the 4T structure on the right, two optically stacked subcells operate through separate terminal pairs at separate maximum power points. The colored rays are qualitative absorption paths; the illustration is not a spectral measurement. The calculated power comparison is in the following panel. [H29] Conceptual illustration prepared with an image-generation tool; it is not a measurement image.

The power cost of current mismatch.

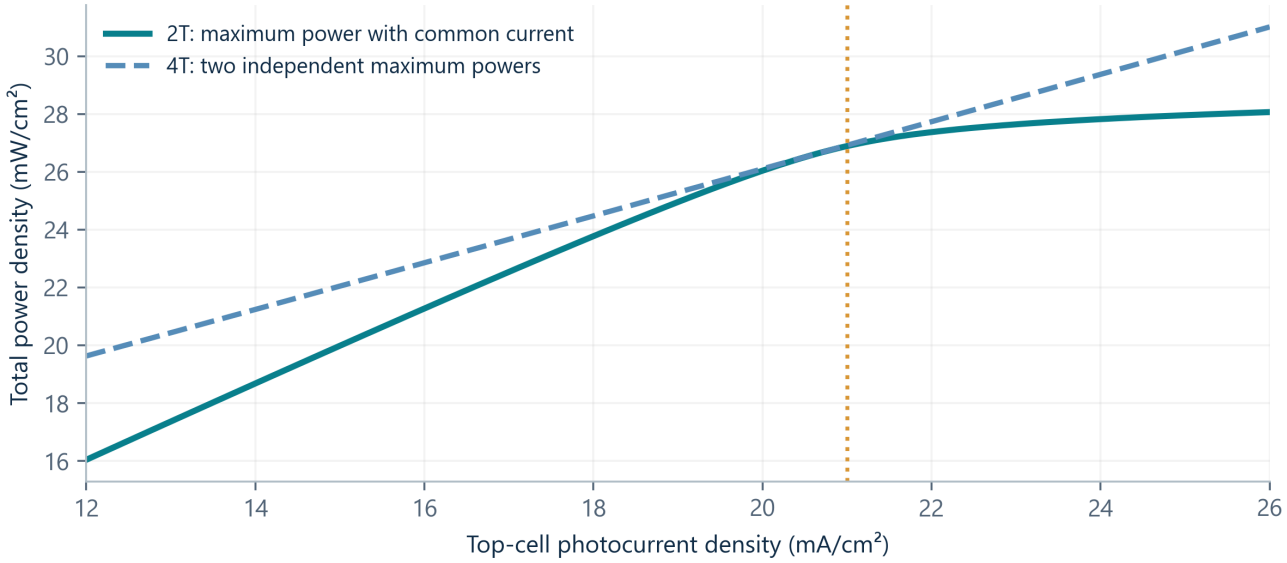


Figure 18 - calculated supplementary panel. Comparison calculated for the same optical input and two ideal diodes. The photocurrent of the bottom cell is kept constant at 21 mA/cm^2; the saturation currents of the subcells are 10^{-13} at the top and 2×10^{-8} A/m^2 at the bottom, and the temperature is set to 298.15 K. The 2T maximum power is determined not only by the smallest short-circuit current but by using both V(J) curves together. [H29]

Breaking the single band gap compromise

In a single-junction device, a low band gap captures more photons but yields a lower voltage and converts excess high-energy photons into heat. A high band gap can provide a high voltage, but it cannot utilize most of the red and near-infrared photons. The purpose of a multijunction device is to distribute this trade-off, inherent in a single absorber, among multiple absorbers that utilize different energy ranges.

The incident light first reaches the top cell, which has a high bandgap, and then the bottom cell. Ideally, the top cell utilizes photons with $E \geq E_{g,top}$, while the bottom cell utilizes photons with $E_{g,bottom} \leq E < E_{g,top}$. In reality, the transparent conductor, transport layers, contacts, and absorber of the top cell also affect the light reaching the bottom cell. The fact that a top cell performs well on its own does not necessarily mean that it is also optically suitable for a tandem configuration.

De Vos's 1980 work is a classic starting point that addresses how, in a tandem detailed balance, the sub-cells can be illuminated not only by the Sun but also by each other's electroluminescence. [H29] This radiative coupling demonstrates why simply summing the results of independent single-junction calculations is not sufficient in all cases.

Two terminals: same current, total voltage

The same current flows through the series-connected sub-cells at the two terminals. The total voltage is given by Vtotal(J) = Vtop(J) + Vbottom(J) - Vconnection(J). The tandem power density is the maximum of the expression p(J) = J Vtotal(J) with respect to the common current density. If J is in A/cm^2, then p is in W/cm^2; the total power is found by multiplying by the common measurement area. Even if the loss of the connecting element is neglected, it is generally not possible for the two cells to reach their respective maximum power points simultaneously.

“Tandem current equals small Jsc” is a useful initial intuition, but it is not a complete operating point model. If effects such as finite shunt, radiative coupling, voltage-dependent collection, and reverse polarization behavior are present, the boundary can differ. The correct approach is to use the voltages of the two sub-cells at the common current. Current matching is not only achieved by selecting the band gaps; thickness and optical reflections also contribute to the same target.

For series connection, the electron flow of one sub-cell and the hole flow of the other must ensure continuity at a suitable interconnection. A tunnel junction or recombination junction performs this electrical function while minimizing light loss. When a new interconnection material is selected, optical transparency, contact resistance, chemical stability, and processing temperature are considered together.

Four terminals: independent power tracking

In a four-terminal configuration, the two sub-cells are electrically independent. The ideal total power density is given by ptotal = max(VtopJtop) + max(VbottomJbottom), and this is multiplied by the common area for the total power. However, the bottom cell’s current-voltage curve must be measured under light that has passed through the top cell. Simply adding the efficiencies of the two cells, each measured separately under full AM1.5G illumination, is equivalent to counting the same photons twice.

Independent power tracking provides flexibility in current mismatch; in return, it may require additional contacts, transparent electrodes, wiring, and power electronics. These can represent minor losses in some devices, but significant losses in others. Determining which topology is better involves comparing not only the cell efficiency but also the total area, optical stacking, and electrical collection protocol.

Three-terminal architectures are also possible. Common contacts or different connection schemes alter the current and voltage constraints. The term “three terminal” alone does not define the measurement protocol; it must be specified which terminals are common and how the two power outputs are used. This area is a research topic that requires careful extension of the standard single-diode concept.

Band gap selection and process compatibility

An ideal spectral matching may suggest a range of band gaps for an efficient top cell. However, the actual optimum is influenced by the top cell's voltage deficit, absorption strength, the optical response of the bottom cell, spectral variation, and manufacturing losses. Selecting a material solely because it is close to the ideal tandem band gap ignores recombination and manufacturability costs.

If the bottom cell in a monolithic stack is fabricated first, the subsequent processing of the top cell should not degrade it. High temperatures can alter doping profiles; solvents can damage the underlying organic or inorganic layer; plasma or sputtering can create interface defects. Mechanical joining can alleviate some of these constraints, but it introduces new optical gaps, adhesion, and thermal expansion issues. Treating the material selection and process sequence as separate entities would be a mistake.

Therefore, the tandem design involves a dual-linked optimization: an optical system that shares the spectrum and an electrical system that operates within the same production chain. It must be demonstrated numerically whether the gain in one system outweighs the loss in the other. Identifying the most sensitive parameters before a broad parameter sweep reduces unnecessary simulations.

Worked example: the cost of a common current

Illustrative example. Consider a top cell with an independent maximum power point of 1.00 V and 18 mA/cm^2, and a bottom cell with 0.60 V and 20 mA/cm^2, under filtered, real-world stacking conditions. The ideal total power at the four terminals is 18 + 12 = 30 mW/cm^2, which corresponds to an input of 100 mW/cm^2 at 30%. In this calculation, both curves are defined under the same optical stacking conditions.

Consider a simple example with two terminals, where at a common current of 18 mA/cm^2, the voltage of the top cell is 1.00 V, and the voltage of the bottom cell is 0.61 V. The power would be 18 × 1.61 = 28.98 mW/cm^2. This number is not the exact solution for the real optimum; the actual J-V curves should be scanned at the common current. However, it simply demonstrates how mismatch can lead to power loss. If there is an additional 20 mV drop in a series interconnection, the loss at that point is 0.018 A/cm^2 × 0.020 V = 0.36 mW/cm^2, which is 0.36 absolute percentage points of efficiency.

In the same example, if the top optical structure reduces the current of the bottom cell from 20 to 17 mA/cm^2, the initial problem is reversed: now the bottom cell is the limiting factor. Therefore, simply stating that a layer "transmits" 95% is insufficient; it is crucial to determine at which wavelengths 5% is lost. Even if the loss in a narrow band beneficial to the bottom cell represents a small fraction of the total optical power, it can disrupt the current matching.

Varying spectrum and actual energy generation

Two-terminal cells that are perfectly matched in the laboratory may not maintain the same matching in the morning or in humid air. Water vapor, aerosols, and the angle of incidence alter the spectrum. For annual energy production, a time-dependent spectral irradiance, temperature, and power tracking calculation is required instead of a single AM1.5G point. High efficiency under standard test conditions are still valuable, but they do not fully explain the annual kilowatt-hour production.

Radiative coupling can mitigate certain mismatches: some of the photons emitted through recombination in the top cell can be absorbed in the bottom cell. This is not free energy generation; it is a transfer from the charge carrier and photon balance of the top cell to the bottom cell. Without specifying the direction, angle, and efficiency with which this occurs, it is unreliable to simply carry over a coupling coefficient to every tandem cell.

Why isn't the tandem power equal to the minimum current multiplied by the sum of Voc?

For each of the two ideal sub-cells, we can write V(J) by reversing the current:

$$V_i(J) = n_i V_T \ln\left[1 + \frac{J_{\mathrm{ph,i}} - J}{J_{0,i}}\right]. \tag{I.9.1}$$

Here, the symbol ni denotes the diode ideality factor of sub-cell i in this equation; it must not be confused with intrinsic carrier density. In a 2T device, the same J passes through both cells, and the total voltage is V1(J) + V2(J). The optimum power is the maximum of this sum multiplied by the current:

$$p_{2T} = \max_J \{J[V_1(J) + V_2(J)]\}. \tag{I.9.2}$$

Multiplying the minimum Jsc by the total Voc establishes an upper rectangle; at the actual maximum, the voltage of each sub-cell is less than Voc. As current mismatch increases, it limits the power curve of the weaker cell; however, the operating voltage of the cell with excess current also changes. Therefore, calculating the loss solely as the "difference between the two currents" is insufficient.

The 4T comparison optimizes the powers of the top and bottom cells independently under the same optical configuration. If only the electrical freedom changes, the sum of the independent maxima cannot be smaller than the maximum under a common-current constraint. However, transparent contacts added to a real 4T stack can introduce parasitic absorption. When different optical structures are used,

automatic superiority of 4T is not mathematically guaranteed. This distinction is the most important check in an architectural comparison.

When the spectrum changes, not only the total irradiance changes, but also the ratio of high-energy to low-energy photons. Two cells that match in a laboratory spectrum may become mismatched due to changes in cloud cover, air mass, and seasonal variations. Therefore, in a tandem design, optimizing the annual energy yield and determining a single STC (Standard Test Condition) point are separate problems. From a research perspective, a robust approach is to first validate the standard point and then model energy generation with location- and time-specific spectra.

Common misconceptions and practice questions

"If I add the efficiencies of two single-junction cells, I will obtain the tandem efficiency" is incorrect. It is also not true that "more junctions always result in a better module"; the ideal thermalization gain is offset by additional optical and electrical losses. A multi-junction configuration modifies the detailed balance assumption for a single-junction cell; it does not violate thermodynamics.

1. In series-connected sub-cells, which quantity is equal, and which is summed? **Answer:** The current is the same, and the voltages are summed with appropriate signs.

2. Under which illumination condition is the four-terminal efficiency sum meaningful? **Answer:** It is meaningful when the top and bottom cell powers are in the same optical stack, and the bottom cell is illuminated with filtered light, with a common incident area/power denominator.

3. At a common current density of 20 mA/cm^2, how much power is lost through a 50 mV interconnection loss? **Answer:** 1 mW/cm^2; one absolute percentage point of efficiency at an input of 100 mW/cm^2.

Reading path: First, examine the historical origins of the tandem detailed balance model ([H29]), followed by the physical classification of advanced concepts ([H30]). For each tandem proposal, clarify the optical stack, terminal circuit, common area, and maximum power collection method using four separate diagrams or equations.

BOOK I · CHAPTER 10 / MATERIALS AND DEVICES

Crystalline silicon: transforming a good semiconductor into a good product

Reading a silicon cell layer by layer

Silicon, represented by the symbol Si, is an element; the silicon dioxide found in sand is not the same as electronic-grade silicon. To manufacture cells, unwanted impurities are reduced, a crystal is formed, and the crystal is cut into very thin slices. This slice is called a **wafer**. A **single crystal** is characterized by the same atomic arrangement over a large volume. In a **polycrystalline** material, there are differently oriented regions, i.e., grains. The electrical effect of the boundaries where the grains meet depends on the structure and impurities.

Let's start by examining a cross-section of a cell, beginning from the side where light enters. On top, there may be a thin coating to reduce reflection. The surface of the silicon can be textured with small pyramids to ensure that the reflected light strikes the surface again. Inside, doping and contact layers establish selective charge collection. Metal fingers carry the collected current to thicker conductive lines. On the back, there is passivation and electrical connection. These are not merely stacked materials; each one is a function that manages a separate loss.

Different questions behind the abbreviations

PERC refers to a cell family that passivates a large portion of the rear surface and establishes electrical contact through local openings. **TOPCon** is a contact approach that combines passivation with charge carrier transport using very thin oxide and doped silicon layers. **SHJ** or **HJT** is a hetero-junction approach that involves forming thin silicon layers with a different structure on crystalline silicon. **IBC** involves placing electron and hole contacts on the rear surface in the form of interweaving strips. The first three approaches primarily focus on contact and surface physics, while the last one focuses on the placement of contacts. In a given architecture, several of these concepts can be used together.

Hypothetical thought experiment: If we reduce the area shadowed by the front metal pattern from 4% to 2%, more light can enter. However, if the same metal is thinner, its resistance may increase. The resulting optical gain can be offset by electrical losses. Therefore, we cannot determine whether the process is effective solely from the surface photograph or the short-circuit current; voltage, fill factor, and total power are

required. Below, we will connect the manufacturing steps to this competition between gain and loss.

A **reference cell** is a control sample produced from the same basic process, used for comparison to assess improvement. A **lot** is a group of samples that share a common production history. Instead of simply selecting the best cell, monitoring the lot distribution reveals whether the successful idea represents a repeatable process.

Comprehension check: what did the new name change?

The term “back contact” for a cell does not, by itself, explain which semiconductor or passivation layers are used. Draw a cross-section and answer the following three questions: where does the light enter, to which contact does each charge carrier go, and where can the metal encounter the wrong charge carrier? You will then have translated the architectural name into its working mechanism.

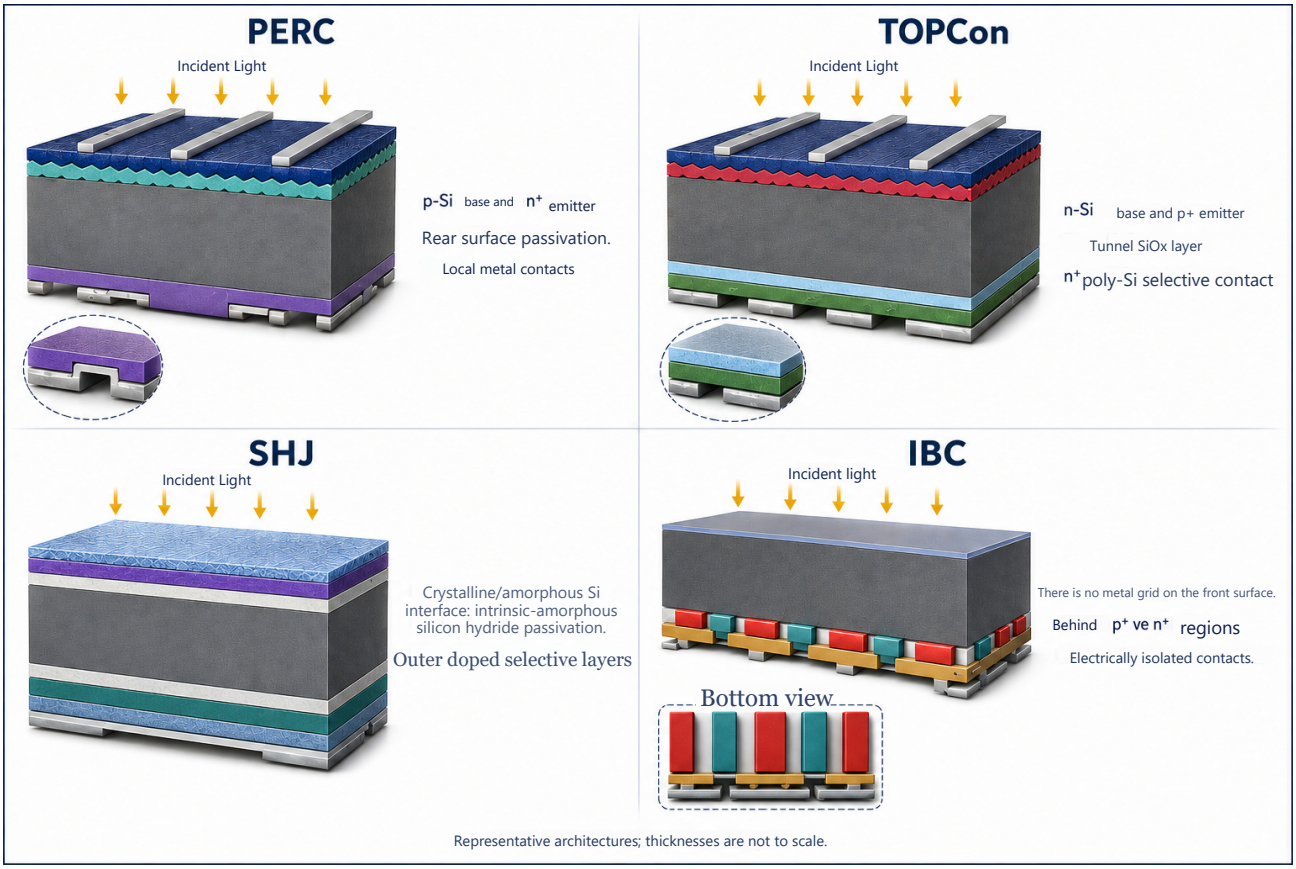


Figure 19. Cross-sections of four common silicon design concepts. Thicknesses are not to scale. PERC highlights rear passivation, TOPCon the tunnel oxide contact, and SHJ the amorphous/crystalline heterostructure. IBC describes the interdigitated arrangement of contacts on the rear and can be combined with other contact physics. The diagrams represent illustrative architectures. [T01] [T02] [T03] [T04] Conceptual illustration prepared with an image-generation tool; it is not a measurement image.

What is silicon's primary advantage?

A photovoltaic technology is not simply composed of a material that absorbs light well. Purification, crystal growth, surface cleaning, doping, passivation, metallization, interconnection, and years of operational experience must all be addressed together. This is the major lesson that silicon teaches researchers: the electronic properties of the material and the manufacturing ecosystem reinforce each other. Due to its indirect band gap, it absorbs light less efficiently than some direct band gap semiconductors; nevertheless, high-quality, large-area wafers, processable surface chemistry, and highly advanced process control create a powerful synergy.

In a silicon cell, the room-temperature band gap of approximately 1.12 eV means that a significant portion of the energy of visible photons is converted into heat. Photons with energy below the band gap do not contribute to ideal interband absorption. These fundamental losses cannot be eliminated by better passivating the surface. In contrast, additional losses caused by defects, surfaces, and contacts can be reduced through engineering. The researcher must first determine which losses are thermodynamic, which are material-related, and which are production-related.

It is beneficial to examine the manufacturing process from a physical perspective. Purification reduces metal impurities that trap charge carriers. Crystal growth controls grain boundaries and dislocations. Wafer cutting creates usable area but can also generate cutting losses and microcracks. Surface texturing facilitates light entry into the cell. Doping determines the majority charge carrier and the junction. Passivation reduces electronic states on the surface. Metallization efficiently conducts electric current outwards. Each process leaves an initial state for the subsequent process; therefore, optimizing the processes as independent units often fails.

PERC, TOPCon, SHJ, and IBC do not refer to the same thing

PERC refers to the passivated emitter and rear cell approach. Protecting most of the rear surface with a dielectric and opening electrical contacts only in specific areas limits the recombination caused by direct metal contact. The cell developed by Blakers and his colleagues in 1989 is a significant early example of this historical development. The conceptual leap here is the inclusion in the design of the understanding that, after a good junction is formed, the rear surface also becomes an effective source of loss. [T01]

TOPCon is a family of passivating contacts that rely on the interplay of a very thin oxide and a doped silicon layer. The oxide surface electronically passivates; appropriate doping and band bending facilitate the transport of one type of charge carrier while suppressing the other. In the 2014 work by Feldmann et al., it was demonstrated that good current transport and low contact recombination can be combined in the same

device. The actual thickness, continuity, local defects, and thermal history of the oxide are important; it is an oversimplification to explain transport in all TOPCon contacts solely as tunneling through an ideal, uniform barrier. [T02]

SHJ is a heterojunction that combines crystalline silicon with thin, hydrogenated amorphous or suitable nanocrystalline silicon layers. The thin intrinsic layer provides passivation, and the doped layers support charge carrier selectivity. An advantage of low-temperature processes is their ability to preserve the lifetime of a good silicon wafer. On the other hand, light loss, transparent conductive oxide resistance, contact resistance, and the temperature budget collectively impose limitations. A 2023 study showed that improving the electrical properties of the nanocrystalline silicon hole contact, without modifying the absorber, resulted in performance enhancement. This indicates that the contact layer is not a passive component. [T04]

IBC refers to the arrangement of electrodes: the electron and hole contacts are located on the rear surface in an interdigitated finger pattern. Front metal shading is eliminated; in return, the rear requires the isolation and patterning of both polarities, as well as the collection of charge carriers over horizontal distances. IBC is not a specific absorber chemistry or a single passivation method; it can be combined with SHJ or other selective contacts. The 2017 study by Yoshikawa et al. provides an original example of combining SHJ with a rear contact topology. The large-area, lifetime, optical, and resistance analyses presented in the publication demonstrate why technology comparisons should not be reduced to a single efficiency number. [T03]

Design	Principal loss targeted	Trade-off to manage alongside it
PERC	Rear surface recombination.	Local contact resistance and patterning.
TOPCon	Selectivity loss at the metal contact.	Oxide integrity, absorption in the doped layer, thermal budget.
SHJ	Surface and contact recombination.	Thin-film optics, TCO, and low-temperature metallization.
IBC	Front metal shadowing	Rear patterning, lateral collection and insulation

Why does a lifetime calculation change the architecture?

A simple model for a thin film with approximately uniform excess charge carrier density and equivalent surfaces is as follows:

$$\frac{1}{\tau_{\text{eff}}} \approx \frac{1}{\tau_{\text{bulk}}} + \frac{2S}{W}. \tag{I.10.1}$$

Here, τ_{eff} represents the effective charge carrier lifetime, τ_{bulk} represents the bulk lifetime, S represents the surface recombination velocity, and V represents the wafer thickness. This expression is not strictly valid for every doping and injection level; it serves to illustrate the magnitude of surface limitation. Consistent units must be chosen: if S is in cm/s, then V must be in cm.

Solved example. For a wafer with a thickness of 150 µm and a bulk lifetime of 2 ms, a value of $W = 0{,}015$ cm is obtained. For a surface recombination velocity of cm/s on both surfaces, the total recombination rate is $500 + 667 = 1167$ s^{-1}, and the effective lifetime is approximately 0.857 ms. When the surface recombination velocity is cm/s, the recombination rate is $500 + 6667 = 7167$ s^{-1} and the lifetime is 0.140 ms. The same quality crystal can exhibit more than six times the difference in effective lifetime solely due to the surface. Purchasing a purer crystal will not yield the expected results if the surface issue is not addressed.

Thinning the wafer reduces raw material consumption; however, it also increases the surface term with the same S value and makes the absorption of long-wavelength light more difficult. Therefore, thinning should be considered in conjunction with improved passivation and light trapping. If the mechanical breakage rate also increases in the thin wafer, the silicon savings per kilogram may not translate into savings per watt of marketable output.

How do you interpret the results of a cell development experiment?

If a new surface treatment increases the V_{oc} value while decreasing the fill factor, it suggests that recombination has decreased, but the transport barrier or series resistance may have increased. Short-wavelength EQE loss may indicate parasitic absorption in the front layers, while long-wavelength loss may indicate insufficient optical path, issues with the back surface, or bulk collection problems. These are diagnostic hypotheses and not conclusive evidence on their own. Reflection, lifetime, dark, and light electrical measurements should be interpreted together.

In silicon research, success often comes not from adding a new element, but from accurately identifying the source of existing losses. If the area-normalized contact resistance, saturation current density, sheet resistance, and optical absorption are measured separately, it can be determined which modification is truly beneficial. In addition to reporting the performance of the best cell, the distribution of cells produced using the same process should also be reported.

Relating the manufacturing steps to their physical functions

The production of a crystalline silicon cell involves more than just creating a p-n junction. The purity of the initial crystal and crystal defects determine the bulk lifetime. The wafer thickness affects material consumption and mechanical strength. Surface preparation and texturing alter reflectivity and the path of light, while also increasing the surface area. Doping and junction formation control charge carrier selectivity and lateral resistance. Passivation layers reduce surface recombination. Metallization should provide low resistance with minimal optical shadowing. Because each step can negate the gains achieved in the previous step, process integration becomes a distinct area of research.

In a PERC structure, the purpose of rear passivation is to reduce the extent to which the metal turns the entire rear surface into a recombination pathway. Local openings maintain electrical contact. In TOPCon, heavily doped polycrystalline silicon with a very thin oxide aims to combine good passivation with carrier transport. In SHJ, a thin intrinsic amorphous silicon layer on the crystalline surface and doped selective layers combine high electronic quality with a low-temperature contact structure. In IBC, moving the front metal to the rear can reduce shading; however, the insulation of the rear p and n contacts and the lateral movement of charge carriers become important. These are not mutually exclusive, comprehensive technology names. [T01] [T02] [T03] [T04]

Why is the metal grid a problem of optimization?

Let s be the distance between the front grid fingers, and Rsheet be the sheet resistance of the surface layer. In a one-dimensional model where a uniform vertical current density J flows laterally to the fingers on both sides, the average ohmic power loss between the fingers is approximately J^2 Rsheet $s^2/12$ per unit area. If the finger width is w, then the shaded fraction is approximately w/s. One increases as s increases, and the other decreases:

$$p_{\text{yanal}} \simeq \frac{J^2 R_{\text{sheet}} s^2}{12}, \qquad f_{\text{golge}} \simeq \frac{w}{s}. \tag{I.10.2}$$

In this simplified derivation, current crowding, the longitudinal resistance of the finger metal, and contact resistance have been neglected. Nevertheless, it demonstrates the basic design principle: a very sparse grid, which aims for zero shading, amplifies lateral transport loss. A very dense grid, on the other hand, blocks light and consumes more metal. For J = 0.04 A/cm², Rsheet = 80 Ω/square, and s = 0.15 cm, the lateral loss is approximately 0.24 mW/cm². If s is doubled, the same model yields 0.96 mW/cm². This

calculation predicts the geometrical effect on the electrical performance before production.

Chemical passivation and field effect are not the same intervention

On the surface, there are atoms with different bonding configurations compared to those within the crystal. The electronic states created by these atoms can capture electrons and holes, thereby facilitating recombination. **Chemical passivation**, for example, reduces these active states by completing the appropriate bonds. **Field-effect passivation**, on the other hand, alters the charge distribution near the surface, reducing the likelihood of two charge carriers being present together in the same loss region. A coating can exhibit both effects; however, knowing only its thickness does not indicate which effect is dominant.

In the figure, **Al_2O_3** represents aluminum oxide; **SiN_x:H** represents hydrogenated silicon nitride; and **a-Si:H** represents hydrogenated amorphous silicon. “Amorphous” indicates the absence of a long-range, ordered crystalline structure. “i” denotes an approximately intrinsic layer, while “n” and “p” indicate the respective doping types. These designations do not necessarily mean that the exact same recipe is used in every cell; they allow for the identification of layer families used for passivation, selectivity, and optical function. [T01] [T02] [T03]

Narrowing the spacing between the metal fingers can shorten the path along which the current flows on the surface; however, it increases the area of the surface covered by the metal. The **sheet resistance** of the surface is the parameter that determines the voltage drop in this lateral current flow. A comparison made with the same area, illumination, and temperature using a control cell shows whether the passivation gain is offset by the metal shadowing or conduction loss.

Self-assessment

1. If the wafer thickness is halved, and the surface velocity remains unchanged, how does the surface-related recombination term change? **Answer:** It doubles; a thinner wafer does not automatically mean a better cell.

2. Can an IBC cell also be an SHJ cell? **Answer:** Yes. IBC defines a specific contact layout, while SHJ defines a heterojunction and passivation approach; they are not mutually exclusive.

3. If a process increases J_{sc} by 1% while V_{oc} and FF remain constant, how much does efficiency increase? **Answer:** It increases by 1% relative. If the initial value is 24%, the new value is 24.24%; the absolute increase is 0.24 percentage points.

BOOK I · CHAPTER 11 / MATERIALS AND DEVICES

Thin films: low material consumption, intense interface physics

What does “thin film” mean, and what does it not mean?

In a **thin-film cell**, the light-absorbing material is formed as a thin layer on a substrate, which can be glass, metal, or a polymer. The substrate is referred to as the **substrate**. Although the substrate can be thick, the active absorber can be very thin; “thin film” does not always imply a flexible or overall thin module. The extent to which the material absorbs light per unit thickness determines the required effective thickness.

The **absorption coefficient** α indicates how quickly the light intensity decreases through the material. In a non-reflective, homogeneous, and single-pass model, the absorbed fraction is 1 - exp(-αd), where d is the thickness, and αd must be dimensionless. **Synthetic example:** for α = 10^{4} cm^{-1} and d = 1 µm = 10^{-4} cm, αd = 1, so the absorption is approximately 63%. In the same model, 3 µm yields approximately 95%. However, increased absorption does not necessarily mean that all the generated charge carriers will reach the contact. The transport distance and recombination still impose limitations.

Translating the material name into chemistry and interface terms

CdTe is cadmium telluride; in its ideal form, the cadmium and tellurium atoms are present in a one-to-one ratio. **CIGS** is an abbreviation for a family of compounds containing copper, indium, gallium, and selenium; the notation $Cu(In,Ga)Se_2$ indicates that indium and gallium can share the same type of crystal lattice sites. The specific ratios chosen affect the band gap and process behavior. In **amorphous silicon**, the atoms are not as regularly arranged over long distances as in a crystal; some bond defects can be mitigated by hydrogenation. These three examples can be found in the same “thin film” production group, but they do not have the same defect chemistry.

The band edges of the film and the adjacent layer may differ. This difference is called **band alignment**. A small barrier for electrons can sometimes reduce loss in the wrong direction, while a large barrier stops beneficial transitions. In the staircase analogy, it is not only the height of the step that matters, but also who passes in which direction. Without separating the energy axis from the physical position axis in the diagram, it cannot be said that “the upper band is better.”

The **window layer** is the layer that is expected to transmit a significant portion of the light to the absorber; however, it is not completely optically lossless. The **buffer layer**

assists in the chemical and electrical matching of the interface. The names indicate their function; their actual contributions are measured depending on the thickness, composition, and processing history.

Comprehension check: Why isn't using less material always cheaper?

As the absorber layer becomes thinner, material consumption may decrease, but this can increase the cost due to challenges in achieving a homogeneous coating, multilayer contacts, low manufacturing yield, or difficult encapsulation. To transition from "a few grams" to the outcome of "cheap electricity," the accepted wattage, process cost, and service life must be calculated together.

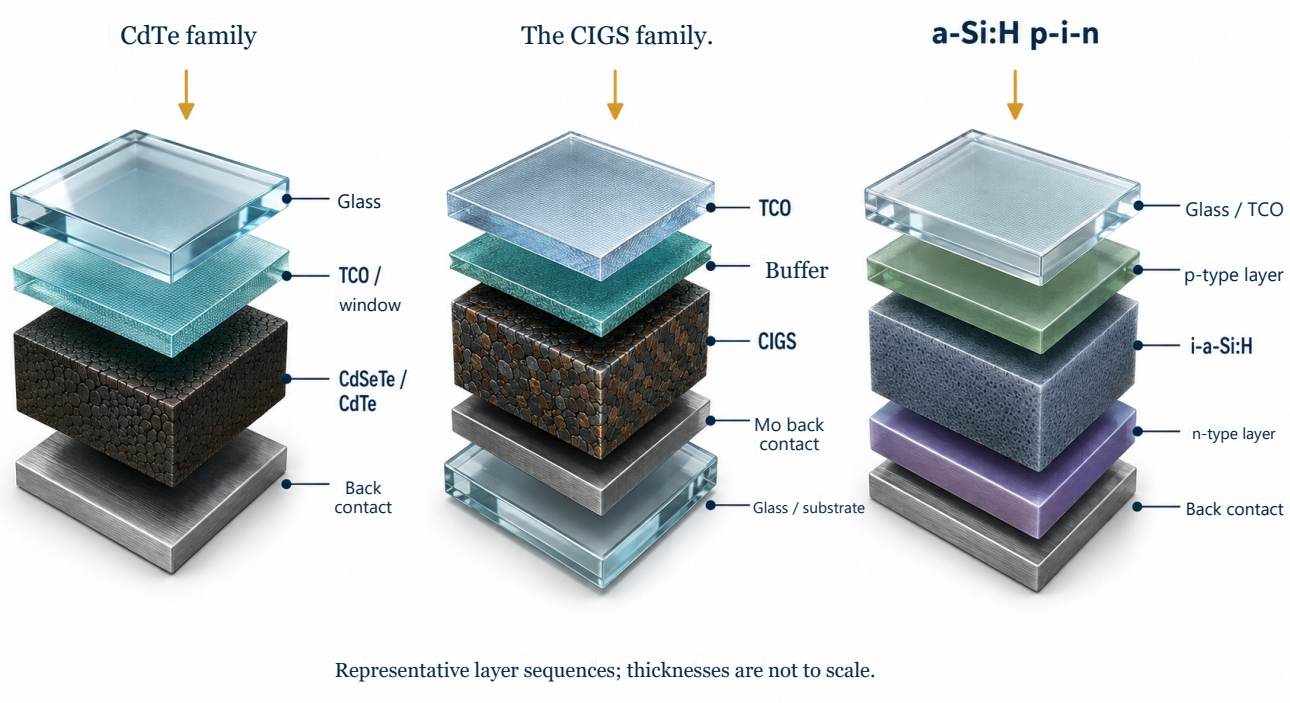


Figure 20. Typical layer sequences for CdTe, CIGS, and amorphous silicon families. The arrow indicates the direction of incident light. The window, buffer, absorber, and back contact have different functions. Thicknesses are not to scale; alternative buffer layers and contacts are possible. [T05] [T06] [T07] Conceptual illustration prepared with an image-generation tool; it is not a measurement image.

Being thin is not an advantage in itself

The thin-film approach involves fabricating a semiconductor on a large supporting substrate, capable of absorbing light over a few micrometers or less. This can reduce material usage, and the cells can be interconnected using lasers. However, as the volume decreases, the importance of interfaces, grain boundaries, and local thickness variations increases. The same average chemical composition can yield different devices with different growth histories.

The Beer-Lambert relation in the absorption physics section provides the initial thickness scale. Measured optical constants and the complete layer stack are required for interference, reflection, scattering, and electrode loss calculations.

Solved example. If the absorption coefficient at a certain wavelength is $\alpha = 10^{4}$ cm^{-1} and the thickness is $d = 2$ μm, then = 2 and the absorption is approximately 86.5%. When the absorption coefficient is 10^{3} cm^{-1} at the same thickness, only 18.1% is absorbed. The statement "Two micrometers is sufficient" is meaningless without specifying a spectrum. Increasing the thickness can improve absorption; if the charge carrier collection length is short, the additional charge carriers generated will recombine.

CdTe: The convergence of band gap engineering and defect chemistry

CdTe is a strong absorber and a direct bandgap semiconductor. Many devices utilize a sequence of glass, transparent conductor, window or buffer layer, absorber, and back contact. The front layer is not merely a layer that transmits light; it determines band alignment, junction recombination, and undesirable current paths. Having a suitable work function for the back metal is not sufficient on its own; surface stoichiometry, intermediate phases, and element migration over time can alter the contact behavior.

Selenium alloying is an instructive example in the context of CdTe. Fiducia and colleagues, in their 2019 study, observed stronger luminescence and a longer charge carrier diffusion length in selenium-containing regions. The result was not only attributed to increased photon absorption due to the reduction in band gap; the contribution of defect passivation was also found. The research methodology that can be derived from this is to separately measure the optical and electronic effects of compositional changes. [T05]

Chemical activation processes can alter grain boundaries and defect populations. The rule "larger grain is better" is not absolute. The recombination activity of a grain boundary arises not only from its geometric size but also from its chemical composition and electrostatic structure. A large grain with low defects but poor contact can perform worse than a network of well-passivated small grains. Similarly, if doping increases the hole density while creating new deep defects, the voltage gain will be limited.

CIGS: composition, location, and history are all important together

In the chalcopyrite family Cu(In,Ga)Se_2, abbreviated as CIGS, the indium/gallium ratio adjusts the band gap. The same average ratio can be produced with different profiles along the depth. A conduction band that increases towards the back surface can reduce the loss of minority electrons as they travel to and are lost at the back contact; however, an increase in the wrong location can turn into a collection barrier. To draw a band diagram, it is not enough to know only the band gap profile; it is necessary to know how the change is distributed between the conduction and valence bands.

A common approximate representation for the alloy range.

$$E_g(x) = (1-x)E_{g,A} + xE_{g,B} - bx(1-x) \tag{I.11.1}$$

where x is the alloy ratio, $E_{g,A}$ and $E_{g,B}$ are the band gaps of the end compounds, and b is the bowing parameter. **Illustrative example:** If $E_{g,A} = 1{,}01$ eV, $E_{g,B} = 1{,}68$ eV, $b = 0{,}15$ eV, and $x = 0{,}30$, then $E_g = 1{,}1795$ eV. These are example parameters; in a real case, the composition, temperature, and ordering state must be measured.

Small amounts of alkali elements strongly affect the performance of CIGS; however, their effects cannot be explained by a universal statement such as “doping is always beneficial.” The 2018 study by Colombara et al. revealed that sodium can alter the mutual diffusion of indium and gallium. When interpreting the alkali effect, it is necessary to monitor not only the final charge carrier concentration but also how the composition profile changes during growth. [T06]

The CIGS researcher also considers the copper deficiency on the surface, possible secondary phases, buffer layer conformity, and the back contact interface. Forcing all elements to fit into a single average EDS count results in a loss of important information. Depth profiling, in-grain/grain boundary differentiation, and measurements in different areas are necessary. The use of indium and gallium also represents a separate supply issue, distinct from the premise that “thin films use less material.”

Amorphous silicon: from initial performance to stable performance

In hydrogenated amorphous silicon, there is no long-range crystalline order. The spreading of electronic states at the band edges and localized defects results in different transport properties compared to crystalline silicon. Hydrogen passivates some of the dangling bonds. Most instructional devices are explained using a p-i-n design, where highly defective doped regions are kept thin, and light is primarily absorbed in the intrinsic region; the electric field assists in the collection of charge carriers.

In their seminal 1977 work, Staebler and Wronski demonstrated reversible changes in conductivity under illumination. This historical finding revealed early on that a measurement taken on the first day might not represent the operational performance. Access to the publisher's full text of the source was not possible during this review; the historical finding was limited to the original author's subsequent explanation and the bibliographic record of the original article. [T07] [T33]

In this class, increasing the film thickness can provide more absorption but may also create collection and stability issues. Microcrystalline or multijunction combinations can alter these balances; however, even though they are all referred to as "silicon," a-Si:H, thin-film microcrystalline silicon, and wafer-based c-Si results should not be placed in a single category. Initial efficiency, light-induced stabilized efficiency, cell area, and module area should be specified separately.

Reading band alignment with the correct signs

In a heterojunction, the conduction and valence bands of the two materials do not necessarily need to be continuous. In the direction of electron transfer from the absorber to the electron-selective layer, the raising of the conduction band can create an energy barrier. A very large barrier limits charge carrier transport at low temperatures or high currents; a distortion can be observed in the J-V curve. Conversely, a large drop in the reverse direction can increase charge carrier densities and the probability of recombination at certain interfaces. Proper alignment cannot be reliably determined simply by subtracting the work functions of the free surfaces.

When an interface is formed, dipoles, chemical bonds, trap charge, and Fermi level equalization can alter the bands. Therefore, an energy level diagram serves as an initial hypothesis. Surface-sensitive measurements such as UPS/XPS, controlled thickness series, and temperature-dependent device data are interpreted together. In photoemission measurements, explicitly stating the energy reference through surface preparation is particularly important. [R07]

In CIGS, the composition gradient allows the band gap to vary with depth. However, the extent to which the increase in band gap occurs in the conduction band versus the valence band determines the charge carrier mobility. Simply plotting Eg(x) to infer the direction of the electric field is insufficient. In the CdTe family, alloying, back contact, and defect chemistry can change simultaneously. When a process alters both the absorption edge and the dopant concentration, as well as the contact resistance, a deconvolution experiment is required to attribute the improvement to a single mechanism. [T05] [T06]

The grain boundary does not always play the same role

In a polycrystalline film, the grain boundary is not simply a “bad region.” The composition, local charge, and potential at the boundary can alter the arrival of charge carriers at that location. Large grains observed on the surface do not guarantee the same crystal structure or low trap density throughout the entire film thickness. A more useful question is under what conditions the boundaries lead to charge carrier loss. Spatially resolved PL, collection maps such as EBIC, and chemical mapping can be used to determine whether the boundary in the topography coincides with the electrical effect at the same location.

Self-assessment

1. Why doesn’t EQE necessarily have to be 90% when absorption is 90%? **Answer:** Some of the absorption may occur in non-functional layers; some of the charge carriers generated in the absorber may recombine without being collected.

2. Why can two CIGS films with the same average Ga ratio produce different voltages? **Answer:** The depth profile, defects, secondary phases, interface band alignment, and alkali history may differ.

3. If the performance decreases under illumination but partially recovers in the dark, how should the measurement be reported? **Answer:** The light/dark cycle, temperature, electrical load, and measurement times should be specified; the recovery should not be presented as a permanent lifetime gain.

BOOK I · CHAPTER 12 / MATERIALS AND DEVICES

III-V and multijunction cells: the cost of spectral splitting

Where does the name III-V come from?

The term III-V refers to semiconductors formed by elements from the traditional III and V groups of the periodic table; the current group numbers are 13 and 15. **GaAs** is gallium arsenide; **InP** is indium phosphide. These are compounds with specific crystal and optical properties. An **alloy** can be formed by multiple elements sharing the same crystal lattice site; the composition ratio is used to adjust the band gap.

These materials provide very strong light absorption and high-quality emissive processes in many designs. However, suitable electronic properties are not the only requirement for production. **Epitaxy** refers to the growth of a crystal layer that follows the crystal structure of the underlying crystal. If the atomic spacing of the underlying lattice differs from that of the overlying lattice, **lattice mismatch** occurs. A very thin layer can accommodate this difference through elastic strain; depending on the thickness and conditions, linear crystal defects called dislocations may form.

Light sharing and lattice matching are separate design problems

In a three-junction cell, the top, middle, and bottom absorbers utilize different energy ranges. The **tunnel junction** is a highly doped semiconductor region that establishes an electrical connection between the series-connected subcells. Quantum tunneling is the phenomenon where a particle can be found on the other side of a barrier even when its energy is insufficient to overcome the classical energy barrier. This connection is expected to not impede current flow and to minimize unnecessary light absorption. Therefore, the intermediate layer is not merely a connecting line in the diagram.

Synthetic example: Let the lattice parameters of two materials be 5.65 and 5.70 angstroms. One angstrom is 10^{-10} meters. The relative difference (5.70 - 5.65)/5.65 ≈ 0.885%. This seemingly small number can be significant in an epitaxial structure. This ratio alone does not determine whether it is “manufacturable” or “not manufacturable”; layer thickness, flexibility, and defect formation are also required. Choosing a more suitable band gap can degrade crystal matching.

A **concentrator** collects light from a larger area using a mirror or lens and focuses it onto a smaller cell. The power incident on the cell increases, but the requirements for optical alignment and thermal management also increase. A cell efficiency obtained under “143 suns” cannot be directly compared with the efficiency of a non-concentrating module. When reviewing the III-V literature, the light intensity, cell

area, number of terminals, and application conditions should be clearly distinguished. [T08]

Comprehension check: Why might a suitable band gap be rejected?

If the top cell you choose promises a higher voltage but creates defects due to incompatibility with the bottom crystal, recombination may increase. For the design to be successful, the optical and electrical gain must be greater than the loss caused by lattice mismatch. The band gap diagram and the lattice matching diagram answer different questions.

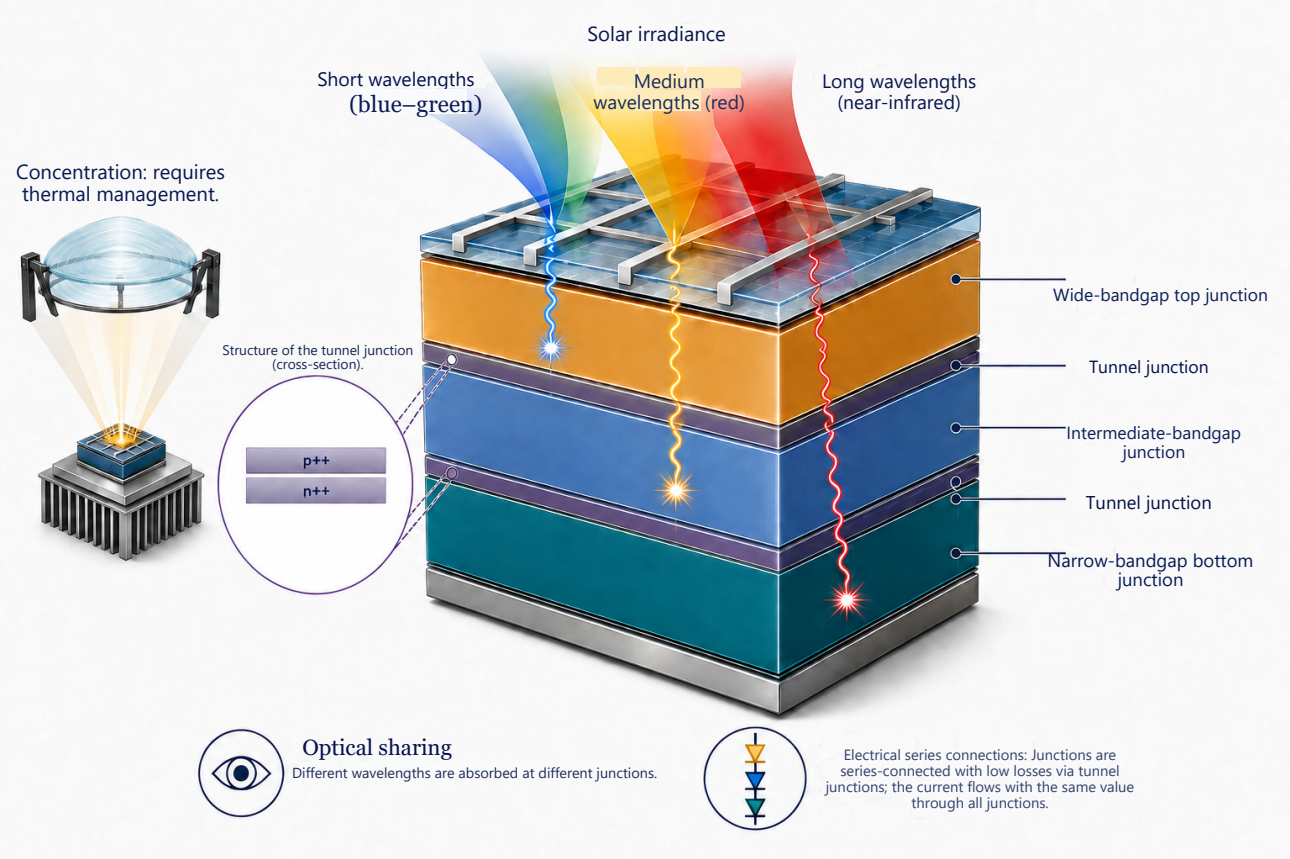


Figure 21. Spectrum and electrical connection sharing in a three-junction III-V device. The band gap decreases from top to bottom; very thin and heavily doped p++/n++ tunnel junctions connect adjacent sub-cells in series. Optical paths and layer thicknesses are not to scale. The concentrator example on the left reminds us of the need for thermal management with increasing current; the ideal voltage gain is given in the following calculation panel. [T08] [T09] Conceptual illustration prepared with an image-generation tool; it is not a measurement image.

Ideal voltage gain of concentration.

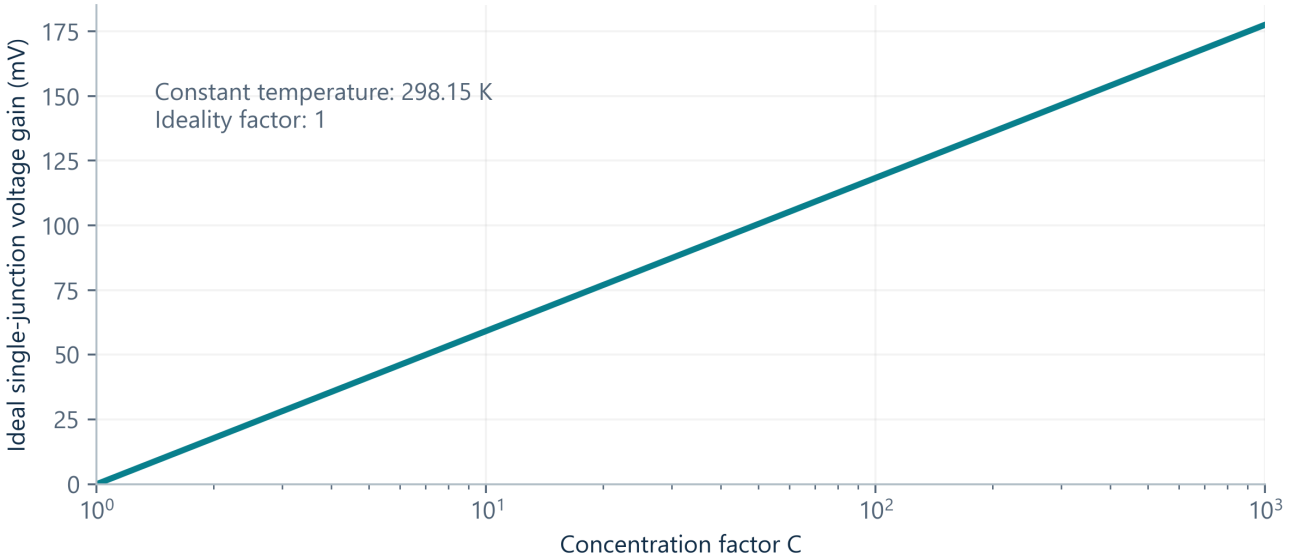


Figure 21 - calculated supplementary panel. The graph is calculated for a single ideal junction at the same temperature using the relationship ΔVoc = VT ln C. The increase in current due to concentration also increases contact and series resistance losses. Since heating is not taken into account here, the curve does not represent the measured performance of a concentrating module. [T08] [T09]

Why should we limit ourselves to a single band gap?

A single junction cannot convert the entire energy of a high-energy photon into electrical work. Charge carriers lose energy as they relax to the band edges, while low-energy photons pass through. Placing a wide bandgap absorber on top and a narrower bandgap absorber below divides the spectrum. Each sub-cell generates its own voltage. This physical principle remains valid even when the materials are not perfect; however, each added junction introduces a new optical, electrical, and manufacturing challenge.

III-V refers to semiconductors composed of elements from groups III and V of the periodic table. GaAs, InGaP, and InGaAs are examples of this material system. By alloying, the band gap and lattice constant can be modified; however, these two properties are not typically adjusted independently. Moving towards a more suitable band gap for an upper cell can introduce lattice mismatch and dislocation density in the substrate.

Epitaxy is the growth of a new crystalline layer, following the crystal structure of the underlying crystal. Lattice mismatch is approximately expressed as $f = (a_f - a_s)/a_s$; a_f is the film, and a_s is the substrate lattice constant. A very thin film can accommodate strain elastically. As thickness and mismatch increase, the strain can relax through dislocation; these defects can reduce charge carrier lifetime. Gradual buffer layers, reverse metamorphic growth, layer transfer, and wafer bonding are

different solutions. Each method has associated costs for additional materials, surface preparation, and manufacturing yield.

Electrical behavior of a series junction

In a two-terminal series device, the same current flows through all sub-cells. In an idealized scenario,

$$V_{\text{tandem}}(J) = \sum_i V_i(J) - JR_{s,A} \tag{I.12.1}$$

It can be written in this form. J represents the current density, V_i represents the voltage of each sub-cell at that current, and $R_{s,A}$ is the area-normalized series resistance. The power density is maximized at $P(J) = JV_{\text{tandem}}(J)$. Simply taking the smallest of the sub-cell currents to estimate the short-circuit current is a rough approximation; for the actual maximum power, all current-voltage curves and possible luminescent coupling are required.

The current must flow between the sub-cells to complete the circuit. A tunnel junction can facilitate the appropriate recombination of charge carriers between two heavily doped regions. This recombination serves the desired electrical connection function and does not represent the same type of loss as non-radiative recombination within the absorber. If the junction cannot handle a high current density or absorbs light, the tandem gain will decrease.

Increasing the absorption of photons destined for another sub-cell in order to enhance the current of one sub-cell can reduce the overall power. Therefore, the optimum thicknesses and band gaps are not the optimum values for a single, independent junction. Furthermore, the current ratio of the sub-cells is altered by the morning, noon, atmospheric water vapor, and aerosol spectrum. Cells that match in the standard spectrum do not match at the same rate throughout the year.

Concentrator efficiency and one-sun efficiency are separate categories

In an original 2020 study, Geisz and colleagues reported a 47.1% conversion efficiency for a six-junction III-V device under 143 suns concentration. This experiment from that year demonstrates the level achievable with multi-junction and optical concentration combined; it does not indicate that a flat panel would have the same efficiency under one sun. The source considers concentration, series resistance and material quality together. [T08]

It can increase both the concentration current and the ideal open-circuit voltage. In the ideal diode approximation, if the temperature is kept constant, then for each junction, approximately

$$\Delta V_{\mathrm{oc}} \approx n \frac{kT}{q} \ln C \tag{I.12.2}$$

This results in the following: n is the ideality factor, k is the Boltzmann constant, T is the absolute temperature, q is the elementary charge, and C is the concentration ratio. **Illustrative example:** If $n = 1$, $T = 298{,}15$, and $C = 100$ are taken, the increase is approximately 0.118 V. However, series resistance loss produces a power loss proportional to the square of the current; if the cell heats up, a portion of the voltage gain is lost. This formula is not a prediction of the performance of a concentrated cell.

The thermal aspect should not be overlooked. Under a hypothetical 100-sun illumination, approximately 10 W of optical power is incident on a 1 cm² cell. Assuming a 45% electrical conversion, this results in approximately 5.5 W of remaining power; most of this is thermal load when reflection and luminescence are neglected. Dissipating this load in a small area requires engineering efforts as significant as optical alignment. Concentrating optics, a tracking system, and cooling are all part of the system, as is the direct beam component of the sky radiation.

For space cells, AM0 is not the same as AM1.5G or the direct irradiance spectrum used on Earth. Power per unit mass, radiation resistance, and reliability are of paramount importance in space. On Earth, however, the energy cost, maintenance, and utilization of diffuse light, as well as power per unit area, are important considerations. The 2022 study by France et al., which reports terrestrial and space spectra as separate results, is a good example of comparative analysis. [T09]

Lattice matching and spectral matching are different constraints

In a multijunction design, if we were to select band gaps solely based on the solar spectrum, we could stack materials that provide each desired band gap. However, in epitaxial growth, lattice mismatch can create strain and dislocations. If dislocations increase recombination, the gain from ideal photon sharing is lost in voltage drop. Metamorphic buffers, or approaches such as inverse growth or device integration, address this material constraint in different ways. [T08] [T09]

The tunnel junction between them is not a simple conductive wire. It provides an electrical connection where electrons from the top cell and holes from the bottom cell can recombine with minimal loss; at the same time, it should absorb as few photons as possible that are intended to reach the bottom cell. A connection with insufficient

current-carrying capacity can lead to voltage drop or an unstable current-voltage curve during operation. Therefore, even if the subcells are individually good, it is not sufficient for the monolithic series to function properly.

When the photon flux in the concentrator increases by a factor of C, the increase in Voc for a single junction at an ideal constant temperature is approximately VT ln C. Conversely, the current increases approximately by C, and the ohmic loss with the same area-specific resistance increases by C^2. Optical gain is also related to thermal management: if the cell heats up, the assumption of constant temperature is violated. Before comparing the concentrated cell in the record table with a module operating under sunlight, these physical conditions must be mapped.

Self-assessment

1. If the efficiency of a concentrator cell is higher than that of a flat-panel cell, can it definitively be said that the material is superior? **Answer:** No. The spectrum, concentration, temperature, area, junction, and number of terminals must be matched.

2. If the independent maximum-power current densities of two subcells are 18 and 21 mA/cm^2, can their two independent maximum powers be added after series connection? **Answer:** No. The total power must be maximized again under the common-current constraint.

3. Is the interface between two semiconductors with the same lattice constant automatically a good one? **Answer:** No. Chemical reactivity, band alignment, polarity, surface termination, and interface defects must also be considered.

Halide perovskites: strong optoelectronics, dynamic chemistry

Perovskite is a family of crystal structures

Although “perovskite” can be used as if it were the name of a single chemical compound, in the context of PV, it most often refers to a family that shares a specific crystal structure. In the ideal $\mathbf{ABX_3}$ notation, A and B represent different-sized positive ion sites, and X represents a negative ion site. In halide perovskites, X is usually associated with iodine, bromine, or chlorine. In common lead-based examples, Pb^{2+} is located at the B site, and a total of +1 charged ions are located at the A site. For one A, one B, and three X, the charge calculation is +1 +2 -3 = 0. This simple neutrality calculation does not prove that every written formula will result in a stable crystal.

FA and **MA** are common abbreviations representing formamidinium and methylammonium ions, respectively; **Cs** represents cesium. In the composition, the A or X sites can be occupied by different species. These changes affect the volume, optical bandgap, crystallization, and mobile ion behavior. Therefore, the statement “We added a little bromine” does not simply refer to a color change; it can affect multiple physical and chemical variables.

Why is the process of film deposition from a solution considered a distinct field of science?

The **precursor** is the initial compound used to form the target material. When the mixture, in which the precursors are dispersed in a **solvent**, is applied to the surface, it initially forms a wet film. As the solvent evaporates, the ion density increases, and small, ordered regions **nucleate**, followed by crystal growth. A **grain** is a region with a common crystal orientation. The presence of voids in the film, the segregation of some components, or the degradation of the interface can negate the benefit of large grains that appear aesthetically pleasing.

The terms **n-i-p** and **p-i-n** indicate the order of the charge carrier selective layers. Here, ‘i’ denotes the absorber layer; however, it does not guarantee that the actual film is a perfect intrinsic semiconductor under all conditions. The **electron transport layer** helps electrons reach the appropriate contact, and the **hole transport layer** helps holes reach the appropriate contact. Each layer is also evaluated in terms of light absorption, chemical compatibility, and processing temperature.

How does the presence of mobile ions affect the measurement?

A **vacancy** in a crystal is a location where the ion that is expected to be present is missing. As neighboring ions move to this location, the vacancy itself can be observed to move in the opposite direction. **Ionic migration** is the redistribution of charge and composition through such atomic movements. It does not necessarily have to occur on the same timescale as electron current.

When rapidly sweeping the voltage, the ion distribution may partially remember the previous condition. Consequently, forward and reverse sweeps yield different curves; this is **hysteresis**. **Synthetic example:** if 22% is observed during a rapid sweep, and 19% is observed during power tracking after a settling period, we cannot use both with the same performance label. This difference alone does not prove a specific ion type; stable measurements and discriminating controls are required. [T12] [T14]

Comprehension check: does a uniform film mean a good cell?

A film that appears to be pinhole-free and has large grains under a microscope does not, by itself, indicate a low density of electrical defects or selective contacts. Correlate the structural image with measurements of luminescence, voltage, steady-state power, and composition. “Improved image” and “the cause of power loss has been eliminated” are separate outcomes.

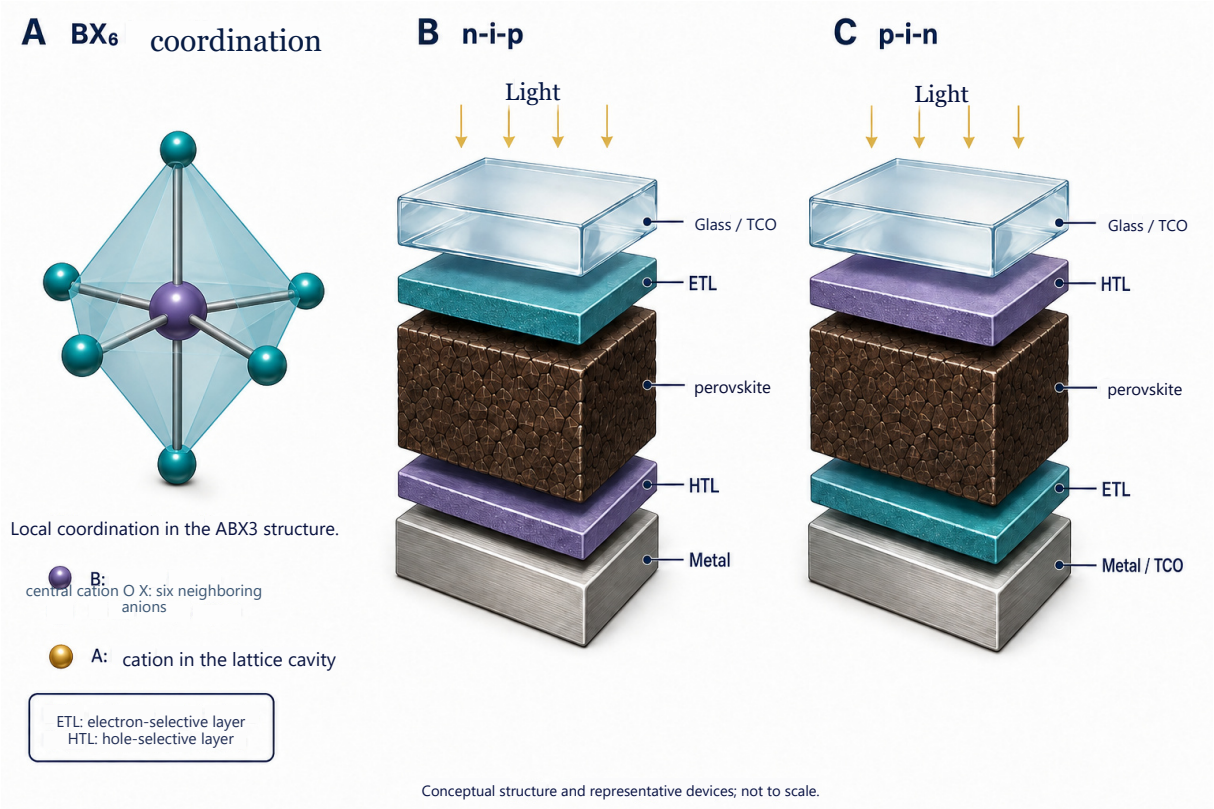


Figure 22. The perovskite structure family and two device orientations. Panel A is a projection of the ideal ABX3 local environment; rotations in real phases are not shown. Panels B and C give the n-i-p and p-i-n layer sequences, starting from the light-entry side. ETL is the electron-selective layer and HTL the hole-selective layer. Layer thicknesses are not to scale. [T10] [T11] Conceptual illustration prepared with an image-generation tool; it is not a measurement image.

Perovskite is a structural family, not the name of a single substance

The term “perovskite” does not refer to a single chemical formula. The halide perovskites commonly used in photovoltaics have an approximate ABX_3 structure: A is usually a monovalent cation; B is a divalent metal such as lead or tin; and X can be iodide, bromide, or a mixture of the two. The B-X octahedral network is crucial in the formation of band edges. The A cation also influences the geometry, phase stability, and dynamics of the network. Therefore, the conclusion that “A contributes little to the band edge and is insignificant” is incorrect.

MA represents methylammonium, and FA represents formamidinium; Cs is cesium. The partial replacement of iodide with bromide generally increases the band gap. Lead-tin mixtures can provide absorbers with narrower band gaps; however, the alloy range does not necessarily have to be linear. When writing the composition, the sum of the coefficients, the halogen ratio, whether the dopant is located within the lattice or on the surface, and the actual phases contained in the film must be clearly stated.

Geometric tolerance factor

$$t = \frac{r_A + r_X}{\sqrt{2}(r_B + r_X)} \tag{I.13.1}$$

It is sometimes used for coarse structural analysis. r_A, r_B, and r_X are effective ionic radii. This indicator does not account for bonding, temperature, molecular orientation, oxidation, or kinetic decomposition. A suitable t value is not proof of a stable film or a synthesizable compound under sunlight. Researchers should use such simple indicators as a screening tool and not as a substitute for an experimental phase diagram.

Key milestones in the development process

The 2009 article by Kojima and colleagues demonstrated that organolead halide crystals could be used in light-sensitized photoelectrochemical devices. Its historical significance lies in the fact that it was one of the starting points for today’s solid-state perovskite cells. The architecture of that device is not the same as that of current solid-state devices; therefore, it would not be appropriate to directly compare its initial performance with the performance of today’s modules. [T10]

The 2012 study by Lee and colleagues is one of the pivotal works demonstrating that perovskite does not necessarily have to function only as a sensitizer but can also perform light absorption and charge transport functions in a solid-state device. The experimental result presented in the original abstract of this article is evidence of a period of very rapid development in the field; it does not mean that any perovskite formulation will automatically result in a good cell. [T11]

The scientific appeal of this rapid development lies in the combination of strong absorption, suitable band gaps, and long charge carrier collection distances in well-prepared films. However, being able to prepare an inexpensive solution does not equate to successfully producing a low-cost, long-lifetime module. Contacts, solvent management, controlled crystallization, encapsulation, containment of toxic elements, and production repeatability determine the actual cost of the product.

Device configuration: n-i-p and p-i-n

When viewed from the light incidence side, in an n-i-p configuration, the electron selective contact is first, followed by the absorber, and then the hole selective contact. In a p-i-n configuration, the order is reversed. Here, "i" refers to the absorber acting as an effectively low-doped region; it does not guarantee that it is a perfect, intrinsic semiconductor. It is considered in the form of a stack: glass/TCO/selective layer/perovskite/counter-selective layer/electrode. Each layer has an optical and chemical function in addition to its electrical function.

For electron transport layers, SnO_2, TiO_2, or suitable fullerene derivatives; for hole contacts, organic molecules, NiOx, or self-assembled molecular monolayers represent different design approaches. This list is not a purchasing recommendation. The suitability of a material is determined by its work function, band alignment, coating compatibility, surface chemistry, and its behavior under heat and light. A thin organic layer can reduce recombination, while if it is too thick or uneven, it can create a transport barrier.

The buried interface is particularly challenging because it cannot be processed directly afterward. As the perovskite film grows on the underlying surface, wetting, nucleation, and chemical bonding occur simultaneously. The 2021 study on the atomic-scale SnO_2/perovskite interlayer provides a unique example of how controlling the buried interface can lead to device performance enhancement. Such findings go beyond the concept of a "new passivation molecule" and teach us how to control the formation of the interface. [T32]

Crystallization: the largest grain does not always make the best film

During film formation, solvent loss, supersaturation, nucleation, growth, and phase transformation occur sequentially. Very rapid nucleation can generate a large number of small grains, while insufficient nucleation can leave voids and uncovered areas in the film. Considering only the large grains in the SEM image as an indicator of success overlooks hidden interface defects and local stoichiometric variations. Continuous coverage, phase purity, orientation, strain, and electronic quality should be measured together.

An additive can simultaneously alter the drying rate, defect passivation, and contact work function. When the efficiency increases, control experiments are needed to attribute the effect to a single mechanism: a similar molecule that provides the same wetting but does not passivate; a process applied only to the bottom contact; equivalent film thickness; different light intensities; and measurements with time resolution. The claim of a specific mechanism requires more experimentation than simply observing the best device performance.

Ion migration and hysteresis

Halide perovskites can contain mobile ionic defects along with electronic charge carriers. The 2015 study by Eames et al. calculated and experimentally correlated the transport associated with iodide vacancies in $MAPbI_3$. This result is specific to a particular composition and mechanism; it is not accurate to extrapolate a single activation energy to all perovskite devices. Interfaces, grain boundaries, and illumination conditions can alter the effective processes. [T12]

A simple thermal activation model has the form $D = D_0 \exp[-E_a/(kT)]$. D is the diffusion coefficient, D_0 is the pre-exponential factor, and E_a is the migration activation energy. **Solved example:** Assume that the pre-exponential factor remains the same, while the barrier increases by 0.10 eV. At 298.15 K, the new/old rate ratio is approximately $\exp(-0{,}10/0{,}02569) = 0{,}020$; a rough 49-fold decrease is expected. However, if the process increases the number of mobile defects by a factor of 100, the total ionic conductivity may still increase. The barrier alone is not a sufficient design target.

When ions accumulate near the contact, the internal electric field and interface recombination can change. The measurement becomes dependent on the scanning direction, speed, and the previous voltage state. However, low hysteresis does not necessarily prove the absence of ion migration. The 2016 experiment by Calado et al. directly addressed this distinction. The occurrence of hysteresis is related to the combined effect of ion movement and the contact and recombination conditions. [T14]

Chemistry under illumination and true stability

In mixed iodide/bromide films, local halogen dissociation can be observed under illumination. The 2015 study by Hoke et al. provides compelling evidence for structural and optical changes that appear and revert under illumination. Even if iodine-rich, narrow band gap regions occupy a small volume, they can collect charge carriers and affect the luminescence spectrum and voltage. Therefore, the dominant PL peak should not be interpreted as representing a homogeneous band gap across the entire film. [T13]

Moisture and oxygen are external factors, while light, temperature, and electrical voltage affect the material within the encapsulation. Using an inorganic A cation can reduce organic volatility; however, it does not spontaneously eliminate halide migration, phase transformation, or metal electrode reactions. “Completely inorganic” is not synonymous with “field-stable.”

The key question regarding stability is: at what voltage and for how long is a specific property maintained? The 2020 consensus document by Khenkin et al. requires clear reporting of light, temperature, humidity, electrical load, encapsulation, and reversible changes. MPP tracking provides an electrical state close to the operating condition. The result of a device stored in the dark is not the lifetime of a device generating power under illumination. [T15]

Considering crystallization in terms of the energy barrier and time scale

In simple homogeneous nucleation, the change in free energy for a spherical nucleus of the new phase with radius r is the sum of the surface cost and the volume gain. When the interfacial energy γ is positive and the volume free energy difference of the new phase, Δgv, is negative:

$$\Delta G(r) = 4\pi r^2\gamma + \frac{4\pi}{3} r^3 \Delta g_v. \tag{I.13.2}$$

By equating the derivative to zero, the critical radius r *= -2γ/Δgv and the barrier ΔG =* $16\pi\gamma^3/(3\Delta g v^2)$ are obtained. In small nuclei below the critical size, the surface energy is dominant; above it, growth becomes more favorable. Supersaturation in the solution, the presence of intermediate phases, and heterogeneous nucleation on the surface alter this picture in the actual film. This model is not a production recipe but rather a starting point that explains why process variables cause certain effects.

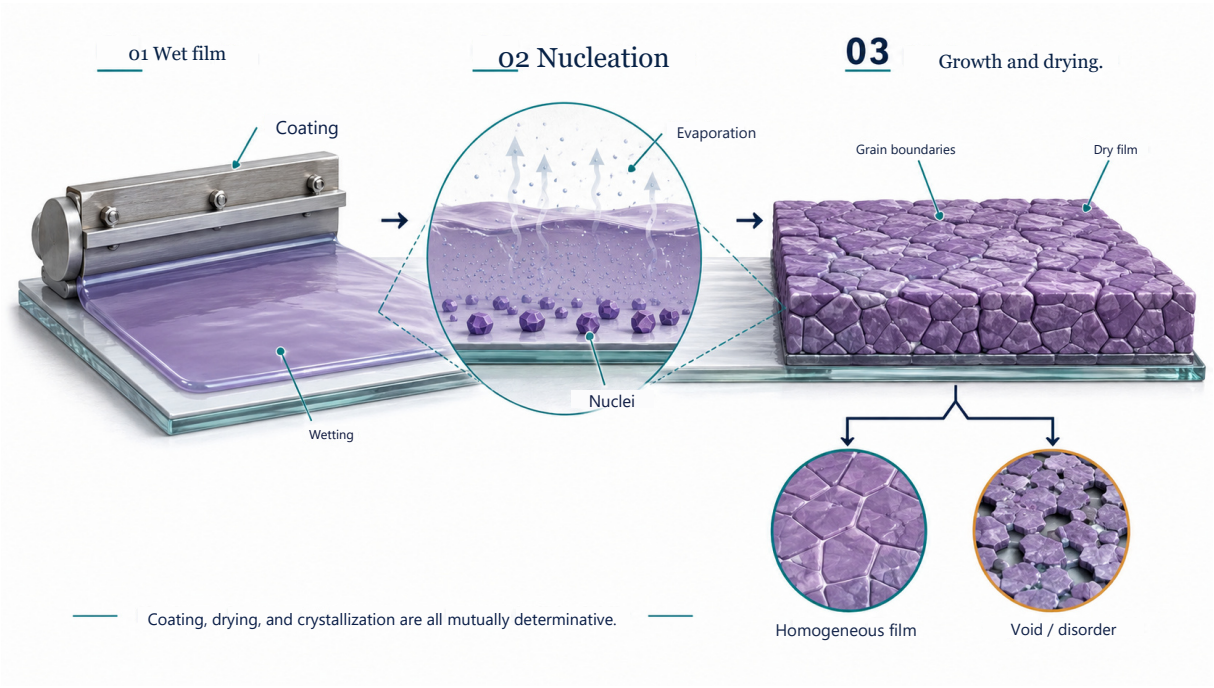


Figure 23. Transition from wet precursor to polycrystalline film. Coating, solvent loss, nucleation, and growth are interconnected. Close-up views illustrate the difference between film continuity and the presence of voids and irregularities; they are not actual microscopy or grain size measurements. The calculation panel that follows also shows the classical energy barrier for a homogeneous spherical nucleus. [T11] [T32] Conceptual illustration prepared with an image-generation tool; it is not a measurement image.

Energy barrier of the critical nucleus.

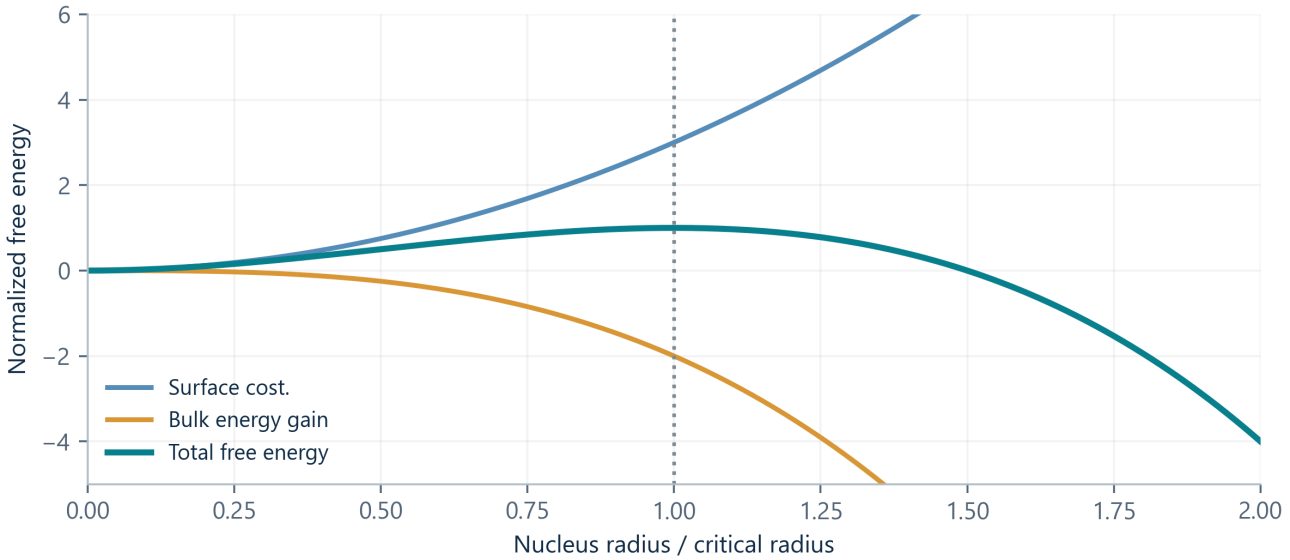


Figure 23 - calculated supplementary panel. In the global and homogeneous nucleation model, the surface term varies with the square of the radius, and the volume term varies with the cube of the radius. For the normalized total of $3x^2 - 2x^3$, the barrier is located at x = 1. In real coated films, heterogeneous nucleation on the substrate and the kinetics of the process are also important. [T11] [T32]

Rapid nucleation can create a large number of initial nuclei; slow growth combined with rapid etchant removal produces different microstructures. However, the “few nuclei, large grains, high efficiency” principle is not a linear rule. Uncoated areas,

residual interphase, surface composition, and adhesion to the transport layer are also important. Two films exhibiting the same optical absorption can yield very different Voc values due to different interface losses. Film evaluation should at least encompass surface coating integrity, phase/composition, optical response, and electronic quality.

Adding ion migration to the transport equation

For a single type of mobile ion, the particle flux is the sum of diffusion and electrical drift in the dilute and isothermal Nernst-Planck approximation. Let z be the number of charges of the ion, ci be its concentration, and Di be the diffusion coefficient:

$$F_i = -D_i \frac{\partial c_i}{\partial x} + \frac{zqD_i}{k_B T} c_i E, \qquad \frac{\partial c_i}{\partial t} = -\frac{\partial F_i}{\partial x}. \tag{I.13.3}$$

The ionic charge, zqci, contributes to the total charge in the Poisson equation. Thus, ions not only produce a slow current but also modify the potential experienced by electrons and holes. In a non-ion-conducting contact, the normal ionic flux can be set to zero; however, if there is a reaction at the interface, this boundary condition is insufficient. The actual mobile species, charge state, and reaction pathway must be determined by independent chemical evidence. [T12] [T14]

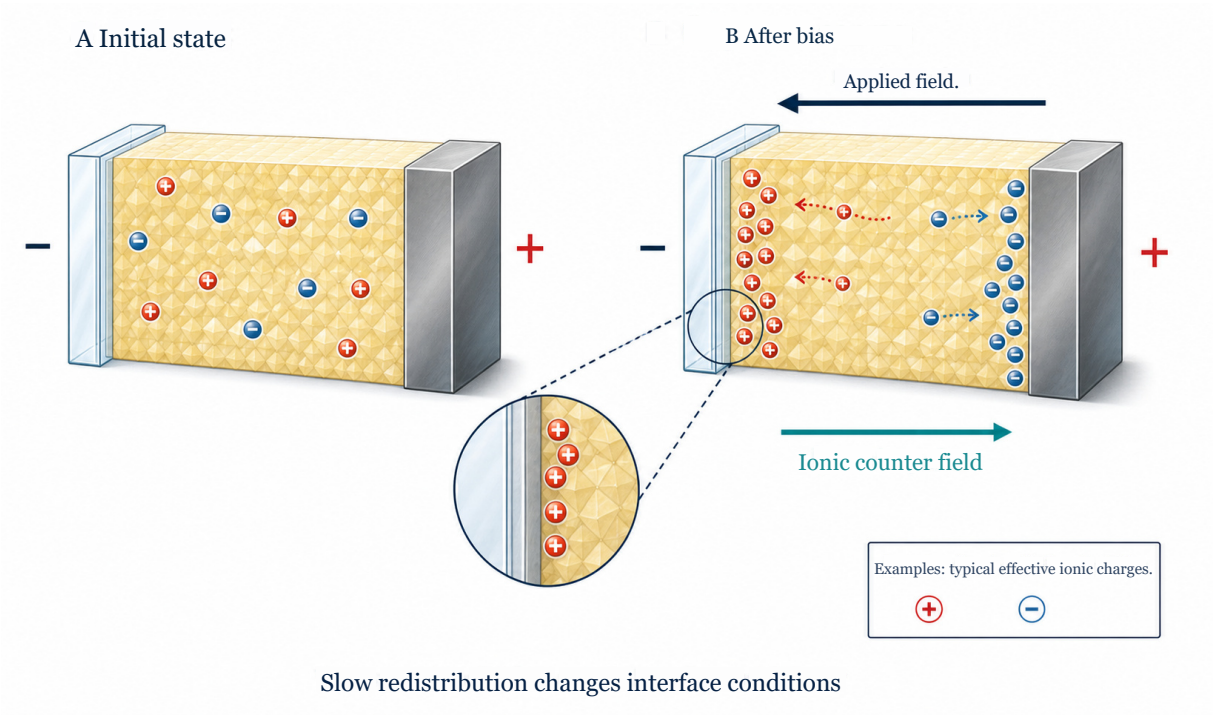


Figure 24. An illustrative diagram of slow ionic redistribution under bias. The applied field, directed to the left, drives positive effective ionic charges to the left interface and negative charges to the right interface; the opposing field created by the accumulation is in the opposite direction. The symbols do not represent a specific ion type or particle count. In a real device, the mobile species, boundary conditions, and electronic response must also be determined. [T12] [T14] Conceptual illustration prepared with an image-generation tool; it is not a measurement image.

Time scale of the measurement with internal relaxation.

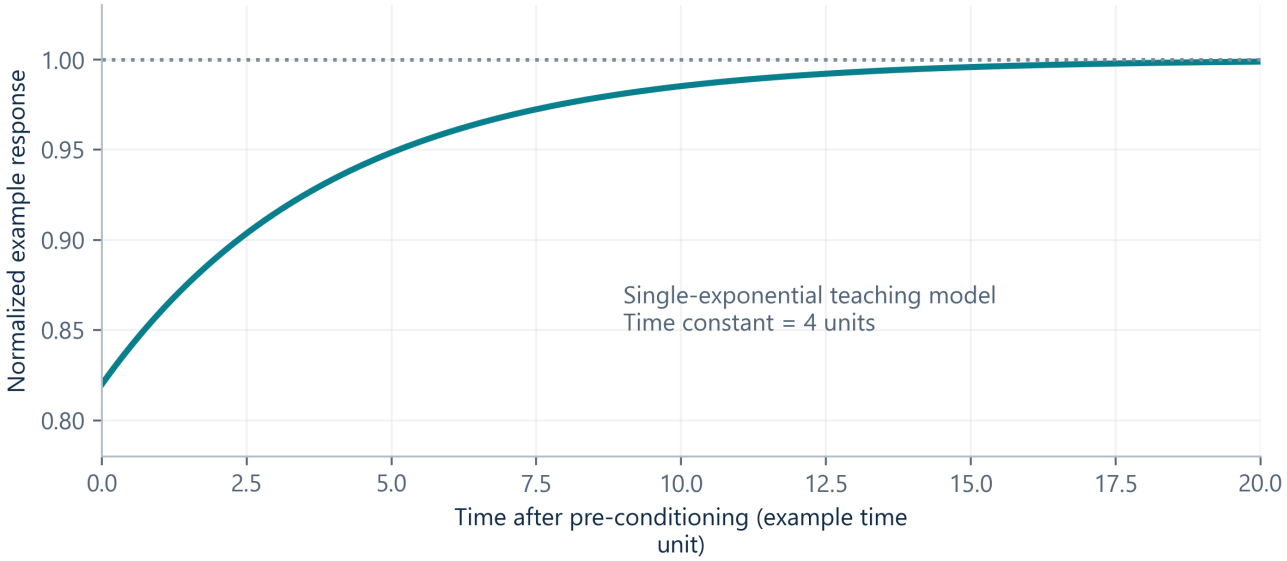


Figure 24 - calculated supplementary panel. The synthetic response y(t) is given by y(t) = 1 - 0.18 exp(-t/4); the time constant is four sample time units. If the duration of a measurement is close to the inner relaxation time, the pre-conditioning and scanning history can affect the result. This curve does not diagnose a specific ion or the kinetics of a real sample. [T12] [T14]

If we consider the film thickness to be d, the diffusion time scale is approximately d^2/D; the drift time under the field may be different. When this scale is much longer or much shorter than the voltage sweep, the hysteresis may appear small. Therefore, a small hysteresis alone does not prove that the ions are immobile. Pre-conditioning, waiting time, scanning direction, and stable MPP measurement are all parts of the same physical process.

Self-assessment

1. If hysteresis has disappeared, does this mean that ion migration has ceased? **Answer:** No; the electrical effect of the ions may have been suppressed by the contact design.

2. If one device remains stable for 1000 hours in the dark and the other remains stable for 300 hours under MPP, which one is more durable? **Answer:** Cannot be determined with the given information; the stress conditions do not match.

3. As PL shifts towards red and the absorption edge remains nearly constant, is a homogeneous band gap reduction the only possible explanation? **Answer:** No; small-volume, low band gap regions can collect charge carriers and dominate the PL.

BOOK I · CHAPTER 14 / MATERIALS AND DEVICES

Perovskite tandem cells: why is simply combining two good cells not enough?

In a perovskite-silicon tandem cell, the processing sequence is important

After the silicon sub-cell is prepared, creating a perovskite top cell on top of it involves subjecting the finished device to new chemical and physical processes. The solvent of the top cell can dissolve the underlying layer; heating it can disrupt the previous passivation; and the surface texture can make it difficult to apply a uniform wet film. **Integration** involves not only stacking the components but also making these processes and functions work together.

The **wide band gap** of the top cell aims to utilize high-energy photons at a higher voltage. However, "wider" is not always "better." If very few photons are absorbed in the top cell, the current of the series circuit will be limited. If too many are absorbed, there may not be enough light remaining for the bottom cell. The layer thickness and composition together determine the current sharing. In mixed halide compositions, compositional degradation under illumination is also investigated.

Which charges meet at the interconnection?

In a 2T tandem cell, one type of charge carrier from a sub-cell completes the electrical circuit in the interconnection region with the opposite charge carrier of the adjacent cell. The **recombination contact** is required here and performs a designed function. It does not have the same design role as the unwanted recombination that occurs within the absorber before reaching the contact. A process cannot be classified as "always bad" without knowing its name, location, and function.

Representative optical balance: Out of 100 photons entering a specific wavelength band, 45 are absorbed in the top absorber, 5 are absorbed in the non-functional contact layer, 10 are reflected, and 40 pass through to the bottom. If the bottom cell collects 75% of these 40 photons in a useful manner, it provides a contribution of 30 electrons from that band. Here, the absorption of 5 photons represents **parasitic absorption**, which is a loss that does not provide useful generation in either the top or bottom cell. This simple count does not include voltage and therefore does not yield tandem efficiency; it shows which layer loses the photons.

A **transparent conductive oxide** is an oxide layer designed to transmit a significant portion of light while conducting electricity; it is abbreviated as TCO. In reality,

absorption, reflection, and sheet resistance occur simultaneously. A thinner TCO layer can increase light transmission but may also increase lateral resistance. Therefore, the performance of the interface cannot be evaluated solely based on the percentage of light transmission.

Comprehension check: after which process step was the gain lost?

If the bottom cell is good, and the top cell is also good in a separate sample, but the tandem cell is performing poorly, then stage the processes. Expose the bottom cell to the solvent, temperature, and deposition conditions of the top layers without adding the absorber, and measure it again. These checks help to distinguish process damage from optical sharing and interconnection losses.

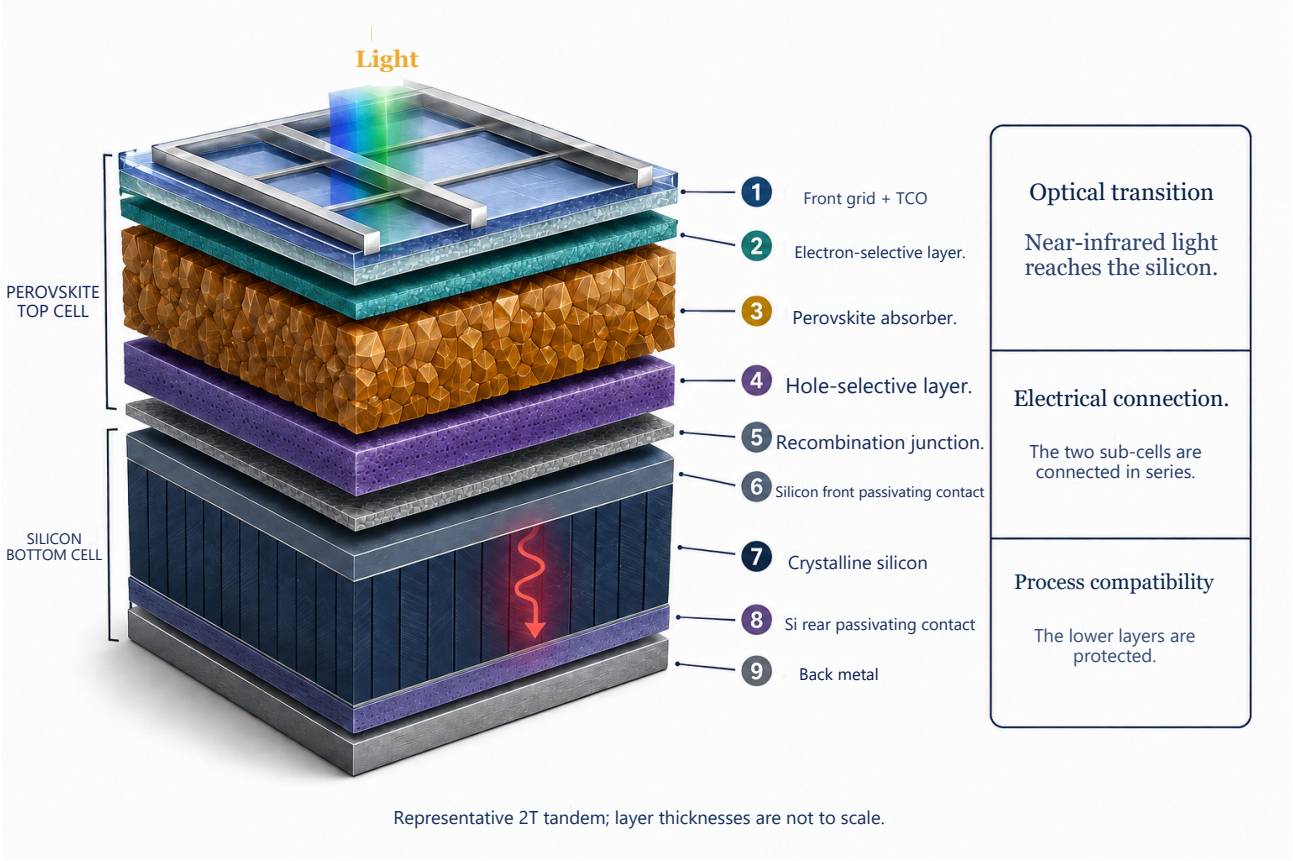


Figure 25. Representative layer cross-section for a monolithic perovskite-silicon tandem cell. The same interlayer must ensure optical transmission, electrical connection, and process compatibility. The depicted p-i-n top cell is only one architectural example; thicknesses and colors are not physical measurements. [T16] [T17] Conceptual illustration prepared with an image-generation tool; it is not a measurement image.

Rethinking the silicon bottom cell

In a perovskite/silicon tandem cell, the top cell utilizes high-energy photons, while the silicon cell utilizes low-energy photons that pass through. The transparency of the top cell is as important as its efficiency. If the top electrode, charge carrier layer, or metal grid absorbs near-infrared photons, the current in the silicon cell will decrease. This loss may not be apparent in a measurement where the top cell is illuminated independently.

The bottom cell does not have the same optimum characteristics as a standard single-junction silicon cell. In a tandem configuration, the spectrum is filtered, the current is generally reduced, the front surface is connected to another stack, and it undergoes additional processing during manufacturing. A texture that is ideal in a single-junction cell can be challenging for uniformly coating the thin top film. While a flat surface facilitates the top film, it can create optical losses; texture improves light input but can lead to thinning or short-circuit risks at the peaks.

Sahli et al.'s 2018 study demonstrated that in a fully textured monolithic perovskite/silicon device, the top layer can be integrated with the existing silicon surface geometry. The key finding here is that the progress in tandem devices is achieved not only through band gap selection but also through the actual surface topography and recombination linkage. [T16]

A fair comparison of two-terminal and four-terminal devices

A two-terminal, or 2T, tandem is a single series circuit. The top and bottom cells carry the same current; the two voltages add. A four-terminal, or 4T, arrangement consists of two independent cell circuits. The top cell is semitransparent; each cell's maximum power is determined separately, accounting for the spectrum reaching the bottom cell. When the area and light input are correctly defined, the powers can be added:

$$\eta_{4T} = \frac{P_{\mathrm{mpp,top}} + P_{\mathrm{mpp,bottom,filtered}}}{P_{\mathrm{in}}}. \tag{I.14.1}$$

There is a single common light input at the denominator. Using the unfiltered power of the bottom cell alone counts the photons twice. Furthermore, if the two cells are in different areas, you cannot simply add their efficiencies; calculations must be performed based on watts, the common aperture area, and optical overlap. The additional cost of the two independent MPP circuits and power electronics must also be explained.

Question	2T	4T
Is a common current required?	Yes.	No.
Can top- and bottom-cell power be maximized independently?	No.	Yes, with the filtered spectrum at the bottom cell
Are intermediate optical layers important?	Yes.	Yes, additional transparent electrodes may be present.
Manufacturing compatibility	Stronger constraints in the common stack	Separate fabrication and optical stacking are possible.
Annual energy-gain assessment	Spectral current matching is critical.	More flexible to spectral variations; system losses persist.

In 2015, Bailie et al. investigated tandem gain by mechanically stacking a semi-transparent top perovskite cell with silicon and CIGS bottom cells. This study serves as a practical, illustrative example of the 4T concept. The fundamental question is not "how good is the top cell?" but rather, "how much more power is generated from the combined light input when the top cell is added?" [T18]

A numerical photon budget

Solved example. Let's assume that the common irradiance is 100 mW/cm^2. The top cell produces 20 mA/cm^2 × 1.05 V = 21.0 mW/cm^2 at its MPP. If the filtered bottom cell produces 18 mA/cm^2 × 0.65 V = 11.7 mW/cm^2, the idealized 4T total is 32.7 mW/cm^2, and the efficiency is 32.7%. This value is not a measured record; it is an exercise in unit and topology.

If the same devices are connected in series, the values of 20 and 18 mA/cm^2 cannot be used simultaneously. For example, if it is assumed that at the common point of 18 mA/cm^2, the upper voltage is 1.08 V and the lower voltage is 0.65 V, then the power will be 18 × 1.73 = 31.14 mW/cm^2. It has not yet been demonstrated that this point is the actual maximum; the entire combined curve must be scanned. The example demonstrates why summing the individual maximum powers in a series circuit is incorrect.

In a tandem design, a small increase in the open-circuit voltage of the top cell is valuable, but the associated current penalty should not be overlooked. For example, suppose a new passivation layer provides a 30 mV gain but reduces the short-circuit current from 19 to 18 mA/cm^2. At an approximate tandem voltage of 1.8 V, the power

impact of this current loss may be greater than the 30 mV gain. The decision to implement this improvement should not be based solely on V_{oc}.

Interfaces and low bandgap perovskites

In their 2020 original study, Al-Ashouri and colleagues demonstrated the simultaneous achievement of rapid hole extraction and low non-radiative recombination using a hole-selective molecular monolayer. This interface modification in a wide bandgap perovskite/silicon tandem resulted in a historical performance improvement. The result suggests that the selective contact can impose a limit, while the perovskite volume remains within the same family. [T17]

In an all-perovskite tandem, the bottom cell is usually a mixed lead-tin perovskite with a narrower band gap. The susceptibility of tin(II) to oxidation makes defect and doping control more challenging. The crystallization rates of the top and bottom layers can also differ. A thick bottom film absorbs more near-infrared light but also amplifies the collection loss caused by the short charge carrier lifetime. Therefore, having a "good band gap pair" is only the initial design requirement.

Zhou et al.'s 2024 study investigated the simultaneous management of crystallization and oxidation in mixed tin-lead films. As a continuation of the current research, the targeted surface transformation study planned for 2026 focuses on preserving the reactive tin-lead surface under combined light-thermal stress. Both sources demonstrate that the problem is not solely related to the initial defect density but also requires controlling the ongoing chemical processes during operation. This brief summary does not claim to reproduce the full experimental methods of the two articles. [T19] [T31]

Do not reduce the interlayer to a single loss number

The middle region of the tandem cell simultaneously constitutes three interfaces: an optical transition, an electrical recombination junction, and a chemical surface where two manufacturing processes converge. If the layer beneath the top cell absorbs near-infrared photons, the current of the bottom cell decreases. If the same layer has high resistance, the fill factor (FF) of the series-connected structure decreases. If the surface treatment degrades the silicon passivation, the open-circuit voltage (Voc) of the bottom cell may also change. These effects cannot be assessed with a single "intermediate layer successful" criterion.

A good experimental sequence checks the electronic quality of the silicon sub-cell before and after the addition of the intermediate layer. Subsequently, it measures the transmittance of the optical stack and the spectral response of each sub-cell. In the final

device, stable power, sub-cell current matching, and temperature dependence are evaluated. If the process temperature or plasma conditions are changed, a control sample with the same total thermal history is required; otherwise, process damage and the effect of chemical layers may be confused.

Luminescent coupling and measurement limits

A photon emitted by the top cell through recombination can be absorbed in the bottom cell and contribute to current. This is called luminescent coupling. In cells with highly efficient radiative emission, treating the bottom cell as an independent filtered device supplied by solar photons transmitted through the top cell can miss this contribution. Conversely, assuming a very large coupling gain for a structure with weak external emission would also be incorrect. Optical escape, the emission spectrum and bottom-cell absorption are modeled together.

In the EQE measurements of the sub-cells, it must be ensured that the other cell does not limit the current with appropriate bias light and electrical conditions. The sub-cell selected for which wavelength range, the light conditions used, and the current corrections are reported. A single J-V curve of the total device does not replace this layer-based characterization. [T28]

Self-assessment

1. For a 23% single-junction top cell and a 25% single-junction silicon cell, is the 4T total 48%? **Answer:** No; the silicon cell must be remeasured under the spectrum filtered through the top cell.

2. Does demonstrating the 2T current matching only under standard spectrum conditions prove annual energy superiority? **Answer:** No; temperature and spectrum change over time, and there are also system losses.

3. Does a full perovskite tandem cell, which uses less silicon, definitely offer greater sustainability? **Answer:** No; the life cycle, including lifetime, manufacturing yield, contacts, solvents, encapsulation, and recycling, needs to be considered.

BOOK I · CHAPTER 15 / MATERIALS AND DEVICES

Organic, dye-based, quantum-dot and emerging absorbers

The processes of light absorption and free charge generation can be separated

We should not directly apply the concepts we learned with silicon to every material. In some materials, light first creates an excitation in which the electron and hole remain bound to each other. This bound pair is called an **exciton**. The **binding energy** is the additional energy required to separate the pair. Dielectric screening affects how strongly the charges feel each other. The movement of an exciton to the contact is not the same transport event as the movement of a free electron.

Organic semiconductors can be made from carbon-based molecules or polymers with tailored electronic properties. Charge separation can be facilitated at the **interface** of **donor** and **acceptor** components. The exciton generated by light must reach this interface without being lost; the resulting separated charge carriers must also travel to the contacts along their respective continuous paths. The microscopic arrangement of the mixture is called the **morphology**. Simply mixing two materials in the same container does not guarantee these charge transport pathways.

Example of diffusion length: If the typical diffusion length of an exciton is 10 nm, and the distance from a point in the donor region to the nearest interface is 100 nm, many excitations may be lost before reaching the interface. A very finely intermixed morphology can reduce this, but it may disrupt the charge transport pathways. The design must address both distances simultaneously; there is no rule that "the smallest region is the best."

The dye and quantum dot establish different task distributions

In a **dye-sensitized solar cell**, the molecular dye absorbs light. The excited electron is transferred to the porous semiconductor under appropriate energy conditions; the electrical state of the remaining dye is replenished by another transport medium. A **redox couple** is the cycle of two chemical states that can accept and donate electrons. The dye, the electron-transporting scaffold, and the charge-replenishing medium perform different functions. Each interface requires energy and rate matching. [T20]

A **quantum dot** is a semiconductor particle so small that its size confines its electronic wave behavior. This **quantum confinement** can alter the optical transition energies in different sizes of the same material. A **ligand** on the surface is a molecule that binds to

the particle and helps it remain stable in solution. However, long organic ligands can hinder electrical transport between neighboring dots. A particle that disperses well during synthesis may not require the same conditions as a particle that conducts current well in a film.

Other absorbers, such as kesterite or antimony selenide, also present separate crystal and defect issues. The abundance of the material is a valuable criterion; however, the desired band gap must be achieved along with low defect losses and suitable contacts. We will compare these families below based on their common solar cell functions.

Comprehension check: the same word may refer to a different step

When it is stated that “charge generation has increased,” does this refer to light absorption, exciton formation, exciton dissociation, or charge collection in the external circuit? In organic and dye-sensitized systems, these steps must be clearly distinguished. Simply measuring a stronger absorption does not prove that more free charge has accumulated at the interface.

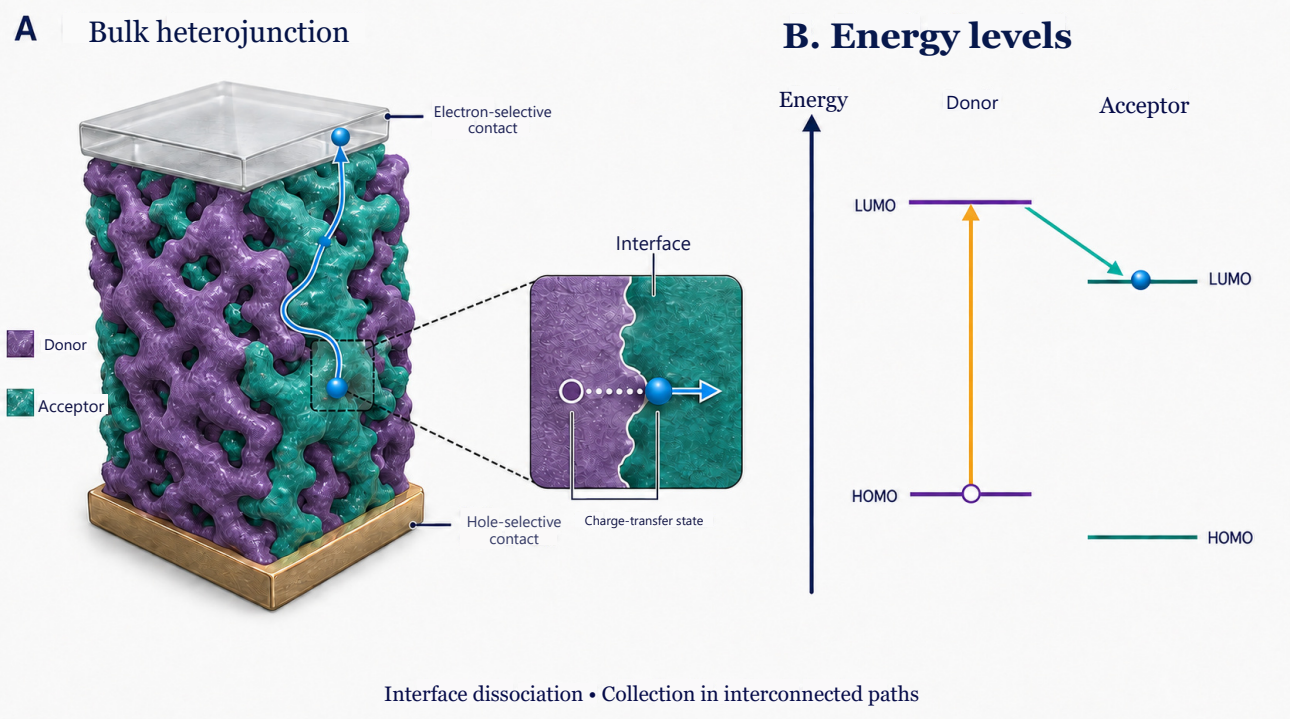


Figure 26. Interface and connected transport pathways in an organic bulk heterojunction. The donor and acceptor phases should form pathways that allow the separated charges to reach their respective selective contacts. The electron-hole pair located in the opposing phases in the close-up view represents a charge transfer state. The HOMO/LUMO ordering and transition arrows on the right are a qualitative energy diagram; the actual energy differences and morphology depend on the material. [T20] Conceptual illustration prepared with an image-generation tool; it is not a measurement image.

Organic photovoltaics: generating the excitation and separating the charge

In organic semiconductors, light often causes bound electron-hole excitation, i.e., the formation of excitons. The nature of dielectric screening and intermolecular coupling affects the spontaneous conversion of this excitation into free charge. The interface between the donor and acceptor components assists in charge separation. Considering the organic device merely as a thin version of a classical inorganic p-n junction obscures many important loss mechanisms.

In a volume heterojunction, the donor and acceptor are mixed at the nanoscale. The goal is to ensure that excitons reach the dissociation interface, and then that electrons and holes are transported to the electrode through their respective continuous networks. If the phases are too coarsely separated, the excitons may disappear before reaching the interface; if they are mixed too thoroughly, the charge transport paths and the regular molecular packing may be disrupted. Morphology, orientation, and stability are as important as the average composition.

Non-fullerene acceptors enabled the enhancement of absorption and energy levels through molecular design. The 2019 Y6 paper by Yuan et al. is a significant and original example of this approach. The results indicate that the molecule's intrinsic absorption, its mixing with a complementary donor, and the film morphology collectively determine the device performance. The same results cannot be expected when using the same molecule with different solvents or contacts. [T21]

The appeal of organic cells lies in their design possibilities, such as flexibility, low mass, color, and semi-transparency. Conversely, oxygen, light, temperature, molecular diffusion, and electrode reactions can limit long-term performance. Indoor applications represent a separate category associated with high efficiency, narrow spectrum, and low light levels; lux is not a unit of luminous intensity, and it is not possible to convert from lux to W/m^2 using a single coefficient without knowing the spectrum.

Dye-sensitized solar cell: separating light absorption from charge transport

In a dye-sensitized solar cell, the molecular dye absorbs light, and the excited electron is transferred to a suitable semiconductor network. The dye is then regenerated by a redox environment or a solid hole carrier. Mesoporous TiO_2 provides a high internal surface area, allowing it to accommodate a large number of dye molecules. The 1991 study by O'Regan and Grätzel marked a historical turning point for this architecture. The cost and energy market context of that paper is specific to 1991; the same economic arguments should not be repeated for today. [T20]

Strong absorption of visible light by a dye alone is not sufficient. Electron injection, dye regeneration, and collection must be fast, while back electron transfer must be slow. The classical energy diagram should facilitate electron transfer from the excited dye to the conduction band of the semiconductor. However, excessive driving energy may result in a reduction of the achievable voltage. The balance between chemical kinetics and energy loss is the central issue.

An illustrative factor decomposition is in the form of $EQE \approx \eta_{\mathrm{abs}}\eta_{\mathrm{inj}}\eta_{\mathrm{coll}}$. Each term is a defined probability; if the processes are strongly coupled, this simple decomposition may not be sufficient. **Solved example:** For absorption 90%, injection 95%, and collection 85%, the EQE is approximately $0{,}90 \times 0{,}95 \times 0{,}85 = 0{,}727$, i.e., 72.7%. Increasing the total to 95% by simply darkening the dye is not possible without addressing these other losses.

Quantum dots: size is a design variable

In quantum dots, the small crystalline size can alter the electronic energy levels. Different sizes of the same chemical composition can provide different spectral absorption. However, the surface-to-volume ratio is large; ligands and surface defects are critical. A long ligand that stabilizes the crystal in solution can hinder electronic transport between neighboring dots in a solid film. Ligand exchange, surface passivation, and conductivity must be managed simultaneously.

One of the investigated pathways is the generation of multiple electron-hole pairs from a high-energy photon. The measurement of an external quantum efficiency exceeding 100% in the 2011 PbSe quantum dot device by Semonin et al. is significant experimental evidence for this physics. This result is not an energy conversion efficiency exceeding 100%: EQE measures the number of charge carriers collected per photon, while power efficiency measures the ratio of output energy to input energy. [T22]

This distinction is often necessary when reading news about new materials. The energy of a photon can be much larger than twice the band gap; the creation of two electron-hole pairs does not violate energy conservation. On the other hand, carrier multiplication must occur over a sufficient portion of the solar spectrum, and the excess charge carriers produced must be rapidly removed. Impressive quantum efficiency at a narrow wavelength does not compensate for low module efficiency over a broad spectrum.

Kesterite and antimony chalcogenides: abundance and electronic quality

Kesterites, such as $Cu_2ZnSn(S,Se)_4$, are being investigated due to their chemical composition, which reduces the need for indium/gallium. However, the multi-component structure leads to numerous possibilities for atoms occupying incorrect lattice sites and the formation of secondary phases. In 2013, Han et al. presented a hybrid functional study that computationally discussed specific deep trap candidates and doping sources within CZTS. This is a prediction of a defect mechanism; it is not, in itself, a measurement of the defect distribution in any real film. [T23]

In layered crystals such as Sb_2Se_3, anisotropic transport and crystal orientation are important. Zhou et al.'s 2015 study demonstrated the relationship between oriented growth and device behavior, and suggested that certain grain boundaries may be less detrimental. The positive material attributes mentioned in the article should not be directly translated into safety regulations applicable to all usage and exposure conditions. Elemental abundance, toxicity, process hazards, and device emissions are separate concerns. [T24]

When selecting an improved absorber, it is beneficial to ask three questions in sequence: Can a real and well-defined phase be produced? Does it maintain charge carriers for a sufficient duration while absorbing enough light? Are these properties maintained under contact, large area, and operating voltage? Only a calculated, suitable band gap addresses a small part of this chain. Progress lies in making visible which link in the chain is causing the failure.

The geometry linking exciton diffusion and charge transport

In an organic absorber, light-induced excitation can initially form a bound exciton, followed by free electrons and holes. Within the exciton's lifetime, it must reach a suitable donor-acceptor interface. For this purpose, the characteristic distance $L_{ex} = \sqrt{(D_{ex} \tau_{ex})}$ is considered. If the areas are very large, some excitations may decay before reaching the interface. If the areas are very small and irregular, the interconnected transport paths for free charges extending to the electrodes may be disrupted.

Therefore, the optimum morphology is not simply "maximum interface area." Sufficient proximity for exciton dissociation, distinct pathways with continuity for electrons and holes, and low recombination are all required together. Facilitating charge transfer by increasing the energy level difference is also not without cost; the available voltage may decrease. In the evaluation of current organic devices, energy loss, morphology, non-radiative transitions, and stability are therefore discussed together. [T20]

In a dye-sensitized cell, the fundamental distinction is made in a different way: the dye absorbs light, injects an electron into the oxide transport network, and the dye is then reduced. Regeneration competes with undesirable back transfer. In a quantum dot film, however, the energy levels, which are adjusted by the nanocrystal size, are considered together with the electronic coupling between neighboring dots and the surface ligands. A dot that exhibits high photoluminescence in solution does not automatically provide good transport in a solid device. [T21] [T22]

Self-assessment

1. Why does continuously increasing the donor/acceptor interface area in an organic film not lead to unlimited gain? **Answer:** The transport networks, molecular order, and recombination also change; the arrival at the interface and the arrival at the electrode are considered together.

2. If EQE is 110%, is the cell's energy-conversion efficiency also 110%? **Answer:** No. The former describes charge generation relative to photon number; the latter is an energy ratio.

3. If an absorber is made of abundant elements, why might it not be low-cost? **Answer:** Purification, difficult phase control, low manufacturing yield, expensive contacts, short lifetime, or complex process costs may be dominant factors.

BOOK I · CHAPTER 16 / MATERIALS AND DEVICES

Optical, contact, and interface engineering: the common language of all technologies

There are three fundamental pathways for a photon

When light strikes a layer, it can be **reflected**, **transmitted**, or **absorbed**. At a fixed wavelength, energy conservation requires that the sum of these fractions equals one. In a stack of layers, the absorption of each layer is summed separately. The charge generated in the absorber can be useful; however, absorption that converts into heat in the metal or contact is mostly parasitic. Therefore, the dark appearance of the cell is not sufficient evidence for high efficiency.

The **refractive index** is an optical quantity that determines the phase velocity of light in a material and its behavior at the interface. In thin films, waves reflected from different surfaces can reinforce or cancel each other out. This phenomenon is called **interference**. An anti-reflection coating can be designed to minimize reflections at a specific wavelength and angle of incidence. However, when considering the entire solar spectrum, all angles, and actual absorption, a single ideal thickness does not solve all conditions.

How can passivation and carrier transport be integrated?

Chemical passivation reduces the density of active dangling bonds. **Field-effect passivation** establishes an electric field that reduces the access of one type of charge carrier to the defective surface. Both methods can be used together. **Contact resistance** describes the electrical cost of traversing the interface, as opposed to the bulk resistance within the material. A small-area contact can leave a very well-passivated surface; however, current crowding and increased resistance loss may occur in the remaining open areas.

Synthetic example: If a coating modification increases the short-circuit current (2%) while other effects on the voltage-current characteristics at maximum power collectively decrease it (3%), the power decreases to approximately $1.02 \times 0.97 = 0.9894$. The result is approximately a 1.06% loss. While it may be true that “we achieved optical gain,” this is not the same as “we improved the cell.” We must specify the metric of the gain each time.

The inputs for the models in this section are the real and imaginary parts of the refractive index, thickness, surface texture, and contact properties. The **imaginary part** of the refractive index is the mathematical component that represents the attenuation of light; it does not imply that the measurement is imaginary. The calculated electric field profile indicates where absorption occurs, and absorption, in turn, indicates the location of carrier generation. The subsequent electrical model calculates how much of these carriers can be collected.

Comprehension check: total absorption increased

If the total absorption increases from 90% to 94%, determine in which layer the new four points are located. If the absorption occurs in the metal or transport layer, the current may not increase. By examining the spectral EQE, reflectance, and optical calculations on a layer-by-layer basis, it becomes possible to distinguish between beneficial absorption and parasitic heat.

Create a balance sheet to track where the photons go

For each wavelength of optical power incident on a cell, the power is distributed among reflection, transmission, and absorption within the layers. The approximate energy balance takes the form $R + T + \sum_j A_j = 1$. R represents reflection, T represents transmission, and A_j represents the fraction absorbed in the j-th layer. The portion that is useful is the fraction that can be converted into electrical power within the absorber; absorption within the metal or TCO is mostly a parasitic loss.

An anti-reflection coating does not necessarily have to increase the cell current in the same proportion as it reduces reflection. The new coating may absorb at shorter wavelengths or direct more photons to regions with lower collection efficiency. The initial experimental closure involves the consistency of these three measurements: spectral reflection/transmission, EQE, and short-circuit current under illumination. The difference between the current calculated from the integral of the EQE with the solar photon flux and the electrical measurement should be investigated, including calibration and area-related issues.

The complex refractive index of a layer is written as $\tilde{n} = n + i\kappa$. n determines the phase advance, and κ determines the absorption; in the relation $\alpha = 4\pi\kappa/\lambda$, the wavelength and length units must be consistent. For thin and uniform stacks, the transfer matrix method is suitable; for complex textures, electromagnetic or ray-tracing approaches are appropriate. Simply taking optical constants from a catalog may conceal the actual differences in density, composition, and roughness of the film.

Light trapping and the cost of surface area

The 1982 analysis by Yablonovitch and Cody is a foundational framework for explaining optical-path enhancement in a thin absorber under suitable ray-optics and randomization assumptions. The familiar ^{2} expression follows from specific ideal light-trapping conditions. It is not an unconditional gain coefficient for every nanopattern, a universal bound for every thickness, or a direct efficiency multiplier. [T25]

Texturing can enable light to travel a longer path inside the material; at the same time, it can increase the actual surface area and make passivation more difficult. If the nanostructure reduces short-wavelength reflection very effectively but also increases surface recombination, the electrical gain can be nullified. Therefore, providing only the number of absorbed photons as the target for optical optimization is misleading. The target should be the maximum power, which is linked to the carrier transport and recombination model.

Solved example. Let a surface modification increase the J_{sc} value from 40 to 41 mA/cm^2 while decreasing the V_{oc} value from 0.72 to 0.70 V; let FF = 0.82 and the input be kept constant at 100 mW/cm^2. The initial power is $40 \times 0{,}72 \times 0{,}82 = 23{,}616$ mW/cm^2; the second power is $41 \times 0{,}70 \times 0{,}82 = 23{,}534$ mW/cm^2. In this example, better optics do not necessarily mean a better cell. The efficiency decreases by approximately 0.082 percentage points.

Contact selectivity: different gateways for the two carriers

A good electron contact allows electrons to exit with low resistance and prevents holes from recombining there. A good hole contact does the opposite. The appropriate work function of a metal serves as an initial indicator; however, at the actual interface, chemical bonds, dipoles, defects, and Fermi level pinning can alter the simple vacuum alignment. Furthermore, under operating conditions, the interface can transform into a different interface over time due to ion migration or diffusion.

The band offset, in itself, is neither good nor bad. A barrier for minority charge carriers can be beneficial, while an excessive barrier for majority charge carriers can be detrimental. A thick thermal barrier combined with a thin tunneling layer will not carry the same current. The evaluation of electrical contact requires considering both the contact-specific resistance and the recombination efficiency. Simply measuring low resistance does not prove that the contact is selective.

Relating voltage loss to luminescence establishes a strong link between the material and the device. Rau's 2007 reciprocity study established the connection between photovoltaic quantum efficiency and electroluminescence under appropriate

assumptions. The non-radiative loss at a fixed radiative reference is expressed as approximately $\Delta V_{\mathrm{nr}} = -(kT/q)\ln \eta_{\mathrm{ext}}$; η_{ext} is the corresponding external luminescence efficiency. The optical reference and operating conditions used must be specified. [T26]

At 298.15 K, increasing the external luminescence efficiency from 10^{-4} to 10^{-3} corresponds to approximately 59 mV less nonradiative voltage loss if the other conditions remain fixed. This alone does not mean that the cell's open-circuit voltage will increase by exactly 59 mV; contact losses, injection level and the optical reference may also have changed. The quasi-Fermi-level splitting measured in a film must be distinguished from the finished device's qV_{oc}. Their difference can provide a research clue about carrier extraction and contact problems.

Do not rely solely on a single graph for diagnosis

An S-shaped current-voltage curve may indicate a carrier-extraction barrier; it should be considered in conjunction with high series resistance, non-photoactive areas, or complex interface behavior. Low shunt resistance suggests a short-circuit-like path; spatial imaging can reveal where it occurs. PL enhancement sometimes reflects defect reduction, and sometimes the inhibition of charge carrier extraction. Examining the same sample under open-circuit and load conditions supports this distinction.

The strongest evidence comes from a variable consistently leaving a traceable mark across different observations. For example, the passivation hypothesis can be supported by increased lifetime, luminescence gain, and voltage increase upon appropriate injection. Conversely, a single surface chemistry measurement alone does not fully explain the device mechanism. Statistical repetition and independent calibration are important, especially for claims of only a few tens of millivolts or a few tenths of a percentage point.

Calculating an antireflection layer

Considering normal incidence and assuming three lossless media: air with refractive index n0, a coating with refractive index n1 and thickness d, and a semi-infinite substrate with refractive index n2. At a single interface, the amplitude of the electric field reflection is rij = (ni - nj)/(ni + nj). The phase change upon a single transmission through the layer is δ = 2πn1d/λ. When we sum the repeated reflections as a geometric series, we obtain the total amplitude and power reflection:

$$r = \frac{r_{01} + r_{12}\exp(2i\delta)}{1 + r_{01}r_{12}\exp(2i\delta)}, \qquad R = |r|^2. \tag{I.16.1}$$

When the quarter-wave condition is met, i.e., d = λ0/(4n1), the phase difference between the two reflections is π. To equalize their amplitudes, an ideal n1 is chosen to be approximately the square root of (n0n2). In the example, n0 = 1, n1 = 2, n2 = 3.5, and d = 75 nm were used. At 600 nm, the reflection without coating is approximately 30.86%, while the reflection with coating is approximately 0.444%. This is a result of using only a single wavelength and the specified fixed refractive indices; in reality, the refractive indices vary with wavelength.

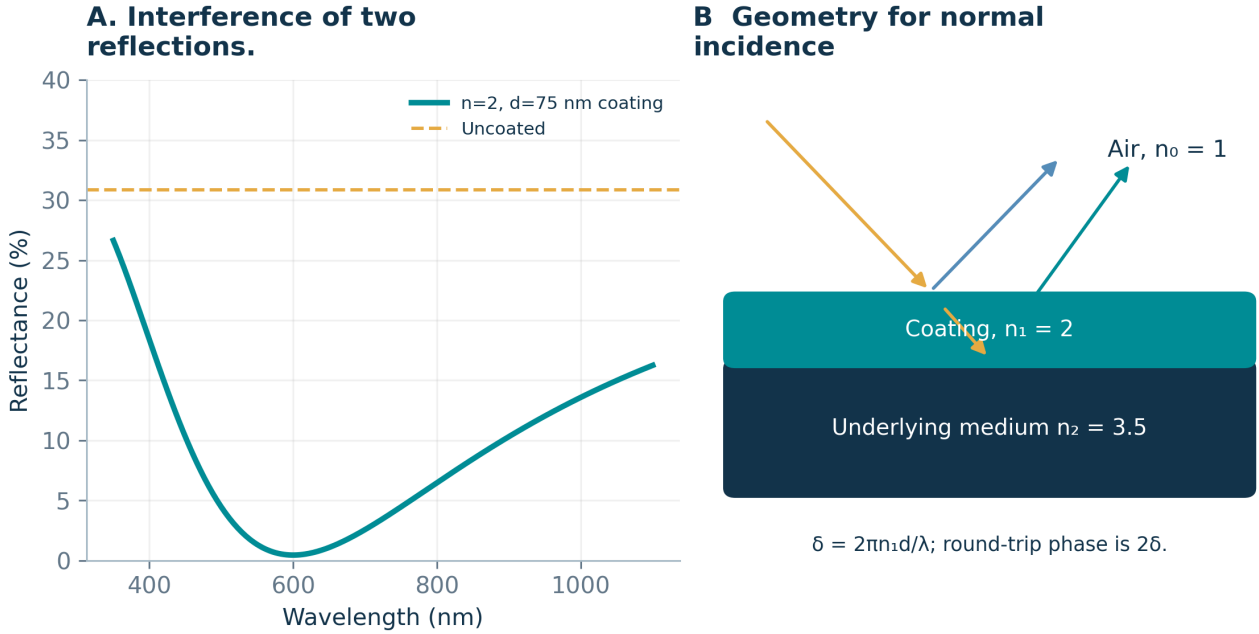


Figure 27. Interference-based reflection reduction. The curve was recalculated from the written amplitude formula. The fact that reflection is very small at one wavelength does not guarantee the same gain across the entire solar spectrum. Panel B illustrates the layer geometry; the angled arrows are for readability, and the calculation is for normal incidence. [B09]

In a multilayer structure, the forward and backward wave amplitudes in each layer are interconnected through boundary conditions and propagation phases. This approach forms the basis of the transfer matrix method. Instead of maintaining coherent interference in optically thick or phase-randomized layers, an appropriate incoherent process is required. It is also incorrect to assume that power transfer in absorbing media depends solely on the square of the field amplitude; the optical flux of the medium must be taken into account. [B09]

The output of the optical model for the device model

If the locally absorbed power density within a film is known, the volumetric generation can be found by dividing it by the corresponding photon energy. This process is integrated over all wavelengths. The result, G(x), is the input for the drift-diffusion model. However, it would be incorrect to add the photons absorbed in the transport layer to the active absorber generation. The optical energy budget should be R + T + total Aj = 1; which Aj contributes to electrical power generation is specified separately.

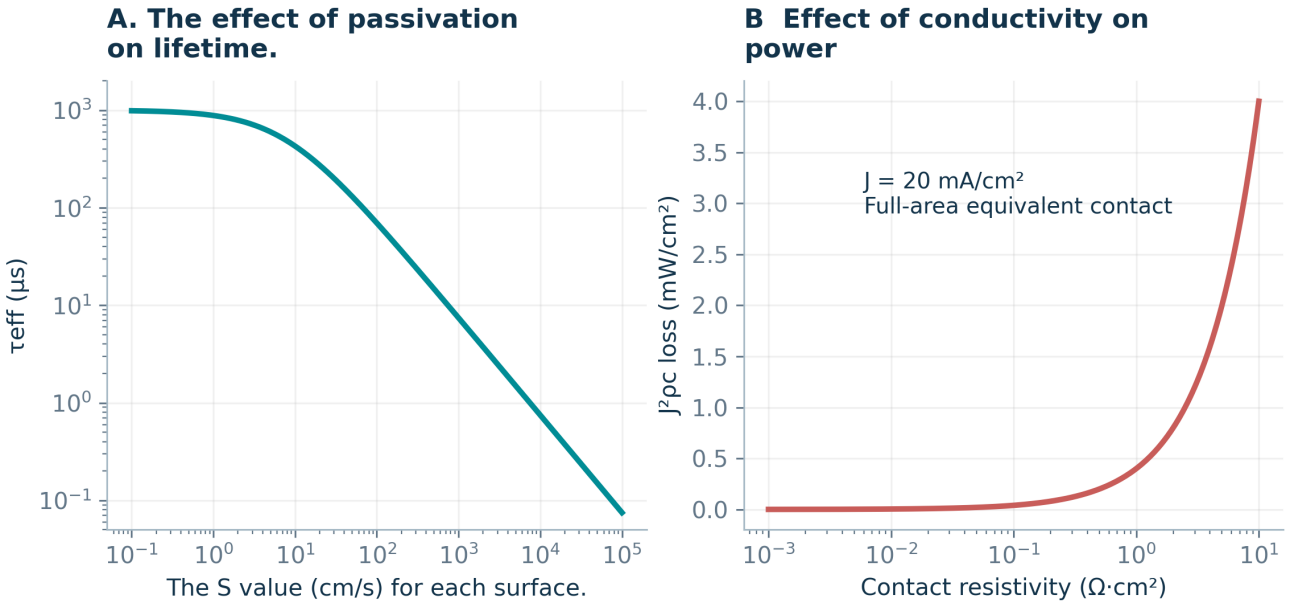


Figure 28. Passivation and conductivity are two distinct design targets. On the left, as S decreases in a 150 µm thick wafer with two equivalent surfaces, the effective lifetime approaches the bulk limit. On the right, the power cost of contact resistance at a constant current is shown. A good contact should be suitable on both axes. Analytical teaching models. [H20] [H21]

Self-assessment

1. The new coating increased the total absorption; however, the current did not increase. What is the first thing to check? **Answer:** Check in which layer the additional absorption is occurring and whether charge carriers are collected from that region.

2. The contact resistance is very low, and the voltage is also low. Is the contact good? **Answer:** Not necessarily; it may be strongly recombining minority charge carriers while allowing majority charge carriers to pass through.

3. With the same radiative reference, if external luminescence efficiency increases by a factor of 100, by how much does nonradiative voltage loss decrease at 25 °C? **Answer:** Approximately $25{,}69 \ln 100 = 118{,}3$ mV.

BOOK I · CHAPTER 17 / MATERIALS AND DEVICES

From the laboratory to the module: area, encapsulation, and sustainable production

What new elements are added when transitioning from cell to module?

A bare cell is not a finished product that can withstand external conditions for years. The **module** brings together electrically connected cells, a glass or other front sheet, interlayer polymers, back protection, and a junction box. **Encapsulation** is the process of protecting the active device within this package. **Lamination** is the integration of layers through a process dependent on temperature, pressure, and time. Electrical insulation, mechanical adhesion, and moisture permeability are as important as optical transmittance.

In a **series connection**, the same current flows through the cells in sequence; the voltages add up. In a **parallel connection**, the terminal voltage is common, and the branch currents are summed. When cells with unequal characteristics are connected, the weaker or shaded section can limit the others. A **bypass diode**, with appropriate design, redirects the current path of a specific cell group when necessary. It is not a material that increases the cell's efficiency; it is a circuit element that helps manage the effects of shading and reverse polarity.

Which area is used to define the efficiency?

The **active area** is the defined region that utilizes light for electrical generation. The **aperture area** is the opening through which light passes in a mask, and it determines the denominator of the measurement. The **total area** is the defined outer area of the product, including edges and non-functional spaces. The areas may not be consistent from one article to another. As the denominator decreases, the percentage reported for the same power increases; however, the physical power does not actually increase.

Synthetic example: If 8 W is measured in a cell area of 0.04 m^2, and the irradiance is 1000 W/m^2, then the efficiency with respect to the cell area is 20%. If the total area of the product, including the spacing between junctions and the frame, is 0.05 m^2, then the same power yields 16% with respect to the total area. We have not yet added any additional electrical or optical losses; the difference arises solely from the geometry.

Water vapor permeability is a property that describes how quickly water can pass through the encapsulant material; it is not an absolute label like “waterproof.” Edge sealing, temperature, and humidity differences also affect ingress. If different layers have different thermal expansion coefficients, daily heating and cooling can create stress. Therefore, the encapsulant is not just a cover, but a mechanical and chemical system that affects the device’s lifespan.

When assessing sustainability, the elements contained in the cell, the energy and solvents used in production, emissions in case of failure, disassembly, and recycling are all considered as separate steps. Using a small amount of a material does not, in itself, necessarily mean that its overall environmental impact is small.

Comprehension check: the small cell is functional, the module is not

Account separately for aperture area, intercell spacing, interconnection resistance, cell matching, and optical changes within the package. These can deteriorate while the efficiency of the cell measured on its own remains unchanged. Trying to improve the module solely by changing absorber chemistry can miss the scale at which the loss occurs.

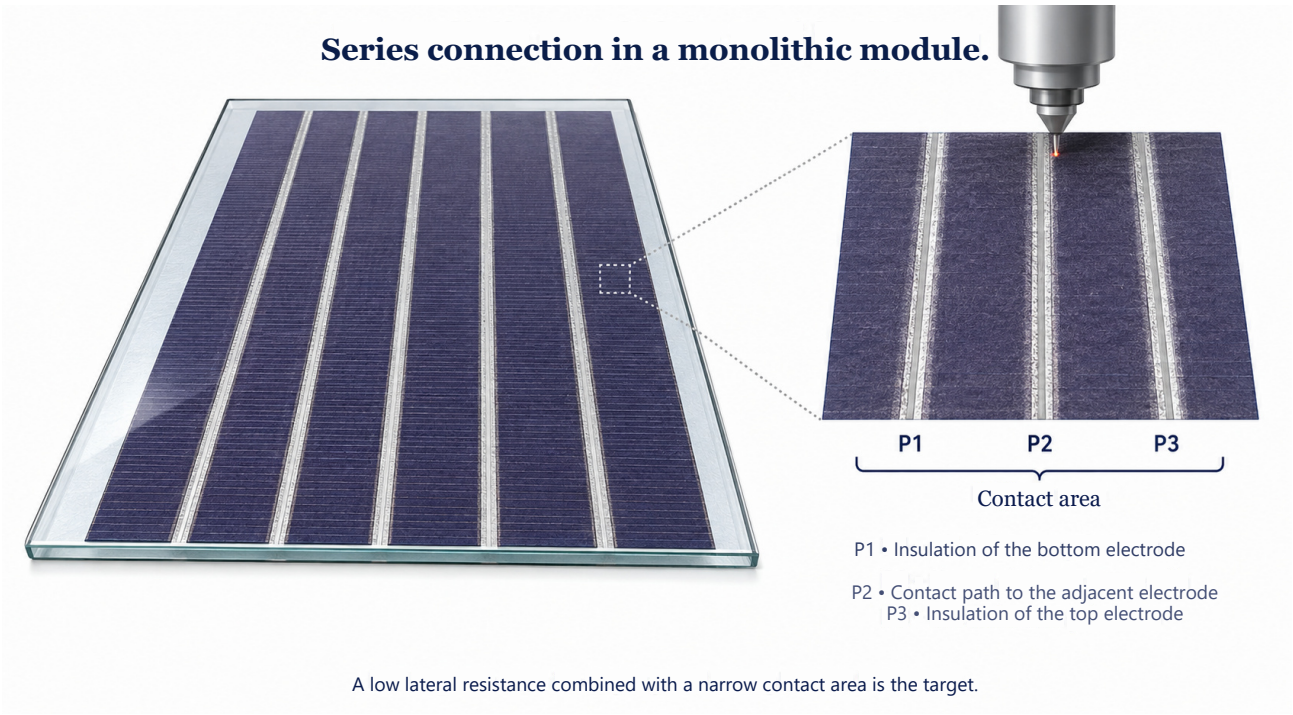


Figure 29. Cell stripes and interconnection traces in a monolithic thin-film module. The top view illustrates the different functions of steps P1, P2, and P3, as well as the inactive interconnection area; it is not a production cross-section showing the scratch depths of the layers. The lines and stripe widths are representative. The following panel calculates the numerical trade-off between geometric fill factor and lateral resistance. [T29] [R34] Conceptual illustration prepared with an image-generation tool; it is not a measurement image.

Stripe width, area loss and resistive loss

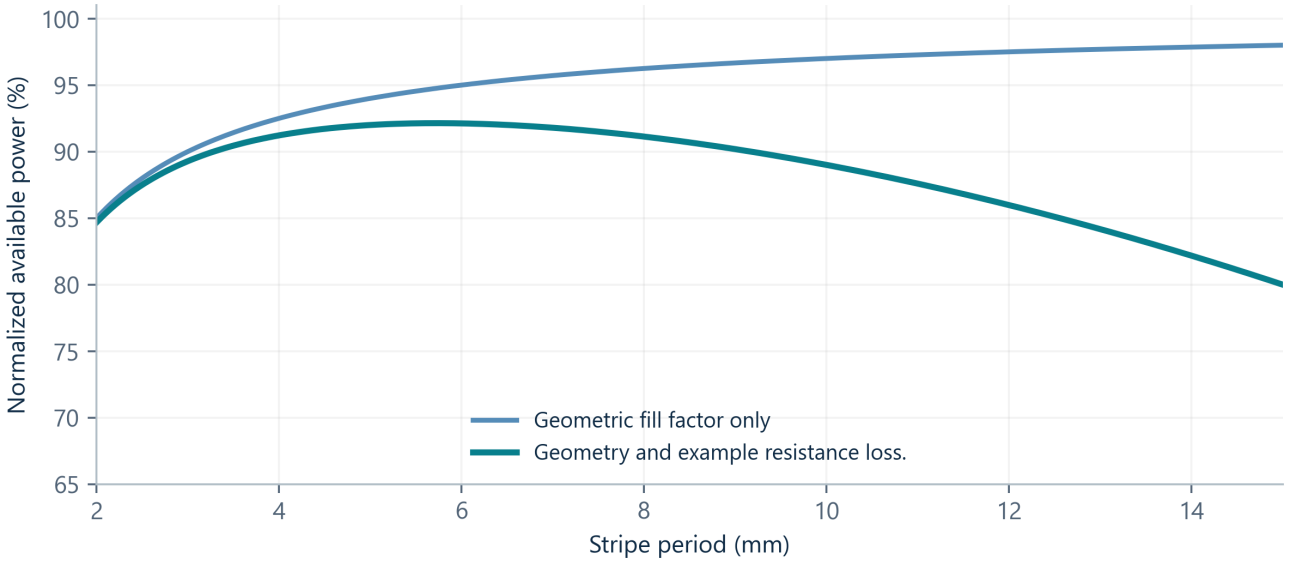


Figure 29 - calculated supplementary panel. The inactive width is 0.3 mm, and the sample resistance loss is assumed to be proportional to the square of the period. A wider stripe increases the geometric fill factor while also increasing the lateral collection loss. The numerically optimal value is not a production recipe or a universal design dimension for a product. [T29] [R34]

Scaling up is not simply about coating a larger film

In a small cell, a single clean area can be selected; in a large area, the probability of encountering thickness variations, dust, scratches, uncoated spots, edges, and connection lines increases. As the cell area increases, the horizontal current path lengthens, and the resistance loss in the transparent electrode may increase. Therefore, thin-film modules are manufactured with patterns that connect smaller sub-cells in series. The pattern consumes active area while reducing electrical loss.

Spin coating is a powerful tool in small-sample research; however, it is not a natural equivalent for large-scale production in terms of material utilization and area geometry. Blade coating, slot-die coating, and vapor-phase processes introduce different control variables. In liquid coating, wetting, flow, drying, and crystallization are managed together. In vacuum processes, source flux, composition control, substrate temperature, and area uniformity become critical. No single method is superior to the others in all circumstances.

Deng and colleagues' 2018 study demonstrated that even a small amount of surface-active component can alter the drying flow and coating behavior. In the same study, results for small cells and larger modules were reported separately. This example illustrates that, instead of directly scaling up the laboratory recipe, it is necessary to revisit and resolve the physics of flow and film formation. [T27]

Active area and aperture area

In a monolithic interconnection, the idealized geometric fill factor can be expressed as $GFF = w/(w + s)$. w represents the effective cell strip width, and s is the total strip width lost for interconnection and insulation. A narrower cell strip can reduce horizontal resistance loss, but it also increases the geometric loss for the same interconnection width. The optimum value is determined by considering both factors together.

Solved example. For $w = 5$ mm and $s = 0{,}5$ mm, the result is $GFF = 0{,}909$. If 25% cell efficiency is assumed for the active regions, then only considering this geometric effect, the aperture efficiency is at most approximately 22.73%. Additional optical and electrical module losses have not yet been added. Therefore, applying the small active area efficiency to the product's outer dimensions overestimates the power.

The defect statistics also vary with area. In the simple Poisson model of independent and uniformly distributed lethal defects, the probability of a defect-free device is $Y = \exp(-DA)$. D is the density of lethal defects per unit area, and A is the device area. If $D = 0{,}001$ cm^{-2} is assumed, then for 100 cm², $Y \approx 0{,}905$ is obtained, and for 1000 cm², $Y \approx 0{,}368$ is obtained. Real defects can cluster, and some can be repaired; this model is not a production forecast but rather a starting point that demonstrates the scale effect.

Encapsulation seals out the environment; do not assume it leaves the internal physics unchanged

Glass, polymer, edge sealing, and barrier layers reduce moisture/oxygen ingress. However, during encapsulation, temperature, pressure, and thermal expansion mismatch are also applied to the device. The weak interface between the absorber and the electrode can delaminate; optical properties can change; and volatile products formed inside can remain trapped within the enclosed volume. A better external barrier is not a solution for all internal degradation mechanisms.

Mariani and colleagues' original 2024 study investigated the importance of low-temperature and low-stress encapsulation for cell and module reliability using different accelerated aging methods. Such a result is evidence for specific batches, encapsulation, and test conditions. Passing an accelerated test alone does not prove a lifespan of decades in another climate. [T30]

The free length change for thermal expansion is in the form of $\Delta L = \alpha_T L \Delta T$. α_T is the coefficient of thermal expansion. If two layers are bonded, their different free expansions create interface stress. Therefore, when selecting materials, it is important to consider not only water vapor permeability but also elastic properties, adhesion

energy, temperature dependence, and changes under UV radiation. A repeated bending test can also demonstrate the combined effect of cracking and chemical degradation in a flexible product.

Toxic element, emission, and recovery

The total mass of a hazardous element within the device is not the exposure itself, but it is also not information that can be ignored. The source and rate of release are investigated in normal operation, breakage, fire, contact with water, and end-of-life scenarios. Before a material is labeled as "environmentally friendly," the different pathways in the production, user, and waste chain must be identified.

Li and colleagues' 2020 study experimentally investigated the possibility of adding a lead-retention function to a perovskite device. This demonstrates an engineering approach that goes beyond simply reducing the total amount of lead. The success of lead retention in a specific damage test does not represent a solution for all damage and waste scenarios; the escaped mass, retention capacity, time, and test environment should be reported. [T28]

Recovering a large amount of glass by weight during recycling and recovering a small amount of metals that are economically or environmentally significant are different targets. Strong adhesion supports a long lifetime but can make it difficult to separate the layers at the end of their use. If a detachable connection, material traceability, and the separability of valuable layers are considered from the beginning in the design, the end-of-life options will be expanded. Conversely, if the field lifetime is shortened in pursuit of ease of recycling, the overall result may worsen.

Instead of considering the cost per watt, think in terms of lifetime energy

A simple material density calculation tests the scale claims. If the hypothetical silver consumption is 10 mg/W, then producing 1 TW of cells per year would require 10,000 tons of silver. This is not a measure of current industrial consumption; it is merely a unit conversion. The fact that a candidate material is inexpensive in a few-gram experiment does not mean that it will have the same supply logic at the terawatt scale. Silver reduction or copper usage is evaluated together with contact quality, diffusion, corrosion, and process cost.

In most cases, the functional unit of a life cycle analysis is the delivered kWh. The production of electricity, material inputs, transportation, installation, maintenance, degradation, lifetime, and end-of-life boundaries should be specified. The IEA PVPS 2020 methodology guide emphasizes these common definitions for evaluating different

PV technologies with consistent assumptions. A good environmental comparison does not only consider the cell's production temperature. [T29]

Illustrative decision example. Module A should generate more energy in the first year in the same area (10%); however, it should have a high production load and lifetime uncertainty. Module B should have a lower initial performance but a longer, proven operational history. The choice cannot be made solely based on initial efficiency: a sensitivity analysis is required based on annual energy reduction, the need for replacement, and the expected service life. The research value of the new technology may be high; its commercial advantage may not yet be proven.

The trade-off between stripe width and series loss

In a monolithic thin-film module, the cells are divided into strips that are connected in series. P1 electrically separates the bottom electrode; P2 creates a path for contact between the layers; P3 isolates the top electrode and active stack from the adjacent strip. The actual scribing sequence and laser process depend on the material system. The main goal is to connect the back electrode of one strip to the front electrode of its neighbor and to prevent unwanted short circuits.

The width of the dead zone is denoted by b, and the stripe period is denoted by s; therefore, the geometric fill factor is approximately 1 - b/s. As s increases, the dead area ratio decreases; however, the carriers travel a longer distance within the transparent electrode. In simple models, the lateral resistance loss increases with s^2. The maximum of the figure arises from the competition between these two effects. No manufacturing dimension should be selected from the graph before both coefficients have been remeasured for the actual optical/electrical stack.

Encapsulation is a mechanical and chemical system

While minimizing water and oxygen permeation is important, encapsulation is not simply an “airtight cover.” The thermal expansion of glass, adhesive, cells, and the back sheet differs. Temperature cycles can create shear stress and connection fatigue. The geometry of the edge seal affects the path water takes. Some degradation products or ions may move under electrical polarization. Therefore, in a stability test, the packaging, edge design, and electrical operating point are part of the device. [T30] [R15]

When a laboratory result is transferred to a module, the repeatability of the process and the defect statistics also change. A short-circuit defect, which is rare in a 1 cm^2 sample, becomes more likely in an area of hundreds of cm^2. Even if the average coating thickness is accurate, the tail of the distribution can determine the yield or reliability.

Therefore, a scale-up study monitors not only the average performance but also the spatial maps, the failure rate of samples, and the variation between production batches.

In a thin-film module, what do P1, P2, and P3 do?

P1, P2, and P3 are the names of three patterning processes used in common monolithic thin-film module fabrication. In a typical glass-superstrate structure, P1 separates the bottom conductive layer between adjacent cell stripes. After the absorber layers are deposited, P2 opens the connection region, allowing the subsequent metal to reach the underlying conductor. After the top conductor is deposited, P3 separates the top contacts of adjacent stripes. Thus, the top contact of one stripe is connected to the bottom contact of the adjacent stripe, and the voltages are summed in series. The details may vary depending on the stacking direction; this description is not a single recipe for all technologies.

Cutting lines and alignment margins convert a portion of the light-receiving area into a **dead area** that does not generate electricity. A narrower pattern can leave more active area; however, the risk of alignment errors, unwanted short circuits, or incomplete separation must also be considered. Therefore, it is necessary to analyze not only the photograph of the module but also the pattern width and the electrical connection function. [T34]

In the packaging diagram, **EVA** is an encapsulant, specifically a polymer called ethylene-vinyl acetate; it is not the only encapsulant used. It provides mechanical bonding and optical transmission between the glass and the cell. Moisture, heat, and chemical reactions can cause this bond and permeability to change over time. **Edge sealing** is a structure that reduces the ingress of the environment, especially from the edges. “Homogeneity” indicates how similar the thickness and properties remain across the area; high average quality does not preclude failure caused by a single weak region.

Self-assessment

1. The active cell efficiency is 24%, and the geometric fill factor is 95%; what is the aperture efficiency after considering only the geometry? **Answer:** 22.8%; other losses have not yet been accounted for.

2. If an encapsulated cell passes the humidity test, does this mean that ion migration has been resolved? **Answer:** No. Ionic processes can continue within the encapsulation due to light, temperature, and voltage.

3. If the material consumption is 5 mg/W, how many tons of material are required for a 2 TW production? **Answer:** 10,000 tons. Multiply mg/W by watts; 1 ton = 10^9 mg.

Scope of the sources for these technology chapters

These chapters represent a teaching synthesis selected from original experimental and theoretical articles, as well as corporate method documents; they do not constitute a comprehensive survey of all PV literature. The source access date is September 7, 2026. Publisher summaries, open-access full texts, and corporate author copies were used in conjunction; articles for which only the abstract was accessible were not presented as if their inaccessible methods or additional data had been reviewed. Dated article results were not labeled as current world records. Numerical exercises are teaching examples derived from explicitly stated assumptions; they are not intended as predictions of candidate material or actual product performance.

Photovoltaic measurement: how the correct value is obtained

A measurement is, first and foremost, a comparison

Shining light on a cell and seeing 24% on the computer is not, by itself, a completed measurement. The displayed ratio depends on the current and voltage sensors, light setting, temperature, and entered area. **Calibration** relates the instrument indication to a known reference. **Traceability** is the documented connection of this reference to higher-level references. **Uncertainty** quantitatively describes the range of values reasonably attributable to the measured quantity. Assuming that “the instrument is correct because it is expensive” cannot replace the verification required by these three concepts.

A **solar simulator** is a light source designed to approximate a specific spectrum and irradiance in the laboratory. A **reference cell** helps to adjust the light with a device of known sensitivity. However, if the reference and test cells respond differently to different wavelengths, the same irradiance indicator does not guarantee the same photocurrent. This difference requires accounting for **spectral mismatch**. The time stability of the lamp and the light distribution in the sample area are also checked separately.

Are voltage and current measured using the same connection?

The **source-measure unit** applies a selected voltage or current and measures the corresponding value; the abbreviation SMU is used. During voltage sweeping, the cell may not immediately reach a stable state at each point. The **settling time** can be affected by the sweep direction and the previous illumination condition. In four-point probing, the cables carrying the current are separated from the cables sensing the voltage; thus, some voltage drops in the cable and contact path interfere less with the measured device voltage.

Synthetic example: When the cell provides 0.60 V and 1 A, the unwanted total resistance of 0.02 ohms in the current path creates a 0.02 V voltage drop. If we measure the voltage from the wrong point, we can calculate the cell's power with a difference of a few percent. This small voltage difference can be greater than the claimed gain of the new material. Therefore, it is risky to interpret the results without understanding the measurement geometry.

Repeatability refers to the closeness of measurements taken under the same conditions. An instrument may consistently display the same error; similar results alone do not constitute proof of accuracy. **Bias** is the effect that systematically shifts the

measurement in one direction. Measuring the same cell five times assesses measurement repeatability, while producing and measuring five independent cells investigates process variability. The uncertainty budget below will explain how these different sources contribute to the overall uncertainty.

Comprehension check: Is it an increase in efficiency, or a change in the denominator?

When a smaller area is entered in the software while the current-voltage data remains the same, the efficiency increases. The physical power has not changed. When comparing old and new results, monitor the raw power, area mask, irradiance, and sample temperature together. The denominator of the measurement is as much a part of the experiment as the numerator.

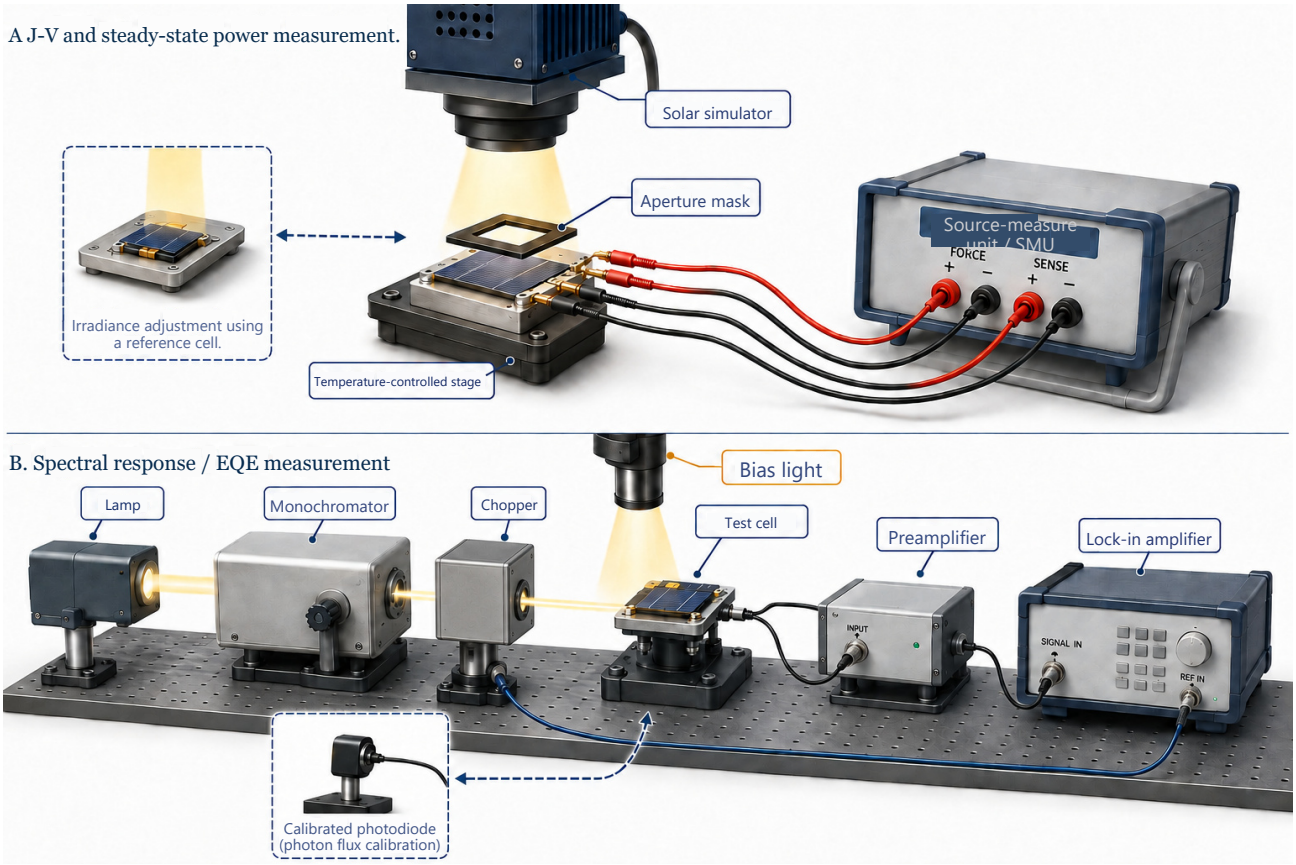


Figure 30. Two complementary measurement setups. The J-V and MPP measurements provide the total power of the device; the EQE measurement examines the origin of the current by separating the photon flux by wavelength. Reference calibration, temperature, area, and bias conditions are part of the setup. Original functional diagrams. [R01] [R02] Conceptual illustration prepared with an image-generation tool; it is not a measurement image.

The efficiency of a solar cell is not solely a characteristic of the device; it is the result produced by the combined effects of clearly defined illumination, area, temperature, electrical history, and the measurement method. Therefore, the researcher's initial question should not be "What percentage?" Instead, the questions should be: "Which device, under which conditions, with which area definition, for how long, and with what uncertainty?" The optical absorption of a material, the photoluminescence of a

film, and the electrical efficiency of a completed device are all different observables. Presenting them within the same graph does not make them interchangeable.

Reading the current-voltage curve as a physical measurement

The current-voltage curve is written as I-V, and the current density-voltage curve is written as J-V. In short-circuit conditions, the voltage is zero, and the measured quantity is I_sc or J_sc. In open-circuit conditions, the external circuit current is zero, and V_oc is measured. The maximum power point is the operating point that maximizes the V × I product in the generation region. It should be noted that the generation current is recorded as negative in some devices; the following equations use the positive magnitude of the generated power.

$$P_{\max} = V_{\mathrm{mpp}} I_{\mathrm{mpp}} \qquad [\mathrm{W}] \tag{I.18.1}$$

$$FF = \frac{P_{\max}}{V_{\mathrm{oc}} I_{\mathrm{sc}}} \qquad (\mathrm{dimensionless}) \tag{I.18.2}$$

$$\eta = \frac{P_{\max}}{G A} \qquad (\mathrm{dimensionless}) \tag{I.18.3}$$

Here, G represents the irradiance [W/m²], A is the specified measurement area [m²], and η is the power conversion efficiency. If J_sc is used, the area definition must remain consistent throughout the calculations. IEC 60904-1 defines the I-V measurement scope for PV devices under natural or simulated sunlight; in this resource, the cell, cell sub-assembly, and module are considered together. The standard's detailed description explicitly states that area measurement, capacitive devices, dark I-V, and spatial illumination non-uniformity are also addressed. This instructional description does not replace the licensed full text of the standard. [R01]

For example, let V_oc = 1.10 V, J_sc = 24.0 mA/cm², and FF = 0.80. When the incident power density is 100 mW/cm², the output is 1.10 × 24.0 × 0.80 = 21.12 mW/cm², and therefore the efficiency is 21.12%. This product serves as a measurable consistency check: if the four numbers in the paper are inconsistent, rounding, area conversion, or table transfer should be investigated. It should also be remembered that the maximum selected from several good points on the curve may be shifted upwards due to noise; appropriate resolution, repetition, and stable operating measurements are required.

Why are area, spectrum, and temperature equally important?

The active area, the region defined by the electrodes, the mask aperture, and the total area of the device are not the same. The collection of light from the unmasked edges, the mask's slope, thickness, and spacing from the sample can introduce significant errors in small devices. The nominal electrode size drawn by the manufacturer should not be used in place of the measured aperture area. The mask's image, dimensions, measurement method, and which area is used in the calculation should be added to the measurement record. The distinction between the total area, the aperture area, and the defined illumination area is also central to the comparison rules in validated efficiency tables. [R37]

Consider the following example: the actual aperture is 0.100 cm^2, the incorrectly used area is 0.095 cm^2, and the measured maximum power is 2.00 mW. The correct efficiency is 20.0%, while the efficiency with the incorrect area is 21.05%. The area reduction of 5% alone resulted in an approximate 1.05 absolute percentage point "improvement." A higher current density alone does not necessarily mean a better semiconductor.

AM1.5G is a spectral reference; the term "1 sun" alone does not specify the spectral shape. A lamp may emit a total of 1000 W/m^2, but it may produce excessive light in one region and insufficient light in another region, where the device absorbs. If the calibration cell and the test device have different spectral responses, the same total irradiance does not guarantee an accurate comparison. Spectral mismatch correction uses the reference spectrum, the simulator spectrum, and the responses of the reference cell and the test device together. It should be stated whether the correction factor is defined as a multiplier or a divisor; a factor obtained from other software should not be applied blindly. NREL's spectral error report examines this issue in the context of GaInAs-based concentrator cells; the lesson learned here is the general principle of spectral mismatch. [R03]

For example, the temperature of the device plane may differ from the temperature of the holder. The lamp heating the sample, the weakness of thermal contact, and the location of the temperature sensor alter the measurement. If the reference is 25 °C, a measurement of 300 K is not the same condition: 25 °C is exactly 298.15 K. If a temperature correction is to be used, the coefficient must be verified for the same technology and within the relevant temperature range. In particular, in multijunction structures, the spectral distribution affects the current of each sub-cell separately; a single reference cell may not provide sufficient calibration information.

Cross-check using EQE and maximum power tracking

The external quantum efficiency EQE(λ) is the ratio of the number of electrons collected from the external circuit per photon incident on the device at a specific wavelength. Its relationship with the spectral response SR [A/W] is given by EQE = SR × h × c / (q × λ), where λ is expressed in meters. The current integrated with the reference photon flux is calculated as follows:

$$J_{\mathrm{sc,EQE}} = q \int \mathrm{EQE}(\lambda)\, \Phi_{\lambda}(\lambda)\, d\lambda \qquad [\mathrm{A/m^2}] \tag{I.18.4}$$

Φ_λ is the photon flux per unit wavelength, time, and area. If spectral data based on nanometers and meters are mixed, it can lead to errors of billions of units. In EQE measurements, the light bias, electrical bias, beam size, and linear response condition are recorded. To measure the sub-cells in series tandems, the other junctions must be biased with appropriate light. The explicit scope of IEC 60904-8 includes the spectral response of linear and non-linear PV devices. [R02]

If J_sc,EQE and the J-V current do not agree, the first explanation is not necessarily “new physics.” First, the area, spectrum, calibration, wavelength range, sample history, and changes under illumination are checked. A lower EQE current may be due to incomplete scanning of the near-infrared region during measurement, a different operating point, or changes in the device over time. EQE also indicates in which spectral region the loss occurs, but it does not, on its own, definitively determine whether the loss is due to absorption or collection.

In devices with slow ionic and capacitive processes, the scanning direction, step size, waiting time at each step, initial voltage, and pre-conditioning affect the J-V curve. The apparent symmetry between forward and reverse scans does not prove the absence of ion movement; ion migration has been experimentally demonstrated in low-hysteresis perovskites. [R14] Therefore, power is monitored over time under appropriate maximum power point tracking. While a stable current at a constant voltage is a useful aid, it is not sufficient if the actual maximum power point is shifting. The delay of the tracking algorithm must be distinguished from the relaxation of the device.

Calculate the uncertainty along with the result

Repeatability is the repeated measurement spread of the device; calibration error may not be included in this. The measurement uncertainty budget includes power measurement, area, irradiance, spectral correction, temperature, and related correlations. For independent small relative uncertainties, it is approximately written as $u_r(\eta)^2 = u_r(P)^2 + u_r(G)^2 + u_r(A)^2$. If there is no independence, covariance terms are added. NIST’s description of uncertainty combination defines this first-order approximation and sensitivity coefficients. [R04]

In the original example, let the standard relative uncertainties be 0.5% for power, 1.0% for irradiance, and 0.7% for area. The sum of the squares within the square root yields 1.319%. The standard absolute uncertainty for efficiency, 20.0%, is approximately 0.264 percentage points. If the U = 2u approach is appropriate, the expanded uncertainty is approximately 0.53 percentage points; the coverage factor and justification are also reported. In this case, the difference between 20.2% and 20.0% cannot be declared as an improvement simply by looking at the point values. If the two devices share the same calibration, the uncertainty of the difference is calculated separately; it may also be incorrect to sum each systematic contribution as if it were two independent errors.

Planning a measurement from start to finish

In a J-V measurement, define the physical object from the data file before proceeding: sample ID, active area, aperture mask, electrode geometry, and the direction of light incidence. The mask's shadow, scattered light, and charge carriers collected from outside the aperture can be significant in small samples. Instead of simply taking the area from the nominal mask design, it is necessary to record the measured size and uncertainty of the aperture used. For temperature, use the appropriate measurement related to the cell temperature, not the ambient air temperature.

After the device is aligned with the reference cell, it is evaluated whether the spectral response of the device differs from the reference. A four-point connection reduces the effect of voltage drop in the current cables on the voltage reading; however, it does not eliminate the cell's own contact resistance. The voltage range, scan direction, dwell time, and pre-conditioning selection are part of the data file. For a device that changes over time, stable tracking around the MPP is required instead of the peak of a single scan. [R01] [R02]

Derive the direction of the spectral mismatch correction

Let's denote the spectral current sensitivity for the test device as S(λ)t and for the reference device as S(λ)r. Let Eref be the reference spectrum, and Elamp be the unscaled spectrum of the lamp. When we adjust the lamp with a factor k so that it produces the same current in the reference cell as the standard spectrum, we have k = integral(Eref Sr) / integral(Elamp Sr). Therefore, the ratio of the current of the test device in the lamp to the current in the reference spectrum is:

$$M = \frac{\int E_{\mathrm{lamp}} S_t \, d\lambda}{\int E_{\mathrm{ref}} S_t \, d\lambda} \frac{\int E_{\mathrm{ref}} S_r \, d\lambda}{\int E_{\mathrm{lamp}} S_r \, d\lambda}. \tag{I.18.5}$$

According to this definition, if M > 1, the lamp test device oversupplies the reference condition; the current corresponding to the reference spectrum is found by dividing the measured current under appropriate linear conditions by M. Some sources define

the correction factor as the inverse of this. Describing the ratio in words instead of copying the symbol prevents errors in sign and direction. When deriving S sensitivity from EQE, S = qλ EQE/(hc) is used; directly multiplying EQE by the energy spectrum omits the photon energy.

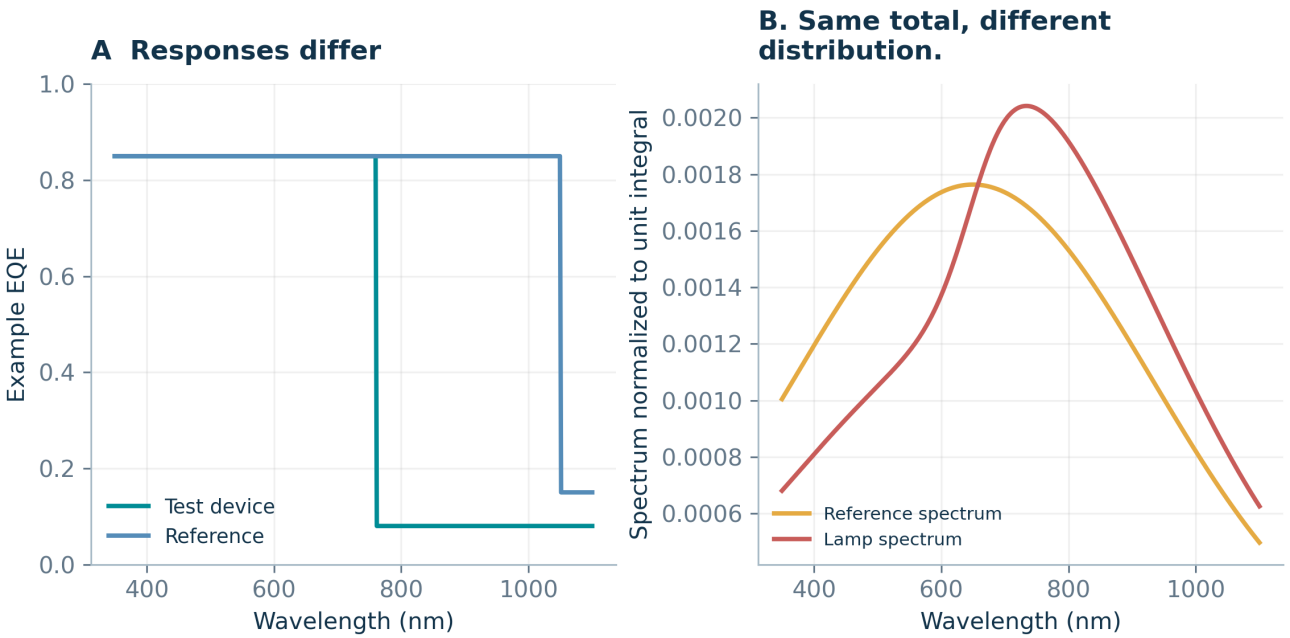


Figure 31. The origin of spectral mismatch. Toward the red end of the spectrum, the test device loses its response before the reference does. A redshift of the lamp spectrum changes the test and reference currents in different proportions even when total irradiance remains unchanged. The curves were created for teaching; the real reference spectrum appears in the preceding physics chapter.

Do not overlook the correlation in uncertainty

Since the efficiency η = Pmax/(GA), the logarithmic small change is dη/η = dP/P - dG/G - dA/A. In the case of independence, the variances are summed; if there is a common calibration or a common geometric method, covariance terms are also included. The general expression for the uncertainty uy^2 is: gradient(f) transpose × Ux × gradient(f), where the output is y = f(x) and Ux is the covariance matrix. [R04]

Comparing two measurements taken with the same lamp on the same day can partially cancel out some common errors in the difference calculation; however, the same error remains in the absolute efficiency uncertainty. Therefore, “the difference between the two cells is very well known” and “both are rated with the same accuracy on an international scale” are different claims. The standard deviation of the repetitions does not represent the entire uncertainty of the device calibration.

Self-assessment

1. **Does normalizing the same cell with a smaller area increase its physical power?** No. The power remains unchanged; J and the calculated efficiency are artificially increased. The area definition in the measurement must be corrected.

2. **For a device where 24% is obtained during reverse scanning and 21% is obtained during MPP tracking, what is the fundamental performance characteristic?** The stable MPP result is used as the basis, specifying the conditions and duration; the scanning result is shown separately as dynamic behavior.

3. **If the EQE current is 8% lower than the J-V current, is it immediately considered a collection loss?** No. First, spectral calibration, area, wavelength range, bias, and device history are matched; then, optical and electrical losses are analyzed.

Why are bias and wiring recorded?

Allowing a device to stabilize at a specific voltage before measurement is called **applying a bias voltage**. This preparation, especially in structures exhibiting slow charging or ion movement, can alter the internal state at the beginning of the scan. The waiting time under illumination should also be recorded similarly. Using the same scan rate does not automatically equalize different initial states.

The wiring affects whether the voltage displayed by the instrument actually corresponds to the voltage at the cell terminals. Separating the voltage drop in the current-carrying cable using separate voltage sensing leads is the purpose of a four-wire connection. After calibrating the light with a reference cell, changing the sample's temperature, area, or connection can alter other links in the measurement chain. Therefore, calibration is not limited to a single certificate page; it is completed with the correct usage conditions.

BOOK I · CHAPTER 19 / MEASUREMENT AND RESEARCH

Characterization: which question does each tool answer?

Characterization is the indirect measurement of an unobservable property

Characterization is the process of defining a sample's structure, composition, and function through measurable signals. Instruments often do not provide a direct answer stating "defect density" or "good interface." Instead, they measure light intensity, electron energy, diffraction angle, or electrical response. We then use a model to relate this signal to a physical property. When the same signal can be generated by several different mechanisms, this is called an **inverse problem**.

XRD is X-ray diffraction. The arrangement of crystal atoms enhances waves scattered at specific angles; the positions and shapes of the peaks provide information about the structure. **SEM** is scanning electron microscopy; it images morphology using signals emitted from the surface. **AFM** is atomic force microscopy, which scans the surface with a tip. We cannot automatically count different chemical substances based on the bright area in the microscope image; the signal type, charging, and topography can also affect the image.

Energy, luminescence, and electrical response

XPS is X-ray photoelectron spectroscopy: it provides information about the elemental and chemical state of the surface, specifically from the energies of the emitted electrons. **UPS** focuses on properties such as valence states and work function, using ultraviolet light in a similar way. The depth probed by these methods and the preparation of the surface are important; the surface composition may not represent the average composition of the entire film.

PL refers to the emission of light from a sample when excited by light, i.e., photoluminescence. **EL** refers to the emission of light when excited by an electric current. **Time-resolved PL** monitors how the signal changes after a short excitation. **Impedance spectroscopy** measures the frequency-dependent response to a small, alternating electrical excitation; models are used to separate resistance, charge accumulation, and slow processes. Frequency is the number of cycles per second. Fitting an equivalent circuit to the data does not prove that each element within it represents a single, real mechanism.

Synthetic diagnosis: Suppose the PL doubles after a surface treatment. Reduced non-radiative recombination is one possible explanation. However, increased absorption of excitation light or increased emission of light reaching the detector can also enhance the signal. If we control the absorbed excitation power and the optical geometry and correlate it with appropriate electrical measurements, the interpretation becomes stronger. Writing down the two explanations we want to distinguish before selecting the instrument transforms the measurement list into a scientific question.

Comprehension check: single peak, single result?

An increase in the intensity of an XRD peak does not always indicate a higher concentration of the target material; crystal orientation can also play a role. Similarly, the smoothing of a SEM image alone does not provide information about the defect capture rate. For each claim, add the sentence: “What signal did the instrument measure, and what feature did I extract using which model?”

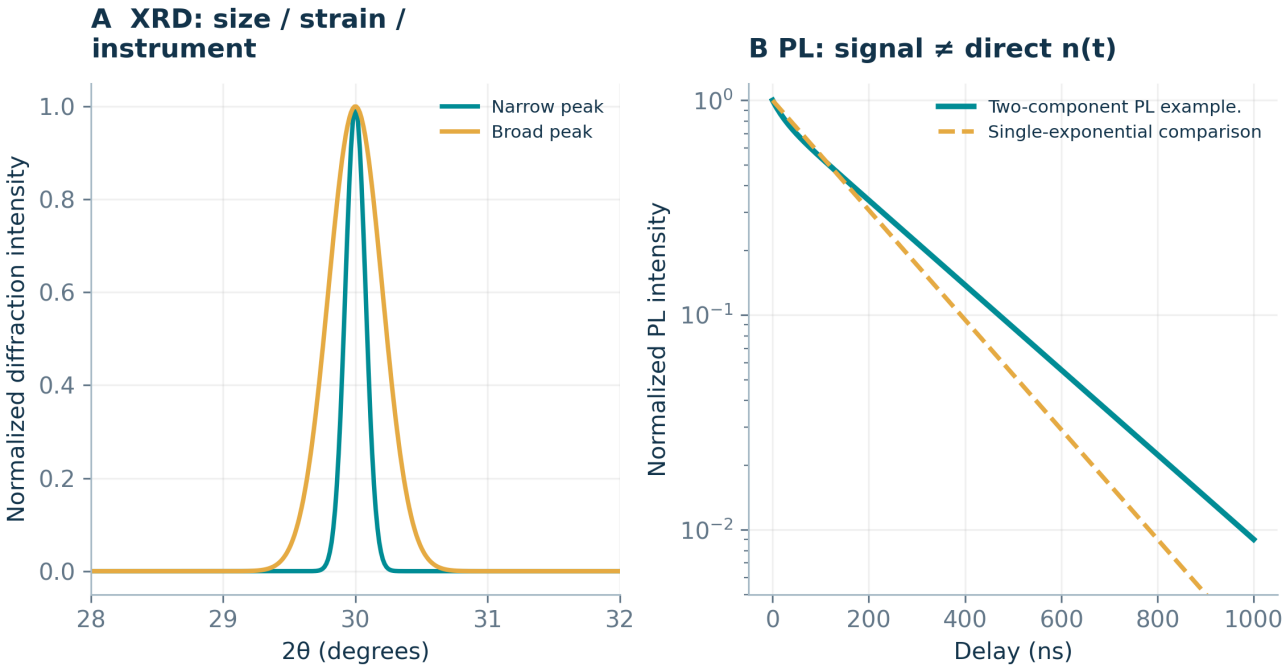


Figure 32. Reading a signal requires a physical forward model. In panel A, the synthetic XRD peaks have different widths; they do not determine the grain size on their own. Panel B compares the single and double exponential forms of the synthetic PL curves. It is not necessary for the PL intensity and the excess charge carrier density to have the same time constant. [R08]

The strength of a research program is not measured by the number of devices it uses. The strength comes from the complementary nature of measurements that test the same hypothesis through different physical channels. Phrases such as “larger grain size,” “longer lifetime,” or “higher binding energy” only become scientific knowledge if it is specified what is being measured, what is being inferred from the model, and which alternative explanations remain open. Material, half-device, completed device, and aged device are different sample classes; these are not compared silently.

Crystal structure and morphology

X-ray diffraction (XRD) measures the scattering trace of the periodic atomic arrangement. The Bragg relation, $n\lambda = 2d \sin\theta$, relates the diffraction angle to the interplanar spacing. The peak position is sensitive to the lattice spacing, the intensity distribution to the atomic arrangement and texture, and the width to factors such as device resolution, coherent region size, and microstrain. A narrowing of a peak alone does not necessarily mean that "defects have decreased." In the Scherrer approach, the size refers to the coherent diffraction region; it is not automatically equated to the geometric grain size observed in SEM.

Preferred orientation in the thin film can weaken some of the expected peaks. The result of "no additional peak" does not prove that there is no secondary phase below the detection limit or that there is no amorphous component. A good analysis includes substrate, electrode, and free charge carrier measurements; if necessary, it is supported by full pattern fitting, standard samples, and independent chemical composition measurements. Since it is possible to fit the pattern with a large number of free parameters when selecting a structural model, chemical plausibility and parametric uncertainty are also controlled.

GIWAXS provides access to the orientation distribution and formation process of thin films by measuring wide-angle scattering with a small incident angle to the surface. The difference between the ring and the arc contains information about the orientation; a curve reduced to a single direction does not represent the entirety of the two-dimensional pattern. In-situ measurements can reveal when solvent evaporation, intermediate phase formation, and crystallization occur during annealing. A study examining precursors containing excess PbI_2 is a concrete example of combining GIWAXS with microscopy and charge carrier collection information to understand performance changes. The methodological lesson here is that the effect of an additive should not be inferred solely from the single XRD pattern of the final film. [R11]

SEM displays the surface morphology and layers in cross-section. Sample preparation, cross-section damage, electron beam degradation, and imaging threshold can affect the results. AFM measures the height topography; the scan area, tip shape, and flattening method can alter the RMS roughness. A single "good" SEM image does not represent the entirety of the sample. The researcher acquires multiple images from random or predefined locations, provides the size distribution, and applies the same analysis settings to the control group. In a film with a cross-sectional appearance of 500 nm, local thinning and pinhole statistics may be more indicative than the average thickness.

Surface chemistry and energy levels

XPS derives elemental and chemical state information from the kinetic energy of photoelectrons. The signal is surface-sensitive; this characteristic is an advantage in interface studies but a limitation when claiming information about the bulk composition. The presence of an oxidized layer on the surface does not necessarily indicate that the entire film is oxidized. Charge correction, energy reference, background, peak shape, and spin-orbit coupling constraints must be clearly stated. Depth profiling is not entirely a passive observation, as reduction or preferential removal may occur during ion sputtering. NIST's practical XPS guide is designed to establish this type of interpretive discipline, from measurement planning to reporting. [R07]

Methods such as UPS and Kelvin probe provide information about the work function and surface energy levels. All values used when drawing an energy diagram must be referenced to the same reference point. Directly transferring the work function of a single film exposed to air to an embedded interface prepared in a vacuum is not reliable. When contact is made, a dipole, chemical reaction, band bending, and Fermi level alignment can occur. Therefore, the inference that "electron affinities are matched, and the interface is lossless" is invalid. Whenever possible, interface formation is monitored with increasing coverage thickness; measurements taken before and after contact are interpreted in conjunction with the device behavior.

From light emission to carrier dynamics

PL is radiative recombination following optical excitation. The PL quantum yield is the ratio of the number of emitted photons to the number of absorbed excitation photons; dividing by the number of incident photons yields a different quantity. The spectral detector response, absorbed power, re-absorption, and photon escape geometry are all part of the measurement. An increase in the raw PL intensity can also be due to stronger absorption. A comparison of unnormalized PL in two samples with different thicknesses or optical stacks is not sufficient.

TRPL tracks luminescence with time resolution. In a simple homogeneous high-injection scenario, if the electron and hole densities are approximately equal, the radiative rate can be scaled with Bn^2, the trap-mediated loss with n/τ, and the Auger loss with Cn^3. Therefore, applying a stronger laser pulse to the same material can alter the observed decay. It is incorrect to unconditionally name the time obtained from a single exponential fit as the "carrier lifetime" of the material. The excitation intensity, pulse repetition, device time resolution, diffusion, and surface recombination are

considered together. A methodological study on PL-based perovskite characterization details the condition dependence of these measurements. [R08]

A typical diagnostic example: a long TRPL is observed in the bare film, while a short TRPL is observed when an electron transport layer is added. One explanation is rapid and efficient electron transfer; the other explanation is increased non-radiative loss at the interface. It is difficult to determine which one is correct in isolation. Under open-circuit conditions, absolute PL/QFLS, V_oc in the completed cell, charge extraction in short circuits, and surface passivation are used together. If PL decreases when a contact is added, and the device V_oc also decreases, the “successful extraction” explanation should be questioned with particular care.

Electroluminescence (EL) is the emission of light under electrical injection. Under appropriate reciprocity assumptions, a connection can be established between optical collection and emission; it is also related to the non-radiative voltage loss and the external emission efficiency. Rau’s reciprocity study establishes this relationship mathematically. [R09] With a constant radiative reference, $\Delta V_{nonrad} = -(kT/q)\ln(\eta_{ext})$. At 298.15 K, kT/q is approximately 25.69 mV: for $\eta_{ext} = 1\%$, the loss is approximately 118 mV, and for $\eta_{ext} = 0.1\%$, it is approximately 177 mV. Here, η_{ext} is the external emission efficiency with the context specified; the PL yield of the bare film does not automatically replace this value. QFLS is the electron and hole quasi-Fermi level separation within the material; it does not necessarily have to be the same as qV_{oc} measured at the external contacts.

Electrical spectroscopy and false precision

DLTS monitors the thermal release behavior of traps after a pulse excitation. Activation energies and trap information are extracted from time constants that vary with temperature, under an appropriate model. Lang’s original work established this approach using high-frequency capacitance transients. [R10] However, the activation energy is not necessarily a direct identification of a specific atomic defect. Multiple defects, distribution, interface effects, and ion movement can yield similar time scales. For identification, evidence from temperature, bias, sample preparation, and independent calculations/chemical interventions is required.

Impedance spectroscopy measures $Z(\omega) = \delta V(\omega)/\delta I(\omega)$. Fitting the frequency-dependent complex response to an equivalent circuit is useful, but a single semicircle does not necessarily correspond to a single physical mechanism. The excitation should be small, the device should remain stationary during the measurement, and the voltage/light history should be preserved. The apparent large or negative capacitance observed in perovskites may arise from slow ionic changes modulating electronic injection; therefore, directly interpreting the circuit parameter

as a large dielectric constant may be incorrect. Ebiadi and colleagues have demonstrated this distinction through transient current measurements. [R12]

When transitioning from the signal to the mechanism, observe the inverse problem

A characterization tool does not directly measure "good material." XRD observes the scattering of photons by the crystal lattice, XPS measures the energies of electrons emitted from near the surface, PL observes luminescent recombination, and electrical measurements observe the carrier and loss components of the entire device. The same microphysical process can alter multiple signals, and the same signal can be generated by multiple microphysical processes.

When deriving a Scherrer-type coherence length from the XRD peak width, it is important that β is in radians, that device broadening is separated, that the shape factor is chosen appropriately, and that the possibility of microstrain is considered. This length does not necessarily have to be the same as the size of all the grains observed under the microscope. Peak intensity is not only related to the phase amount; preferential orientation and measurement geometry can also vary. Therefore, automatically translating the growth of a single peak into the statement "crystallinity has increased" is insufficient.

Why can lifetime not be read directly from PL decay?

Let's assume that in a uniform volume, at a single injection level, the instantaneous PL signal is proportional to radiative recombination: $I_{PL} \approx Bnp$. Since $p \approx p_0$ in low-level doping, the signal is approximately proportional to Δn. If $\Delta n = \Delta n_0 \exp(-t/\tau)$, then PL also decays with the same time constant. In high-level injection, when $n \approx p \approx \Delta n$, $I_{PL} \approx \Delta n^2$; the same charge carrier decay now yields $\exp(-2t/\tau)$ in PL. The measured exponential lifetime may be half the charge carrier lifetime.

In reality, transport, surface loss, photon recycling, and injection-dependent recombination also modify this simplified model. The purpose of this derivation is not to simply multiply every PL curve by two; rather, it is to establish a clear forward model between the signal and the desired physical quantity. Different excitation intensities, front/back illumination, and passivation control allow for testing this model. [R08]

Choosing a measurement that distinguishes a mechanism

Observation	At least two possible explanations.	Discriminating control
Voc increased.	Bulk loss decreased; contact loss decreased	PL/QFLS comparison of bare film and contacted stack
FF increased.	The series resistance decreased; the recombination rate changed.	Suns-Voc/pseudo-JV and steady-state J-V combined
Jsc increased.	Optical generation increased; collection improved	EQE, reflectance and wavelength-dependent collection
The PL signal disappeared.	Faster charge extraction; a new loss pathway	Control with selective and blocking contacts; device Voc
The XRD peak narrowed.	The coherent region has grown; the strain has decreased.	Instrument correction and analysis of multiple peaks

The measurements in the table are not interchangeable. For example, removing the load in an open circuit does not generate external current; the PL quenching of the contacted film should not be directly interpreted as evidence of high power. The researcher first establishes the boundary conditions of the measurement, and then interprets the signal.

Self-assessment

1. **Can it be said that as the XRD peak narrows, the charge carrier lifetime increases?** No. The peak width includes structural and device-related contributions; charge carrier dynamics are measured separately.

2. **Is the quenching of PL upon contact addition a good sign?** It cannot be determined in isolation. Beneficial charge transfer and detrimental interface recombination must be distinguished.

3. **If impedance matching is very good, does that prove the mechanism?** No. Alternative circuits and physical models must be tested and distinguished using independent time-domain and operating condition data.

Imaging, charge extraction, and controlled intervention

Heterogeneity refers to the non-uniformity of properties within a sample. The thickness, chemical composition, or electrical response may vary; therefore, local information obtained through microscopy is complemented by measurements taken across the entire area. **Charge extraction** is the process of transferring the generated charge carrier from the absorber to a neighboring layer or to an external circuit. An increase in the extraction rate can lead to a decrease in luminescence; however, a similar decrease can also result from increased recombination. A single PL curve cannot distinguish between these two explanations.

By **intervention**, we mean a controlled change that specifically tests one of these explanations. For example, passivation is applied to one sample of the same film, while the optical conditions of the other are matched and kept as a control. Then, the luminescence, voltage, and extracted charge are compared together. The **forward model** calculates the expected signal from the assumed mechanism; the **inverse problem** investigates which mechanisms are possible from the measured signal. A conceptual example curve does not replace measurement data from a real sample.

Durability: from one-hour curves to service life

Lifetime is more of a metric definition than a specific date

Whether a module is considered “durable” depends on how well it maintains its functionality. The initial maximum power can decrease over time; insulation can degrade; layers can delaminate. The thresholds for these outcomes are different. **Degradation** is the change in properties over time; **failure** is the point at which a defined function or safety criterion is no longer met. A slow power loss and a sudden electrical failure may not result in the same lifetime distribution.

T80 is the time it takes to reach 80% from the selected initial power. It should be specified whether the initial value represents the first measurement or the end of a stabilization period. **Synthetic example:** if the initial value is 10 W, the threshold is 8 W. If 8.5 W is measured after 200 hours and 7.5 W after 300 hours, and assuming a linear change between these two points, T80 is approximately 250 hours. If the actual change is not linear, this is only an estimate; more frequent data or a suitable model is required.

What do we write if no fault is detected after the test?

If, after a 1000-hour test, the sample still provides 90% power, it is not written that “T80 = 1000 hours.” The threshold was not reached within this time; it can be stated that “T80 is longer than 1000 hours under these test conditions.” Such records, where we observe the limit instead of the exact lifetime, are called **censored data**. Silently removing a sample that was taken out of the test early from the data set can make the durability appear better than it actually is.

Accelerated aging involves studying a degradation process in a shorter time frame by applying high temperature, humidity, light, or electrical stress. The **activation energy** is a model parameter that relates the chosen process rate to its temperature dependence. If the same mechanism applies, the rates at different temperatures can be correlated. However, if a new reaction starts at a high temperature, we may no longer be accelerating the same degradation process, but rather triggering a different failure mode. Converting a test hour to a field year using a universal coefficient is not accurate.

ISOS is a family of defined research protocols, particularly used in the stability assessment of developing cells. **IEC qualification tests** evaluate whether a design passes specific tests according to the conditions of the relevant standards. These tests

address different questions. Passing a qualification test alone does not guarantee a specific service life under certain field conditions. Below, the test objective, stress condition, and reported threshold will be kept separate. [R05] [R06]

Comprehension check: can recovery conceal a failure?

When the device is allowed to rest in the dark and some of the power is recovered, distinguish between reversible changes and permanent losses. Reporting only the measurements taken after resting can obscure the actual performance during operation. It is necessary to maintain a record of the operating, resting, and measurement history on the same timeline.

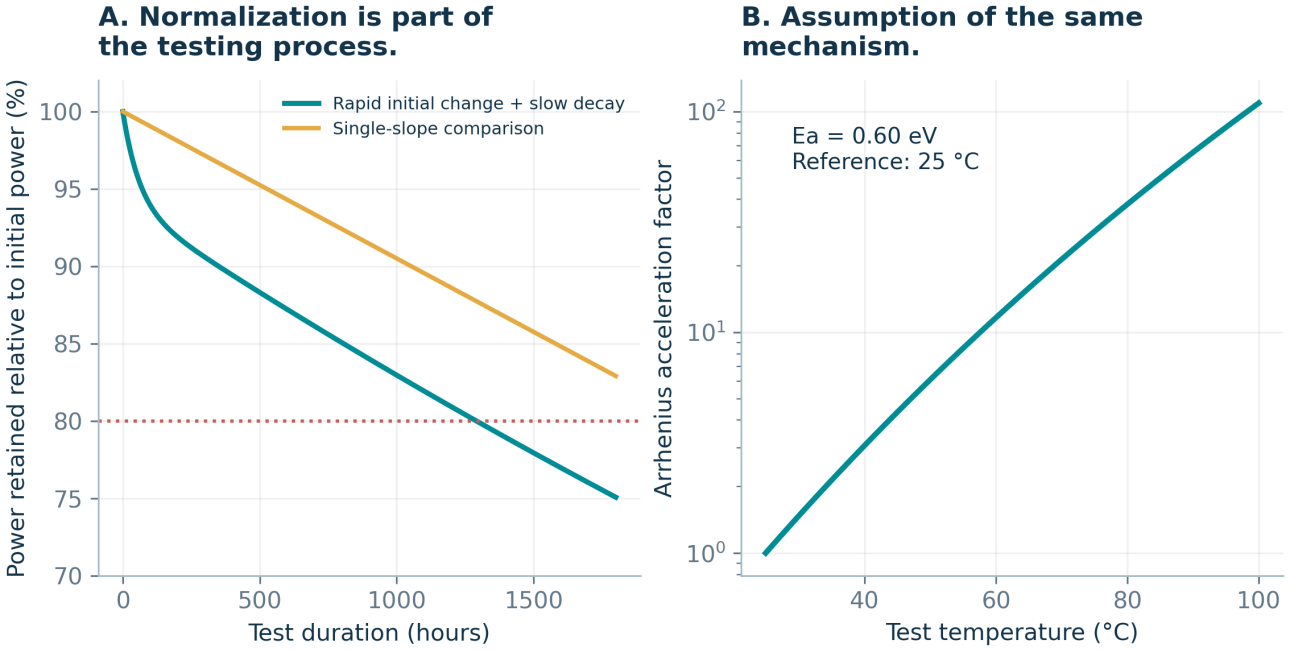


Figure 33. Analyze the stability in terms of time and mechanism. Panel A shows two synthetic power curves, one with and one without an initial change; Panel B shows the Arrhenius factor with an activation energy of 0.60 eV. The accelerated aging curve, referenced at 25 °C, is based on the assumption that only the same mechanism is sustained. [R05] [R16]

Efficiency describes what the device does at a specific point in time; durability describes how well it can maintain that same performance over time. In cell development, high initial efficiency and slow degradation converge on the same target function: total energy generated. A device that is initially more efficient but degrades rapidly may produce less electricity than a more modest but stable device. Therefore, durability studies should not be a postponed “additional test”; rather, it should be integrated into the design of the material, interface, metal contacts, encapsulation, and operating conditions.

There is not a single cause for degradation

Moisture and oxygen can reach the active layer, altering the interface chemistry or accelerating metal corrosion. Thermal diffusion affects ion movement, reaction rates, and mechanical stress. Light can initiate photochemical pathways that are not observed in the dark by generating new charge carriers. Electrical bias can alter the distribution of charged defects and interface reactions. A condition in which a component is safe on its own may not be safe when combined with other stresses: a result of "temperature resistance in the dark" does not necessarily imply "resistance during operation under illumination."

In silicon modules, cell cracks, connection issues, encapsulant and backsheet degradation, corrosion, and potential-induced effects are investigated. In thin-film and emerging technologies, in addition to these, different migration and interface mechanisms are studied. Their frequency of occurrence varies depending on the technology, production batch, and environment. The IEA PVPS module failure study provides a broad institutional framework demonstrating that failures should be addressed not only through electrical characterization but also through methods such as visual inspection and imaging. A universal degradation rate cannot be derived from this. [R15]

In addition to the presence of ionic movement in perovskites, a mechanism must be established to explain device failure. Mobile species can alter the local field, accumulate at interfaces, or combine through chemical reactions. Eames and colleagues' calculation and experimental study of ion transport represent early examples of correlating the atomic barrier with the device timescale. However, a single migration barrier does not determine the entire device lifetime; the density of mobile defects, the connectivity of the path, and the actual boundary conditions are also required. [R13]

ISOS and IEC do not serve the same purpose

The ISOS approach aims to evaluate research samples in a more comparable manner under different stresses such as storage, light, temperature, and external environment. Simply stating the name of the test is not sufficient; the atmosphere, relative humidity, sample temperature, light spectrum, electrical load, encapsulation, measurement range, and number of samples must be specified. The consensus text adapted for perovskites specifically addresses the unique challenges of these materials, such as dynamic behavior and recovery. Aging under MPP for a functioning device is a different experiment than holding it in an open circuit. [R05]

IEC 61215 is a family of standards related to the design qualification and type approval of terrestrial PV modules. The open IEC catalog explicitly states that these tests are not

interpreted as quantitative predictions of module lifetime. Therefore, passing a series of tests does not equate to the conclusion that "this technology will operate for so many years." Specific module design, bill of materials, and manufacturing changes are important in the context of qualification. In this book, the standard's explicit scope is confirmed; no unseen article numbers, mandatory test thresholds, or certification compliance are invented in the full text. [R06]

A good research program first investigates the mechanism at the cell level, and then tests it in an encapsulated mini-module and a full module. A small cell with open edges and a well-encapsulated module have different pathways for moisture ingress. Encapsulation that works well in a small sample may behave differently in a large panel in terms of edge length/area ratio, thermal expansion, and mechanical load. Glass, adhesive, and sealant are also part of the design in terms of optical loss, chemical interaction, and recyclability.

T80, recovery and censored data

T80 indicates the time at which the performance drops to the selected initial reference value, 80%. It must be clearly stated whether "initial" refers to the first measurement, the first stable plateau, or the value after the first rapid drop. Different initial definitions can yield different T80 values for the same device. Concealing the actual initial efficiency and only showing the normalized curve weakens the energy assessment. Both absolute power/efficiency and normalized power should be presented; pauses, periods of no measurement, and dark recovery should be kept visible.

If a device retains 92% of its initial performance after 1000 hours and does not reach the threshold defined by the selected T80 during the monitored period, it can be stated that "T80 > 1000 hours, under these test conditions"; however, the exact value of T80 will not be measured. Knowing only the final data point is not sufficient: the device may have fallen below the threshold and recovered at an earlier time. When the experiment ends without observing the threshold, the duration observation is right-censored. Excluding the worst examples from the measurement and plotting only the average of the remaining ones creates artificial durability. It is important to preserve the information about when and why devices that failed were removed from the data set. If a device has completely lost electrical connection, it is not correct to represent this as a simple lack of efficiency measurement.

Exemplary energy scenario: The efficiency of cell A decreases linearly from 24% to 18% over 1000 hours, and that of cell B decreases from 22% to 21%. Under constant illumination of 1000 W/m^2, the average efficiencies are 21% and 21.5%, respectively. The energy for one square meter is approximately 210 and 215 kWh. In this limited

scenario, the initial leader, A, produced less energy. If the actual curve is not linear, a numerical calculation of the time integral is required, including dark intervals and changes in irradiance.

Valid transfer of accelerated testing

For a simple thermal process, the rate can be modeled as $k(T) = k_0 \exp[-E_a/(k_B T)]$. If the same mechanism remains dominant, the process is accelerated at high temperatures. However, overcoming a phase transition, shifting the encapsulant to a different regime, or initiating a new reaction can decouple the laboratory test from the field mechanism. It is not possible to extract the activation energy from a single temperature point. At multiple temperatures, with sufficient samples and similar failure signatures, the model should be tested; the effects of humidity, light, and voltage are evaluated separately.

In the original calculation, let $E_a = 0.60$ eV, the ambient temperature be 298.15 K, and the test temperature be 358.15 K. Then, $AF = \exp[(E_a/k_B) \times (1/298.15 - 1/358.15)]$ is approximately 50. This is only the rate ratio if the assumed single mechanism is valid. Automatically converting 1000 hours to a 50,000-hour service lifetime ignores the unknown duty cycle and other failure modes. If E_a itself is uncertain, AF changes exponentially; the lifetime estimate should be reported with the model and uncertainty rather than as a single number.

Field studies are necessary to test the laboratory model. The night-day cycle, seasonal temperature, pollution, precipitation, light spectrum, and actual electrical load all have a combined effect. The IEA PVPS lifetime report addresses the technical, economic, and user-dependent aspects of the “end-of-life” definition, as well as the relationship between physical models and system energy calculations. [R16] As a didactic application, the failure definition is first frozen, and then it is compared whether the same chemical/electrical signature appears in both laboratory and field samples. The acceleration factor is not transferred unless a match is demonstrated.

Choosing the baseline and threshold in a T80 calculation

Let the time series of power be $P(t)$. When normalized with respect to the beginning, $p(t) = P(t)/P(0)$, T80 can be reported as the time at which $p(t)$ first reaches 0.8. Normalizing with respect to another reference after the rapid initial change will produce a different metric; this should be given a different name, and the initial value should not be hidden. If the sample is still above the threshold at the end of the test, the final value is not an estimate of the lifetime. If the threshold is never exceeded, it can only be said that T80 is greater than the observation period.

If a sample partially recovers in the dark, a day-night cycle with continuous illumination will not produce the same data. Temperature, humidity, and electrical charge are also not independent parameters of the test; one can influence the effect of the other. ISOS conditions are useful for comparable research reporting; the purpose and scope of IEC module qualification tests are different. The standard heading in the catalog does not replace unread normative clauses. [R05] [R06]

Avoid misinterpreting the Arrhenius plot and developing a false sense of confidence

Let the rate constant for a single effective mechanism be kdeg = k0 exp[-Ea/(kBT)]. The acceleration factor between two temperatures is obtained by subtracting the logarithms:

$$AF = \frac{k_{\text{test}}}{k_{\text{use}}} = \exp\left[\frac{E_a}{k_B}\left(\frac{1}{T_{\text{use}}} - \frac{1}{T_{\text{test}}}\right)\right]. \tag{I.20.1}$$

For Ea = 0.60 eV, a factor of approximately 50 is found for the operating temperature of 25 °C and the test temperature of 85 °C. However, before estimating the service life, it must be verified that the same degradation mechanism dominates at both temperatures when this ratio is extrapolated over time. If a new phase, a different electrode reaction, or another moisture-related pathway emerges at high temperatures, the single Ea extrapolation becomes invalid. Even observing consistent slopes at a minimum of three temperatures does not represent all field conditions; a mechanism analysis and correlation with actual field data are required. [R16]

In lifetime data, not only the average but also the distribution is important. A small number of early failures can be masked in the average power curve. Maintaining a serial record for each sample, along with a clear record of samples removed from testing or for which measurements were terminated, and the classification of failure modes, determines the reproducibility of the research.

Self-assessment

1. **Does 95% performance retention after 1000 hours prove a 25-year lifetime?** No. It is only an observation under the specified test conditions; the mechanism and acceleration model must be validated for transfer to field conditions.

2. **Why should T80 be specified with an initial definition?** Re-normalizing after the initial drop can alter the time and the actual energy loss.

3. **If the dark thermal test yields good results, but the MPP light test yields poor results, does this indicate a contradiction?** Not necessarily. Light and electrical operation can activate different or combined degradation mechanisms.

Distinguishing between initial degradation and permanent degradation

In the literature, **burn-in** refers to the initial change observed during the first operation or pre-conditioning. Initially, the power may decrease rapidly and then change more slowly; some effects may partially reverse with dark storage or re-conditioning. This does not mean that every initial drop is harmless or reversible. During measurement, the initial power, the selected reference power, and any recovery are recorded separately.

The **threshold** is the limit chosen for the lifetime criterion. Therefore, the starting point used for 80% in T80 affects the result. At the end of the experiment, for a sample that has not yet reached the threshold, only the lifetime information exceeding the observation period is available. It is incorrect to include this sample in the average as if it had failed on that day, or to consider it as having an infinite lifetime.

First-principles materials research: the power and limits of DFT

What does DFT attempt to calculate?

The properties of a crystal arise from the quantum interactions of the atomic nuclei and electrons. Directly tracking the motion of all electrons is too computationally expensive for most real solids. **Density functional theory**, or DFT, reformulates the problem by relating the ground-state energy to the electron density. **Electron density** describes how many electrons are present in each small region of space. In this book, DFT is not used as a "write the chemical formula, get the efficiency" machine.

A **functional** is a mathematical rule that takes an entire function as input, rather than a number. For practical calculations involving electron exchange and correlation effects, approximate functionals are selected. **PBE** is the name of such a common approach. **Self-consistency** is the iterative process that ensures the potential generated by the calculated density yields the same density. **Geometry optimization** involves modifying the atomic positions and, if necessary, the cell size in a way that minimizes the forces. This process may stop at the nearest local minimum and does not guarantee finding the best result among all possible structures in nature.

Why do numerical settings appear to have a physical effect?

In the computer, we represent the crystal with a finite number of waves or spatial points. The **cutoff energy** determines how much detail is retained in the plane wave representation. The **k-point mesh** is a sampling of the periodic electronic states of the crystal at different wave vectors. The **pseudopotential** groups some of the effects near the nucleus into a more economical representation. If these settings are insufficient, the small energy difference between materials may arise from numerical error.

Example of synthetic convergence: the energy difference between the same two structures yields 40, 28, 25, and 24 meV/atom in more refined settings. Because the last two values converge, the numerical sensitivity of this observable decreases in that range. The result is not that the "true energy difference is exactly 24"; the error of the chosen functional and the presence of other competing phases still exist. **Convergence** is the model's numerically consistent solution; whether the model accurately represents nature is a separate challenge.

Formation energy compares a compound with selected elemental reference states. The **convex hull** is the lowest-energy boundary of competing phase mixtures that can give the same overall composition. Being above the hull indicates an energetic benefit

from decomposition within the specified pool and model. A **phonon** is a quantized mode of crystal vibrations; a vibrational calculation examines the structure's response to small displacements. These three checks ask different questions, and none alone constitutes successful experimental synthesis.

Comprehension check: the calculation has "successfully" completed

The program running without errors does not necessarily mean that the physical result has been verified. The chemical definition of the structure, the forces, the convergence of the energy difference, competing phases, and the limitations of the approach used should be examined separately. Distinguish between the generation of the file and the establishment of scientific evidence.

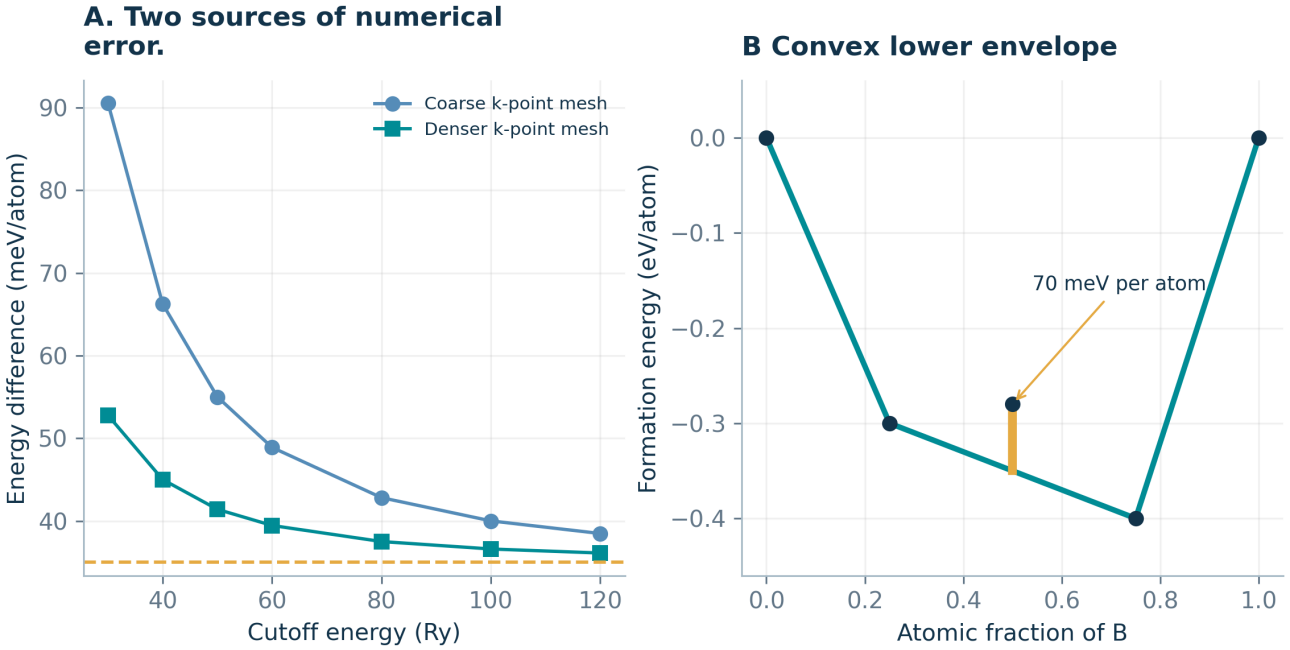


Figure 34. Testing DFT results at two distinct scales. Panel A shows the effect of cutoff energy and the k-point mesh; panel B shows the relation between energy and the lower envelope. All numbers are synthetic. The candidate in panel B lies 70 meV/atom above the envelope; this is not a decomposition time. [R18] [R19] [R20]

Computational discovery is a more challenging task than simply writing numerous formulas and calculating band gaps. A single formula does not tell us where the atoms are located, what arrangement they form, which phases they compete with, or which defects will annihilate the charge carriers. DFT provides a physical model for a significant portion of these questions; however, each result still has limitations in terms of method, structure, convergence, and temperature. The flawless execution of an electronic structure calculation does not necessarily mean that the calculated structure can be fabricated in the laboratory.

First, define the structure, then consider the energy

In the initial structure, the chemical formula, number of atoms, cell vectors, coordinates, occupancies, charge state, and magnetic state must be clearly defined. A crystallographic file exhibiting partial occupancy does not spontaneously transform into a physically disordered alloy in a standard periodic DFT calculation. Regular supercells, sampled configurations, or appropriate disorder models are required. SQS aims to represent selected correlations of a random alloy in a small cell; a single SQS does not guarantee a representation of the entire configuration space. The cell size and sampling selection are tested. [R24]

Geometric relaxation searches for a local minimum. Convergence from a starting point does not prove that the globally lowest energy structure has been found. Different initial volumes, symmetries, atomic arrangements, and physically reasonable magnetic orderings can be tried. A calculation that does not converge is not necessarily due to an "unstable material": the electronic solution, the geometry algorithm, or the chosen method may have failed. Force and stress convergence alone only indicates that a stationary point has been approached in the degrees of freedom being examined; an evaluation of the local minimum requires energy curvature with respect to relevant structural distortions and appropriate phonon analysis. The synthesis route and competing phases are separate issues.

Semi-local exchange-correlation functionals, such as PBE, are a common starting point due to their computational cost and scope. The original formulation of PBE is based on the generalized gradient approximation. [R17] However, the Kohn-Sham eigenvalue difference does not automatically correspond to the measured optical or quasiparticle band gap. Hybrid functionals, GW, or other suitable methods can reduce different sources of error; no method guarantees an accurate result for all chemistries. Spin-orbit interaction in heavy elements, magnetic order and correlation in transition metals, and dispersion in weakly bound systems require attention.

Convergence and comparable energy

The plane-wave cutoff, k-point mesh, electronic threshold, force tolerance, smearing, pseudopotential, and cell size converge according to the target size. Even when the change in total energy is small, stress or phonons can still change. The SSSP study demonstrates the importance of using phonons, pressure, bands, and other criteria together, rather than evaluating pseudopotentials with only a single energy test. [R19] The convergence budget should be stricter than the calculated smallest meaningful difference; a 20 meV/atom method uncertainty does not allow for a definitive decision for an ordering of 5 meV/atom.

Lejaeghere and his colleagues' inter-code comparison demonstrated that the numerical convergence of different DFT implementations can be systematically tested for a defined problem. Such validation is not proof that the same functional fully represents the experimental reality. [R18] It is possible for two codes to agree under the same incorrect physical assumption. Therefore, the scientific literature distinguishes between numerical reproducibility and physical validation; independent verification is not limited to simply running the same input on different computers.

Formation energy, phase diagram, and free energy

The formation energy measures the gain with respect to elemental references. A negative formation energy does not indicate that the compound will not decompose into other compounds. The convex hull represents the lowest energy among phase mixtures that yield the same overall composition. E_hull = E_candidate - E_best_mixture, calculated per atom in the same units. An incomplete pool of competing phases can falsely elevate the convex hull and make the candidate appear better than it is. Therefore, possible binary, ternary, and higher-order compounds, alternative polymorphs, and the calculation methods for the references are examined.

Original example: Let the energy value of the AB_2 candidate be -0.80 eV/atom, and let the best A-B phase mixture that yields the same composition be -0.86 eV/atom. The energy of the candidate above the convex hull is 0.06 eV/atom = 60 meV/atom. Since there are three atoms in one formula unit, the difference favoring decomposition is 0.18 eV/formula unit. Despite the negative formation energy, the candidate does not belong to the thermodynamic ground state. This result alone does not prove the impossibility of synthesis; there are metastable phases that can be kinetically stabilized. Sun and colleagues' study on metastability shows that the observed scale of metastability depends on the chemistry; a universal rule of "it can definitely be synthesized below this meV" cannot be derived. [R20]

The total energy at zero Kelvin is not the free energy at the operating temperature. Vibrational, configurational, magnetic, and, if necessary, electronic entropy contributions can become significant. G is considered with components such as G ≈ E + F_vib - T S_config + pV; the same contribution should not be counted twice. In synthesis, which is in equilibrium with an open gas reservoir, the chemical potential, temperature, and partial pressure are the determining factors. Since the equilibrium against phase separation and the possibility of formation during the process are different problems, the synthesis window is not simply derived from the band structure at room temperature.

Phonons and finite temperature

Phonon calculations investigate the force response to small atomic displacements. Imaginary frequencies indicate that the chosen structure may be unstable with respect to the corresponding distortion within the harmonic approximation. First, numerical aspects such as the supercell, k/q mesh, force accuracy, and acoustic sum rule are examined. Stability at only the Γ point does not cover the entire Brillouin zone. If the soft mode is real, the atoms can be moved along that mode, and a structure with lower symmetry can be searched for. The phonon calculation study by Togo and Tanaka explains the fundamental tools of these types of calculations in the study of structure and thermodynamics. [R21]

A harmonically unstable high-temperature phase can be stabilized by anharmonic effects; conversely, a harmonically stable structure can undergo chemical degradation under illumination. In molecular dynamics, not fragmenting for 10 or 20 picoseconds is not proof of long-term durability. The timescale, sample volume, and barriers must be considered for observing rare events. The simulation thermostat, time step, and initial configuration are also recorded. Instead of stating “AIMD stable,” it is more informative to specify the duration, temperature, cell, and observed structural metrics.

Defects, ion migration, and the actual interface

The typical notation for the defect formation energy is as follows:

$$\Delta H_f(D^q) = E_{\text{defect}} - E_{\text{pristine}} - \sum_i n_i \mu_i + q(E_F + E_{\text{VBM}}) + E_{\text{correction}} \qquad [\text{eV}] \qquad \text{(I.21.1)}$$

In this equation, q is the dimensionless integer representing the defect charge in units of the elementary charge; it differs from the symbol q used for the elementary charge constant in other sections. E_F is the Fermi energy measured with respect to the top of the valence band, and E_VBM is the top of the valence band in the common energy reference. Here, n_i is chosen as a positive value for the number of atoms added to the supercell; other sign definitions are possible but must be explained. The defect charge alters the chemical potentials and the Fermi level. In charged supercells, finite-size and potential alignment corrections are necessary. The transition level, capture coefficient, and defect density are different quantities; the mere finding of a deep level does not provide the recombination rate. Freysoldt and colleagues compile the theoretical and numerical foundations of point defect calculations. [R22]

For migration, only the initial and final energies are not sufficient; the highest point of the path in between must be determined. Methods such as the climbing-image NEB search for saddle points along the selected path. Alternative paths, charge states, and defect concentrations should also be investigated. [R23] In the original scale

calculation, if a transition attempt of 10^{13} s^{-1}, a barrier of 0.50 eV, and a temperature of 300 K are chosen, the Arrhenius rate scale for a single attempt is approximately 4×10^{4} s^{-1}. This is the atomic jump scale; it is not the transition time of an ion across the film or the device lifetime. For long-range movement, the path geometry, random walk, and the number of mobile species are required.

In the interface model, surface termination, lattice mismatch, artificial strain, charge transfer, dipole, and chemical reactions are defined. Simply juxtaposing the band edges of individual materials with respect to the vacuum is only a preliminary step. Setting optimistic limit values for device parameters without evaluating interface defects and selective contact behavior breaks the chain of evidence. All inputs, software version, pseudopotential ID, raw output, and analysis script are stored; the results table alone does not guarantee reproducibility.

Distinguishing between numerical convergence and model accuracy

In DFT calculations, if increasing the cutoff energy or the k-point grid does not change the result, it indicates that the chosen approach has been numerically converged. However, this alone does not necessarily mean that the result reflects the properties of the real material. The exchange-correlation approximation, spin-orbit coupling, temperature, disorder, and defect structure are all separate physical choices. These choices should be kept consistent, especially when comparing the band structure of heavy-element absorbers. [R17] [R18] [R19]

If the quantity to be compared is the total energy difference, the convergence test should be performed directly on that difference. While there may be a large common error in the total energy of each phase, the difference can remain small; conversely, the ordering can change at the level of a few meV/atom, even if the individual energies appear stable. Calculating the reference phases with different numerical settings introduces a non-physical shift into the phase diagram. Consistent potentials for the same type of atom and sufficient convergence should be the common basis of the phase space.

From the geometry of the lower convex hull to a decomposition reaction

In a binary A-B system, let the energy of a candidate with a composition of xB = 0.50 be -0.28 eV/atom. If there are phases at xB = 0.25 with -0.30 and at xB = 0.75 with -0.40 eV/atom, a mixture with equal atomic ratios provides the same total composition at -0.35 eV/atom. The energy of the candidate above the hull is 0.07 eV/atom. This difference indicates the existence of a lower-energy decomposition combination at the same composition; it does not indicate at what rate the candidate will decompose.

In the multicomponent case, the same principle applies to linear programming: select non-negative amounts of the reference phases, conserve the element amounts, and minimize the total energy. When a previously missing competing phase is added, the lower envelope may decrease; therefore, a zero difference within a restricted pool of phases does not guarantee stability in the complete chemical system. When entropy and the chemical potentials of the environment are included, the relevant thermodynamic potential also changes. [R20]

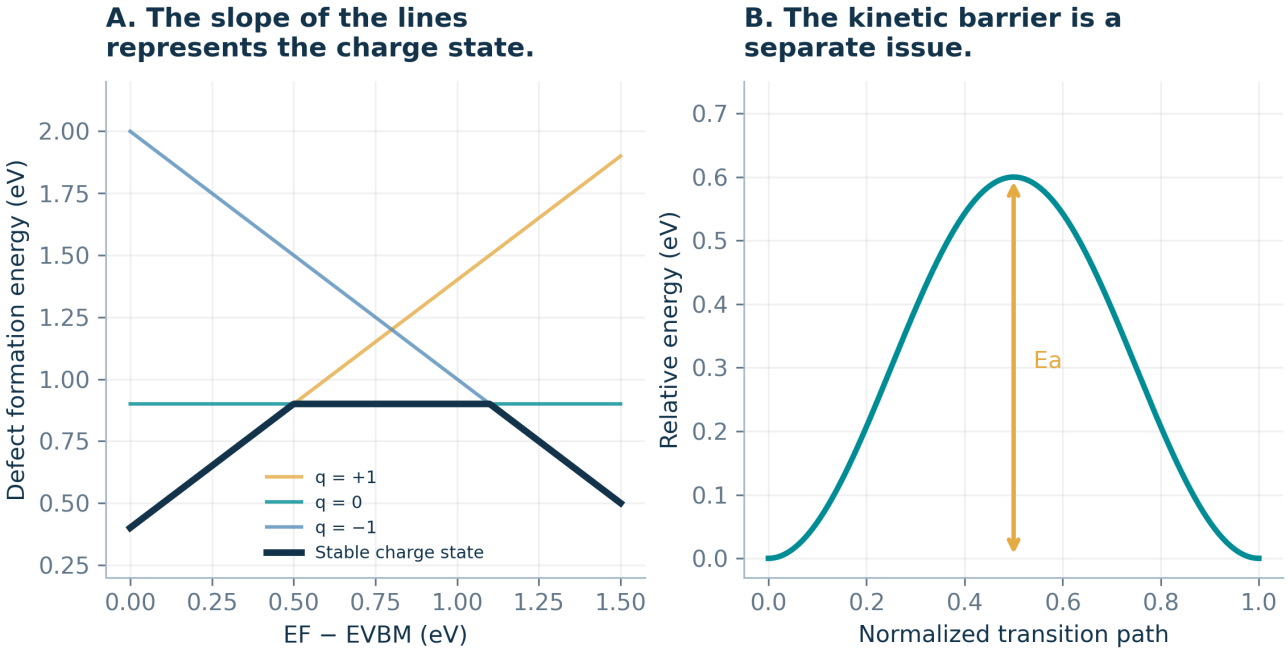


Figure 35. The defect formation energy and the kinetic barrier have different roles. In panel A, the slope of the formation energy with respect to the Fermi level represents the number of charges associated with the defect; the lower envelope indicates the stable charge state. In this synthetic example, the transitions occur at 0.50 and 1.10 eV. Panel B shows an example path with a 0.60 eV barrier; it is not the output of a real NEB calculation. [R22] [R23]

Phonon stability and defect charge states

The reduction of forces during structural relaxation indicates that a stationary point has been reached. The eigenvalues of the curvature matrix with respect to small displacements are related to the square of the vibrational frequencies. Negative curvature appears as an imaginary frequency in the harmonic model. Such a mode suggests that the selected structure can relax in that direction; however, numerical noise, insufficient supercells, and anharmonic stability at finite temperatures are also considered. The harmonic zero-temperature analysis alone does not represent the phase lifetime at the operating temperature. [R21]

The defect formation energy adds to the energy difference between defective and defect-free cells, including the atomic reservoirs and the electron reservoir. Due to the linear EF term associated with the electron reservoir, the charge states have different slopes. The thermodynamic transition level is where two charge states have equal formation energies; it is not the same magnitude as the optical transition or charge

carrier capture barrier. It is possible for a defect with low formation energy to occur frequently, but to determine its effect on recombination, the capture physics must also be considered. [R22]

Self-assessment

1. **Does a negative formation energy prove phase stability?** No. It is necessary to compare it with all relevant phase mixtures that yield the same composition.

2. **If two DFT codes yield the same band gap, does this validate the experimental band gap?** No. It only indicates numerical convergence; a common modeling error may still be present.

3. **If phonons are clean and a short, trouble-free AIMD run is achieved, are we ready for the lab?** Not on its own. Competitive phases, defects, the synthesis window, the interface, and practical limitations must also be evaluated.

Explaining the concepts of magnetic state and anharmonicity

The quantum property of the electron, called **spin**, contributes to magnetic behavior. In a structure, the arrangement of local magnetic moments in the same direction, in opposite directions, or in another configuration can change the total energy. The prompt “Define the magnetic state” indicates that, especially in materials where such options are physically possible, one should not treat a single initial configuration as representative of all possibilities. It is not claimed that strong magnetism is present in every PV material.

The **harmonic approximation** assumes that the energy increases approximately parabolically with small displacements of the atoms. In this case, the normal modes in which the atoms vibrate together, and their frequencies, can be calculated; the quanta of these vibrations are called **phonons**. **Anharmonicity** refers to the fact that this simple parabola is not sufficient for larger displacements or in some soft structures. Vibrations can interact with each other, and the effective forces can change with temperature. Therefore, the harmonic behavior at zero temperature is not the same as the structural behavior at high temperatures; they are not the same answer to the same problem. [R21]

Numerical **convergence** means that the result we are interested in changes sufficiently little when the mesh, cutoff energy, or tolerance is chosen more strictly. This does not necessarily mean that the model accurately represents nature. An incorrect physical approach can converge to a very precise number. Model error, synthesis behavior, and experimental validation must be examined separately, beyond numerical convergence.

From material to cell: optical and electrical modeling

Which components does a device model combine?

The optical model first calculates how light enters the layers and at which location it is absorbed. This result becomes the **generation profile** for electron-hole pairs per unit volume per unit time. The electrical model then solves the charge densities, electric field, charge carrier flow, and recombination together. **Drift** is the net transport caused by the electric field; **diffusion** is the net transport caused by the charge carrier density difference. The accounting of charges entering, leaving, being generated, and being lost at each point is maintained by the **continuity equation**.

The **Poisson equation** relates the charge distribution to the electrostatic potential. The **boundary condition** specifies what happens at the edges of the model: such as contact voltage, charge carrier transport, or surface recombination velocity. The same intrinsic material parameters can yield different power outputs under different contact conditions. Therefore, simply inputting the band gap and lifetime does not fully define the cell.

How does a computer solve the model of a continuous film?

The **mesh** consists of calculation points placed along the thickness or on the surface. **Discretization** is the process of transforming continuous equations into relationships between these finite points. **Synthetic example:** If we initially divide a 1 μm film into 10 equal segments, each segment will be 100 nm. If a significant change near the contact occurs within 5 nm, this mesh cannot resolve it. We refine the mesh and check that the results for current, voltage, and charge conservation remain unchanged. It is not assumed that the solution is sufficient just because the graph appears smooth.

Parameter refers to a material or interface property that is input into the model. **Sensitivity** indicates how much a small change in a parameter affects the output. **Identifiability** refers to whether different parameters can be individually extracted from the measurement. For example, a better contact with a poorer bulk lifetime can explain a single J-V curve in a similar way. In this case, a very good curve fit is not sufficient to determine which mechanism is correct.

The “calibration” of a model involves adjusting its parameters to fit specific data. **Validation** tests whether it can also explain data from different conditions that were not used in the calibration. Testing a model fitted to a specific temperature under

different light intensities and temperatures is a robust check. We should interpret the model's power gain prediction as a range within the parameter uncertainties.

Comprehension check: is there only one correct parameter set?

Choosing the best fit with more decimal places does not solve the problem if two different sets of parameters describe the same curve. Find a measurement condition where the two models diverge: different irradiance, temperature, or time response. Selecting the new measurement to highlight this divergence connects the modeling to the experiment.

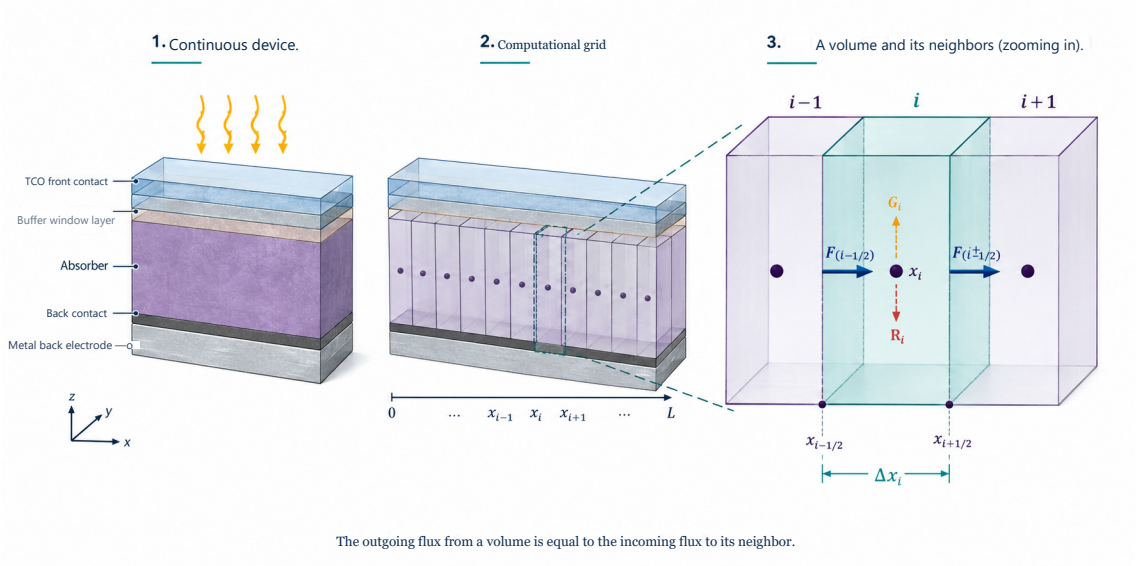


Figure 36. From a continuous device description to a conservative finite-volume calculation. The central mesh is enlarged on the right to show volume i and its neighbors. F represents particle flux through the faces; Gi and Ri represent generation and recombination within the volume. Inflow through the left face and outflow through the right face are balanced together. Read this panel in terms of particle conservation rather than a current sign convention. [R25] [R26] [R27] Conceptual illustration prepared with an image-generation tool; it is not a measurement image.

In the figure, F represents the particle flux; it should not be confused with the sign of the electric current. In a one-dimensional network, the average electron density in a volume i changes with the flux difference across the two surfaces and the volume-internal generation-loss:

$$\frac{dn_i}{dt} = \frac{F_{i-1/2} - F_{i+1/2}}{\Delta x_i} + G_i - R_i, \qquad J_n = -qF_n. \tag{I.22.1}$$

When adjacent volumes use the same surface flux, the contributions of the internal surfaces cancel each other out when the equations for all volumes are summed. Thus, only the input-output across the boundary and the total generation-loss remain. The basis of numerical conservation is this common surface calculation, which is more robust than simply obtaining a smooth curve at each node. [R25] [R27]

A semiconductor that absorbs light well is not necessarily a good solar cell. Photons must be absorbed in the active layer, charges must be separated, they must reach the

selective contacts without recombination, and they must be able to deliver work to the external circuit. Assuming that one link in this chain is ideal can obscure the success of the others. The goal of device modeling is not to produce a desired efficiency, but to show which loss is dominant and which experiment can isolate it, using measured or justified parameters.

First, the optical energy budget

In a passive optical stack, the reflection R, transmission T, and the sum of absorptions in all layers must conserve energy at each wavelength: R + T + ΣA_i = 1. Light absorbed in the active layer is a candidate for useful generation; light absorbed in the metal or transport layer is generally a parasitic loss. The term “total absorption 95%” does not provide sufficient information about the device current without specifying in which layer it occurs. If diffuse scattering is present, the measurement geometry and tools such as the integrating sphere used are also important.

For a single-pass, non-reflective, and homogeneous layer, A ≈ 1 - exp(-αd) can be written. In the original example, for $\alpha = 10^5$ cm^{-1} and d = 300 nm = 3×10^{-5} cm, αd = 3, and A is approximately 95.0%. When $\alpha = 10^3$ cm^{-1} with the same thickness, A is approximately 2.96%. This comparison explains why weak absorption near the band edge determines the thickness and light-trapping design. If there are multiple reflections and interferences in the actual device, this simple expression is not sufficient.

In planar layers, the transfer matrix method can be used, while in textured or nanostructured systems, an appropriate wave optics or ray tracing approach can be employed. The refractive index n(λ), extinction coefficient κ(λ), thickness, and surface geometry are obtained from measurements or explicitly defined calculations. In thick and irregular layers, the coherence assumption is revisited. Solcore is an example of an open-source tool developed to combine material and solar cell models at different scales; when used, it reports which sub-model is selected and which limits apply. [R26]

Generation, transport and recombination

The generation profile G(x) [cm^{-3} s^{-1} or m^{-3} s^{-1}] is obtained from the local absorption of the optical model. The electrical model must use the same unit system. In a one-dimensional drift-diffusion model, the electrostatic potential is determined by the Poisson equation, and the electron and hole currents are determined by the transport equations:

$$\frac{d}{dx}\left(\varepsilon\frac{d\psi}{dx}\right) = -\rho. \tag{I.22.2}$$

$$J_n = q\mu_n nE + qD_n\frac{dn}{dx}. \tag{I.22.3}$$

$$J_p = q\mu_p pE - qD_p\frac{dp}{dx}. \quad \text{(I.22.4)}$$

E = -dψ/dx; μ is the mobility, and D is the diffusion coefficient. The continuity equations relate the spatial variation of the current through G and recombination R. The sign convention must be fixed from the beginning. In a steady state, the conservation of the total current throughout the device provides a strong check for the mesh and solver validation. If the boundary conditions at the contacts are not physically chosen, obtaining a very accurate solution in the internal region is not sufficient for accurately modeling the device.

Radiative recombination can be written as R_rad = B(np - n_i^2). The SRH model accounts for the effects of trap-assisted capture and release; Auger recombination can become significant at high charge carrier densities. Interface recombination should not arbitrarily contribute to the bulk defect density. The selectivity of transport layers, energy barriers, contact resistance, and shunt paths are separate physical contributions. SCAPS's original work involves the modeling of polycrystalline semiconductor cells; SIMsalabim is an example of a tool representing open-source drift-diffusion solvers. The tool name does not replace model validation. [R27] [R25]

Increasing the thickness does not always yield the desired result

The diffusion length, L = √(Dτ), provides a rough estimate for charge carrier collection. Under classical, non-degenerate conditions, the Einstein relation is D = μkT/q. In the original example, if μ = 10 cm^2/Vs, T = 298.15 K, and τ = 100 ns, then D is approximately 0.257 cm^2/s, and L is approximately 1.60 μm. If the lifetime decreases to 1 ns, then L becomes approximately 0.160 μm. With all other conditions remaining the same, a 500 nm film may be promising for collection in the first case, but more challenging in the second. However, this calculation provides a scaling intuition, as the electric field and contact boundaries will modify the actual collection length; it does not replace device simulation.

An increase in thickness enhances light absorption but can also increase bulk recombination, carrier transport distance, and manufacturing challenges. In very thin films, pinholes, shunts, and optical escape can be significant. Therefore, the optimum thickness is not simply chosen based on α. If a design study keeps mobility and defect density unrealistically constant while varying the thickness, the result is stated as "optimum under these parameters." If, in an experiment, changes in thickness also alter the morphology and interface, the effects are analyzed separately.

The inverse problem: different models that explain the same curve

In the forward problem, parameters are given, and the J-V curve is calculated. In the inverse problem, an attempt is made to extract the parameters from the measured curve. This process is often non-unique: higher mobility combined with shorter lifetime can yield similar collection behavior under certain conditions; interface losses and bulk traps can explain the same V_oc drop. Fitting four summary numbers with five free parameters may appear flawless but can be scientifically weak. More important than the number of parameters is the independent sensitivity of the measurement to each parameter.

A distinctive example of non-uniqueness: suppose the experiment only constrains the product $L^2 = D\tau$. $D = 0.10\ cm^2/s$, $\tau = 100$ ns, and $D = 1.0\ cm^2/s$, $\tau = 10$ ns yield the same L^2 value. It is impossible to distinguish between the two from a single measurement. Independent mobility or time-resolved measurements could break this equivalence. If the error function of a model has a long, flat valley, writing the best point with many digits does not create additional information. The confidence region, parameter correlations, and alternative fits should be shown.

A practical solution is to explain the dark and illuminated J-V curves, different light intensities, temperature, EQE, absolute PL, and transient response using common physical parameters. Releasing all parameters freely for each new data type reduces the testing power. First, calibration is performed with a subset of the data; then, the curve under different conditions is predicted and subsequently measured. Validation requires successful prediction of behavior that has not been previously shown to the model.

Tandem and module interconnection

For a two-terminal series tandem, current matching is a fundamental constraint; simply summing the individual maximum powers of the sub-cells does not yield the power of the series device. In a simplified analysis, the sub-cell voltages are summed at a common current, and the total power is maximized over this common current. In a four-terminal configuration, independent electrical operation is possible, but optical filtering, interconnection, and power electronics losses must still be considered. The comparison should clearly state the number of terminals and the number of independent MPP circuits.

In uncertainty propagation, physically plausible common distributions are used instead of a single “ideal” set of parameters. If the band gap, absorption, and mobility are correlated by the same chemical change, they should not be chosen independently at random. The result shows which parameter influences the decision, in addition to the efficiency distribution. Thus, an expensive new calculation or measurement is directed

to where it will reduce the uncertainty the most. Priority is given to information that can change the result, rather than to the most aesthetically pleasing simulation curve.

Transforming the numerical device model into a solvable problem

Describing a one-dimensional device solely by its thickness, band gap, and mobility is insufficient. First, the coordinates, contacts, band edges, dielectric permittivity, doping, and fixed charge are determined. Then, G(x) is established from the optical model, and R(n, p, x) is defined based on the selected mechanisms. The electron and hole current densities, along with Poisson's and continuity equations, are solved simultaneously. The charge carrier density or flux boundaries at the contacts determine the physical meaning of the model.

In finite volume discretization, the current difference across each small cell's two faces is equal to the net generation within the volume. For an electron in a steady state, $J_{n,i+½} - J_{n,i-½}$ is approximately $q(R_i - G_i)\Delta x_i$. Neighboring cells share the same interface current. When all cells are summed, the internal face currents cancel each other out, leaving only the external contacts and the total generation/loss. This is the origin of the conservation check. [R25] [R26] [R27]

The model must satisfy at least the following constraints: zero net current in dark thermal equilibrium; optical power balance; stable output when the mesh is refined; total electrical current independent of position; expected analytical behavior at simple boundaries such as zero loss or low area. A numerical convergence message does not replace these checks.

Let's examine the optimization of thickness using an analytical example

Let light enter at x = 0, and let the electron collection surface be at x = d. Let's choose a reflectionless $G(x) = \alpha\varphi \exp(-\alpha x)$ and a sample collection model $P_{col}(x) = \exp[-(d - x)/L]$. The fraction collected per incident photon is the integral of these two functions:

$$F(d) = \frac{\alpha \exp(-d/L)}{\alpha - 1/L} \left[1 - \exp\left(-[\alpha - 1/L]d\right)\right]. \tag{I.22.5}$$

This expression is written as $\alpha = 1/L$; at that point, the limit is $\alpha d \exp(-d/L)$. For $\alpha = 2\ \mu m^{-1}$ and L = 1 µm, $F(d) = 2[\exp(-d) - \exp(-2d)]$. When we set the derivative to zero, we find d = ln 2 µm = 0.693 µm, and the maximum F = 0.5. Optical absorption, on the other hand, continuously increases with thickness. It is thus clear how a larger collected current can result from greater absorption within the same device.

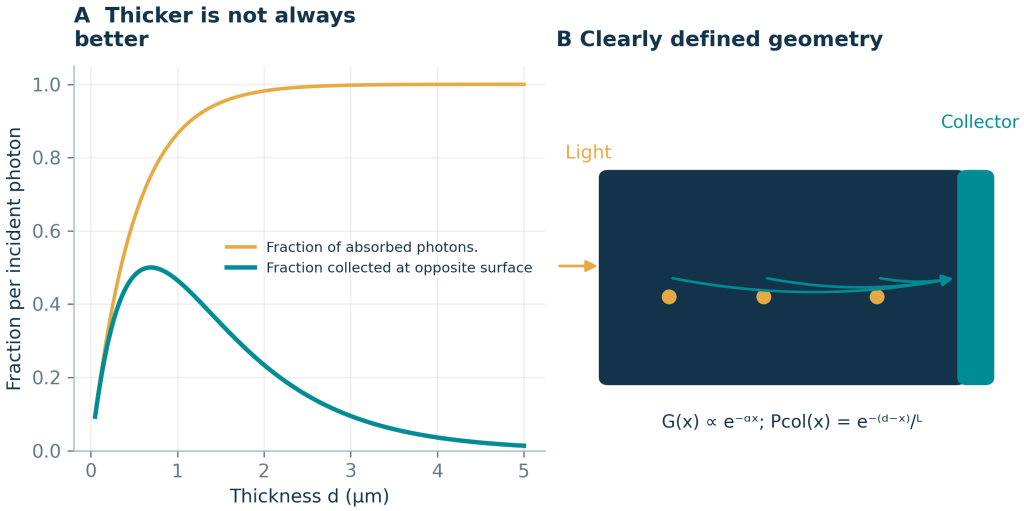


Figure 37. An example of an optimum thickness with explicitly defined geometry. On the left, the absorption increases monotonically, while the fraction reaching the back collector passes through a maximum. The geometry and formula on the right use $\alpha = 2\ \mu m^{-1}$ and $L = 1\ \mu m$. The exponential collection probability is a teaching model; it does not replace the Poisson-transport solution of a real heterostructure.

If we had chosen Pcol = exp(-x/L) in the semi-infinite model with the collector on the front side, we would have obtained a different thickness dependence. This comparison teaches an important research habit: before believing in an optimum, draw the geometry, boundary and loss mechanism that produce that optimum.

Self-assessment

1. **If the total absorption is 95%, is the EQE also 95%?** No. It is necessary to consider in which layer the absorption occurs and how much of the generated charge is collected.
2. **Does a very good fit to a single J-V curve uniquely determine the physical parameters?** Generally, no. Additional measurements with independent sensitivities are required.
3. **In a series-connected tandem cell, are the maximum power values of the individual sub-cells simply added together?** No. The total voltage and power must be calculated under the condition of a common current.

What do the optical constant, mesh, and verification represent?

The **optical constants** of a layer describe the propagation and attenuation of light within the material. The refractive index is related to the phase advancement of light, and the extinction coefficient is related to absorption; both can be wavelength-dependent. Two films of the same thickness but with different optical properties may not generate the same number of charge carriers. Therefore, it is necessary to use the generation profile as input for the electrical model.

The **numerical grid** divides the continuous space into small, discrete regions for computation. The current leaving the common surface of two adjacent volumes must

be consistent with the current entering the other; otherwise, the calculation behaves as if it were creating or destroying charge. Grid refinement, unit, and conservation checks test numerical consistency. **Independent validation** involves testing the model's prediction with a measurement that was not used in the fitting process. A parameter set that describes a single curve very well may fail at a different temperature; the quality of the fit alone is not proof of the mechanism.

Let's also clarify the symbols at the boundary. The **Dirichlet condition**, for example, specifies that the contact potential is held at a certain value. The **Neumann condition** specifies the normal derivative at the boundary, or the flux associated with it; in an appropriate model, zero flux can represent an insulating boundary. The **Robin condition** relates the value to the normal derivative; the recombination flux proportional to the excess of charge carriers on the surface is one of its physical examples. ΓD, ΓN, and ΓR are the names of the boundary segments to which these different conditions are applied. These are not new material layers; they describe how the calculation area interacts with the outside.

Searching for materials with machine learning: from prediction to evidence

What does machine learning learn?

Machine learning encompasses methods that utilize input-output relationships from examples to generate predictions for new inputs. The input is referred to as a **feature**, and the value being predicted is called the **target**. For example, composition and certain structural information can be the input, while the calculated band gap can be the target. The model learns this target. If the target is only the calculated band gap, the model's output is not directly the synthesizability, actual defect behavior, or cell efficiency.

The **training set** is the data used to learn the parameters. The **validation set** assists in model and parameter selection. The **test set** is kept separate from the selection process to measure the final performance. **Overfitting** is learning the details of the training examples and failing on new examples. A measure of successful learning is not only explaining the known data but also working well on a properly separated new case.

Why does data leakage sometimes appear to yield good results?

Data leakage refers to the indirect inclusion of information that will not be known during prediction into the model selection or inputs. **Synthetic example:** Let's take measurements from ten different regions of the same film and randomly divide the rows into training and testing sets. The model has already seen training regions that are very similar to the film in the test set. As a result, it may overestimate the success in predicting a new production lot. The division unit should be a real independent specimen or lot, not a row.

Calculations involving very similar compositions within the same material family or different calculation records for the same structure can lead to similar problems. We must specify in advance which “new” situation we want to generalize to: a new measurement point, a new batch, a new composition, or an entirely new structural family? These are different tests. [R29]

Uncertainty estimation attempts to express the model’s confidence as a range; the agreement of this confidence with the actual error frequency must also be tested. An **out-of-distribution sample** is a condition that is significantly different from the training data. The fact that the model appears confident in such a sample does not necessarily mean that it is reliable.

Active learning selects the next calculation or experiment based on the information that the results will provide. The candidate with the highest predicted value may not be the same as the candidate that reduces the most uncertainty. Allocating some of the research budget to improving a well-known region and some to exploring an uncertain area is a design question. Predicted candidates are ranked; they do not replace experimental evidence.

Comprehension check: which achievement was reported?

If a model accurately predicts a band gap, can we say that it has "found a good solar cell"? No. The band gap is just one of the inputs for absorption and energy sharing. If there are no phase, defect, interface, manufacturing, and stability targets, then success in those areas has not been measured.

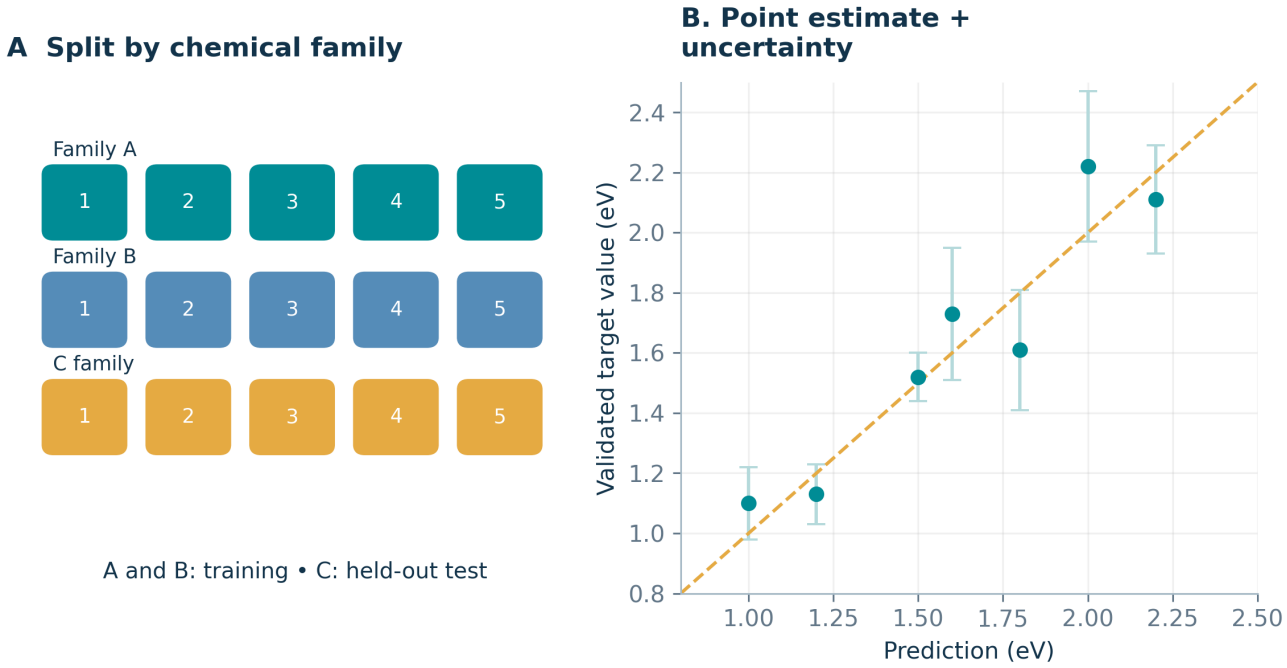


Figure 38. The data split must match the research question. Panel A illustrates holding out an entire chemical family for testing. Panel B shows a prediction and its uncertainty; the numbers are synthetic. The reliability of an interval is assessed by a coverage test on held-out data. [R28] [R29]

Machine learning can improve the order in which expensive calculations and experiments are performed. This role is important because the candidate space is very large. However, the model's task is not the same as the ultimate claim of the research. A model may predict the formation energy; the researcher desires a synthesizable, stable, low-defect, and appropriately interfaced solar cell. There are many steps in between. Extending the single task that the model solves well to the entire chain is one of the most common semantic shifts in computational research.

What does the data set actually represent?

For a data row, both the chemical formula and the source are important. Was the energy obtained experimentally or calculated? Which functional, pseudopotential, spin state, and geometry were used? How were convergence failures handled? Different structures of the same compound are distinct physical examples; repeated copies of the same structure are not independent examples. If the "band gap" column is a mixture of optical measurements, PBE eigenvalue differences, and hybrid calculations, the model's target becomes ambiguous. It is not possible to eliminate label noise by using a larger network.

Negative results should be visible in the data set. If unsuccessful syntheses, unstable relaxations, samples that fall outside the measurement range, or deviations from the process conditions occur, the model will only learn about the world of successful publications. "This could not be produced with this method" is not the same label as "the material is impossible." Failure in the laboratory record can be due to the solvent, atmosphere, equipment, or process window. The usable learning target should express the result and its conditions together.

Data leakage and spurious generalization

Data leakage refers to the inclusion of information in the training or model selection process that should not be available during testing. Randomly splitting slightly corrupted copies of the same structure, distributing samples from the same experimental batch to both training and testing, or learning normalization across the entire dataset can lead to overly optimistic scores. Selecting features and models by repeatedly examining the test results also compromises the independence of the test. Kapoor and Narayanan systematically investigated this problem in science based on machine learning, finding that it is widespread and takes many forms. [R29]

In PV research, partitioning should be appropriate for its intended use. For generalizing to a new laboratory batch, a batch-based approach is meaningful; for generalizing to new chemistries, a chemical family-based approach is meaningful; and for generalizing to future candidates, a time-based evaluation may be meaningful. Completely excluding all new elements from the training set is too strict, but it is a necessary constraint in some tasks. The result of random partitioning is still useful, but it only provides information about new samples with similar distributions. The term "general purpose" does not guarantee accuracy outside of the distribution.

In the original example, 2000 rows are generated when 20 small perturbations are created for each of the 100 main structures. When a random 80%/20% split is performed, most of the test structures have siblings in the training set. The model can achieve high accuracy without learning the new main structure. Separating the main structures into their respective groups provides a better test for the actual

generalization problem. The same logic applies to a large number of solar cells cut from the same substrate and to repeated data derived from the same article.

A good regression score is not discovery success

The mean absolute error indicates how much, on average, the target is incorrectly predicted. However, if the decision is made based on a threshold, false positives may be more significant. The Matbench Discovery study distinguishes between formation energy prediction and thermodynamic stability classification, and between retrospective testing and prospective searching; it demonstrates that a low regression error may not prevent a high number of false positives near the threshold. [R28] Therefore, precision, recall, false positive rate, cost per successful calculation, and top-k enrichment are selected in conjunction with the task.

Original Bayes example: Suppose only 1% of 10,000 candidates truly meet the target. If the sensitivity is 90%, then 90 out of 100 true positives will be detected. If the specificity is 95%, then 5% of the 9900 negatives, or 495 candidates, will be false positives. Out of the 585 selected candidates, only 90 are correct: the positive predictive value is 15.4%. Although it appears that "accuracy is very high," most of the experimental budget may be spent on unsuccessful candidates. If the specificity increases to 99%, then 99 false positives remain, and the rate increases to 47.6%. In rare target scenarios, the base rate cannot be ignored.

Uncertainty can be conceptually separated into epistemic uncertainty, which arises from a lack of knowledge or model deficiencies, and aleatoric uncertainty, which stems from inherent variability in the data or process. Ensemble spread or the standard deviation provided by a model does not automatically represent a calibrated confidence interval. Whether the predicted intervals actually achieve the specified coverage rate is measured on independent data. If multiple models use the same training set and similar architectures, they can collectively err in the same direction. Approaches such as conformal methods also have their own assumptions regarding exchangeability and distribution; their guarantees are not unlimited under distribution shift.

The proper role of universal interatomic potentials

An interatomic potential predicts energy, forces and sometimes stress. These can reduce the computational cost of structural relaxation or molecular dynamics. The model in its standard form does not produce band gap, optical transition strength, defect capture coefficient, or PV efficiency. Interpreting the outputs of an energy model as these electronic quantities is a categorical error. Coordination, oxidation state, charge, surface, and interfaces, which are outside the scope of training, should also be tested. Success in three-dimensional crystals does not guarantee the same success in sparse surface chemistry.

The practical procedure is as follows: first, the formula and structure are chemically verified; then, the model's training similarity and uncertainty are evaluated; low-cost screening is performed; selected candidates are checked using independent and convergent calculations. Writing the model output as "priority candidate with this score under this model" instead of "stable material" preserves the level of evidence. DFT verification is also not synthesis evidence. If the label chain is maintained at each step, negative results become valuable data for the next model.

Active learning and reproducibility

In active learning, the model selects the candidate from which the next calculation or experiment will yield the most benefit. Simply selecting the candidate with the highest predicted efficiency may repeatedly exploit the same chemical region. Uncertainty, diversity, cost, and practical feasibility are considered together. The learning target can be established in a decision-oriented manner: the question "which inexpensive test will eliminate this family?" is sometimes more valuable than the question "which candidate has the highest score?" The identity of the samples, preparation conditions, and reasons for failure for experimental feedback are maintained in a machine-readable format.

The FAIR principles aim to ensure that data is findable, accessible, interoperable, and reusable. It is not exactly the same as open access; even restricted data can have declared access conditions and sufficient metadata. [R30] The research package stores the data version, partition list, preprocessing steps, random seeds, software versions, model weights, hardware specifications, and the date of the last evaluation. The SHA-256 hash of a file is used to verify that the file has not been changed; it does not prove that the information within it is correct. Producing the same result from the same input is reproducibility; success in an independent laboratory is a higher level of evidence.

Formulate the generalization question before data partitioning

The question, "Does the model identify the unknown material?" can have several different meanings. Predicting a new composition within the same chemical family, transitioning to a new crystal prototype, and predicting an entirely new element combination are not the same tasks. Random row splitting, if it distributes near-variant samples of the same material for training and testing, may yield good results in the first task but may provide little information about the third. The type of split should be chosen based on the type of generalization that the research will use. [R28] [R29]

Scaling, feature selection, and hyperparameter tuning are performed without looking at the test set. If the model is regularized, it is also investigated whether information from the test label was used during regularization. Multiple models originating from the same source should not be treated as independent specimens. Identifying duplicates based on composition, structure, and source ID is a scientific part of data cleaning.

Linking predictive uncertainty to selection

If a model generates two predictions, such as 1.40 ± 0.05 eV and 1.45 ± 0.40 eV, selecting based solely on the proximity to the average ignores the uncertainty. The probability of hitting the target range, the computational cost, and the distance from unknown chemistry can be evaluated together. For this, the coverage of the error bars should be tested on held-out data: for example, do the ranges called 90% actually cover approximately 90% of the results? A narrow, uncalibrated range merely gives the appearance of high confidence.

In active learning, repeatedly calculating the model's most preferred candidates can narrow the known region. Examples with high expected success, high uncertainty, and high chemical diversity can be included in a selection batch. The goal is not only to improve the prediction score but also to gather information that will change the research decision. After each new calculation, the data version, selection rule, and validated result are saved, thus distinguishing between retrospective successful candidate selection and prospective prediction. [R30]

Self-assessment

1. **Does a model with a low average energy error correctly select all stable candidates?** No. Errors near the threshold and the base rate of candidates determine the false positives.
2. **Can different perturbations of the same structure be present during training and testing?** If the goal is to generalize to a new structure, they should be grouped together and separated; otherwise, leakage may occur.
3. **If the universal potential has been adequately relaxed, has a PV material been found?** No. Evidence regarding electronics, defects, interfaces, synthesis, and devices is still lacking.

Experimental design and statistics: how do you distinguish an effective change?

Why can we not immediately interpret a difference as an effect?

When the efficiencies of two cells differ, the variation may be due to the starting material, the conditions of the day, or a measurement difference. The **experimental unit** is the smallest unit to which the process is applied independently. Multiple measurement points on the same wafer do not represent multiple independent wafers. The **control group** is a reference that matches the conditions outside the process as closely as possible for comparison. The **factor** is the condition we change; the **response** is the result we measure.

Randomization reduces the accumulation of sequence-dependent effects by randomly assigning the order of processing or measurement for the groups. **Blocking** involves making comparisons within a known source of variability, such as day, lot, or device. The goal of both methods is not to randomly generate samples, but to manage the sources that confound the effect of interest. [R31]

Mean, variability, and independent replication

The **average** is the sum of the values divided by the number of values. The **standard deviation** describes the typical spread around the average of the measurements. **Synthetic example:** Let three independent cells, 20%, 21%, and 22%, yield data. The average, 21%, has a sample standard deviation of 1 percentage pointage point. This deviation does not mean that the data are 1% wrong; it summarizes how different the three cells are from each other. The uncertainty of the average estimate also varies with the number of samples and independence.

The **confidence interval** is a range based on the coverage property of the selected statistical method for repeated sampling. Simply writing a single average with more decimal places does not increase confidence. The **p-value** is related to the probability of observing the obtained data or more extreme data under a specific null hypothesis and assumptions; it is not the probability that the hypothesis is true. **Effect size** describes the magnitude of the difference. A very small difference, even if statistically significant, may be insignificant in practice; a large-seeming but uncertain difference may require new data.

Interaction refers to the phenomenon where the effect of one factor depends on the level of another factor. For example, doping may be beneficial at a low annealing

temperature but detrimental at a high temperature. Testing doping at only a single temperature does not reveal the overall effect. A **factorial design** systematically tests combinations of factor levels. Below, we will arrange the numbers in a predetermined experimental design to make a decision.

Comprehension check: twenty measurements or two experiments?

If ten points are measured on a control wafer and a process wafer, there are not twenty independent process replicates. These points represent the within-wafer variability. To evaluate the repeatability of the process on different wafers, independent wafer productions are required. In statistics, the unit that needs to be counted correctly is not the number of rows in the table.

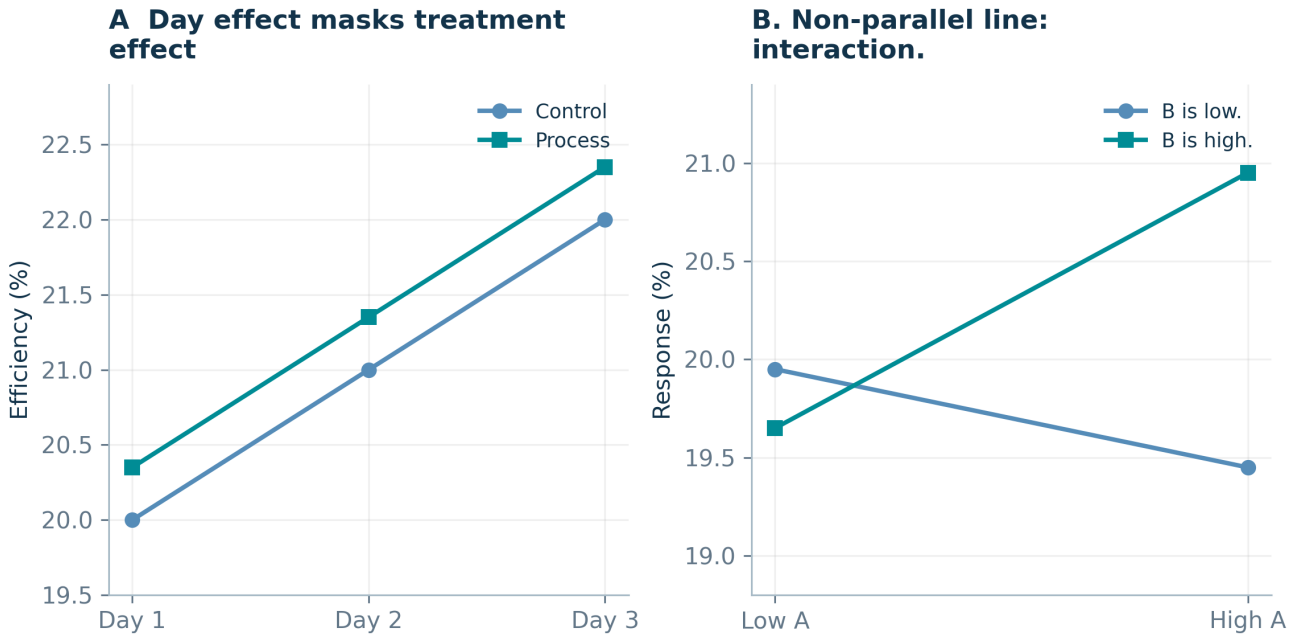


Figure 39. Illustrative examples of blocking and interaction. In panel A, the day effect is large, and the difference between treatments within the same day is +0.35 percentage points. In panel B, the effect of one factor changes sign depending on the level of the other factor. All responses were generated using explicit formulas. [R31]

The costly part of laboratory research is not just the use of equipment; it's the weeks spent chasing down spurious causal conclusions. When a new dopant yields higher efficiency, it may indeed be effective. However, it could also be that the humidity decreased on the same day, the solution age changed, the annealing plate behaved differently, or the operator applied a better film coating. Statistics should be used not as an additional tool that produces a nice p-value afterward, but as a way of thinking that distinguishes between these alternatives when designing the experiment.

Distinguish the experimental unit from repeated measurements

Eight pixels on a substrate are often not the result of eight completely independent fabrication experiments. They share the same solution, coating step, and annealing process. Obtaining 50 J-V curves from the same cell does not measure fabrication variability; it measures the device's measurement and time-dependent behavior. When reporting the sample size, the number of independent solutions, substrates, fabrication batches, and devices should be specified separately. Otherwise, technical replicates are treated as if they were independent samples, and the uncertainty is reduced.

Original example: Let 23.0% represent 12 pixels from a single doped substrate, and 22.0% represent 12 pixels from a control substrate produced on a different day, and calculate the average. Although the total appears to be "n = 24," the doping effect is intertwined with the day and substrate effects. On the same day, under the same controlled conditions, doping and control should be randomly distributed across multiple independent substrates. Repeating the experiment over multiple days will show whether the results are consistent despite production variability. If analysis is to be performed at the pixel level, the hierarchical structure must be taken into account.

Randomization, blocking, and blind analysis

Randomization reduces the systematic clustering of unknown factors within a group. Blocking organizes known nuisance factors: days, batches of solution, or furnace positions can be blocked. Producing both control and intervention within each block helps to separate day-to-day variation from group differences. NIST's design of experiments resources address random block and factorial designs for this purpose. [R31] Randomization is not about leaving all conditions random and uncontrolled; it is about neutralizing the order of assignment within a defined arrangement.

When blind analysis is possible, sample labels can be hidden from the person making the image segmentation or curve exclusion decision. Acceptance/rejection criteria are written without looking at the data; for example, a broken measurement contact, an obvious physical short circuit, or a calibration failure. Being "low efficiency" in itself is not a reason for rejection. The rejected data and the reason for rejection remain in an accompanying file. Criteria determined before the sample is produced are more robust than rules that are adapted to the result later.

Changing individual variables may lead to overlooking the interactions between them

In a two-factor experiment, the four combinations of low/high levels of factors A and B are measured together. If the effect of one factor depends on the other, there is an interaction. The coded model and line graph at the end of the section set up this calculation step by step.

When there are three or four factors, a full factorial experiment can be costly. Fractional designs can be used when the interactions between effects are known; the interacting effects are then tested later with a separate experiment. After the screening phase, the response surface and the optimal region can be investigated. However, the point that appears optimal in the initial small data set may be a result of noise. The selected condition is verified in new and independent production batches. The samples used in the optimization and the verification samples serve different purposes.

Effect size, uncertainty, and selection bias

Reporting only the best cell for a group conceals the distribution. The average/median, spread, all data points, efficiency, V_oc, J_sc, FF, and production success are all useful when considered together. The champion cell is a probabilistic outlier; a group that produces more cells may simply find a higher champion due to the larger sample size. “The best of 8 cells in the control group, and the best of 80 cells in the intervention group” is not a fair process comparison. An independently certified record is one question, and the advantage of a repeatable process is another.

In the original independent-group analysis, let there be 10 independent samples in each of the two groups, with standard deviations of 0.5 percentage points and a difference between the means of 0.6 points. The standard error of the difference is $\sqrt{(0.5^2/10 + 0.5^2/10)} \approx 0.224$ points. Within the appropriate approximate t-interval, the 95% confidence interval is approximately 0.6 ± 0.47 points. This is an illustrative scenario where the samples are independent and the model assumptions are reasonable; it cannot be directly applied to the pixels of a single substrate. In a paired design, the variability of the within-block differences should be used.

The p-value assesses the extent to which the data deviates from what is expected under the null hypothesis and the model; it is not the practical magnitude of the effect or the probability that the hypothesis is true. If numerous additives, annealing processes, solvents, and criteria are tested, and only the one with the lowest p-value is selected, the risk of false discovery increases. The primary endpoint is pre-selected, and multiple comparisons and exploratory analyses are explicitly stated. An effect may be statistically significant but insignificant due to production costs and lifetime

degradation; the decision criterion should encompass both scientific and practical objectives.

The intervention chain for the causal mechanism

The “doping → large grain → high efficiency” chain comprises three separate claims. It must be individually verified that doping alters the grain size, the grain size affects the relevant electrical loss, and this change leads to efficiency. If doping also alters the surface chemistry, energies, and crystallization rate, then grain size may only be an accompanying indicator. For the mechanism, control doping, along with distinct interventions such as the same morphology but different chemistry, dose series, reversal, or different preparation methods, are valuable.

The researcher can propose an alternative explanation for each hypothesis and identify observable parameters to differentiate between them. For example, is the improvement in V_oc due to bulk passivation or contact selectivity? An absolute PL/QFLS comparison of the bare film, single-contact stack, and complete device, followed by contact modification, provides a pathway. If the same model cannot explain all the results, the hypothesis is not forced; the uncertainty and failure to explain are noted. If a negative result is well-designed, it indicates which approach should be abandoned.

Cost-effective and decisive experiment selection

The answer to every problem is not simply a larger dataset. If the fundamental claim is the existence of a phase, then a reliable phase definition is required first; if the claim is reduced interface loss, then a measurement sensitive to that loss is required first; if the claim is lifetime, then operation under the relevant stress is required first. The value of an experiment is assessed by the expected information gain, cost, and the ability to change the decision. A pre-written stopping rule prevents endless adjustments when the result is negative. If there is a genuine repair hypothesis, the new experiment is opened as a separate hypothesis; the old, unsuccessful result is not deleted.

Difference within the block: a simple yet powerful calculation

Over the three production days, the control efficiencies were 20.00%, 21.00%, and 22.00%, respectively; and the processed samples for the same day were 20.35%, 21.35%, and 22.35%. The day effect changes by 2 percentage points, while the processing effect is +0.35 percentage points for each block. However, if we compare the control of the first day with the processed sample of the last day, we see a difference of +2.35 points; most of this difference is not related to processing. The matched difference within the block partially eliminates the common day condition.

In a real experiment, independent production replicates are required each day. In the model $y_{ij} = \mu + \beta_{treatment} + b_{day} + \varepsilon_{ij}$, the day term represents dependence between samples from the same day. Ten scans of the same cell do not count as ten independent production replicates.

Interaction calculation for a two-factor experiment

Let's code the factors at a low level as -1 and at a high level as +1. The model $y = \beta_0 + \beta_A A + \beta_B B + \beta_{AB} AB$ implies that the effect of one variable depends on the other. In the figure, $\beta_0 = 20$, $\beta_A = 0.2$, $\beta_B = 0.3$, and $\beta_{AB} = 0.45$ were chosen. When B is low, increasing A reduces y by 0.5 points; when B is high, the same intervention increases y by 1.3 points. Changing a single variable might lead one to believe that this discrepancy is due to a change in mechanism; a factorial design makes the interaction visible. [R31]

In this example, the four-corner responses are 19.95, 19.45, 19.65, and 20.95, respectively. However, simply publishing the best corner does not teach the process window. The center points provide information about the curvature, the repetitions predict the noise, and the random sequence reduces the mixing of drift with the factors over time. The research question shifts from "which recipe yields the highest value?" to "which effect is repeating under which condition?"

Self-assessment

1. **Does having 20 pixels on a substrate represent 20 independent manufacturing iterations?** Mostly no. Due to the shared manufacturing history, group/hierarchy is taken into account.

2. **What should be reported if the doping effect disappears with temperature?** The interaction and the conditions under which the advantage is observed; not an unconditional, general improvement.

BOOK I · CHAPTER 25 / MEASUREMENT AND RESEARCH

From cell to module, to the field, and throughout the lifecycle

There is a relationship between cell efficiency and daily energy output

The power of a cell under standard conditions does not mean that it will operate at the same power level at all times outdoors. The sun's position, clouds, soiling, temperature, shading, and the device's operational status all affect the output. **Nominal power** is the power rating under specific reference conditions. **Energy generation** is the sum of the actual power curve over time. Its unit is kWh, which is different from the power unit, kW.

Synthetic day: Assume a system generates an average of 1 kW for two hours, 2 kW for the next three hours, and 0.5 kW for the last hour. The daily energy would be $2 \times 1 + 3 \times 2 + 1 \times 0.5 = 8.5$ kWh. Using the average for several hours is an approximation of the integral. It is also necessary to clearly state how this summation handles negative nighttime measurements, downtime, or missing data.

What does the denominator of the performance ratio represent?

Reference yield is the equivalent number of hours obtained by dividing the total irradiation on the module plane by the selected reference irradiance. **Specific energy yield** is the ratio of energy to the installed rated power; it is expressed as kWh/kWp. The **performance ratio** compares the actual specific yield with a radiation-based reference. It summarizes many system losses together and does not isolate the specific mechanism responsible. The temperature correction and measurement method used should also be specified.

A **bifacial module** can also utilize light coming from the rear side. The proportion of light reflected from the ground depends on the surface's reflectivity, the mounting height, and the spacing. The surface's reflectivity ratio is called **albedo**. Therefore, the fact that the same module produces different amounts of energy in different terrains does not necessarily mean that the material has changed.

Life cycle assessment encompasses the selected environmental impacts from raw material extraction to production, use, and end-of-life recycling within defined boundaries. The **functional unit** is the basis for comparison; for example, 1 kWh of electricity delivered. The **energy payback time** is the time it takes for the energy used in production to be offset by the energy generated during use, under specific

calculation conditions; it is not the same as the material investment payback time. **LCOE** correlates the costs over the lifetime with energy production in a defined economic model. Different service life, financing, and irradiance assumptions yield different results for the same technology.

Comprehension check: Does higher efficiency imply a lower impact?

An increase in efficiency can reduce the area required for the same power output. However, if production energy demand rises substantially or lifetime deteriorates, the environmental impact per kWh may increase. It is not possible to conclude that a system is "more sustainable" without comparing efficiency, production energy, and lifetime energy within the same system boundaries.

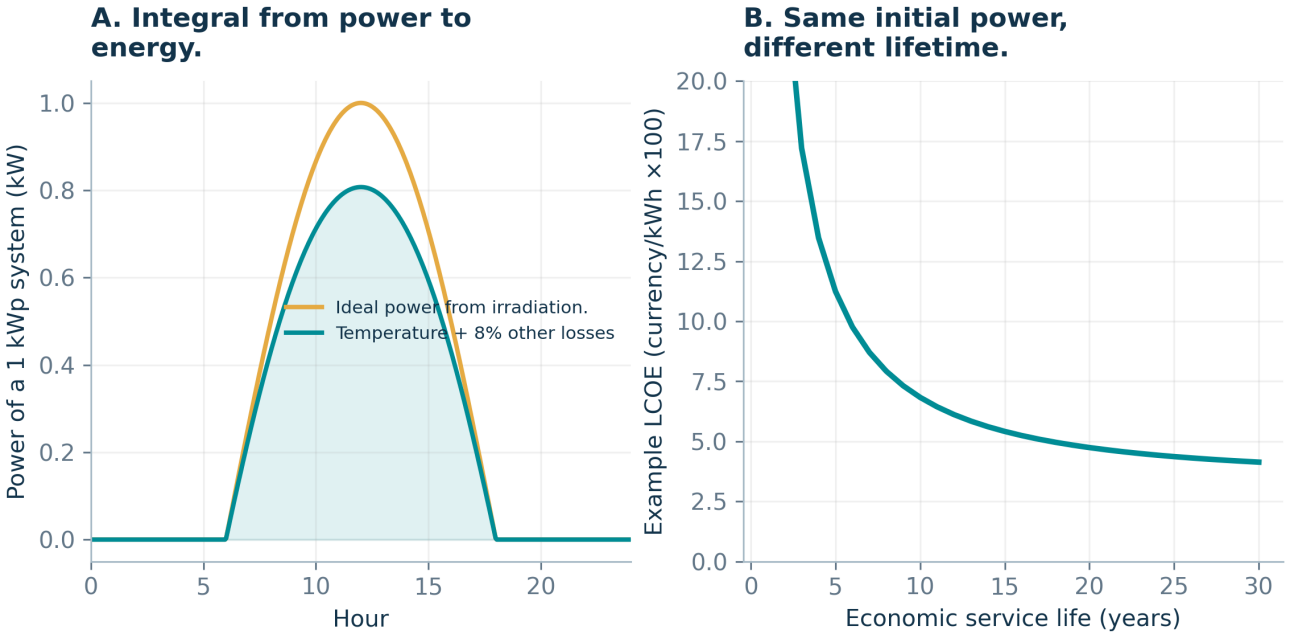


Figure 40. From initial power to lifetime energy. Panel A represents the temperature and loss calculation for a synthetic day at 1 kWp. Panel B illustrates the lifetime impact on the LCOE under selected cost/production assumptions; it is not a market forecast. The calculation inputs are clearly provided in the section. [R32] [R34]

A cell with an area of one square centimeter is a powerful tool for testing physical principles; it is not a power plant or a commercially viable panel. Scaling up does not simply involve geometrically expanding the same cell. The current collection distance, transparent electrode loss, metal shading, coating homogeneity, edge areas, interconnections, and manufacturing defects all change with scale. Therefore, material efficiency, cell efficiency, module efficiency, energy yield, and economic consequences should be considered as separate steps.

Cell-to-module losses

Series-connected cells carry the same current; a weak or shaded cell can limit the entire array. Bypass diodes provide protection in certain shading conditions, but they do not eliminate energy loss. In thin-film modules, the lines used for monolithic interconnection and the dead areas reduce the geometric fill factor. In crystalline silicon modules, the spacing between cells, the connection strips, and the encapsulation optics are evaluated. During the cell-to-module transition, some optical gains may also occur; representing the entire effect with a single, fixed loss percentage is only a rough approximation.

In the original area calculation, let the active cell area efficiency be 25%, the effective geometric fill factor be 92%, and the other electrical/optical factor be 0.97. Using a simple separable approximation for the module, we get $0.25 \times 0.92 \times 0.97 = 0.2231$, which is 22.31%. This is not an estimate for a real product, but rather a calculation demonstrating how losses are multiplied in a chain. As the area definition changes, the cell efficiency should be compared with the total module area. A higher active-area efficiency at the expense of a larger dead area may negate the advantage at the panel level.

At the production scale, the process window becomes critical. Instead of the optimal thickness for a single device, the thickness distribution across a large area, coating lines, solvent drying dynamics, particles, and defect density are controlled. Manufacturing yield is the ratio of the number of accepted products to the total production; it should not be confused with electrical conversion efficiency. If a small performance improvement results in a very high defect rate, it may not provide a cost advantage. Process cycle time, energy consumption, material usage per square meter, and recovered scrap are recorded together.

STC power and annual electricity generation are different quantities

Standard test conditions are necessary for comparing devices. In the field, however, irradiance, spectrum, angle of incidence, temperature, wind, soiling, and shading constantly change. Inverter efficiency and power curtailment, cable losses, and maintenance downtime also affect the delivered electricity. In bifacial modules, rear-side irradiance depends on ground reflection, height, and array geometry. In tandem cells, a changing spectrum can affect current matching. Therefore, the annual energy production ranking of two technologies cannot be definitively determined based solely on STC performance.

IEC 61724-1 clearly defines the terms, equipment, and methods used in the performance monitoring and analysis of PV systems. [R32] Researchers must organize data logging with regular timestamps, device plane irradiance, appropriate temperature measurements, and system operating status. Missing data is not equivalent to zero production. Sensor drift, maintenance, inverter shutdowns, and data communication issues should be marked separately. To accurately determine the root cause of a failure in the field, electrical power generation and meteorological measurements must be correlated on the same time base.

Specific yield and performance ratio

The final yield Y_f = E_AC / P_STC [kWh/kWp], the reference yield Y_r = H_POA / G_STC [h], and the performance ratio PR = Y_f / Y_r [dimensionless] can be defined. H_POA is the time integral of irradiance on the module plane [kWh/m^2]; G_STC = 1 kW/m^2 is assumed. It is clearly stated whether the power rating used is for DC, whether the energy delivery is AC, and where the system boundary is located. PR is not a cell efficiency; it summarizes the total loss behavior of the system compared to the expected energy under reference irradiance.

Original example: A 10 kWp system should produce 14,000 kWh of AC per year, with annual plane-of-array irradiation of 1700 kWh/m^2. Then, Y_f = 1400 kWh/kWp, Y_r = 1700 h, and PR = 1400/1700 ≈ 82.35%. The PR values of two different climates should not be directly converted into a quality ranking; weather conditions such as temperature affect the ratio. NREL's PR report, adjusted for weather conditions, describes a method to reduce this bias. [R33] Simply writing "adjusted PR" without specifying the correction and reference weather file used is not acceptable.

To determine the degradation rate, seasonal variations, soiling, interruptions, sensor calibration, and initial transients are analyzed. Before attributing a year's low production to material degradation, irradiance and operational availability are checked. Linearly extrapolating a few months of trend data over decades may not be reliable. Annual energy predictions involve uncertainty due to the selection of the climate file, model error, and long-term variability. If terms like P50 or P90 are used, the probability definition and the uncertainties covered must be clearly stated.

LCOE: the bridge from efficiency to cost

The simplified tiered electricity cost can be expressed as follows:

$$\mathrm{LCOE} = \frac{C_0 + \sum_t C_t/(1+r)^t}{\sum_t E_t/(1+r)^t}. \tag{I.25.1}$$

C_0 represents the initial investment, C_t represents the maintenance/replacement/operating cost, E_t represents the delivered electricity, and r represents the discount rate. If the units are cost in a currency and energy in kWh, the result will be currency/kWh. Nominal prices should be matched with the nominal rate, and real prices should be matched with the real rate. The module price is only a part of the system cost; higher area-based efficiency can reduce land and installation costs, but this effect depends on the application. Presenting a single LCOE number when lifetime and energy production are uncertain is misleading.

In the original illustrative example, the initial cost of a 10 kWp system is 10,000 monetary units, the annual maintenance cost is 150, the energy generated in the first year is 14,000 kWh, the duration is 20 years, and the discount rate is 5%. Assuming no degradation or change, the annuity factor is approximately 12.462. The present cost is 10,000 + 150 × 12.462 ≈ 11,869; the present energy is 14,000 × 12.462 ≈ 174,468 kWh; the LCOE is approximately 0.0680 monetary units/kWh. This is not a price study. The result changes when degradation, inverter replacement, and lifetime uncertainty are added; the assumptions are stored in a table.

Life cycle and recycling

Life cycle assessment (LCA) evaluates the environmental impacts within the system boundary, from raw material extraction to production, transportation, installation, use, and end-of-life. The functional unit can be a module or a watt; in most cases, delivered kWh is more informative for comparing electricity services. The electricity mix in production, efficiency, site irradiance, lifetime, and recycling assumptions affect the outcome. The IEA PVPS 2024 information note presents this assessment framework in the context of current technology inventories. From this, a single carbon intensity is not derived for each country and technology. [R34]

In the original scale calculation, let the production and life cycle load be 1000 kg CO_2-equivalent/kWp, and the lifetime production be 30,000 kWh/kWp. This yields 0.0333 kg/kWh, which is equal to 33.3 g CO_2-equivalent/kWh. If the actual lifetime is halved and all other conditions remain the same, the load per unit of energy will approximately double. This simple result demonstrates the environmental importance of durability. When calculating the energy payback time, it should be considered whether the energy input is primary or final energy, and the compared electricity conversion should be consistent.

A high mass recovery rate in recycling does not necessarily mean that all valuable or hazardous components are recovered. While glass and the frame may constitute the majority of the mass, the loss of silver, semiconductors, or trace elements can be significant from both an economic and environmental perspective. The purity of the

recovered materials, the level of reuse, and the energy and chemical consumption are evaluated. The IEA PVPS module recycling LCA report demonstrates that these processes are a separate subject for environmental assessment. [R36] Good design addresses the tensions of making a device both long-lasting and repairable and easily disassembled from the outset; the term “recyclable” is not a complete result without a functioning collection and processing chain.

Including temperature and irradiance in the same energy calculation

In a simple initial approximation, the instantaneous power P(t) is written as approximately PSTC [G(t)/GSTC][1 + γP(Tc(t) - 25 °C)] multiplied by other loss coefficients. Here, γP is the relative temperature coefficient. For example, -0.35%/K means -0.0035 per Kelvin; directly using the number -0.35 would create a hundredfold error. The cell temperature Tc is not the ambient temperature. Wind and mounting conditions alter the difference between the two.

For the 1 kWp system in the figure, the daytime irradiance was selected in a sinusoidal form between 06:00 and 18:00. The daily energy obtained solely from irradiance is approximately 7.64 kWh. When the cell temperature is 25 + 35G/GSTC and other losses are considered as 8%, approximately 6.35 kWh is obtained. This difference cannot be seen by simply comparing the power at noon; an integral over the entire day is required. This is not a local weather forecast but a synthetic day used to illustrate the calculation method.

Discounting the numerator and denominator together in LCOE

In an electricity cost calculation, the investment occurs at the initial moment, while operating expenses and production costs accrue over the years. Using the same discounting rule:

$$\mathrm{LCOE} = \frac{C_0 + \sum_{t=1}^{N} C_t/(1+r)^t}{\sum_{t=1}^{N} E_t/(1+r)^t}. \tag{I.25.2}$$

The teaching scenario in the figure uses an initial investment of 700 currency units for 1 kWp, annual expenses of 12 units, an initial year production of 1600 kWh, an annual production loss of 0.5%, and a discount rate of 6%. This results in an approximate value of 0.04364 currency units/kWh over 25 years. This number is not an investment proposal specific to a country or time period. For example, the lesson demonstrates how shortening the lifespan increases the energy cost, even with the same initial efficiency.

The stakeholder also plays an important role in life cycle assessment. kg CO2-equivalent/module and g CO2-equivalent/kWh answer different questions. For the second metric, the production region, electricity mix, transportation, on-site energy, service life, and end-of-life scenario are required. A technology that uses fewer materials in cell production may not maintain the same advantage per kWh if its lifespan or on-site production is low. [R34] [R36]

Self-assessment

1. **Is the efficiency of a 25% cell the same as the efficiency of a 25% module?** No. Area coverage, interconnection, and optical and electrical effects must be taken into account.

2. **PR = 82%, does this mean that the cell has an efficiency of 82%?** No. PR is the performance ratio, which normalizes the system energy with respect to irradiation and the installed reference power.

3. **Does the 90% mass recovery in recycling indicate that all valuable materials are recovered?** No. Recovery is evaluated on a component-by-component basis, considering purity and the environmental/cost burden separately.

Availability and daily integral

Availability describes the proportion of the expected production time during which the system can operate. Production may stop due to a connection failure or maintenance while the sun is shining. Modeling this downtime solely as cloud cover loss is misleading. Irradiance, temperature, shading, and operational interruptions are separate input parameters.

The **daily integral** represents the summation of power over time throughout the day. If power is measured in kilowatts and time in hours, the result is energy in kilowatt-hours. A system that produces 2 kW for one hour and then 3 kW for the next hour will generate 5 kWh in those two hours; multiplying the peak value of 3 kW by 24 hours does not represent the daily production. The annual energy calculation follows the same logic, extending it across seasons, interruptions, and degradation over time. This example calculation explains the summation concept; it is not a production forecast for a specified location and year.

BOOK I · CHAPTER 26 / RESEARCH PRACTICE

From literature review to research question

What type of information does the article provide?

An **original research article** answers a specific question with new experiments, calculations, or analyses. A **review** brings together many studies; it is valuable for understanding the scope of a topic, but it may not be the primary source for a particular piece of information. A **preprint** is a text shared before the peer-review process is complete. **Supplementary information** includes methods, additional measurements, and details that do not fit in the main article. A **patent** is a technical document containing a claim for legal rights; it is not an independent performance verification. A **datasheet** presents the properties of a product under specified conditions. We should not consider these types as equivalent under a single “source” heading.

We cannot assess the reproducibility of an experiment by simply looking at the title or abstract of a publication. **DOI** is the persistent digital object identifier that uniquely identifies a publication. It helps in finding the correct version of the text. A **citation** indicates the source upon which a claim or method is based; it does not automatically imply that the source's result is correct. The author's claim, the presented data, and our derived conclusions should be kept separate.

Reading a paper in three passes

In the first pass, identify the question, the device type, and the main result. In the second pass, read the figures along their axes: which quantity was measured, which condition was kept constant, what do the error bars represent, and how many independent specimens are there? In the third pass, return to the method: is the layer sequence, processing history, area, light, temperature, and analysis definitions sufficient to reconstruct the result? If there is missing information, noting this is not a failure in reading, but rather a determination of the limits of inference.

Exemplary claim: “The new dopant increased efficiency.” Let’s convert this into a testable form: which dopant, in which absorber, at what concentration, and was it compared to an undoped control with the same solvent history? Is the gain observed across the entire distribution, or only in the best cell? Is it stable power, or a swept value? With these questions, the claim becomes a measurable and falsifiable proposition.

A **research gap** is not a word or formula that has never been used before. It can be a specific problem that existing evidence cannot explain or differentiate. For example, is the effect of the dopant due to defect reduction or a change in the crystallization rate? A control sample that distinguishes between the two explanations can create a more valuable research question than simply "trying a new dopant."

Comprehension check: follow the citation chain

Before using the efficiency value you see in a compilation, refer to the original article, and if necessary, the certificate. The rounded value in the compilation may belong to a different area or light category. If you have only read the abstract of the source, do not claim that the method details have been verified.

When starting research, the problem is often not the inability to find articles. The problem is the inability to distinguish which of the many articles actually answers a specific question. A review article provides a map of the field; an original article provides evidence for a specific claim; supplementary information provides details about the methodology; and open data provides an opportunity to recalculate some claims. Reading these as if they were a single type of source is inefficient.

Read an article in three rounds

In the first round, read the title, abstract, main figures, and conclusion. Write a one-sentence claim: for example, "The interface treatment reduces non-radiative recombination in specific cells." Simultaneously, write the scope of the claim: film, partial stack, full cell, or module. In the first round, do not decide if the mechanism is correct; simply determine what the author intended to demonstrate.

In the second round, proceed to the method and additional information. Determine the sample size, the number of independent production batches, the measurement sequence, the area mask, the light spectrum, the temperature, and the statistics. Record the difference between the "best cell" and the "average cell." Even if the number of devices is n=30, if these devices come from a single coating batch, it does not count as thirty independent experiments for production repeatability.

Read the figures that test the mechanism in the third round. Does the claim of contact improvement rely solely on higher photoluminescence, or have selectivity and transport losses also been investigated? Does the claim of crystal growth rely solely on surface photography, or have phase, texture, and composition also been measured? Consider whether there is an alternative to the author's proposed mechanism that explains the same data.

When concluding a study, three things should remain: what you learned, what remains unclear, and what the next experiment will investigate. Summarizing a study is not the same skill as evaluating it. A summary recounts the author's journey; an evaluation asks whether that journey was sufficient to reach a conclusion.

Source family tree

When you reach a table in a compilation, refer to the table for the critical value. If the value in the original article was taken from another study, continue the chain of references. In which sample and with which method did the value appear? It is easy to combine two different columns of a compilation to create a "super material" that has never actually been produced: the best mobility can be taken from a single crystal, the best lifetime from another film, and the best band gap from another composition. These are not a set of compatible parameters for a single device.

Secondary sources play an important role; however, if a numerical result is being determined, the end of the source chain must be defined. Conversely, it is not necessary to rediscover every fundamental equation. For established physics, a reliable textbook is a more accurate starting point than an original article for a specific new device result. Luque and Hegedus' handbook covers technology and engineering, while Würfel and Würfel's book provides a complementary reading path, extending from physical principles to advanced concepts. Here, they are recommended solely based on the publisher's scope information. [B04] [B05]

How should a record efficiency be interpreted?

A "record" graph provides an idea about the rate of discovery, but it is not, on its own, a ranking of investment, scalability, or field lifetime. The competition between a small-area research cell and a commercially available module is not the same. A cell category may have attracted more researchers and investment over the years. Before interpreting the slope of the graph as an inherent superiority of the material, consider the research effort and the measurement categories.

Independent performance tables and laboratory charts are valuable for source selection. The JRC record for Version 68 indicates that the study compiles independently verified cell and module performance data and reviews new entries after January 2026. This sentence does not imply that all results in a specific table were obtained under the same area, topology, or light intensity. Table footnotes are part of the research. [B03]

Innovation and utility

A new formula does not necessarily imply a useful PV material. A novel arrangement of a known compound may be scientifically interesting, but it must be demonstrated that it represents a genuinely different physical state. For the same chemical composition, polymorphism, site ordering, disorder, strain, surface termination, and heterostructure can create different objects. Innovative research cannot be conducted without clearly defining which of these objects it is.

In the search, synonyms, reduced and expanded formulas, prototypes, solid solution families, equivalent element sequences, and possible decomposition products should be used. The absence of results only indicates that no results were found under the recorded searches. The database scope, language, indexing delay, and access restrictions introduce uncertainty. Patentability and freedom to operate are also distinct issues that require expert evaluation and are not a natural outcome of a literature review.

Application: one-page article summary

For an article, fill in the following fields: complete citation; DOI; access date; main claim; sample description; nearest control; device area; light and temperature; measurement method; number of independent batches; distribution; strongest figure; weakest assumption; open data; missing information for reproduction; subsequent distinguishing test. The summary should not exceed one page. The goal is not to compress the text, but to select the key information.

Exercise: The efficiencies of two articles are 24.0% and 24.4%. Is the second article better? Answer: One cannot decide based solely on these numbers. The area, measurement, stabilization, uncertainty, distribution, and control conditions are required. If the first result is from a large area and is independently certified, and the second result is from a small area and is a single scan, then the ranking depends on the scientific question.

BOOK I · CHAPTER 27 / RESEARCH PRACTICE

How is a research program established?

Structuring a research program as a sequence of decisions

A research program is not a list of all possible measurements. The **objective** is the specific problem we want to solve. The **hypothesis** is a testable explanation related to this problem. The **criterion** is the observable outcome by which the explanation will be evaluated. The **decision gate** is the evidence required before proceeding to the next expensive step. Distinguishing these four concepts prevents the objective from being silently changed when no results are obtained.

Synthetic example: The voltage in a cell is low. Let's assume the initial hypothesis is that surface recombination is dominant. Using the same base material, we can modify the surface treatment and measure the lifetime and voltage together. If the contact resistance also changes, we will check the power separately. If there is no voltage gain, we will not change the initial criterion by saying, "but the surface is brighter." The initial hypothesis may not be supported; this is the result that guides the subsequent experiment.

Sometimes, the control sample is more valuable than the new sample

The **reference process** is the initial pathway from which we can consistently obtain similar outcomes. If the variability of the reference itself is unknown, it becomes difficult to isolate the effect of the new process. A **discriminatory experiment** selects a condition where competing explanations predict different outcomes. The **stopping criterion** specifies in advance the point at which further work will no longer yield evidence that supports the objective. Stopping is not deleting the data; it is preserving the negative finding, along with the method and scope used.

For a new absorber, the initial considerations are its chemical definition, followed by phase and structure, optical and electrical properties, interface and device characteristics, and then questions related to scale and lifetime. This sequence is not entirely rigid; a cheap and decisive interface incompatibility can be checked early on. However, a result calculated at one stage cannot be presented as if it were obtained through experimentation at another stage. The **level of evidence** clarifies with which calculations, observations, or independent verifications the claim is supported.

A **reproducible workflow** includes not only the final graph but also the raw data, sample identification, processing sequence, analysis description, and software version. Can someone else obtain the same result from the same inputs? Are they observing a similar physical effect with a different device and sample? These two questions do not

represent the same validation; they both test different risks associated with the research.

Comprehension check: what would make you abandon your idea?

After stating your hypothesis, also state the observation that would disprove it. If no result can alter the hypothesis, then the experimental question is not yet sufficiently well-defined. A pre-defined control and stopping criterion reduces the tendency to select only positive results.

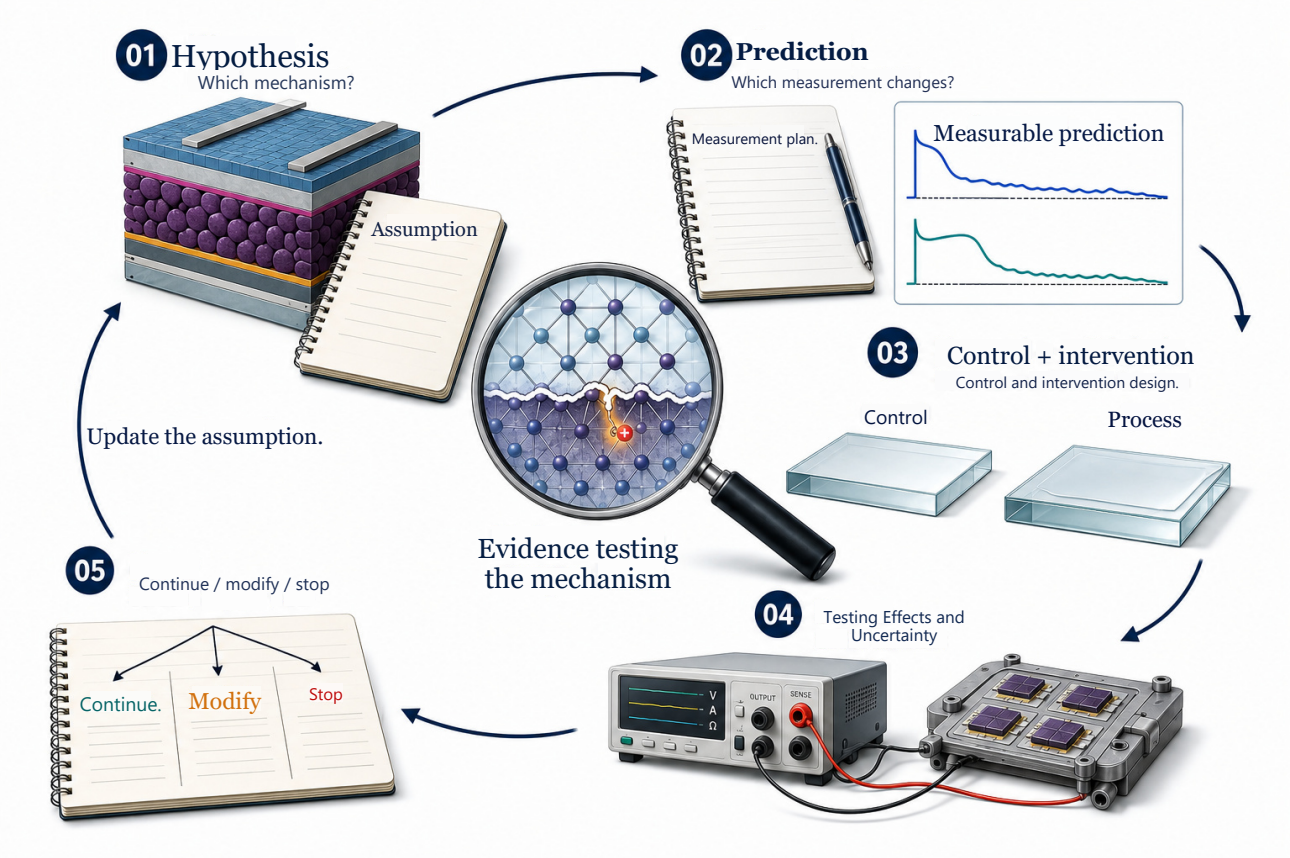


Figure 41. The research cycle that tests the mechanism. The hypothesis is translated into a measurable prediction; control and intervention samples are compared using repeated measurements; the effect is evaluated with its associated uncertainty. The result leads to a decision to continue, modify, or terminate. Schematic signals and devices are not actual data from an experiment. [R30] [R31] Conceptual illustration prepared with an image-generation tool; it is not a measurement image.

A good research question is not left as broad as “can we improve the efficiency?” For example, the question “does this change in the top transport layer reduce non-radiative interface loss without increasing transport resistance, using the same absorber and production batch?” can be tested. The variable, control, mechanism, and success criterion are all included in the same sentence. Trying to directly optimize a mechanism that you cannot measure may lead you to chase after a measurable proxy indicator.

Measure the bottleneck, then select the method

If a cell's short-circuit current is lower than expected, starting a new DFT campaign may not be the cheapest first step. EQE together with reflectance and parasitic-absorption measurements can separate optical and collection losses more directly. If Voc is low, voltage as a function of light intensity, luminescence and structures with controlled contacts may be more informative. If FF is low, series resistance, shunting, barriers and time dependence are separated. The choice of tool depends on the uncertainty, not on the researcher's favorite software.

Equating the success of a study with the computation time or the number of measurements is misleading. Success lies in reliably obtaining information that will influence the decision-making process. Twenty similar scans may repeat the same systematic error; a single, well-designed control can reveal that error. Additional data is only as beneficial when it tests a new independent variable, a different condition, or another component of uncertainty.

Example design: a passivation additive

Consider a hypothetical scenario where a dopant increases Voc. The hypothesis is that the dopant reduces recombination at the interface. Alternatives include the dopant altering the absorber composition, modifying the optics, temporarily affecting the ion distribution, or changing the measurement preconditioning. Rephrasing these alternatives prevents you from hastily selecting a mechanism when a positive result is observed.

The control group should use the same solvent, duration, temperature, and processing sequence. Samples are produced in multiple independent batches, and each batch includes both control and intervention groups. The measurement sequence is randomized. The primary output is predetermined; for example, a stabilized MPP efficiency after a specific protocol. Voc, FF, EQE, and luminescence can be secondary outputs. Failed or short-circuited devices are not simply discarded; manufacturing yield is also a result.

For the mechanism claim, simply increasing the primary output is not sufficient. The fact that the EQE remains largely unchanged can weaken the optical alternative, but it does not eliminate it on its own. The voltage increase in the complete device and the quasi-Fermi level separation in the partial device structure are considered together. The persistence of the gain after stabilization tests the transient conditioning explanation. Different additive amounts provide clues about the mechanism, but selecting the optimal point after numerous experiments requires a separate validation set.

The stopping criterion is defined in advance. If the additive works only in one batch, its benefit disappears in stabilized measurements, or it causes severe degradation under

humidity or heat, a higher efficiency in a sweep is not sufficient to continue the program. A different hypothesis can be formulated; this does not mean that the previous hypothesis has been validated.

Example design: a new absorber

The initial decision for a new compound may not be to calculate the electron bands. First, the atomic and charge balance, known main phases, coordination, competing compounds, and chemical accessibility are evaluated. Even if the formula is correct, if the crystal structure is uncertain, calculating the band gap for a single random structure does not define the target object. A multi-digit number output from a machine does not reduce the uncertainty in the input object.

The least expensive discriminating test is sometimes a balanced decomposition channel. The presence of a significant energy disadvantage within this channel can reduce the priority of that structure. However, a limited channel test does not represent the entire phase diagram. Conversely, the absence of problems in the channel does not necessarily confirm its synthesizability. Subsequently, a systematic set of competing phases, structural convergence, dynamic behavior, electronic quality, and defects are considered. At each step, the rationale for undertaking the next expensive step should be documented.

When working in the laboratory, the sample to be delivered, the expected phase, the characterization package, the acceptance criteria, the raw data, and the repetition conditions are defined in advance. The statement “Synthesize this material and measure its efficiency” leaves the scope undefined. Material synthesis, thin film formation, contact development, and solar cell optimization are different stages. The success criterion should reflect this distinction. The book teaches this scientific scope rather than providing a recipe for a chemical operation.

Stages of evidence from idea to product

A research idea begins as a clear hypothesis. Computational screening provides evidence for the properties under investigation, given the selected model and inputs. Material-level studies examine the structure, phase, optical, and transport behavior; interface studies investigate the interaction of adjacent layers; device studies test the current, voltage, and steady-state power of the completed cell. Independent experimental repetition investigates whether a result can be observed with different samples and measurement setups. Product validation further includes large-area testing, production repeatability, environmental conditions, and durability. These represent a general thought process used in this book; they are not a new standard or formal certification classification.

Let us make this distinction concrete. Even for a compound calculated to have a suitable band gap, successful synthesis may still be unknown. Strong luminescence

from a synthesized film does not determine the efficiency of a cell with contacts. A high independently measured cell efficiency does not show that a mass-produced module has the same efficiency or lifetime. At every stage, the claim is limited to the scope of the available observation. [R18] [R30]

Define the success target not by selecting a universal percentage, but by specifying the conditions of the application. In the comparison, the light spectrum and intensity, sample temperature, whether it is a cell or a module, the definition of the area, concentration, number of terminals, power collection method, and stable measurement conditions must be specified. A direct conclusion of superiority cannot be drawn from two numbers in mismatched categories. When production acceptance and service life are added to the success achieved under standard conditions, it can be seen whether the target truly meets the product requirements. [R01] [R06]

Minimum outline of the final report

Report the research question, experimental or computational protocol, origin of the input data, comparison, units and conditions, uncertainty, raw data links, and failures together. For a result to be reproducible, code alone is not sufficient; it is also necessary to specify which file was used, with which version, and with which assumptions. Storing negative results prevents the same failed hypothesis from becoming expensive to repeat under a different name.

Exercise: A model indicated very high efficiency for 10 out of 1,000 candidates. What should be the first step? Answer: Check whether the target is actually the measured cell efficiency, the training domain, data leakage among similar candidates, and the physical consistency of the inputs. Then, perform the cheapest independent discriminating test. Starting the expensive calculations for just those 10 candidates directly could amplify the model's error.

A twelve-week study route for researchers

Select the learning outcome before the schedule

The twelve weeks outlined in this section do not guarantee expertise from scratch. It serves as an example for establishing a study schedule. Someone studying electricity and semiconductors for the first time may take longer to complete each step; access to a laboratory or prior knowledge of mathematics will affect the duration. The measure of completing a week is not the number of pages covered, but the amount of work you can accomplish independently.

Learning outcome is an observable statement of skill: such as “I can calculate power from a J-V graph” or “I can identify an error in the definition of ‘area’ in an article.” “I understand perovskites” is too broad. If we break down the outcome into smaller tasks, we can identify any missing prerequisite knowledge. For example, if there is an error in the efficiency calculation, the problem may not be the cell physics, but rather the conversion from cm^2 to m^2.

Three working notebooks

In a **concept notebook**, define the term in your own words and provide a counterexample. Use the fact that the power in a short circuit is zero as a counterexample to the statement “high current means high power.” In a **calculation notebook**, keep the knowns, unknowns, units, assumptions, process, and result separate. In a **evidence notebook**, record the source of the claim you read, an example, and the conditions to which it can be generalized. Repeating the same topic in these three formats transforms memorization into application.

Example study session: First, read the one-page introductory explanation; then, close the figure and create your own drawing; next, repeat the calculation by slightly modifying the numbers in the book; finally, interpret a similar figure from a different publication. If you obtain an incorrect result, instead of immediately copying the solution, trace back the units and assumptions. Identifying at which step of the solution the unknown concept arises will define your new learning target.

The following table outlines the suggested sequence for these skills. Before proceeding to the advanced modeling stage, it is necessary to establish a basic energy and charge balance. Computational route can begin without a laboratory; however, experimental skills are acquired through appropriate training, equipment, and supervised practice.

This book provides explanations but does not constitute training in the actual use of a device.

Comprehension check: If you get stuck, where should you go?

If an equation is not understood, first write down the unit of each symbol, and then the measurable meaning of the variable. If these are established, proceed to the mathematical step; if not, return to the concept section. Fixing the missing link instead of reading more pages will increase the pace of subsequent sections.

This program is not a guarantee of proficiency; it is a study schedule that transforms the book into a tool for active learning. It is a suggested starting point for a reader who can dedicate approximately eight to twelve hours per week. Simply reading the book without recalculating the equations and thoroughly examining a real paper at the methodological level is not sufficient. Measure progress not by the number of pages completed, but by the small research outputs produced.

Week	Focus	Tangible output.
1	History, energy-power distinction, spectrum.	Annotated timeline; eV-nm conversion table.
2	Bands, Fermi level, p-n junctions, and contacts.	Explain equilibrium and illuminated band diagrams with your own drawings
3	Transport, recombination, J-V	Determine Voc, Jsc, FF, and efficiency from the synthetic diode curve.
4	Detailed balance and voltage loss.	Explain the assumptions of an ideal upper limit in a single page.
5	Silicon and thin films.	Compare losses and manufacturing for two cell architectures
6	Perovskite and tandem	Optical and electrical circuit diagram for 2T and 4T.
7	Measurement and characterization.	Complete measurement conditions and uncertainty sheet for an article.
8	Durability and module.	State which lifetime claim is not supported by a particular aging experiment.
9	DFT, defects, phase stability.	Competing explanations and a convergence plan for a candidate.
10	Device modeling and ML.	Analysis of parameter sensitivity and data leakage.
11	Design of experiments and field	A research proposal with controlled, predefined stopping criteria.
12	Independent reproduction	Recalculate a bounded result from an open-access paper; report differences

Three final projects

The first option is device physics: assess the current consistency in an openly available J-V and EQE data set. If spectral data is unavailable, do not state that the current is definitively verified; instead, specify what data is required. Investigate and report the extent to which different sets of parameters fit the same J-V curve, and report the limit of identifiability.

The second option is materials research: for a known PV absorber, compile the literature on structure, competing phases, band gap, and defects into an evidence map. Instead of forcing an average for conflicting values, explain the differences with method, temperature, sample, and compositional variations. You don't have to propose a new structure; accurately defining a known uncertainty is a research skill in itself.

The third option is reliability: re-examine a clear aging study. Extract the initial efficiency, conditioning, light/heat/humidity/load, interruption, sample size, and the definition of T80. Show how different initial points affect the T80 for the same data. List the missing variables for transferring the result to field lifetime.

Reading order and the role of tools

Use the physics textbook, a recent review on the technology, the original article on the mechanism you have chosen, and additional data for numerical results together. Calculators like PV Lighthouse are useful for testing basic trends; however, the output obtained without understanding the assumptions is not an independent validation. First, test the calculator on a known boundary condition. [B06]

When discussing with an expert, ask "which observable quantity's uncertainty is hindering our decision?" before asking "which software should I learn?" The software may change, but the ability to formulate the question correctly remains. In the later stages, update the literature review at regular intervals; studies conducted after the cut-off date of this book will not be included here.

BOOK I · CHAPTER 29 / RESEARCH PRACTICE

Clear limitations of the research and future perspectives

Asking which problem the “new” thing solves

The open frontiers of PV research exist at several different scales. A material may exhibit lower voltage loss; a contact may use less metal; a coating may be produced more quickly; a module may have a longer lifetime. Each of these can represent progress. However, success in one area does not automatically guarantee success in the others. When making claims about the future, we must first determine which loss or cost will be reduced.

A **hot-carrier cell** aims to utilize the excess energy of a photo-excited charge carrier before it thermalizes with the lattice. **Carrier multiplication** is the mechanism by which multiple electron-hole pairs are generated from a single, sufficiently energetic photon. An **intermediate band** is the concept of using low-energy photons in multiple steps with suitable electronic states within the normal band gap. These concepts are not stand-alone technologies; their speeds, selectivity, losses, and overall power balance must be evaluated.

Why is quantum yield not energy efficiency?

Teaching example: Let’s assume that a 3 eV photon generates two pairs. If each pair can transfer 0.5 eV of energy in the external circuit, the total electrical energy is 1 eV; the energy ratio for this photon is approximately 33%. Two pairs mean two charge carrier cycles per photon; this is not the “200% energy efficiency.” Furthermore, the generation of excess pairs and their collection at the contact are separate efficiency steps. This distinction is particularly important in unconventional conversion mechanisms.

Technology maturity describes the scale and conditions under which the concept is demonstrated. The steps include a single sample, independently measured cell, pilot production, and continuous commercial output. **Trade-off** refers to the deterioration of one criterion while another is improved. An example is that higher efficiency may require a narrower process window or more expensive equipment.

Instead of limiting the next research question to achieving the “highest percentage,” we can define it conditionally: within a specific area, with a specific production time and material budget, achieve a certain level of stable power and a certain durability

criterion. Although this sentence may seem less ambitious, it determines how the experiment should be designed and whether a result truly represents progress.

Comprehension check: which model class has changed?

If the new mechanism uses a different assumption than the single-junction limit, state this explicitly. Then, calculate the additional losses and the actual net power of the new mechanism. Changing the assumption regarding a theoretical limit does not mean that advantage has been realized in the manufacturing process.

In photovoltaics, there is no single, ultimate problem. As one technology improves in efficiency, it can create new challenges in terms of scale, manufacturing tolerance, material density, lifetime, or recyclability. Reducing the future of research to solely achieving the highest cell efficiency obscures these interdependencies. The following questions are not predictions or promises of success, but rather a framework for defining research problems.

Beyond silicon, together with silicon

The accumulated knowledge of the silicon-based industry necessitates that any new material not only compete physically but also in terms of manufacturing. The tandem concept offers the opportunity to reduce the loss of high-energy photons by utilizing the existing bottom cell. However, the top cell must generate a higher voltage, which should outweigh the losses associated with additional optical layers and interconnections. Current matching, seasonal spectrum, temperature coefficients, manufacturing yield, and the aging of the tandem module must be addressed collectively.

Theoretically, three or more junctions can utilize the spectrum more effectively; however, this comes at the cost of increased material compatibility, interconnection, and manufacturing challenges. The scientific value of an architecture stems not from the number of junctions it has, but from what it gains in terms of net reduction of losses. Writing down the question “which loss does this new layer reduce, and which loss does it add?” for each new layer clarifies the design.

The real research gap for new absorbers

For a new material to be worth investigating, it doesn't necessarily have to be the best in every metric. Low-temperature production, adaptation to a specific spectrum, low toxicity, flexibility, or a specific integration advantage can create different targets. However, the target must be defined from the outset. The suitable band gap and optical environment for the power source of an indoor sensor differ from those of an outdoor power plant. It is incorrect to directly compare an illumination given in lux with AM1.5G without knowing the spectrum.

It is not sufficient to determine toxicity solely based on the element's name; the compound's form, usage amount, leakage pathway, and life cycle are also important. Conversely, high efficiency does not eliminate environmental concerns. Studies examining the terawatt-scale demand for metals and transport layers demonstrate that material selection and recycling should be addressed from the beginning of the design process. This resource is used here only to frame the importance of the resource demand question. [B07]

Alternative conversion mechanisms

Concepts such as the intermediate band, hot charge carriers, multiple exciton generation, singlet fission, and bulk photovoltaic effect are valuable from a fundamental physics perspective. In each case, the goal is to utilize energy or charge carrier distribution differently than in a standard single-junction device. Observing a microscopic mechanism does not necessarily mean that a net energy gain is demonstrated in the complete device. Absorption, selective extraction, loss channels, solar irradiance, and the overall power balance of the device are considered together.

This book is not a detailed monograph on these specializations. The physics limits section provides a starting point for further reading. When examining a new mechanism, determine which detailed balance assumption has changed, what additional device condition that change requires, and whether the experiment was conducted at a realistic operating intensity. The statement "exceeds the SQ limit" alone is not a research explanation.

Thinking in terms of the system

Combined use with agricultural land, building surfaces, floating systems, and low-light applications introduce different design criteria. In addition to power per area, parameters such as transparency, color, load, maintenance, access, and ecosystem conditions can also become important. The cell researcher does not necessarily need to perform the entire system engineering; however, they need to know what constraints the target application imposes.

Power electronics, grid flexibility, and storage influence the value of energy in high PV penetration scenarios. This book is not a power electronics design guide or a handbook on grid connection regulations. From a materials research perspective, the lesson is this: higher test efficiencies do not necessarily translate to more valuable energy per hour. The time at which energy is produced, its availability, and system losses determine the ultimate benefit.

Final exercise: your own research statement

Once you have finished reading the book, write down the following five sentences. What physical object am I investigating? Which observable quantity do I want to improve? What is the most plausible alternative explanation? Which is the most cost-effective discriminating test? At which outcome will I stop? If these sentences can be completed with numerical conditions and controls, then you will have moved beyond simply having a topic and will have formulated a viable research question.

BOOK I · CHAPTER 30 / STUDY AND REFERENCE

To analyze a device from start to finish

The first ten minutes with a device dossier

In this section, we will examine a single example from start to finish. First, we need the **sample ID**: which film or cell, which production day, which layer sequence? Then comes the **measurement ID**: which light source, temperature, area, scan, and device? If we do not separate the sample from the measurement, we may mistakenly treat records of the same cell under different conditions as if they were different samples.

Raw data refers to the numbers recorded by the device. **Processed data** is the recorded data that has undergone correction, normalization, or the application of a model. The fact that a curve has been divided by an area does not prove that the area was entered correctly. A **derived quantity** is a result, such as efficiency, FF, or lifetime, calculated from the raw measurements. It should be possible to trace the result back to the input data from which it was derived.

The initial filter is to ensure the numbers match

Synthetic pre-check: Let's assume that a maximum power of 6 mW is measured for an aperture area of 0.25 cm^2. The power density is 24 mW/cm^2. If the irradiance is 100 mW/cm^2, then the efficiency is 24%. If the text states 26%, is there another area, irradiance, or measurement that explains this difference? First, the definition and arithmetic are checked. Searching for new physics is a later task.

Next, we perform a **cross-check**: does the expected short-circuit current from the spectrum and EQE correlate with the J-V measurement? Does the steady-state power support the maximum obtained from the rapid scan? The agreement of a measurement with a quantity obtained through another physical method provides stronger confidence than relying on a single graph. However, using the same erroneous value in two calculations does not constitute independent validation.

In the final stage, we list the explanations. For low FF, the cause could be series resistance, a shunt, or a transport barrier. Which additional measurement will differentiate between these possibilities at the lowest cost? This selection is based on the concept of **information value**: prioritize the measurement that will change the decision, rather than the most detailed device characterization. The following case will demonstrate how this transition from preliminary checks to the research plan is made.

Comprehension check: trace a number backward

From the efficiency in a specific case to the maximum power, from the power to the current and voltage at the same operating point, and from the current density back to the area and current. If each step can be linked to the same sample and conditions, the calculation chain is traceable. If a link is missing, that missing step must be completed before proceeding to the result.

Seeing an increase in a cell's efficiency is just the beginning. Research aims to determine the mechanism behind the increase and whether it can be replicated in other samples. In this section, we will compare three synthetic devices within the same framework. In one, the recombination rate decreases, while in the other, the contact resistance decreases. Both achieve almost the same efficiency; nevertheless, the researcher's subsequent experiment should be different.

Define the data and assumptions

For the three devices, let the temperature be 298.15 K, Jph = 40 mA/cm^2, the diode ideality factor be 1, rsh = 3000 $\Omega \cdot cm^2$, and the irradiance be 100 mW/cm^2. In the control case, J0 = 10^{-12} A/cm^2 and rs = 1.5 $\Omega \cdot cm^2$ are selected. In the passivation scenario, only J0 is reduced by a factor of five. In the contact scenario, only rs is reduced to 0.4 $\Omega \cdot cm^2$. These parameter changes do not imply that a real process affects only this variable; they are designed to study the mechanisms separately.

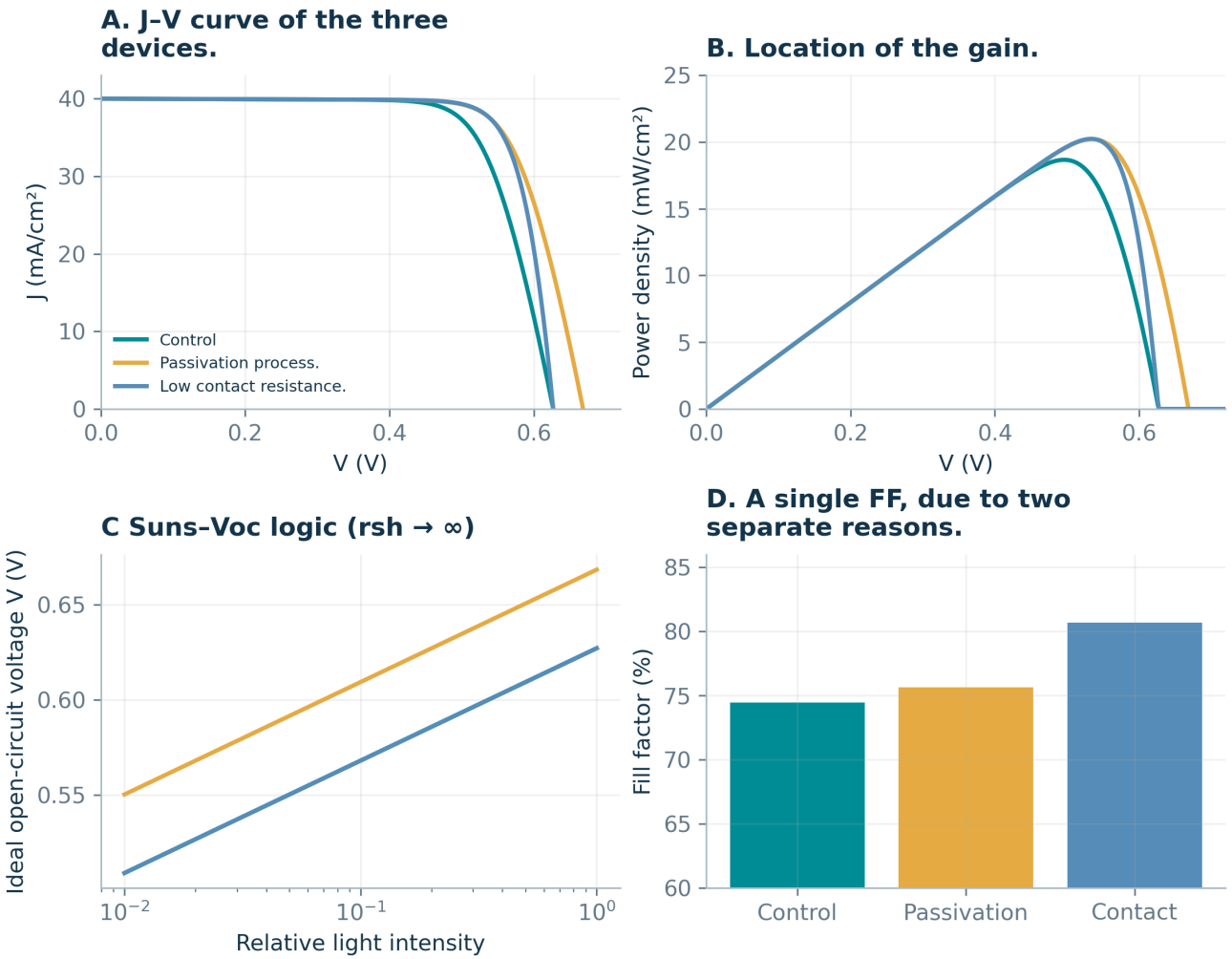


Figure 42. The same efficiency, different physics. Panels A and B are exact single-diode solutions for three devices. Panel C is the Suns-Voc thought experiment, calculated with parallel leakage neglected; while passivation increases the voltage, a pure series resistance change does not affect the open-circuit voltage. Panel D shows that FF can be affected by both mechanisms. All curves are synthetic. [B11]

Device	Voc (V)	Fill Factor (%)	Efficiency (%)
Control	0,62708	74,46	18,668
Passivation scenario.	0,66842	75,67	20,220
Contact scenario	0,62708	80,70	20,239

The multi-digit numbers in the table do not represent measurement accuracy; they are control values of the numerical model. In all three cases, Jsc remains approximately 40 mA/cm^2. In the passivation scenario, Voc increases by approximately 41.34 mV. The simple logarithmic expectation is VT ln 5 = 41.35 mV; there is a small difference in the complete solution due to finite parallel leakage. In the contact scenario, since the external J is zero in the open circuit, the Jrs drop is zero; Voc remains unchanged. When current is drawn, the internal voltage drop decreases, so MPP and FF improve.

How would we test the first claim made in the article?

If an author states that "interface passivation increased the efficiency by almost two points," the mere increase in the final efficiency does not prove the mechanism. In this example, a simple contact improvement could also produce a similar result. For the initial differentiation, we look at Voc and FF together. An increase in Voc may be consistent with a reduction in recombination; however, an increase in optical generation or a temperature difference could also change the voltage. Therefore, the same Jsc and the same temperature conditions are controlled.

In the second step, the contact-free film, the half-stack, and the complete device are compared. If the film's PL/QFLS improves but the Voc does not, it is likely that material gain is being lost at the contact. If the FF increases without a change in Voc, the contact or transport explanation becomes more plausible. However, this inference is merely a suggestion for a new measurement; it is not a definitive diagnosis in itself. The explanation is narrowed down through several mutually consistent measurements.

In the third step, the performance with reduced resistance effects is investigated using the Suns-Voc or a suitable pseudo-JV approach. A significant difference between the full J-V and pseudo-JV curves may indicate transport losses. Here, the light-induced collection dependence on voltage, ionic effects, and parallel leakage, among other model parameters, are checked. Not all measurement techniques rely on the same assumptions; the fact that different techniques yield different results may not solely be due to device errors.

With a limited budget, which experiment should be prioritized?

First, we select the inexpensive measurement that differentiates the explanations. Before synthesizing a new material, a temperature-controlled, stable J-V measurement, EQE integral, and repeatable Voc measurement can be performed on the same device. Then, a film/contact control suitable for the selected mechanism is established. If the two explanations describe the same data, we look for a condition in which they predict different results, such as light intensity, temperature, layer thickness, or contact variation.

Hypothesis	The expected change in this example.	Observation used for refutation.
Only J0 decreased.	Voc increases; Jsc remains approximately constant.	Unchanged Voc at a calibrated temperature
Only rs decreased	FF increases; Voc remains the same.	Significant and repetitive increase in Voc.

Hypothesis	The expected change in this example.	Observation used for refutation.
Only optical generation increased	The EQE integral and Jsc increase.	Only the FF gain is observed under the same EQE/Jsc conditions.
Incorrect measurement area	The J values and the efficiency scale shift.	Difference disappears after independent mask/area measurement

This table does not exclude the possibility of the effects coexisting in a real device. On the contrary, it indicates when a single-effect explanation should be abandoned. As research progresses, the complexity of the model should increase in accordance with the data that necessitates it.

Contents of a reproducible work package

The raw J-V and time series data, along with records of the used aperture area, irradiance, and temperature, sample IDs, and processing batches, are stored together. The analysis is performed in a separate file without modifying the raw data. For each graph, the samples that were excluded and the reasons for their exclusion are recorded. The main result is based not only on the best cell but also on the distribution of independent production repetitions. Failed samples are as valuable as the most successful samples for understanding the underlying mechanism.

The same principle was followed in the numerical example of this book: the data spectrum, the shape generation code, the parameters used, and the calculation results were kept separate. Graphs were not subsequently used for manual numerical corrections; tables were generated from the solutions of the same equation. Reproducing a curve and proving a real material mechanism are different stages; a controlled experiment lies between the two.

BOOK I · CHAPTER 31 / STUDY AND REFERENCE

Solved research problems

Formulating the problem before solving the equation

Solved problems are not just exercises in finding the correct number. In each problem, first write down the **knowns** and the **unknown**. Then, state which condition the equation you used requires. Convert to the same system of units, perform the calculation, and consider in which range the result should be reasonable. Finally, report the answer with the appropriate number of significant figures. **Significant figures** represent the discipline of not writing down artificial precision that is not supported by the inputs.

Example of unit conversion: 500 nm, 0.5 µm, and 5×10^{-5} cm are all equivalent lengths. If the absorption coefficient is given in cm^{-1}, the thickness must be converted to centimeters. In the exponential expression, αd must be dimensionless. Directly substituting the µm value can result in a unit error of ten thousand; even if the result falls between 0 and 1, the calculation may be physically incorrect.

The meaning of mathematical tools

Derivative is the local rate of change of a quantity with respect to another. If the voltage increases from 0.50 to 0.51 V while the current decreases from 30 to 29 mA, then the slope in this small interval is approximately -100 mA/V. This finite difference aims to approach the local derivative as the interval is reduced. **Integral** is the sum of small contributions. The integral of power with respect to time is energy, and the integral of current with respect to time is charge. **Square root** asks which number, when multiplied by itself, produces the given value. The appearance of the square root in the diffusion length is related to the fact that when time is doubled, the diffusion distance generally increases by the square root of two, rather than by a factor of two.

Logarithms transform multiplication into addition. The equation ln(ab) = ln(a) + ln(b) illustrates this property. The physical ratio within a logarithm must be dimensionless; “ln(5 volts)” is not a valid expression on its own. In a correct expression, the voltage may be divided by a reference voltage. This check allows one to notice lost scales when copying the equation.

Instead of simply writing “24” at the end of a problem, specify “the current in the selected single-pass, reflection-free model.” The model’s limitations are part of the solution. Subsequent solutions will repeat this practice with different materials, measurements, and research decisions.

Comprehension check: test a limiting case

In the absorption model, as the thickness approaches zero, the absorbed fraction should approach zero, and as it becomes very large, it should approach a maximum of one. If a formula or calculation does not satisfy these simple limits, it indicates that the unit, or the model setup is incorrect. Limit cases serve as an independent verification tool, regardless of the calculator used.

The objective of this section is to go beyond simply finding a number. In each solution, first a model is selected, then the units are defined, and finally the result is interpreted physically. The numbers are for instructional purposes. If you choose a different model for a problem, you may obtain a different result; you should explain the difference based on the assumptions made.

Problem 1 - Is the absorption thickness consistent with the collection length?

Let the α value of an absorber at a specific wavelength be 2×10^{4} cm^{-1}. Determine the thickness required to achieve 95% absorption in a single pass. If D = 0.5 cm^2/s and τ = 20 ns, calculate the diffusion length. Can a good cell result be obtained from these values?

Solution: From the equation $1 - \exp(-\alpha d) = 0.95$, we get $d = \ln 20/\alpha = 1.498$ μm. $L = \sqrt{(D\tau)} = \sqrt{(0.5 \times 20 \times 10^{-9})}$ cm = 1 μm. The optically required thickness is greater than the diffusion length in this model. This suggests that there may be collection losses in the neutral region. However, the device efficiency cannot be calculated without knowing the internal field, contact direction, generation profile, and surface losses. The cheapest next step is to compare the EQE and voltage-dependent collection for a series of thicknesses.

Problem 2 - How much does an aperture-area error change efficiency?

Let Pmax = 20 mW and G = 100 mW/cm^2 be measured. Assume that the area was mistakenly taken as 0.90 cm^2, while the actual area is 1.00 cm^2. What are the reported and actual efficiencies?

Solution: The incorrect efficiency is $20/(100 \times 0.90) = 22.22\%$; the correct efficiency is 20.00%. The error is +2.22 percentage points, or approximately 11.11% relative. It is wrong to assume an efficiency error of exactly 10% just because the stated area is 10% too small; area appears in the denominator. This example shows why active area, aperture area and total device area are defined separately.

Problem 3 - Inferring ERE from nonradiative voltage loss

If the non-illuminated voltage loss is 150 mV at 298.15 K, what is the ERE? If this loss decreases to 100 mV, by how many times does the ERE increase?

Solution: ERE = exp(-ΔV/VT). For 150 mV, exp(-0.150/0.0256926) is approximately 0.002914, which means 0.2914% is obtained. A 50 mV improvement corresponds to approximately a 7.00-fold increase in ERE, as calculated by exp(0.050/VT). This logarithmic relationship explains why a significant relative improvement in radiative emission can result in only tens of mV in voltage. If the optical escape conditions change during the comparison, the same ratio cannot be directly inferred regarding internal recombination.

Problem 4 - Loss cost due to front grid spacing

Let J = 35 mA/cm^2, Rsheet = 100 Ω/square, and s = 1.2 mm. In a one-dimensional model between the fingers, what is the lateral loss? How does this ratio change if s = 1.8 mm?

Solution: In centimeters, s = 0.12. J^2 Rsheet $s^2/12$ = 0.000147 W/cm^2, which is 0.147 mW/cm^2. When the distance is increased by a factor of 1.5, the loss increases by a factor of 2.25, reaching 0.331 mW/cm^2. Conversely, the shading fraction for the same finger width decreases by one-third. For the overall optimum, these two losses should be compared in the same power unit.

Problem 5 - The sign of the slope of the defect formation energy

Let the formation energies of the two charge states be H+(EF) = 0.4 + EF and H0(EF) = 0.9 eV. EF is measured in eV from the top of the valence band. What is the thermodynamic transition level, and what is the stable charge state at EF = 0.2 eV?

Solution: Since the equality is 0.4 + EF = 0.9, the transition occurs at 0.5 eV. For EF = 0.2, H+ = 0.6, H0 = 0.9 eV; the +1 charge state has a lower energy. The positive slope indicates that the formation cost of the positive charge state increases as the electron reservoir changes. This level is not a direct PL peak energy or a charge carrier trapping barrier.

Problem 6 - Energy above the hull and kinetic stability

Let the formation energies of the xB = 0.25 and 0.75 phases be -0.30 and -0.40 eV/atom, respectively. The xB = 0.50 candidate has an energy of -0.28 eV/atom. Calculate the energy difference above the lower envelope; can the decomposition time at room temperature be determined from this difference?

Solution: Compositional balance is satisfied by an equally weighted mixture. The mixing energy is -0.35 eV/atom, and the driving force is 70 meV/atom. This represents the thermodynamic driving force within the selected phase pool. For the

decomposition time, diffusion, nucleation, and reaction barriers are required; comparing the driving force with kBT alone does not yield a timescale of hours or years.

Problem 7 - Uncertainty and significant figures

Let the independent relative standard uncertainties of current, voltage, area, and irradiance be 0.5%, 0.2%, 0.7%, and 1.0%, respectively. If the efficiency is 25%, what is the combined standard uncertainty and the expanded uncertainty with k = 2?

Solution: $\sqrt{(0.5^2 + 0.2^2 + 0.7^2 + 1.0^2)} = 1.334\%$ is the relative standard uncertainty. In efficiency units, this is 25 × 0.01334 = 0.334 percentage points. With k = 2, it becomes approximately 0.667 percentage points. The approximate report can be given in the form 25.0% ± 0.7, along with the coverage approach and the k value. If there is a common error or correlation, the sum of independent squares must be modified.

Problem 8 - Daily energy and performance ratio

For a system with a nominal power of 5 kWp, assume a daily plane-of-array irradiance of 6 kWh/m^2 and an AC output of 24 kWh. Calculate the performance ratio, taking the reference irradiance GSTC = 1 kW/m^2.

Solution: The final yield Yf = 24/5 = 4.8 kWh/kWp. The reference yield Yr = 6/1 = 6 hours. PR = 4.8/6 = 0.80, which means 80%. This value encompasses the optical, thermal, electrical, and availability effects simultaneously. Do not interpret the PR values of different seasons as solely due to equipment degradation without considering temperature and data selection.

Problem 9 - Interaction between two factors

In the model y = 20 + 0.2A + 0.3B + 0.45AB, A and B take on values of -1 or +1. Does increasing A from a low value to a high value have an effect that depends on B?

Solution: The response difference caused by changing A is Δy = 2(0.2 + 0.45B). For B = -1, the change is -0.5 points, and for B = +1, the change is +1.3 points. Therefore, the statement “increasing A is detrimental” or “beneficial” is incomplete on its own. The result depends on the level at which B is chosen. The physical interpretation could be, for example, that the process temperature produces different responses in different surface chemistries; this interpretation should be tested experimentally.

Problem 10 - From Measurement to Research Decision

After the new contact was applied, the fill factor (FF) increased by three points; Voc and the EQE integral remained unchanged. Let the first hypothesis be that the contact resistance decreased, and the second hypothesis be that light absorption increased. Which observation would differentiate between the two hypotheses?

Solution: Since the EQE integral remains unchanged, the explanation that “only absorption increased” becomes less plausible. The unchanged Voc and increasing FF are more consistent with improvements in contact/transport. A subsequent experiment could involve measuring contact resistance or performing a suitable pseudo-JV comparison. The mechanism cannot be definitively determined without verifying the same irradiance and temperature, as well as repeatability between samples and a stable MPP. A good response does not simply select a hypothesis; it also indicates which experiment would disprove it.

A reading template for studying an article

Once you finish reading the article, prepare a one-page research note including: the main physical claim; the cross-section of the device under investigation; the definition of the sample and control; the primary performance metric; the most important raw graph; the forward model used by the author; an alternative explanation; a differentiating experiment; and missing information needed for replication. Then, update the same note with additional information from the article. The title and abstract serve only as an introduction to this work.

When incorporating a new method from the literature into your own work, first reproduce the initial control. If the control does not work, it is difficult to interpret the success or failure of the new process. Keep records of each parameter change individually; understanding why negative results are negative yields more transferable knowledge than searching for the best cell by randomly changing the conditions.

BOOK I · CHAPTER 32 / STUDY AND REFERENCE

Symbols, units, and a Turkish-English glossary

Turning the glossary from a word list into a working tool

A symbol does not have a single, universal meaning. **G** can represent the irradiance on a surface in W/m^2 in one section, and the volumetric charge carrier generation rate in cm^{-3} s^{-1} in another. **R** can represent resistance, reflectance, or recombination rate. Instead of memorizing the letter alone, remember it along with its definition and unit. If similar letters are used in the same equation, subscripts and context provide differentiation.

Subscript indicates the type of quantity: sc for short circuit, oc for open circuit, and mpp for maximum power point. **Superscript** can sometimes indicate a power, sometimes a charge state, or sometimes a descriptive label. In cm^2, the superscript 2 denotes an area unit; in Pb^{2+}, the superscript 2+ denotes the ion's charge state. These should not be interpreted as the same operation. Greek letters are also just symbols: η for efficiency, τ for lifetime, and λ for wavelength are frequently used in this book.

Converting units line by line

Since 1 m = 100 cm, 1 m^2 = 10,000 cm^2. Therefore, 1 A/m^2 = 0.1 mA/cm^2: multiply by 1000 when converting amperes to milliamperes, then divide by 10,000 when converting the area denominator from square meters to square centimeters. The conversion 1000 W/m^2 = 100 mW/cm^2 follows the same logic. Applying the length conversion factor only once to an area unit is one of the most common errors.

The term **density** also requires a denominator. Current density is the current per unit area, and carrier density is the number per unit volume. Mass density is the mass per unit volume. The statement "density increased" is incomplete without specifying which quantity and denominator are being referred to.

When learning the English equivalent, match concepts rather than words. "Yield" can refer to the acceptance rate in production or the amount of production in a specific period. "Lifetime" can refer to the microscopic lifespan of excess charge carriers or the service life of a product over many years. Using the dictionary equivalent along with the scale and unit in the text helps prevent this confusion in translation and literature review.

Comprehension check: identify the incorrect equation

40 mA/cm^2 is not equal to 40 A/m^2; it is equal to 400 A/m^2. Also, 1 cm^2 is not equal to 0.01 m^2, but rather 0.0001 m^2. Clearly stating the unit conversion at each step allows us to identify errors of several orders of magnitude in the efficiency before even plotting the graph.

Unit ledger

1 eV = 1.602176634 × 10^{-19} J; q = 1.602176634 × 10^{-19} C; h = 6.62607015 × 10^{-34} J s; c = 299792458 m/s. Using these SI definition values, hc is approximately 1239.841984 eV nm. The Boltzmann constant k = 1.380649 × 10^{-23} J/K; k/q is approximately 8.617333262 × 10^{-5} V/K. 25 °C = 298.15 K, and kT/q is approximately 25.693 mV. [B08]

1 cm^2 = 10^{-4} m^2; 1 mA/cm^2 = 10 A/m^2. 1000 W/m^2 = 100 mW/cm^2. For Jsc = 40 mA/cm^2, Voc = 0.70 V and FF = 0.80, the maximum power density is 22.4 mW/cm^2; the efficiency at this irradiance is 22.4 percent. This numerical shortcut depends on the irradiance being 100 mW/cm^2. The same shortcut does not apply at a different irradiance.

Differentiate between percentage and percentage point: an increase in efficiency from 20% to 22% is a 2 percentage point increase, which is a 10% relative increase compared to the initial value. The phrase “2% improvement” is ambiguous without specifying which of these two meanings is intended. Energy density, power density, power per unit mass, and power per unit area are also different performance metrics.

Key symbols

Symbol	Meaning	Common unit
E, Eg	Photon energy, band gap.	eV or J
λ, ν	Wavelength, frequency	nm; Hz
G	Irradiance or volumetric generation rate, depending on context	W/m^2 or cm^{-3} s^{-1}; define it precisely.
Φ	Photon flux or spectral photon flux.	m^{-2} s^{-1}; specify separately whether per unit energy or wavelength
J, I	Current density, current	mA/cm^2; A
V, Voc	Voltage, open-circuit voltage.	V
P, η	Power, power conversion efficiency.	W; dimensionless or in percent.

Symbol	Meaning	Common unit
n, p	Electron and hole density.	cm^{-3}
μ, D, τ, L	Mobility, diffusion coefficient, lifetime, diffusion length.	cm^2/Vs; cm^2/s; s; cm
α, d	Absorption coefficient, thickness.	cm^{-1}; cm
Rs, Rsh	Series and shunt resistance	Ω; for area-normalized resistance, Ω cm^2
ε, ψ	Dielectric permittivity, electrostatic potential	F/cm; V
u, U	Standard uncertainty, expanded uncertainty	Same unit as the result

Bilingual glossary of terms

Turkish / abbreviation	English	Meaning in research
Fotovoltaik	Photovoltaic	Direct conversion of light into electricity
Soğurucu	Absorber	Layer intended to absorb useful photons
Bant aralığı	Band gap	Energy difference between electronic band edges
Doğrudan / dolaylı aralık	Direct / indirect gap	Distinguishes the momentum condition for the transition
Eksiton	Exciton	Bound electron-hole pair
Taşıyıcı	Charge carrier	Electron or hole participating in the current.
Katkılama	Doping	Impurities that control the charge carrier concentration and type.
Fermi seviyesi	Fermi level	Electronic chemical potential at equilibrium
Kuazi-Fermi ayrışması	Quasi-Fermi level splitting	Difference in non-equilibrium electron and hole potentials.
Yeniden birleşme	Recombination	Loss of electron-hole population.
Işınımsal yeniden birleşme	Radiative recombination	Recombination channel involving photon emission
Işınımsız yeniden birleşme	Non-radiative recombination	Energy being lost through channels other than photons.
SRH	Shockley-Read-Hall	Defect-mediated recombination model.
Auger	Auger recombination	The channel through which energy is transferred to another charge carrier.
Pasivasyon	Passivation	Reducing the effect of electrically harmful states

Turkish / abbreviation	English	Meaning in research
Seçici kontak	Selective contact	Conducting one charge carrier while blocking the other.
Bant hizalanması	Band alignment	Interlayer electronic energy relationship.
Arayüz	Interface	The region where two materials meet.
Tane sınırı	Grain boundary	The region that separates different crystal orientations.
Boşluk kusuru	Vacancy	Missing atom at a crystal lattice site
Antisite	Antisite defect	An atom occupying a site intended for a different type of atom.
İyon göçü	Ion migration	Movement of ions or ionic defects.
Kısa devre akımı	Short-circuit current	Current at zero terminal voltage
Açık devre gerilimi	Open-circuit voltage	Voltage at zero net terminal current
Dolum faktörü, FF	Fill factor	Pmax/(Voc Isc); if expressed in terms of power density, it becomes pmax/(Voc Jsc).
MPP / MPPT	Maximum power point / tracking	Maximum power point and tracking
PCE	Power conversion efficiency	The ratio of output electrical power to input light power.
EQE	External quantum efficiency	Ratio of collected electrons to incident photons
IQE	Internal quantum efficiency	Quantum efficiency relative to the defined absorbed-photon population
PL / TRPL	Photoluminescence / time-resolved PL	Light-induced emission and time response.
EL	Electroluminescence	Light emission under electrical excitation
PLQY	Photoluminescence quantum yield	The ratio of emitted photons to absorbed pump photons.
ERE	External radiative efficiency	External radiative recombination fraction; not identical to PLQY
Histerezis	Hysteresis	The result depends on the measurement history.
Spektral uyumsuzluk	Spectral mismatch	Mismatch of the source and device response with the reference
Aperture alanı	Aperture area	Measurement area defined by an optical aperture
Aktif alan	Active area	The definition of a specific active region may not encompass the entire device area.
STC	Standard test conditions	Defined reference spectrum, irradiance and temperature

Turkish / abbreviation	English	Meaning in research
AM1.5G	Air mass 1.5 global	Reference terrestrial global spectral distribution
AM1.5D	Air mass 1.5 direct	Reference direct spectral distribution
Tandem	Tandem	Stacked subcells using different spectral regions
2T / 4T	Two / four terminal	Distinction in electrical terminals and circuit topology
Akım eşleme	Current matching	Common-current constraint of series-connected subcells
Şönt	Shunt	Undesired parallel leakage path.
TCO	Transparent conducting oxide	Transparent conducting oxide
ETL / HTL	Electron / hole transport layer	Electron/hole transport layer
PERC	Passivated emitter and rear cell	Silicon architecture with rear passivation.
TOPCon	Tunnel oxide passivated contact	Passivated contact with a thin oxide
SHJ	Silicon heterojunction	Silicon heterojunction architecture.
IBC	Interdigitated back contact	Interdigitated rear-contact geometry
DSSC	Dye-sensitized solar cell	Dye-sensitized solar cell
BHJ	Bulk heterojunction	Organic donor-acceptor blend network.
DFT	Density functional theory	Framework for calculating the electronic ground state
SOC	Spin-orbit coupling	Spin-orbit interaction
Konveks zarf	Convex hull	Lowest-energy envelope of mixtures of phases
Fonon	Phonon	Crystal vibration mode
Metastabilite	Metastability	Locally stable state outside global equilibrium
SQS	Special quasirandom structure	Representation of disorder using selected correlations.
NEB	Nudged elastic band	The transition path and energy barrier method.
Sürüklenme-difüzyon	Drift-diffusion	Transport model driven by electric fields and density differences
TMM	Transfer matrix method	Solution method for layered optical structures.
UQ	Uncertainty quantification	Quantitative calculation of uncertainty.
OOD	Out of distribution	Outside the training distribution
Veri sızıntısı	Data leakage	Improper transfer of test information into model training
Tanımlanabilirlik	Identifiability	Ability of the data to distinguish parameters

Turkish / abbreviation	English	Meaning in research
Tasarım yeterliliği	Design qualification	Adequacy of a design under specified tests
T80	Time to 80 percent	The time it takes for the performance to degrade to 80 percent of the defined initial performance.
PR	Performance ratio	System performance normalized to reference irradiance
LCOE	Levelized cost of electricity	The ratio of discounted costs to discounted energy.
LCA	Life cycle assessment	Calculation of environmental impacts over the life cycle
EPBT	Energy payback time	The time required for the energy input to be recovered through production.

References and access notes

How should the bibliography be used?

The entries in this section are not a list of names, but rather a trail of claims made in the text. The code in square brackets leads you to the entry, and the entry leads to the DOI or institutional link. The **year of publication** indicates when the work was published; the **date accessed** indicates when the link was checked while this compilation was being prepared. Since current web pages can change, we should not interpret both as being the same date.

A record's description note specifies the access limit. If it states "summary reviewed," it does not imply that the entire methodology section was read. A "standard catalog entry" serves to verify the scope and version of the standard; it does not mean that all mandatory items are included here. Listing a further reading book does not imply that all of its chapters are reproduced in this work.

When citing, distinguish between the book's explanation and the original experimental result. If you are using the book to explain a concept, cite the book; if you are using the original data or evidence related to a specific cell's efficiency or mechanism, cite the original article. Both can be used together. This way, the educational synthesis and the originator of the initial measurement remain visible.

In this revision, the accessible pages of Becquerel's 1839 text for historical experiments, as well as Adams-Day's brief original statement, have also been examined. This scope is clearly stated in the source notes. The aim is to identify which experiment the text refers to, rather than relying solely on popular historical timelines for the details of the chemical process. No claim is made that the entire PV literature or the entire historical archive has been exhaustively scanned.

Comprehension check: what does a reference substantiate?

A citation does not automatically verify all the sentences associated with it. When using a specific number, check whether the source actually provides that number with the same conditions, definition, and sample. If the source cannot be found, leaving it unspecified is a more accurate research practice than adding another link that appears to support it.

Historical sources, original studies, and institutional reference records. The sources in the basic compilation were accessed on September 7; additional historical checks were conducted on September 8, 2026. Listing a source does not necessarily mean that its

full text, which may not be accessible, has been reviewed; usage limitations are specified in the notes below.

[B01] Photovoltaics Report, updated 14 July 2026
Fraunhofer ISE; PSE Projects GmbH (2026). Institutional report
https://www.ise.fraunhofer.de/content/dam/ise/de/documents/publications/studies/Photovoltaics-Report.pdf
The PDF and update date have been verified; it provides a concise overview of market and resource utilization. It is not a standalone, matched record certificate.

[B02] Snapshot of Global PV Markets 2026
IEA PVPS (2026). Institutional market report.
https://iea-pvps.org/snapshot-reports/snapshot-2026/
The official summary page and the main PDF have been checked. The summary graph indicates 607-698 GW, while the main text reports approximately 608 GW for the lower value; 698 GW is the upper estimate. PDF: https://iea-pvps.org/wp-content/uploads/2026/04/Snapshot-of-Global-PV-Markets-2026.pdf

[B03] Solar cell efficiency tables: Version 68
M. A. Green; E. D. Dunlop; M. Yoshita; N. Kopidakis; K. Bothe; G. Siefer; J. Y. Jiang (2026). Table of independently verified results.
https://doi.org/10.1016/j.joule.2026.102494
The official JRC146451 bibliography and scope record has been verified: https://publications.jrc.ec.europa.eu/repository/handle/JRC146451. Detailed record area/uncertainty values were not transferred from here.

[B04] Handbook of Photovoltaic Science and Engineering, Second Edition
A. Luque; S. Hegedus (editors) (2011). Further reading.
https://doi.org/10.1002/9780470974704
The publisher's bibliography and scope have been verified; it is not claimed that the full text has been scanned.

[B05] Physics of Solar Cells: From Basic Principles to Advanced Concepts, Third Edition
P. Würfel; U. Würfel (2016). Further reading.
https://www.wiley-vch.de/en?isbn=9783527413126&option=com_eshop&view=product
The publisher's bibliography and scope have been verified; it is not claimed that the full text has been scanned.

[B06] PV Lighthouse: Equivalent circuit and research calculators
PV Lighthouse (Continuously updated resource). Research tool official website.
https://www.pvlighthouse.com.au/equivalent-circuit
The tool's scope was checked; its outputs do not substitute for independent verification.

[B07] The Resource Demand of Terawatt-Scale Perovskite Tandem Photovoltaics
L. Wagner; J. Suo; B. Yang; D. Bogachuk; E. Gervais; R. Pietzcker; A. Gassmann; J. C. Goldschmidt (2023). Record of the original work's pre-print submission.
https://arxiv.org/abs/2306.13375
The preliminary title and source request scope have been verified; the numerical source request has not been transferred.

[B08] The International System of Units (SI), 9th edition
BIPM (2019; updated online edition.). Official SI reference source.
https://www.bipm.org/en/publications/si-brochure
Source for the definition constants of SI units.

[B09] Multilayer optical calculations
Steven J. Byrnes (2016; v5 (2020)). Explicit technical derivation.
https://arxiv.org/abs/1603.02720
In the v5 HTML text, normal incidence, Fresnel amplitudes, phase, and coherent/incoherent range were verified. The lossless single-layer example in the book is an original numerical recalculation.

[B10] ASTM G173 reference spectra: pvlib data representation and get_reference_spectra
pvlib python contributors; ASTM G173 reference data (Accessed in 2026). Open reference data
https://pvlib-python.readthedocs.io/en/stable/reference/generated/pvlib.spectrum.get_reference_spectra.html
A 2002-line CSV file was used: https://raw.githubusercontent.com/pvlib/pvlib-python/main/pvlib/data/ASTMG173.csv. Local file SHA-256: 91964ac23c0ec82dbbda4a7f160a5f5faf551dfe18ffae7e2446d74b57ee7859. It was compared with the institutional spectrum definition H09.

[B11] pvlib.pvsystem.singlediode - single diode equation
pvlib python contributors (Accessed in 2026). Official vehicle documentation.
https://pvlib-python.readthedocs.io/en/stable/reference/generated/pvlib.pvsystem.singlediode.html
The parameters and equation range of the single-diode equivalent circuit were checked. The current density format and curves in the book were generated using an independent root-solving method.

[B16] Solar Photovoltaic Cell Basics
U.S. Department of Energy (Accessed in 2026). Introductory teaching material from an institution
https://www.energy.gov/cmei/systems/solar-photovoltaic-cell-basics
Accessed for basic cell operation and types of technology. Not all record/market statements from the updated page were incorporated into this revision. Accessed: September 8, 2026.

[B17] Solar Photovoltaic Performance and Efficiency Basics
U.S. Department of Energy (Accessed in 2026). Introductory teaching material from an institution
https://www.energy.gov/cmei/systems/solar-photovoltaic-performance-and-efficiency-basics
Used to check the definition of efficiency and the current-voltage-power relationship. The quantitative examples are teaching examples created for this book. Accessed: September 8, 2026.

[H01] The History of Solar
U.S. Department of Energy, Energy Efficiency and Renewable Energy (Year not specified). Institutional timeline
https://www1.eere.energy.gov/solar/pdfs/solar_timeline.pdf
The 12-page publicly available PDF has been verified. It was used for the historical milestones of 1839 and 1883; however, the exact year of publication could not be verified in the document. The outdated future predictions and record tables in the document were not used as current information.

[H02] Effect of Light on Selenium During the Passage of an Electric Current
Willoughby Smith (1873). Primary historical publication.
https://doi.org/10.1038/007303e0
Nature 7, 303; February 20, 1873. The title, date, and DOI were verified through the publisher's index and bibliographic record. A brief historical context is provided for distinguishing devices that generate energy through photoconductivity; a complete review of the article is not claimed.

[H03] Referee's report on The action of light on selenium by William Grylls Adams and R. E. Day
Henry Enfield Roscoe; The Royal Society Archives (1876). Primary archival record
https://makingscience.royalsociety.org/items/rr_7_429/referees-report-by-henry-enfield-roscoe-on-a-paper-the-action-of-light-on-selenium-by-william-grylls-adams-and-r-e-day
The record of the referee report dated August 7, 1876, confirms the connection to the publication of the relevant work in the 1877 Philosophical Transactions, DOI 10.1098/rstl.1877.0009. It was used to distinguish between the date of the experiment/presentation and the date of publication.

[H04] A New Silicon p-n Junction Photocell for Converting Solar Radiation into Electrical Power
D. M. Chapin; C. S. Fuller; G. L. Pearson (1954). Primary device article.
https://doi.org/10.1063/1.1721711
Journal of Applied Physics 25(5), 676-677; May 1954. The authors, institution, title, pages, and DOI were verified through bibliographic records. Automated access to the publisher's full text could not be provided; 6%'s historical context was supported by H08.

[H05] Experimental silicon solar cell
Smithsonian Institution, National Museum of American History (Year not specified). Museum artifact and historical record.
https://www.si.edu/object/nmah_713146
The indexed description of the Smithsonian collection record has been verified. It was used in the context of Chapin, Fuller, Pearson, and Ohl; the direct automatic opening of the page resulted in a temporary error.

[H06] The 1905 Papers - Annus Mirabilis of Albert Einstein
Library of Congress (Year not specified). Institutional archive and reading guide.
https://guides.loc.gov/einstein-annus-mirabilis/1905-papers
The institutional record describing Einstein's 1905 paper on the light quantum/photoelectric effect and its Princeton translation has been verified. It was used for a brief historical context; the distinction between the external photoelectric effect and the PV device represents the original instructive explanation.

[H07] Vanguard Satellite, 1958
NASA (2015). Institution's historical record.
https://www.nasa.gov/image-article/vanguard-satellite-1958/
The launch date of March 17, 1958, and the information regarding the first solar-powered satellite were confirmed on the NASA website. No further claims were made regarding its current orbital status.

[H08] Deployment of Solar Photovoltaic Generation Capacity in the United States
David Hart; Kurt Birson (2016). Academic institution report prepared for the DOE.
https://www.energy.gov/sites/prod/files/2017/01/f34/Deployment%20of%20Solar%20Photovoltaic%20Generation%20Capacity%20in%20the%20United%20States.pdf
George Mason University, June 2016; a 48-page PDF document was released. Early transition from space to terrestrial applications, Bell Labs, approximately 6%, and a brief overview of the federal R&D context. This is not a current source for cost or market data.

[H09] Reference Air Mass 1.5 Spectra
National Laboratory of the Rockies, formerly NREL (Year not specified). Institutional reference spectrum and data description.
https://www.nlr.gov/grid/solar-resource/spectra-am1.5
On the live page, ASTM G173, 37-degree surface, specified atmospheric conditions, spectral units, and the SMARTS model were validated. The source page was presented under the name NLR and at the address where the old NREL links were redirected. It was used to explain that the standard spectrum does not represent universal weather conditions.

[H10] The International System of Units - SP 330, Section 2
National Institute of Standards and Technology (2019). Official SI definitions.
https://www.nist.gov/pml/special-publication-330/sp-330-section-2
The precise SI values of the speed of light, Planck's constant, the elementary charge, and Boltzmann's constant were verified. The thermal voltage used in the illustrative numerical examples was calculated independently of these constants.

[H11] Fundamentals of Photovoltaics - Calendar and Readings
MIT OpenCourseWare (2013). University course syllabus.
https://ocw.mit.edu/courses/2-627-fundamentals-of-photovoltaics-fall-2013/pages/calendar-readings/
The lesson sequence for source material, optical management, excitation, charge separation, and advanced topics has been confirmed. Reading guidance was not used for current technology records.

[H12] Band Gap
PVEducation (Year not specified). Original teaching material.
https://www.pveducation.org/pvcdrom/pn-junctions/band-gap
The content regarding band gap, valence/conduction band, and electron/hole definitions has been reviewed. More advanced theory and numerical examples constitute the original instructional synthesis.

[H13] Absorption Coefficient
PVEducation (Year not specified). Original teaching material.
https://www.pveducation.org/pvcdrom/pn-junctions/absorption-coefficient
The wavelength- and material-dependent definition of the absorption coefficient was verified. The absorption thickness example, 90%, was calculated using hypothetical values selected for this book.

[H14] Equilibrium Carrier Concentration
PVEducation (Year not specified). Original teaching material.
https://www.pveducation.org/pvcdrom/pn-junctions/equilibrium-carrier-concentration
The fundamental concepts of equilibrium charge carrier density and the mass-action relationship were reviewed. The values of ni and dopant concentration in the book are presented as a clear, didactic assumption.

[H15] The Theory of p-n Junctions in Semiconductors and p-n Junction Transistors
William Shockley (1949). Primary theoretical article.
https://doi.org/10.1002/j.1538-7305.1949.tb03645.x
Bell System Technical Journal 28(3), 435-489; the abstract and publication details on the publisher's page have been verified. It was used as the historical basis for the junction potential, minority charge carrier diffusion, and the rectification relationship.

[H16] Diffusion
PVEducation (Year not specified). Original teaching material.
https://www.pveducation.org/pvcdrom/pn-junctions/diffusion
The concepts of density gradient and diffusion were reviewed. The book expands on the original pedagogy with discussions and calculations related to continuity and boundary conditions.

[H17] Statistics of the Recombinations of Holes and Electrons
William Shockley; W. T. Read Jr. (1952). Primary theoretical article.
https://journals.aps.org/pr/abstract/10.1103/PhysRev.87.835
Physical Review 87, 835-842. The publisher's record and abstract page have been opened. It was used to explain the original source of the SRH mechanism; the book is not a translation of an article.

[H18] Electron-Hole Recombination in Germanium
R. N. Hall (1952). Primary theoretical publication.
https://journals.aps.org/pr/abstract/10.1103/PhysRev.87.387
Physical Review 87, 387; July 15, 1952. The citation and DOI were verified with the publisher; full-text access was restricted. This was used for the historical origin of the SRH nomenclature.

[H19] Improved quantitative description of Auger recombination in crystalline silicon
Armin Richter; Stefan W. Glunz; Florian Werner; Jan Schmidt; Andrés Cuevas (2012). Institutional record of the primary research article.
https://publica.fraunhofer.de/entities/publication/80c799ad-9546-4dc3-8a7c-b24c4c1ccfe7
Physical Review B 86, 165202; DOI 10.1103/PhysRevB.86.165202. The abstract and authors listed in the Fraunhofer database were verified. It was used for 300 K conditional injection/doping-dependent parameterization; the coefficients were not transferred to another temperature.

[H20] Surface Recombination
PVEducation (Year not specified). Original teaching material.
https://www.pveducation.org/pvcdrom/pn-junctions/surface-recombination
The definition of surface recombination and its relationship with lifetime was reviewed. A two-surface sheet calculation, assuming a uniform charge carrier density, was developed for this textbook.

[H21] Charge Carrier Separation in Solar Cells
Uli Würfel; Andres Cuevas; Peter Würfel (2015). Institutional record of the primary theoretical article.
https://publikationen.bibliothek.kit.edu/1000058630
IEEE Journal of Photovoltaics 5(1), 461-469; DOI 10.1109/JPHOTOV.2014.2363550. The KIT record was verified; the author's description of selective conductivity and quasi-Fermi gradient in the open-access copy of the article was reviewed. The source-specific summary was kept brief.

[H22] Solar cell fill factors: General graph and empirical expressions
Martin A. Green (1981). Primary theoretical article.
https://doi.org/10.1016/0038-1101(81)90062-9
Solid-State Electronics 24(8), 788-789. The citation and the PDF copy of the original article, available at the academic institution, were verified. It was used to determine the origin of the ideal FF approach; the complete MPP example was calculated using an independent root-finding method.

[H23] IV Curve
PVEducation (Year not specified). Original teaching material.
https://www.pveducation.org/pvcdrom/solar-cell-operation/iv-curve
The definitions of short circuit, open circuit, and maximum power point were reviewed. The numerical cell data in the book is an illustrative model, not a record of an experiment.

[H24] Quantum Efficiency
PVEducation (Year not specified). Original teaching material.
https://www.pveducation.org/pvcdrom/solar-cell-operation/quantum-efficiency
The definitions of external and internal quantum efficiency have been reviewed. The spectral band current calculation is an independent instructional example.

[H25] Detailed Balance Limit of Efficiency of p-n Junction Solar Cells
William Shockley; Hans J. Queisser (1961). Primary theoretical article.
https://doi.org/10.1063/1.1736034
Journal of Applied Physics 32(3), 510-519. The title and abstract of the original article, as well as the 6000 K/300 K assumptions, were verified against the copy in the USPTO public archive. The book contains a brief reference to the original historical result; the lengthy explanations represent the original, didactic derivation of the general equilibrium physics.

[H26] Tabulated values of the Shockley-Queisser limit for single junction solar cells
Sven Rühle (2016). Primary calculation article.
https://doi.org/10.1016/j.solener.2016.02.015
Solar Energy 130, 139-147. The abstract, title, DOI, and publisher information were verified. AM1.5G was used as the basis for the band gap-dependent table scope; complete tables were not presented as recalculated or verified records in this session.

[H27] The chemical potential of radiation
Peter Würfel (1982). University copy of the original theoretical paper.
https://www.unife.it/scienze/astro-fisica/insegnamenti/ottica-applicata/materiale-didattico/sorgenti-assolute/Wurfel.pdf
Journal of Physics C: Solid State Physics 15, 3967-3985; DOI 10.1088/0022-3719/15/18/012. The university copy and the publisher's abstract were verified. It was used for a brief explanation of the generalized Planck approach.

[H28] Reciprocity relation between photovoltaic quantum efficiency and electroluminescent emission of solar cells
Uwe Rau (2007). Primary theoretical article.
https://harvest.aps.org/v2/journals/articles/10.1103/PhysRevB.76.085303/fulltext
Physical Review B 76, 085303; the publisher's full-text endpoint was verified. For a concise reference regarding reciprocity and the Voc/electroluminescence relationship; the number of ERE samples was calculated independently at 298.15 K.

[H29] Detailed balance limit of the efficiency of tandem solar cells
Alexis De Vos (1980). Institutional record of the primary theoretical article.
https://biblio.ugent.be/publication/207802
Journal of Physics D: Applied Physics 13(5), 839-846; DOI 10.1088/0022-3727/13/5/018. The author confirmed the date and details of the UGent registration; the publisher-provided abstract confirmed the scope of the electroluminescent coupling between sub-cells. Older theoretical efficiency figures were not transferred as modern AM1.5G records.

[H30] Advanced Concepts, Part 1 - Lecture 15, MIT Fundamentals of Photovoltaics
Joseph T. Sullivan; MIT OpenCourseWare (2011). University lecture notes.
https://ocw.mit.edu/courses/2-627-fundamentals-of-photovoltaics-fall-2013/54a21db9c8e8a6a5b181807080da4f20_MIT2_627F13_lec15.pdf
The 44-page PDF document was last updated on November 3, 2011, and is presented on the 2013 course page. It was used to guide students towards more advanced concepts. The outdated performance and cost tables in the notes were not considered as current information.

[H31] Mémoire sur les effets électriques produits sous l'influence des rayons solaires
Edmond Becquerel (1839). Exact replica/transcription package of the original historical text.
https://www.becquerel-prize.org/pdf/2020_02_10_History_PV_BECQUEREL_prize.pdf
C. R. Acad. Sci. Paris 9, 561 and onwards. The original pages 561-565 of the accessed package were visually inspected: two-compartment setup, cover and light control, surface cleaning, AgCl-coated platinum experiment. This access to the package does not imply that the entire 1839 archive has been inspected. Accessed: September 8, 2026.

[H32] The action of light on selenium (Abstract)
W. G. Adams; R. E. Day (1876-1877). Original short research paper.
https://ese.nju.edu.cn/_upload/article/files/1a/d6/bd70f7454528b852ea0fd22758b6/e30147ef-ddc7-45a1-ae41-29fdba6bcfdb.pdf
Proceedings of the Royal Society of London, 25, 113-117. The text indicates it was received on May 18, 1876; the archive volume record is from 1876-1877. The complete text of the accessed short communication was checked; it should not be presented as if the entire 37-page Philosophical Transactions article was read. The galvanometer experiment without a battery and the check of three samples to which no current was previously applied are on pages 115-116. Accessed: September 8, 2026.

[T01] 22.8% efficient silicon solar cell
Andrew W. Blakers; Aihua Wang; Adele M. Milne; Jianhua Zhao; Martin A. Green (1989). Original experimental article; author's institutional bibliographic record.
https://researchportalplus.anu.edu.au/en/publications/228-efficient-silicon-solar-cell/
Historical development of PERC technology. The ANU record has been confirmed as a live record; the complete experimental methods were not disclosed. The efficiency value in the title refers to a study from a specific date and is not the current record.

[T02] Carrier-selective contacts for Si solar cells
F. Feldmann; M. Simon; M. Bivour; C. Reichel; M. Hermle; S. W. Glunz (2014). Original experimental article.
https://doi.org/10.1063/1.4875904
Applied Physics Letters 104, 181105. The publisher's summary and bibliographic data have been verified; historical evidence of passivation and carrier balance in TOPCon contacts.

[T03] Silicon heterojunction solar cell with interdigitated back contacts for a photoconversion efficiency over 26%
Kunta Yoshikawa and colleagues (2017). Original experimental article.
https://www.nature.com/articles/nenergy201732
Nature Energy 2, 17032. Publisher's summary and figure captions accessed; combination of SHJ and IBC topologies and reporting of the area. No claim is made that the entire full text of the subscription-based article was read.

[T04] Silicon heterojunction solar cells with up to 26.81% efficiency achieved by electrically optimized nanocrystalline-silicon hole contact layers
Hao Lin, Miao Yang, Xiaoning Ru, and colleagues. (2023). Original experimental article.
https://www.nature.com/articles/s41560-023-01255-2
Nature Energy 8, 789-799. The results, methodology, and relevant electrical analysis sections from the publisher were accessed. In the text, only the nanocrystalline hole contact mechanism was briefly mentioned; the number in the title does not represent the current record.

[T05] Understanding the role of selenium in defect passivation for highly efficient selenium-alloyed cadmium telluride solar cells
Thomas A. M. Fiducia, Budhika G. Mendis, Kexue Li, and colleagues. (2019). Original experimental article.
https://www.nature.com/articles/s41560-019-0389-z
Nature Energy 4, 504-511. Publisher's summary and figure captions; the effect of defect passivation of selenium outside the optical range. A link to the author's corrections from May 28, 2019, was found on the page; the text only conveys the summary findings of the current page.

[T06] Sodium enhances indium-gallium interdiffusion in copper indium gallium diselenide photovoltaic absorbers
Diego Colombara, Florian Werner, Torsten Schwarz, and colleagues. (2018). Original experimental article; open access.
https://www.nature.com/articles/s41467-018-03115-0
The relationship between the sodium effect, compositional diffusion, and processing history. Open access publication consulted; a general alkali-ion mechanism was not claimed.

[T07] Reversible conductivity changes in discharge-produced amorphous Si
David L. Staebler; Christopher R. Wronski (1977). Original experimental article; full-text access restricted.
https://doi.org/10.1063/1.89674
Applied Physics Letters 31, 292-294. The DOI link resulted in an error; the title, author, year, and DOI were verified against the bibliographic record. The historical fact is further supported by the original author's description of T33; the full text, which was not accessible, was not considered as read.

[T08] Six-junction III-V solar cells with 47.1% conversion efficiency under 143 Suns concentration
John F. Geisz, Ryan M. France, Kevin L. Schulte, and colleagues. (2020). Original experimental article.
https://www.nature.com/articles/s41560-020-0598-5
Nature Energy 5, 326-335. Publisher page verified. It was used solely for teaching the concept of a six-junction concentrator device and category differentiation, dating back to 2020; it does not represent a solar panel efficiency or claim a current record.

[T09] Triple-junction solar cells with 39.5% terrestrial and 34.2% space efficiency enabled by thick quantum well superlattices
Ryan M. France; John F. Geisz; Tao Song; Waldo Olavarria; Michelle Young; Alan Kibbler; Myles A. Steiner (2022). Original experimental article.
https://doi.org/10.1016/j.joule.2022.04.024
Joule publisher's summary and author's pre-print accessed at arxiv.org/abs/2203.15593. It supports the separate reporting of AM1.5G and AM0 results, as well as quantum well interval tuning. The numbers in the title refer to the dates of the results.

[T10] Organometal Halide Perovskites as Visible-Light Sensitizers for Photovoltaic Cells
Akihiro Kojima; Kenjiro Teshima; Yasuo Shirai; Tsutomu Miyasaka (2009). Original experimental article.
https://pubs.acs.org/doi/10.1021/ja809598r
Journal of the American Chemical Society, 131, 6050-6051. Publisher's abstract, authors, and publication date accessed; limited use with a historical photoelectrochemical sensitizer architecture.

[T11] Efficient hybrid solar cells based on meso-superstructured organometal halide perovskites
Michael M. Lee; Joël Teuscher; Tsutomu Miyasaka; Takurou N. Murakami; Henry J. Snaith (2012). Original experimental article; original abstract available via PubMed.
https://doi.org/10.1126/science.1228604
Science 338, 643-647. The original author's abstract and bibliographic record were verified via pubmed.ncbi.nlm.nih.gov/23042296/; no claim of full method access was made.

[T12 / R13] Ionic transport in hybrid lead iodide perovskite solar cells
Christopher Eames; Jarvist M. Frost; Piers R. F. Barnes; Brian C. O'Regan; Aron Walsh; M. Saiful Islam (2015). Original computational and experimental article; open access.
https://www.nature.com/articles/ncomms8497
Nature Communications 6, 7497. Hole-assisted ion transport for a specific MAPbI3 system: computational and kinetic experimental correlation. It was not used as a single universal barrier for all perovskites. Nature Communications 6, 7497; an original study that combines first-principles calculations and experimental kinetics for ion migration.

[T13] Reversible photo-induced trap formation in mixed-halide hybrid perovskites for photovoltaics
Eric T. Hoke; Daniel J. Slotcavage; Emma R. Dohner; Andrea R. Bowring; Hemamala I. Karunadasa; Michael D. McGehee (2015). Original experimental article; open access.
https://pubs.rsc.org/en/content/articlelanding/2015/sc/c4sc03141e
Chemical Science. Publisher's summary and article PDF search text accessed; example of light-reversible decomposition and optical switching in mixed halide perovskites.

[T14 / R14] Evidence for ion migration in hybrid perovskite solar cells with minimal hysteresis
Philip Calado; Andrew M. Telford; Daniel Bryant; Xiaoe Li; Jenny Nelson; Brian C. O'Regan; Piers R. F. Barnes (2016). Original experimental and device modeling paper; open access.
https://www.nature.com/articles/ncomms13831
Nature Communications 7, 13831. Publisher and PMC full text verified; it supports the idea that low hysteresis does not necessarily imply the absence of ion migration. Nature Communications 7, 13831; an original experiment demonstrating that low hysteresis does not preclude ion migration.

[T15 / R05] Consensus statement for stability assessment and reporting for perovskite photovoltaics based on ISOS procedures
Mark V. Khenkin and colleagues. (2020). Researcher consensus and methodology document.
https://www.nature.com/articles/s41560-019-0529-5
Nature Energy 5, 35-49. Open access publisher sections; reporting on light, heat, humidity, load, MPP, and reversible change. It was not presented as a regulation or a definitive field lifetime model. Nature Energy 5, 35-49; the ISOS framework serves as a method source for the operating load, MPP, and outdoor performance transfer. Not all sections were derived from this single source.

[T16] Fully textured monolithic perovskite/silicon tandem solar cells with 25.2% power conversion efficiency
Florent Sahli and colleagues (2018). Original experimental article.
https://www.nature.com/articles/s41563-018-0115-4
Nature Materials 17, 820-826. Publisher's summary and page verified; historical example of a recombination junction with a textured monolithic stack. No current record claim.

[T17] Monolithic perovskite/silicon tandem solar cell with >29% efficiency by enhanced hole extraction
Amran Al-Ashouri and colleagues (2020). Original experimental article; original abstract and institutional author copy.
https://doi.org/10.1126/science.abd4016
Science 370, 1300-1309. The original abstract was verified at pubmed.ncbi.nlm.nih.gov/33303611/, and the institutional author copy was confirmed. The relationship between hole extraction/contact loss using a molecular monolayer; the cited record number was not used as an up-to-date reference in the text.

[T18] Semi-transparent perovskite solar cells for tandems with silicon and CIGS
Colin D. Bailie and colleagues (2015). Original experimental article.
https://pubs.rsc.org/en/content/articlehtml/2015/ee/c4ee03322a
Energy & Environmental Science 8, 956-963. Publisher's text accessed; 4T teaching method via semi-transparent top cell and mechanical stacking.

[T19] Mixed tin-lead perovskites with balanced crystallization and oxidation barrier for all-perovskite tandem solar cells
Jin Zhou, Shiqiang Fu, Shun Zhou, and colleagues. (2024). Original experimental article; open access.
https://www.nature.com/articles/s41467-024-46679-w
Nature Communications 15, 2324. Publisher's summary and open access; mixed tin-lead crystallization and Sn(II) oxidation. The chemical synthesis procedure was not reproduced.

[T20] A low-cost, high-efficiency solar cell based on dye-sensitized colloidal TiO2 films
Brian O'Regan; Michael Grätzel (1991). Original experimental article.
https://www.nature.com/articles/353737a0
Nature 353, 737-740. The publisher's summary and bibliographic details have been verified; this provides historical evidence for the dye-sensitized porous TiO2 architecture. The economic context of 1991 has not been updated.

[T21] Single-Junction Organic Solar Cell with over 15% Efficiency Using Fused-Ring Acceptor with Electron-Deficient Core
Jun Yuan, Yunqiang Zhang, Liuyang Zhou, and colleagues. (2019). Original experimental article.
https://doi.org/10.1016/j.joule.2019.01.004
Joule 3, 1140-1151. Publisher's article text and abstract accessed; Y6 non-fullerene acceptor and morphology/absorption relationship. No source-specific synthesis method or long-term results transfer was performed.

[T22] Peak external photocurrent quantum efficiency exceeding 100% via MEG in a quantum dot solar cell
Octavi E. Semonin; Joseph M. Luther; Sukgeun Choi; Hsiang-Yu Chen; Jianbo Gao; Arthur J. Nozik; Matthew C. Beard (2011). Original experimental article; original abstract available via PubMed.
https://doi.org/10.1126/science.1209845
Science 334, 1530-1533. The original author's abstract was verified via pubmed.ncbi.nlm.nih.gov/22174246/. Distinguishing energy efficiency from EQE; no module record was obtained from the narrow spectral data.

[T23] Deep electron traps and origin of p-type conductivity in the earth-abundant solar-cell material Cu2ZnSnS4
Dong Han; Y. Y. Sun; Junhyeok Bang; Y. Y. Zhang; Hong-Bo Sun; Xian-Bin Li; S. B. Zhang (2013). Original computational article.
https://journals.aps.org/prb/abstract/10.1103/PhysRevB.87.155206
Physical Review B 87, 155206. The publisher's summary has been verified. It was explicitly classified as a hybrid functional defect prediction, and not presented as a direct defect measurement of the actual film.

[T24] Thin-film Sb2Se3 photovoltaics with oriented one-dimensional ribbons and benign grain boundaries
Ying Zhou, Liang Wang, Shiyou Chen, and colleagues. (2015). Original experimental and computational article.
https://www.nature.com/articles/nphoton.2015.78
Nature Photonics 9, 409-415. Publisher's summary and figure captions accessed; discussion of stripe orientation and grain boundary physics. The toxicity assessment in the source was not adopted as a universal safety provision.

[T25] Intensity Enhancement in Textured Optical Sheets for Solar Cells
Eli Yablonovitch; George D. Cody (1982). Original theoretical article; author's university archive.
https://optoelectronics.eecs.berkeley.edu/ey1982ieeeed292.pdf
IEEE Transactions on Electron Devices 29, 300-305. The indexed content of the institutional PDF has been verified; it was emphasized that the $4n^2$ approach represents an assumed optical limit. There is no claim of a universal limit for general nanophotonics.

[T26 / R09] Reciprocity relation between photovoltaic quantum efficiency and electroluminescent emission of solar cells
Uwe Rau (2007). Original theoretical article.
https://journals.aps.org/prb/abstract/10.1103/PhysRevB.76.085303
Physical Review B 76, 085303. Publisher's summary and APS author text accessed. Reciprocity, external luminescence, and voltage loss were used with the formula, assuming a constant optical reference and validity. Physical Review B 76, 085303; publication and open access original text record verified. Used with the assumption of reciprocity relations.

[T27] Surfactant-controlled ink drying enables high-speed deposition of perovskite films for efficient photovoltaic modules
Yehao Deng; Xiaopeng Zheng; Yang Bai; Qi Wang; Jingjing Zhao; Jinsong Huang (2018). Original experimental article.
https://www.nature.com/articles/s41560-018-0153-9
Nature Energy 3, 560-566. The publisher's summary, results, and author information were verified through a live search; a direct link resulted in an error. It was used for the small-cell/large-module distinction and flow-drying control.

[T28] On-device lead sequestration for perovskite solar cells
Xun Li; Fei Zhang; Haiying He; Joseph J. Berry; Kai Zhu; Tao Xu (2020). Original experimental article.
https://www.nature.com/articles/s41586-020-2001-x
Nature 578, 555-558. Publisher's summary and article information accessed; device-level lead retention approach. No claim of zero emissions or complete safety in all damage scenarios.

[T29] Methodology Guidelines on Life Cycle Assessment of Photovoltaic 2020
IEA PVPS Task 12 uzman grubu (2020). Corporate methodology guide.
https://iea-pvps.org/key-topics/methodology-guidelines-on-life-cycle-assessment-of-photovoltaic-2020/
Official page accessed. Functional unit, system boundaries, production location, lifetime, degradation, and energy production assumptions should be clearly reported. It was not used as a source for current prices or market share.

[T30] Low-temperature strain-free encapsulation for perovskite solar cells and modules passing multifaceted accelerated ageing tests
Paolo Mariani, Miguel Ángel Molina-García, Jessica Barichello, and colleagues. (2024). Original experimental article; open access.
https://www.nature.com/articles/s41467-024-48877-y
Nature Communications 15, 4552. Publisher's open access text; low-temperature encapsulation, thermomechanical compatibility, and multiple tests. Accelerated testing did not correlate with decades of field life.

[T31] Highly stable all-perovskite tandem solar cells with targeted conversion of tin-lead surfaces
Nannan Sun, Sheng Fu, Yunfei Li, and colleagues. (2026). Original experimental article.
https://www.nature.com/articles/s41566-025-01815-w
Nature Photonics 20, 273-279; published February 5, 2026. Publisher's summary and institutional author record verified. This is only a brief example demonstrating the protection of a reactive tin-lead surface under light-heat conditions; it is not a current record or a detailed chemical application procedure.

[T32] Perovskite solar cells with atomically coherent interlayers on SnO2 electrodes
Hanul Min, Do Yoon Lee, Junu Kim, and colleagues. (2021). Original experimental article.
https://www.nature.com/articles/s41586-021-03964-8
Nature 598, 444-450. The publisher's summary and article details have been verified; this is an example of embedded interface engineering. It is not claimed that the complete method and all supplementary data have been reviewed.

[T33] Optically Induced Conductivity Changes in Amorphous Silicon: A Historical Perspective
David L. Staebler (1997). The original researcher's historical account.
https://www.cambridge.org/core/journals/mrs-online-proceedings-library-archive/article/abs/optically-induced-conductivity-changes-in-amorphous-silicon-a-historical-perspective/834195C6D952A5863FDDD22BE4F63D58
MRS Online Proceedings Library 467, 3; 1997 conference publication, Cambridge, accessed online on February 15, 2011. The author's account of their own discovery and the explanation of reversibility complete the T07 access restriction. Publisher's abstract accessed.

[T34] Inverted perovskite solar modules with 99.3% geometrical fill factor via nanosecond single laser patterning
Andrés E. R. Soto; Vera C. M. Duarte; Adélio Mendes; Luísa Andrade (2025). Original research
https://www.nature.com/articles/s44172-025-00512-4.pdf
Communications Engineering 4, 198. doi:10.1038/s44172-025-00512-4. The P1, P2, and P3 functions and the active/dead area description on the first two pages were checked; the numerical performance results were not included in this supplementary explanation. Accessed: September 8, 2026.

[R01] IEC 60904-1:2020 - Photovoltaic devices - Part 1: Measurement of photovoltaic current-voltage characteristics
International Electrotechnical Commission (2020). Standards catalogue entry
https://webstore.iec.ch/en/publication/32004
The open IEC catalog scope was verified; compliance was not checked on a full-text or item-by-item basis.

[R02] IEC 60904-8:2014 - Photovoltaic devices - Part 8: Measurement of spectral responsivity of a photovoltaic device
International Electrotechnical Commission (2014). Standards catalogue entry
https://webstore.iec.ch/en/publication/3879
The spectral response range for both linear and nonlinear devices was verified using the open catalog; the complete standard text was not examined.

[R03] Effects of Spectral Error in Efficiency Measurements of GaInAs-Based Concentrator Solar Cells
C. R. Osterwald, M. W. Wanlass, T. Moriarty, M. A. Steiner, K. A. Emery (2014). Institutional report
https://www.nrel.gov/docs/fy14osti/60748.pdf
NREL/TP-5200-60748; the indexed title, author, and spectral error text of the report were verified. Direct PDF opening resulted in an error during this scan; specific concentrator data were not transferred.

[R04] Combining uncertainty components
National Institute of Standards and Technology (Year not specified). Institutional method source.
https://physics.nist.gov/cuu/Uncertainty/combination.html
Propagation of uncertainty, sensitivity coefficients, and an explicit institutional description of covariance; undated, accessible page.

[R06] IEC 61215-1:2021 - Terrestrial photovoltaic modules - Design qualification and type approval - Part 1: Test requirements
International Electrotechnical Commission (2021). Standards catalogue entry
https://webstore.iec.ch/en/publication/61345
The open catalog has been verified; the catalog states that it does not provide a quantitative estimate of module lifetime. No claim of compliance with full standards or test thresholds is made.

[R07] Practical Guides for X-Ray Photoelectron Spectroscopy: First Steps in Planning, Conducting, and Reporting XPS Measurements
D. R. Baer et al. (2019). Method article
https://www.nist.gov/publications/practical-guides-x-ray-photoelectron-spectroscopy-first-steps-planning-conducting-and
NIST publication record; DOI 10.1116/1.5065501. The XPS planning and reporting framework was validated.

[R08] Photoluminescence-Based Characterization of Halide Perovskites for Photovoltaics
T. Kirchartz, J. A. Márquez, M. Stolterfoht, T. Unold (2020). Method compilation.
https://advanced.onlinelibrary.wiley.com/doi/abs/10.1002/aenm.201904134
Advanced Energy Materials, 1904134; the publisher's record and indexed measurement description have been verified. Selected method as a reference for the condition dependence of PL/TRPL.

[R10] Deep-level transient spectroscopy: A new method to characterize traps in semiconductors
D. V. Lang (1974). Bibliographic record of the original article.
https://doi.org/10.1063/1.1663719
Journal of Applied Physics 45, 3023-3032. Verified via DOI and original bibliographic record; direct access to the publisher's full text was unsuccessful.

[R11] Understanding how excess lead iodide precursor improves halide perovskite solar cell performance
B.-W. Park et al. (2018). Original research article
https://www.nature.com/articles/s41467-018-05583-w
Nature Communications 9, 3301. An example of a method that combines GIWAXS, electron microscopy, and charge collection.

[R12] Origin of apparent light-enhanced and negative capacitance in perovskite solar cells
F. Ebadi, N. Taghavinia, R. Mohammadpour, A. Hagfeldt, W. Tress (2019). Original research article
https://www.nature.com/articles/s41467-019-09079-z
Nature Communications 10, 1574; visible capacitance separation with a slow ionic/electronic response, as confirmed by the authors and in the main text.

[R15] Review of Failures of Photovoltaic Modules
M. Köntges et al.; IEA PVPS Task 13 (2014). Institutional report
https://iea-pvps.org/wp-content/uploads/2020/01/IEA-PVPS_T13-01_2014_Review_of_Failures_of_Photovoltaic_Modules_Final.pdf
IEA-PVPS T13-01:2014; corporate report on module failure mechanisms: a single universal degradation rate was not assigned to any specific technology.

[R16] Service Life Estimation for Photovoltaic Modules
IEA PVPS Task 13 (2021). Institutional report
https://iea-pvps.org/key-topics/service-life-estimation-for-photovoltaic-modules/
IEA-PVPS T13-16:2021; end-of-life definitions, degradation models, and the relationship between service life and energy.

[R17] Generalized Gradient Approximation Made Simple
J. P. Perdew, K. Burke, M. Ernzerhof (1996). Original research article
https://journals.aps.org/prl/abstract/10.1103/PhysRevLett.77.3865
Physical Review Letters 77, 3865; the original publication of the PBE functional.

[R18] Reproducibility in density functional theory calculations of solids
K. Lejaeghere et al. (2016). Institutional record of the original article.
https://www.nist.gov/publications/reproducibility-density-functional-theory-calculations-solids
Science, DOI 10.1126/science.aad3000; NIST institutional record and self-verification. Numerical reproduction deviated from physical accuracy.

[R19] Precision and efficiency in solid-state pseudopotential calculations
G. Prandini, A. Marrazzo, I. E. Castelli, N. Mounet, N. Marzari (2018). Original research article
https://www.nature.com/articles/s41524-018-0127-2
npj Computational Materials 4, 72; SSSP multiple convergence criteria.

[R20] The thermodynamic scale of inorganic crystalline metastability
W. Sun et al. (2016). Original article, author's copy.
https://perssongroup.lbl.gov/papers/sun-2016-metastability.pdf
Science Advances 2, e1600225; author's LBL institutional copy, a scale related to metastability in chemistry.

[R21] First principles phonon calculations in materials science
A. Togo, I. Tanaka (2015). Method article, author version.
https://arxiv.org/abs/1506.08498
Scripta Materialia, DOI 10.1016/j.scriptamat.2015.07.021; the bibliography and content of the author's version have been verified.

[R22] First-principles calculations for point defects in solids
C. Freysoldt, B. Grabowski, T. Hickel, J. Neugebauer, G. Kresse, A. Janotti, C. G. Van de Walle (2014). Method compilation.
https://doi.org/10.1103/RevModPhys.86.253
Reviews of Modern Physics 86, 253; defect formation energy and the finite-size/chemical potential framework.

[R23] A climbing image nudged elastic band method for finding saddle points and minimum energy paths
G. Henkelman, B. P. Uberuaga, H. Jónsson (2000). Bibliographic record of the original article.
https://doi.org/10.1063/1.1329672
Journal of Chemical Physics 113, 9901-9904; bibliographic record and original method title verified, publisher's direct access failed.

[R24] Special quasirandom structures
A. Zunger, S.-H. Wei, L. G. Ferreira, J. E. Bernard (1990). Original research article
https://journals.aps.org/prl/abstract/10.1103/PhysRevLett.65.353
Physical Review Letters 65, 353; the original SQS method, which represents random alloy correlations using a small structure.

[R25] SIMsalabim: An open-source drift-diffusion simulator for semiconductor devices
M. Koopmans, V. M. Le Corre, L. J. A. Koster (2022). Research software article.
https://joss.theoj.org/papers/10.21105/joss.03727
Journal of Open Source Software 7(70), 3727; an open-source software and publication record for one-dimensional drift-diffusion.

[R26] Solcore: A multi-scale, python-based library for modelling solar cells and semiconductor materials
D. Alonso-Álvarez et al. (2017). Preprint on research software
https://arxiv.org/abs/1709.06741
Author's pre-print 2017; journal publication 2018. A multi-scale optical/electrical tool is provided as an example, but it does not guarantee the accuracy of a specific version.

[R27] Modelling polycrystalline semiconductor solar cells
M. Burgelman, P. Nollet, S. Degrave (2000). Original article, author's copy.
https://users.elis.ugent.be/ELISgroups/solar/projects/scaps/Burgelman%20TSF%202000a.pdf
Thin Solid Films 361-362, 527-532; original author's copy from the SCAPS page of Ghent University.

[R28] A framework to evaluate machine learning crystal stability predictions
J. Riebesell et al. (2025). Original research article
https://www.nature.com/articles/s42256-025-01055-1
Nature Machine Intelligence 7, 836-847; Matbench Discovery. Distinction between formation energy/stability, regression/classification, and prospective evaluation; a correlation was observed.

[R29] Leakage and the reproducibility crisis in machine-learning-based science
S. Kapoor, A. Narayanan (2023). Research review
https://pmc.ncbi.nlm.nih.gov/articles/PMC10499856/
Patterns 4, 100804; DOI 10.1016/j.patter.2023.100804. Data leakage typology and challenges in scientific reproducibility.

[R30] The FAIR Guiding Principles for scientific data management and stewardship
M. D. Wilkinson et al. (2016). Paper on fundamental principles
https://www.nature.com/articles/sdata201618
Scientific Data 3, 160018; FAIR data management principles are not unconditionally equated with open access.

[R31] NIST/SEMATECH e-Handbook of Statistical Methods - Choosing an experimental design
NIST/SEMATECH (Year not specified). Institutional handbook
https://www.itl.nist.gov/div898/handbook/pri/section3/pri3.htm
An open-source repository for random block, factorial, and response surface designs. The numerical examples in this section are original, illustrative calculations.

[R32] IEC 61724-1:2021 - Photovoltaic system performance - Part 1: Monitoring
International Electrotechnical Commission (2021). Standards catalogue entry
https://webstore.iec.ch/en/publication/70170
The scope of the open catalog has been verified, including terminology, equipment, and analysis methods for monitoring. RLV catalog entry: no claim of full-text item matching.

[R33] Weather-Corrected Performance Ratio
T. Dierauf, A. Growitz, S. Kurtz, J. L. Becerra Cruz, E. Riley, C. Hansen (2013). Institutional report
https://www.nrel.gov/docs/fy13osti/57991.pdf
NREL/TP-5200-57991, April 2013; a corporate methodology report that minimizes the impact of weather conditions on the performance ratio (PR) comparison.

[R34] Fact Sheet: Environmental Life Cycle Assessment of Electricity from PV Systems
IEA PVPS Task 12 (2024). Institutional fact sheet
https://iea-pvps.org/fact-sheets/fact-sheet-environmental-life-cycle-assessment-of-electricity-from-pv-systems/
May 2024 information note; within the context of LCA boundaries and technology inventory. No current market price or universal carbon intensity claim was used.

[R36] Life Cycle Assessment of Current Photovoltaic Module Recycling
IEA PVPS Task 12 (2018). Institutional report
https://iea-pvps.org/wp-content/uploads/2020/01/Life_Cycle_Assesment_of_Current_Photovoltaic_Module_Recycling_by_Task_12.pdf
IEA-PVPS T12-13:2018; environmental assessment of recycling. The concept of component value was conceptually separated from mass recovery.

[R37] Solar cell efficiency tables (Version 60)
M. A. Green, E. D. Dunlop, J. Hohl-Ebinger, M. Yoshita, N. Kopidakis, K. Bothe, D. Hinken, M. Rauer, X. Hao (2022). Study of comparison and measurement methods.
https://doi.org/10.1002/pip.3595
It was used for defining areas and measurement/comparison methods; it was not presented as a current record table. Publication and JRC institutional records were verified.